The potential involvement of semicarbazide-sensitive amine oxidase-mediated reactions and aldehyde stress in the aggregation, cytotoxicity and clearance of beta-amyloid related to Alzheimer's disease

A Thesis

Submitted to the College of

Graduate Studies and Research

in Partial Fulfillment of the Requirements

for the Degree of Doctor of Philosophy

in the Department of Pharmacology

University of Saskatchewan

Saskatoon

By

KUN CHEN

Fall 2009

PERMISSION TO USE

In presenting this thesis in partial fulfillment of the requirements for a Postgraduate degree from the University of Saskatchewan, I agree that the Libraries of this University may make it freely available for inspection. I further agree that permission for copying of this thesis in any manner, in whole or in part, for scholarly purposes may be granted by Dr. Peter Yu, who supervised my thesis work, or in his absence, by the Head of the Department of Pharmacology, or the Dean of the College of Medicine at the University of Saskatchewan. It is understood that any copying, publication, or use of this thesis or parts thereof for financial gain shall not be allowed without my written permission. It is also understood that due recognition shall be given to me, and to the University of Saskatchewan in any scholarly use which may be made of any material in my thesis.

Requests for permission to copy or to make other use of material in this thesis in whole or part should be addressed to:

Head of the Department of Pharmacology
University of Saskatchewan
Saskatoon, Saskatchewan S7N 5E5

ABSTRACT

Beta-amyloid (Aβ) remains to be the focus of research interest of the pathogenesis of Alzheimer's disease (AD). Aβ is subject to oligomerization and its polymers are cytotoxic. Advanced aggregation leads to formation of senile plaques. Depositions of Aβ surrounding the cerebral vasculature, *i.e.* cerebral amyloid angiopathy (CAA), occur in most AD patients. The occurrence of Aβ aggregation in AD brains is not due to over-expression of amyloid precursor protein in most cases of AD. Factors influencing Aβ polymerization are yet to be established.

Aldehydes are highly reactive. They can cause protein crosslinkage. It is interesting to study whether endogenous aldehydes may be involved in Aβ polymerization process. In order to investigate the potential interaction of endogenous aldehydes with Aβ and their effects on its aggregation, various techniques including thioflavin T fluometry, dynamic light scattering, circular dichroism and atomic force microscopy were employed to assess Aβ aggregation at different stages. Formaldehyde, methylglyoxal, malondialdehyde and 4-hydroxyl-nonenal were found to enhance Aβ β-sheets formation, oligomerization and fibrillogenesis *in vitro*. The sizes of the oligomers are increased after interaction with the aldehydes. Lysine residues of Aβ were identified to be the primary site of interaction with aldehydes by forming Schiff bases, which may subsequently lead to intra- and inter-molecular crosslinkage. Aldehydes can also crosslink Aβ with other proteins such as apolipoprotein E and α2-macroglobulin (α2M), to form large complexes. Results suggest that aldehydes substantially increase the rate of Aβ oligomerization at each stage of fibrillogenesis.

The native and formaldehyde-modified Aβ oligomers were isolated by size exclusion chromatography and their cytotoxic effects towards SH-SY5Y neuroblastoma cells were assessed using MTT, LDH and caspase-3 activity assays. The aldehyde-modified oligomers are slightly but significantly more cytotoxic compared to the native oligomers. Since aldehydes significantly increase the production of Aβ oligomers, an increase in aldehydes would enhance the total cytotoxicity, suggesting that aldehydes may potentially exacerbate neurovascular damage and neurodegeneration caused by Aβ.

Low-density lipoprotein receptor related protein-1 (LRP-1) plays a crucial role in Aβ clearance *via* the cerebral vasculature. Semicarbazide-sensitive amine oxidase (SSAO) and LRP-1 are both richly expressed on the vascular smooth muscle cells (VSMCs). We demonstrated that

SSAO-mediated deamination affects LRP-1 function using isolated VSMCs. Formaldehyde at low concentrations decreases LRP-1-mediated uptake of α2M, a substrate of LRP-1 and a carrier for Aβ. Methylamine, an SSAO substrate that is converted to formaldehyde, also inactivates LRP-1 function, but not in the presence of an SSAO inhibitor. Increased SSAO-mediated deamination can potentially impair Aβ clearance *via* LRP-1.

In conclusion, aldehydes derived from oxidative stress and SSAO-mediated deamination induce Aβ aggregation, enhance Aβ cytotoxicity and impair Aβ clearance. The exclusive localization of SSAO on the cerebral vasculature may be responsible for the perivascular deposition of Aβ, *i.e.* CAA, which is associated both with vascular dementia and with AD. Vascular surface SSAO may be a novel pharmacological target for the treatment of AD.

ACKNOWLEDGEMENT

First, I would like to thank my supervisor, Dr. Peter Yu, for his supervision, ongoing encouragement and unwavering support, professionally, financially and personally, throughout the course of my PhD studies. Dr. Yu guided me through this path of training during which not only my professional knowledge has been greatly extended, but also he believed in my potential to independently develop my ideas on this thesis project, and by supporting me to participate in international and local academic conferences. He has been always approachable and patient, which has strengthened my commitment in research. Dr. Yu's passion on science, diligence and high standard for excellence has always been inspiring and stimulating to me. His excitement by new findings spreads to everyone in his laboratory. Dr. Yu is truly an excellent example of a great scientist, trustworthy and respected by all his peers and students. More importantly, Dr. Yu is more than a supervisor and scientist for me. He is caring for other people and willing to provide his help at his best. He never loses sight of the truly important things in life.

I would also like to acknowledge the support of my committee members: Drs. Richardson, Wu, Sawicki, and Nazarali. They were available for guidance whenever necessary. I greatly appreciate the time and constructive advice from my external reviewer, Dr. Tieu, from University of Rochester. I am particularly thankful to Dr. Tuchek, who has always been helpful and encouraging to me when I transferred from the Department of Psychiatry to the Department of Pharmacology.

Throughout my PhD training, I have been most fortunate to work with coworkers: Michael Kazachkov, Zhongjian Jiang, Lixin Lu, Stephanie Johnson, Zaiping Liu and Linda Huang. Their help in countless ways was crucial in building the depth and breadth of this thesis. We also shared a memorable friendship. I would also like to acknowledge the tremendous help provided by Heather Schultz, the source of joy of our daily life.

Finally, I would like to acknowledge those closest to me: my parents. Their continued support and unwavering faith in me during every day of this long educational odyssey is my ultimate drive.

TABLE OF CONTENTS

LIST OF FIGURES AND TABLES

LIST OF ABBREVIATIONS

Aβ	β-amyloid
AD	Alzheimer's disease
AFM	Atomic force microscopy
AGE	Advanced glycation end products
AO	Amine oxidase
ApoE	Apolipoprotein E
APP	Amyloid precursor protein
BBB	Blood-brain barrier
BSA	Bovine serum albumin
C1q	Complement component 1q
CAA	Cerebral amyloid angiopathy
CBF	Cerebral blood flow
CD	Circular dichroism
CHAPS	3-[(3-Cholamidopropyl)dimethylammonio]-1-propanesulfonate
CNS	Central nervous system
CO_2	Carbon dioxide
CSF	Cerebral spinal fluid
DEVD-pNA	Asp-Glu-Val-Asp-p-nitroaniline)
DLS	Dynamic light scattering
DM	Diabetes mellitus
DMEM	Dulbecco's Modified Eagle's Medium
ECL	Enzymatic chemiluminescence
EDTA	Ethylenediaminetetraacetic acid
EM	Electron microscopy
ER	Endoplasmic reticulum
FAD	Flavin adenine dinucleotide
FBS	Fetal bovine serum
FMOC	9-Fluorenylmethyl chloroformate
HBSS	Hank's balanced salts solution
HCl	Hydrochloric acid
HEPES	4-(2-Hydroxyethyl)piperazine-1-ethanesulfonic acid, N-(2-Hydroxyethyl)piperazine-N′-(2-ethanesulfonic acid)
HFIP	1, 1, 1, 3, 3, 3-Hexafluoro-2-propanol

HNE	4-Hydroxy-2-nonenal
HPLC	High performance liquid chromatography
IDE	Insulin-degrading enzyme/insulysin
LDH	Lactate dehydrogenase
LDL	Low density lipoprotein
LPO	Lipid peroxidation
LRP	LDL receptor-related protein
LTP	Long-term potentiation
α2M	α2-Macroglobulin
MAO-A/B	Monoamine oxidase A/B
MDA	Malondialdehyde
MTT	3-[4, 5-dimethylthiazol-2-yl]-2, 5-diphenyl-tetrazolium bromide
$NaBH_4$	Sodium tetrahydridoborate
NaCl	Sodium chloride
NAD+	Nicotinamide adenine dinucleotide
NFT	Neurofibrillary tangles
NMR	Nuclear magnetic resonance
NSAIDs	Non-steroidal anti-inflammatory drugs
OD	Optical density
PBS	Phosphate-buffered saline
RAGE	Receptor for advanced glycation end products
RAP	Receptor-accociated protein
Rh	Hydrodynamic radius
ROS	Reactive oxygen species
SDS	Sodium dodecyl sulfate
SEC	Size exclusion chromatography
SSAO/VAP-1	Semicarbazide-sensitive amine oxidase/vascular adhesion protein-1
TBS(T)	Tris Buffered Saline (Tween-20)
ThT	Thioflavin T
TMA	Tetramethylammonium chloride
TPQ	2, 4, 5-trihydroxyphenylalanine-quinone
VSMC	Vascular smooth muscle cell

1. INTRODUCTION

1.1 Alzheimer's Disease

1.1.1 History

In 1906, a German psychiatrist, Alois Alzheimer reported a case of a dementia patient, Mrs. Auguste Deter from the Frankfurt Asylum, to the German Medical Society. He described the patient's symptoms including memory decline and noncognitive behavioral features. Alzheimer also presented their association with neuropathological changes: senile plaques and neurofibrillary tangles (Alzheimer, 1906). Since this presentation, the symptoms and pathological changes of presenile dementia have been used to diagnose Alzheimer's disease (AD).

1.1.2 Symptoms and Pathophysiology

AD is a neurodegenerative disease. It is the most common form of dementia accounting for 60% to 80% of all dementia cases (Fratiglioni et al., 1999). Its prevalence increases with age. For Canadians, 7.7% of the population older than 65 develop AD or related diseases and it increases to 33% among those older than 85 (Ebly et al., 1994). In other words, as the average life expectancy increases, so does the disease incidence.

There are three types of AD, namely, familial, early-onset and late-onset AD, depending on the age of onset. In the first type, about 90% of AD cases are diagnosed after age 65, which are categorized as late-onset/sporadic AD. In the second type, less than 10% of cases are diagnosed before age 65, which are categorized as early-onset AD. Less than 1% of AD cases are diagnosed with early-onset familial AD as the last type. Strong genetic links are associated with early-onset and familial AD (Bertram and Tanzi, 2008).

The characteristic symptom of AD is gradual memory loss. Therefore, the current diagnostic criteria (the Diagnostic and Statistical Manual of Mental Disorders) are based on the impairment of memory and learning abilities. Overall, both the long-term and short-term memory are impaired in AD (Sartori et al., 2004). Other symptoms include deterioration in language skills and cognitive functions related to speaking, reading and writing are all affected, eventually

leading to complete loss of speech (Frank, 1994). Very frequently, neuropsychiatric manifestations, including depression, aggression and anxiety, develop with the memory loss (Mitrushina et al., 1994; Tatsch et al., 2006).

The pathology of AD involves degeneration of neurons and synaptic connections in the cerebral cortex as well as certain subcortical regions. In turn, the degeneration leads to memory loss and atrophy in the temporal and parietal lobe, and is observed as shrinkage of brain in patients (Wenk, 2003). Autopsy from AD patients exhibits two histopathological hallmarks: senile neuritic plaques and neurofibrillary tangles (NFT).

There are three major types of plaques: diffuse, neuritic and cerebrovascular. Diffuse plaques lack the amyloid core and the abnormal dystrophic neurites seen in neuritic plaques and possess amorphous appearance. It is presumed that the diffuse plaques represent the early phase of plaque formation. The neuritic plaques have a dense core of amyloid surrounded by abnormal neurites (aggregates of axons and dendrites containing lysosomes, mitochondria and paired helical filaments), microglia and astrocytes that form a spherical shape. The diameters of neuritic plaques range from 50 to 200 μm (Mandybur and Chuirazzi, 1990). Cerebrovascular plaques are the amyloid deposits associated with capillaries and arterioles in the cerebral cortex of up to 90% of AD patients (Mandybur, 1975; Yamada et al., 1987; Ellis et al., 1996).

The other histopathological hallmark of AD, the NFT, is comprised of paired helical filaments in the cell body and axon and is formed by hyperphosphorylated tau protein (Grundke-Iqbal et al., 1986a; Grundke-Iqbal et al., 1986b; Lee et al., 1991). Tau is a protein associated with microtubules in neurons. It interacts with tubulin, facilitates its assembling, and stabilizes the microtubules. Hyperphosphorylated tau reacts rapidly with each other to form filaments especially in large pyramidal cells (Terry et al., 1991).

1.1.3 Aetiology and Potential Mechanisms of Late-Onset AD

The aetiology of late-onset AD is not fully understood. Current hypotheses about the causes of the disease are focused on β-amyloid (Aβ) and formation of senile amyloid plaques, or on tau and the accumulation of NFT. These aggregated proteins were thought to cause degeneration of synapses and neurons, which consequently cause cognitive impairment (Selkoe, 1991; Roher et al., 1993; Selkoe, 1994; Hardy and Selkoe, 2002). A variety of factors may be involved in this

process including oxidative stress, inflammation, metal ions and so on (Subbarao et al., 1990; Pappolla et al., 1992; Behl et al., 1994; Breitner, 1996; Deibel et al., 1996).

1.1.4 Amyloid Hypothesis

Aβ aggregation can trigger formation of NFT (Lue et al., 1999; Datki et al., 2004). Therefore, the amyloid hypothesis has proposed that Aβ aggregation is the upstream origin of other relevant pathologic changes such as NFT, oxidative stress, inflammation and degeneration of synapses and neurons, eventually leading to AD (Neve and Robakis, 1998; Hardy and Selkoe, 2002; Sommer, 2002).

1.1.4.1 Aβ Production

Aβ is a peptide composed of 39 to 43 amino acids from proteolysis of a large transmembrane glycoprotein, amyloid precursor protein (APP) (Selkoe, 1991). APP is encoded by a gene on chromosome 21, and is expressed in all cell types. It is localized on the plasma membrane as well as endosomes and shifts between them (Koo and Squazzo, 1994). In the brain, it contributes to neuronal migration and synapse formation (Priller et al., 2006; Young-Pearse et al., 2007). Its function in the peripheral system is unclear.

The proteolytic processing of APP is mediated by secretase enzymes. Three types of secretase have been identified: α-, β- and γ-secretases. α-secretase is located on the plasma membrane and cleaves APP between residues 16 and 17 of the Aβ sequence to form the sAPPα, which inhibits Aβ formation (Verbeek et al., 1997). sAPPα is involved in cell adhesion and exhibits neuroprotective properties (Selkoe, 1994). β-secretase, also known as beta-site APP cleaving enzyme, is expressed on the Golgi apparatus and endosomes, and cleaves APP between residues 596 and 597 to form a 99-amino acid membrane-bound fragment containing the C-terminus of Aβ peptide (Nunan and Small, 2000). Following cleavage by β-secretase, this fragment is further cleaved transmembranely on endosomes by γ-secretase, localized in endoplasmic reticulum (ER), lysosomes and cell membrane, to form the N-terminus of Aβ (Wolfe et al., 1999). The γ-Secretase is able to cleave APP at different sites, between residues 637 and 639, to generate Aβ monomers of different lengths (Shi et al., 2003; Wolfe, 2006). The products of APP cleavage are either secreted into the extracellular compartment or degraded by intracellular proteolytic enzymes.

Among the Aβ species, $A\beta_{1-40}$ is the predominant form and $A\beta_{1-42}$ accounts for 10% of total secreted Aβ (Dovey et al., 1993; Asami-Odaka et al., 1995; Citron et al., 1996). Despite its lower amount, $A\beta_{1-42}$ appears to be the major amyloid component in senile plaques (Roher et al., 1993; Iwatsubo et al., 1994). Plaques associated with walls of cerebral blood vessels, known as cerebral amyloid angiopathy (CAA), contain high levels of $A\beta_{1-40}$ compared with $A\beta_{1-42}$ (Joachim et al., 1988; Prelli et al., 1988; Suzuki et al., 1994; Alonzo et al., 1998; Zipfel et al., 2009). AD patients with certain APP mutations in the mid-region of Aβ develop more CAA than senile plaques not associated with cerebral vessels (Levy et al., 1990). Hence, APP produced on cerebral vasculature may be cleaved differently from that on neurons and astrocytes. Interestingly, initial $A\beta_{1-42}$ deposition around cerebral vasculature triggers massive accumulation of $A\beta_{1-40}$ (Alonzo et al., 1998). In APP transgenic mice, an elevated ratio of Aβ 40:42 in brain extracellular pools and a decreased 40:42 ratio in the cerebral spinal fluid (CSF) are associated with increased CAA formation (Fryer et al., 2003; Fryer et al., 2005).

1.1.4.2 Factors Affecting Aβ Production

Genetic Links

Early-onset and inherited familial AD account for less than 10% of all AD cases. These cases are known to be associated with increased Aβ production. Mutations of genes encoding APP, presenilin 1 and presenilin 2 have been identified (Bertram and Tanzi, 2004). For instance, presenilins are proteins located near the catalytic center of γ-secretase (Wolfe et al., 1999; Hansson et al., 2004). Presenilin mutations cause altered γ-secretase activity (Berezovska et al., 2000), increased Aβ production (Scheuner et al., 1996; Ikeuchi et al., 2003) and alterations in the $A\beta_{1-42}/A\beta_{1-40}$ ratio (Borchelt et al., 1996; Kaneko et al., 2007). On the other hand, APP mutations cause increased APP expression, increased Aβ production and secretion (Mullan et al., 1992; Felsenstein et al., 1994). These findings have provided remarkable insights into AD pathology and a great number of transgenic mouse models have been created representing Aβ deposition and AD pathology (Duff and Suleman, 2004; Marjanska et al., 2005; Muyllaert et al., 2006; Crews et al., 2008).

The ε4 allele of apolipoprotein E (ApoE) has been consistently found as a predisposing factor for late-onset AD in various studies (Saunders et al., 1993; Strittmatter et al., 1993; Montine et

al., 1997; Holtzman et al., 2000). ApoE is the main apolipoprotein in the central nervous system (CNS), secreted by astrocytes and microglia. It is a crucial component of triglyceride-rich lipoproteins mediating cholesterol transport in the brain and the peripheral system. It has three isoforms: ApoE2, ApoE3 and ApoE4 respectively coded by ε2, ε3 and ε4 alleles (Das et al., 1985). Carriers of ε4 allele have a more than 2-fold risk of developing AD, whereas ApoE2/3 seems to have preventive effect on AD (Corder et al., 1993; Corder et al., 1994; Hofman et al., 1997; Bonarek et al., 2000). The ε4 allele is strongly associated with increased Aβ aggregation in mouse models of AD (Holtzman et al., 2000; Buttini et al., 2002). Over the past 10 years, more than 20 non-ApoE loci have been identified that are significantly associated with late-onset AD (Bertram et al., 2007), such as genes encoding angiotensin converting enzyme-1, cholesterol 25 hydroxylase, sortilin-related receptor and transferrin (Lee et al., 1999; Kehoe et al., 2003; Rogaeva et al., 2007; Zerbinatti et al., 2008). Overall, the identification of gene mutations associated with late-onset AD is based on and guided by various hypotheses of AD pathology, including Aβ degradation and clearance, signal transduction, cholesterol metabolism and metal homeostasis. Whether these genetic mutations play a crucial role in AD pathogenesis, particularly in Aβ production, requires further studies.

ApoE, Low Density Lipoprotein Receptor-related Protein-1 and Cholesterol Metabolism

ApoE seems to influence APP processing and increase Aβ production (Masinovsky et al., 1990; Vincent and Smith, 2001; Ye et al., 2005). This effect is mediated by the low density lipoprotein (LDL) receptors, particularly the LDL receptor-related protein-1 (LRP-1) pathway (Li et al., 2001; Herz and Bock, 2002; Ye et al., 2005). LRP-1 has diverse ligands including ApoE, α2-macroglobulin (α2M), lactoferrin and APP (Herz, 2001; Li et al., 2001). LRP-1 plays a central role in the transport of lipoproteins composed of ApoE and cholesterol. Interestingly, polymorphism of LRP-1 gene is associated with late-onset AD (Kang et al., 1997; Baum et al., 1998; Lambert et al., 1998a). LRP-1 and APP are co-localized on the plasma membrane and endosomes. As a result, LRP-1 either directly interacts with the extracellular domain of APP or indirectly with the intracellular tail of APP *via* an adaptor protein (Trommsdorff et al., 1998; Kinoshita et al., 2001). By interaction with APP, LRP-1 influences APP processing, endocytic trafficking and turnover, which subsequently affects Aβ production (Kounnas et al., 1995; Ulery et al., 2000; Pietrzik et al., 2002; Pietrzik et al., 2004).

In humans, high levels of plasma cholesterol have been identified as a risk factor for AD (Notkola et al., 1998). Patients treated with cholesterol-lowering statins have significantly reduced incidence of AD (Jick et al., 2000; Wolozin et al., 2000). Cholesterol is also abundantly present in the brain with a slow turnover (Dietschy and Turley, 2001). The homeostasis of cholesterol in the brain is separate from the peripheral system due to function of the blood brain barrier (BBB). Cholesterol in the brain is synthesized locally and eliminated by brain-specific mechanisms. It is endocytosed by ApoE-LRP interaction and converted into 24(S)-hydroxycholesterol (Dietschy and Turley, 2001, 2004). The imbalance of cholesterol metabolism seems to contribute to AD pathogenesis. For example, alteration in the level of cellular cholesterol affects APP processing (Bodovitz and Klein, 1996; Racchi et al., 1997). Elevated level of cholesterol is able to increase Aβ production in cell, rabbit and mouse models (Sparks et al., 1994; Refolo et al., 2000). Similarly, suppression of *de novo* cholesterol synthesis leads to decreased Aβ production (Simons et al., 1998). One potential mechanism by which cholesterol affects APP processing is that cholesterol increases β- and γ- secretase activities, resulting in more Aβ formation (Frears et al., 1999; Fassbender et al., 2001; Wahrle et al., 2002).

In summary, ApoE, LRP-1 and cholesterol appear to be involved in AD pathology by affecting Aβ production. Not only are they involved in Aβ production, but also in Aβ aggregation, clearance, cytotoxicity and oxidative stress.

1.1.4.3 Aβ Aggregation

Under physiological conditions, soluble monomeric $A\beta_{1\text{-}40/42}$ is predominately formed in unfolded random coils with almost no α-helix or β-sheet structures (Kelly, 1998; Smith, 1998; Kirkitadze et al., 2001). When accumulated, Aβ monomers initially undergo a serial conformational change before folding into β-sheets (Thunecke et al., 1998).

Two hydrophobic regions on the Aβ molecule are critical for its aggregation, particularly in the initial phase (Balbach et al., 2000; Ma and Nussinov, 2002; Soto, 2003; Liu et al., 2004). The first region is residues 17 to 21 (LVFFA). These residues are all hydrophobic amino acids. This region generates a hydrophobic core for subsequent protein folding and "seeds" of aggregation. Interestingly, the $F^{19}F^{20}$ dipeptide in this region aggregates by itself to form stiff nanotubes, which further stabilizes Aβ aggregation (Reches and Gazit, 2003). Another hydrophobic region

is residues 31 to 35 (IIGLM). This region forms a reverse turn that forms antiparallel strands with surrounding residues and facilitates the aggregation (Bond et al., 2003).

After the initial conformational changes, the hydrophobic regions are exposed to each other. These hydrophobic regions form the intra- and intermolecular β-sheet structure (Carrell and Lomas, 1997; Capaldi and Radford, 1998). β-sheet (both parallel and antiparallel) formation is crucial for this stage. Driven by hydrophobic force, Aβ monomers assemble into dimers, trimers, tetramers, and then soluble oligomers (composed of 5 to 16 Aβ monomers). Such a nucleation step is the rate-limiting step representing the lag phase of Aβ aggregation (Merlini and Bellotti, 2003). After the concentration of Aβ oligomers reaches certain threshold, the oligomers as building blocks will further assemble into protofibrils and then fibrils (Lomakin et al., 1996; Harper et al., 1997; Bitan et al., 2001). The chronic aggregation of Aβ with itself as well as with other molecules such as lipoproteins and cholesterol eventually leads to the formation of senile plaques. The process of Aβ aggregation is summarized in Figure 1.

The structures of amyloid fibrils have been elucidated from studies using electron microscopy (EM), X-ray diffraction, circular dichroism (CD) and Fourier transform infrared spectroscopy (Naiki et al., 1989; Lomakin et al., 1996; Naiki and Nakakuki, 1996; Makin and Serpell, 2005). A structural model of Aβ fibrils was proposed by combining results from X-ray diffraction, EM and nuclear magnetic resonance (NMR) as shown in Figure 2 (Petkova et al., 2002). Briefly, the intermolecular backbone is composed of hydrogen bonds. A cross-β unit has a double-layer structure with a hydrophobic core and hydrophobic surface formed by residues 12 to 24 and 30 to 40. Residues 12 to 24 and 30 to 40 display β-strand conformation and they form parallel β-sheets *via* intra- and inter-molecular hydrogen bonds. Lysine 28 and aspartate 23 are the only charged residues in hydrophobic core responsible for intramolecular salt-bridge formation. Region of residues 25 to 29 forms a β-turn on the peptide backbone, which facilitates the side-chain-side-chain interactions by bringing two β-sheets in contact. Cross β-units further stack up by juxtaposing the hydrophobic surfaces leading to fibril growth in diameters.

With the development of more advanced structural technologies, smaller intermediate species have been identified during the early phase of aggregation. Fibrils are composed of unbranched protofibrils attached laterally or twisted together (Walsh et al., 1999; Kirkitadze et al., 2001). Typical protofibrils of $A\beta_{1\text{-}40}$ are around 4 nm in diameter, 20 to 70 nm in length with a

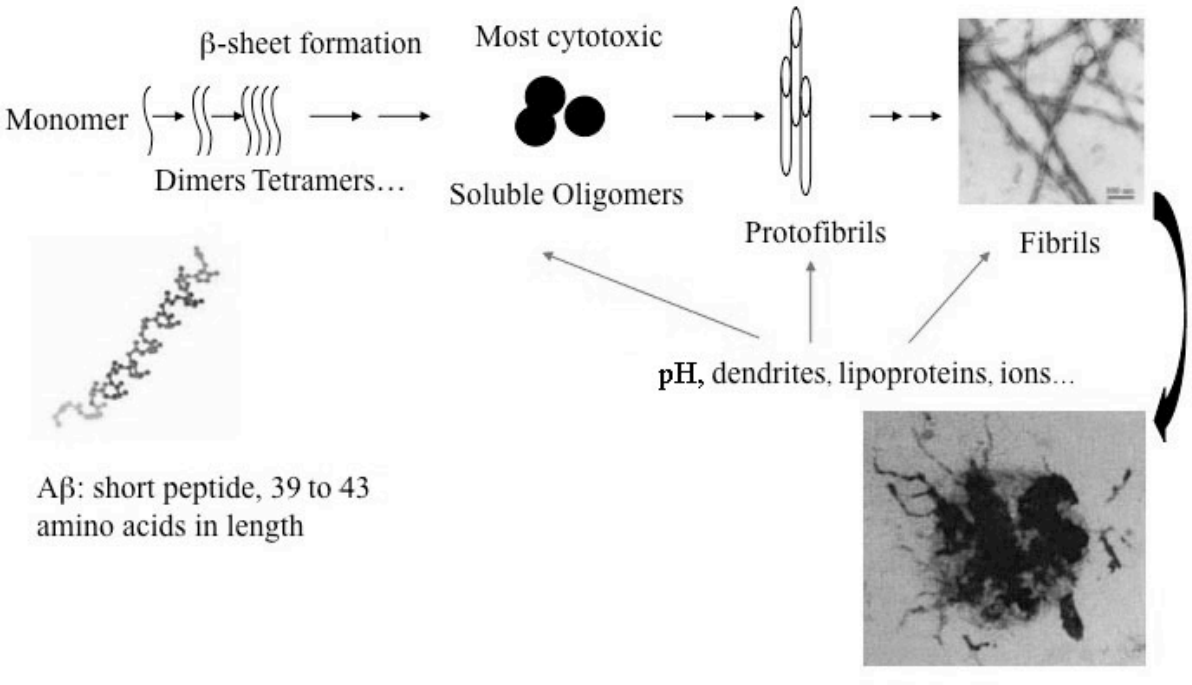

Figure 1. Process of Aβ aggregation. Aβ monomers assemble into dimers, trimers, tetramers and oligomers (up to 16'mers) by β-sheet structure formation, driven by hydrophobic force. Oligomers further aggregate to form protofibrils and fibrils. A number of factors such as pH, lipoproteins and ions affect this process, which eventually leads to the formation of senile plaques as seen in AD.

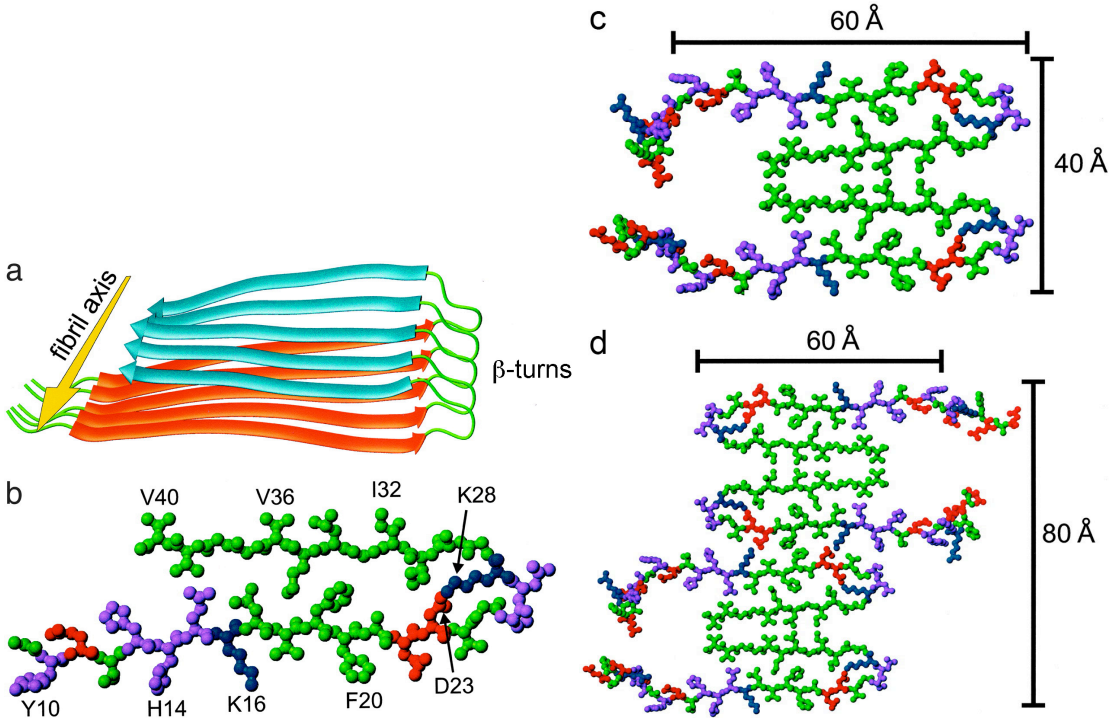

Figure 2. A structural model of $A\beta_{1\text{-}40}$ fibrils derived from NMR and EM (Petkova et al., 2002). (a) A cross-β unit composed of several $A\beta_{1\text{-}40}$ monomers. The direction of the long axis of the fibrils is indicated by the arrow. (b) $A\beta_{1\text{-}40}$ viewed down the long axis of its fibril. Residues 1 to 8 (Asp-Ala-Glu-Phe-Arg-His-Asp-Ser) are omitted as they display fully disordered conformation. (c, d) Cross-sections of $A\beta_{1\text{-}40}$ fibril formed by lateral association of β-units. Residues 1 to 8 are included in randomly assigned conformation.

periodicity of around 20 nm and have a stable core structure (Harper et al., 1997, 1999; Kowalewski and Holtzman, 1999; Kheterpal et al., 2003).

Soluble Aβ oligomers, formed before the protofibrils and composed of 5 to 16 Aβ monomers, have also been identified. They have a spherical structure with diameters ranging from 2.7 to 5 nm (Huang et al., 2000; Bitan et al., 2001; Urbanc et al., 2004). The oligomerization processes of $A\beta_{1-40}$ and $A\beta_{1-42}$ are different (Bitan et al., 2003; Urbanc et al., 2004). $A\beta_{1-40}$ tends to form more dimers and less pentamers compared to $A\beta_{1-42}$. The Aβ pentamer has a hydrophobic core with a hydrophilic surface formed by N-terminal residues (Urbanc et al., 2004). As shown in Figure 3a and 3b, $A\beta_{1-42}$ pentamers are less spatially condensed than those of $A\beta_{1-40}$. Therefore, the hydrophobic core of $A\beta_{1-42}$ pentamers is more exposed to each other leading to faster aggregation.

The oligomerization and fibrillogenesis of Aβ are observed not only in AD. It has been proposed that most proteins are potentially amyloidogenic under certain conditions (Stefani and Dobson, 2003). A number of diseases, including AD, type 2 diabetes, Down's syndrome, Parkinson's disease, Huntington's disease and Creutzfeldt-Jakob disease, are associated with amyloidosis in which different amyloidogenic proteins deposit in tissues and organs. To date approximately 20 proteins that are distinct in sequences and structures have been discovered associated with amyloidoses, such as Aβ, tau, islet amyloid polypeptide, α-synuclein, polyglutamine, human insulin and prion peptide. These depositions are generally observed in the extracellular compartment but exceptions have been found, such as NFT in AD (Grundke-Iqbal et al., 1986b) and Lewy bodies composed of α-synuclein in Parkinson's disease (Serpell et al., 2000).

Amyloidoses share some similarities. The general model of protein misfolding is summarized in Figure 4. First, initial conformational changes of the proteins into partial folding state are required for subsequent aggregation. Secondly, soluble amyloid oligomers form during aggregation and they represent the primary cytotoxic species. These oligomers of different proteins exhibit a common and unique conformation-dependent structure regardless of their primary sequences (Kayed et al., 2003). They are capable of increasing the conductance of plasma membrane (Kayed et al., 2004). These findings suggest that these diseases share a common mechanism of cytotoxicity. Thirdly, the fibrils of different proteins have similar morphologies with a twisted and filamentous structure.

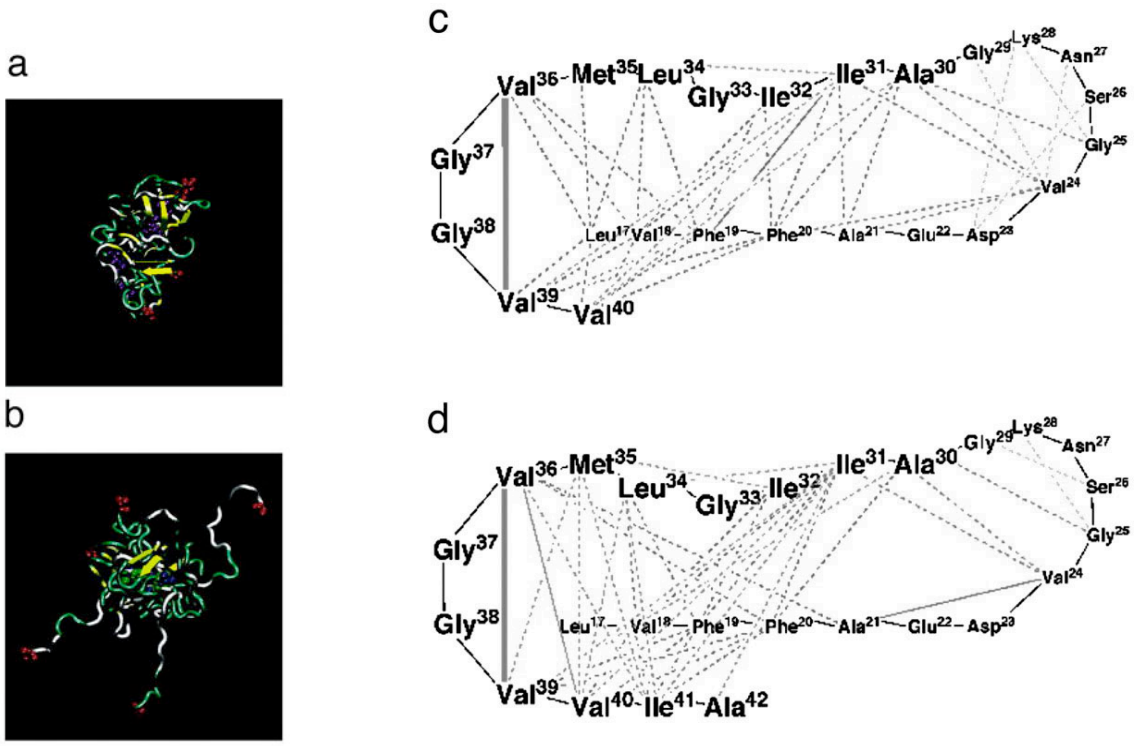

Figure 3. A structural model of Aβ pentamers derived from discrete molecular dynamics (Urbanc et al., 2004). (a) $A\beta_{1\text{-}40}$ pentamers. (b) $A\beta_{1\text{-}42}$ pentamers. In the $A\beta_{1\text{-}42}$ pentamer, the tails and spheres extending out from the hydrophobic core represent the N-terminal Asp-1. (c) Intramolecular contacts within $A\beta_{1\text{-}40}$ pentamers. (d) Intramolecular contacts within $A\beta_{1\text{-}42}$ pentamers. Weaker and stronger hydrophobic interactions are represented by dashed and solid lines, respectively. Glycine-37-glycine-38 in $A\beta_{1\text{-}42}$ pentamer is critical for a β-turn that is important in pentamer formation.

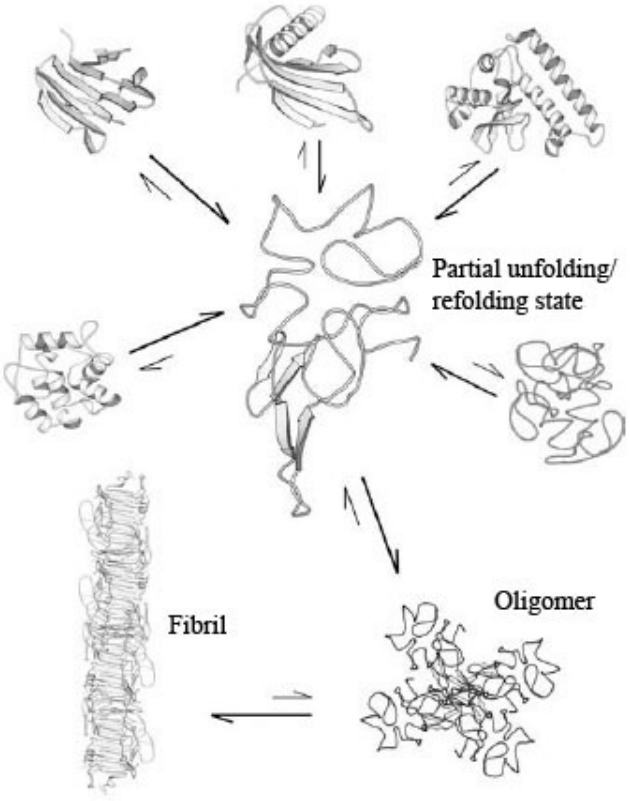

Figure 4. The general model of protein misfolding (Uversky, 2003). At the initial stage of misfolding, native soluble proteins with either globular or unfolded structures enter a partial folding state, followed by nucleation, oligomerization, fibrillogenesis and fibril elongation. Each step during this process is likely to be reversible with unknown relevant equilibrium constant. The oligomers are presented as a tetramer for convenience only and will vary depending on each protein.

1.1.4.4 Technologies of Structural Analysis Applied in the Present Aβ Aggregation Investigation

The development of high-resolution technologies has made it possible to assess Aβ aggregation at various stages.

Circular dichroism (CD) spectroscopy has been widely used to study the transition of random coils and α-helices of Aβ monomer into β-sheet structure during its aggregation (Huang et al., 2000; Syme et al., 2004). A solution of macromolecules absorbs the left- and right-handed polarized light differently dependent on structural asymmetry. CD spectroscopy measures the absorption of polarized light of wavelength from 190 nm to 260 nm and compares the differences in absorption between left- and right-handed light. CD spectra vary according to compositions of secondary structures present in peptides, proteins and nucleic acids. Therefore, the analysis of CD spectra can yield valuable information on secondary structures of biological macromolecules such as:

- Percentage of each secondary structure in solution
- Thermodynamic and solvent effects (pH, salt and organics) on the confirmation of macromolecules
- Kinetic information on protein folding, unfolding and aggregation
- Effects of chemical denaturants on protein stability and aggregation
- Protein-protein interactions.

The limitation of CD spectroscopy is the inability to provide direct information on sizes of particles. EM is useful for observing the morphology and the dimensions of Aβ fibrils, but it is not practical for real-time kinetic studies (Iwata et al., 2001a; Pallitto and Murphy, 2001). Dynamic light scattering (DLS) can overcome such difficulties. DLS uses a beam of monochromatic laser light that is scattered by micron-sized particles undergoing Brownian motion in solution. The laser light is scattered into a random pattern of spots varying in shape, size and intensity. The fluctuation of photon intensity of scattered light is analyzed. The resulting spectrum can provide relative information on the sizes of biomolecules, for example, the distribution of molecular sizes in solution. It is suitable to study particles with diameters ranging from submicron to several microns. Therefore, DLS is applied in protein characterization such as confirmation, crystallization, structural stability and aggregation. It is also used in studying

macromolecular complexes as well as biological and synthetic polymer characterization. DLS applied in studying the oligomerization and fibrillogenesis of Aβ has provided information on sizes of Aβ oligomers and fibrils, its nucleation rate and elongation rate (Lomakin et al., 1996; Thunecke et al., 1998).

Atomic force microscopy (AFM) is applied in studying protein structure, protein-protein interactions and surface properties of materials at atomic to micron level (Stolz et al., 2000; Nazem and Mansoori, 2008). The mechanism of AFM is illustrated in Figure 5. The instrument is composed of a sensitive cantilever with an ultra-fine tip at the end, a laser source and a photodetector. The cantilever is brought in close proximity to samples absorbed onto a smooth surface (*e.g.* mica) and moves across sample surface by lines. At atomic level, the repulsive force between the tip and sample surface is maintained constant. Therefore, AFM is capable of observing macromolecular structures at a level of sub-nanometer to microns. A laser beam is directed to the top of cantilever. As the cantilever moves, the constant force causes vertical displacement measured by laser deflection. The deflection is measured by a position-sensitive photodetector. The topography of samples is rastered from single-line scans.

The AFM instrument housed at the Saskatchewan Structural Sciences Center, University of Saskatchewan, can be operated in two modes, namely, contact mode and alternating-contact mode. In the contact mode, the force between the tip and sample surface is kept constant during scanning by maintaining a constant deflection. This mode is not appropriate for scanning soft samples due to the contact between tip and sample that distorts surface morphology.

In alternating-contact mode, the cantilever is externally oscillated close to its resonance frequency. During scanning, the oscillation gets modified by the force of tip-sample interaction. More commonly, the changes in oscillation amplitude (also known as intermittent contact or tapping mode) are analyzed. With respect to reference of the external oscillation, the changes in oscillation amplitude can provide information on the sample topography. Furthermore, under tapping mode, changes in the phase of oscillation can be used to discriminate between different types of materials on the surface. The alternating-contact mode exerts lower lateral force on samples and is widely used in imaging of biological samples.

Compared to EM that provides two-dimensional images, AFM can generate true three-dimensional images without special sample treatment as required by EM. Studies using AFM to observe Aβ aggregation have yielded useful information on the sizes of Aβ oligomers,

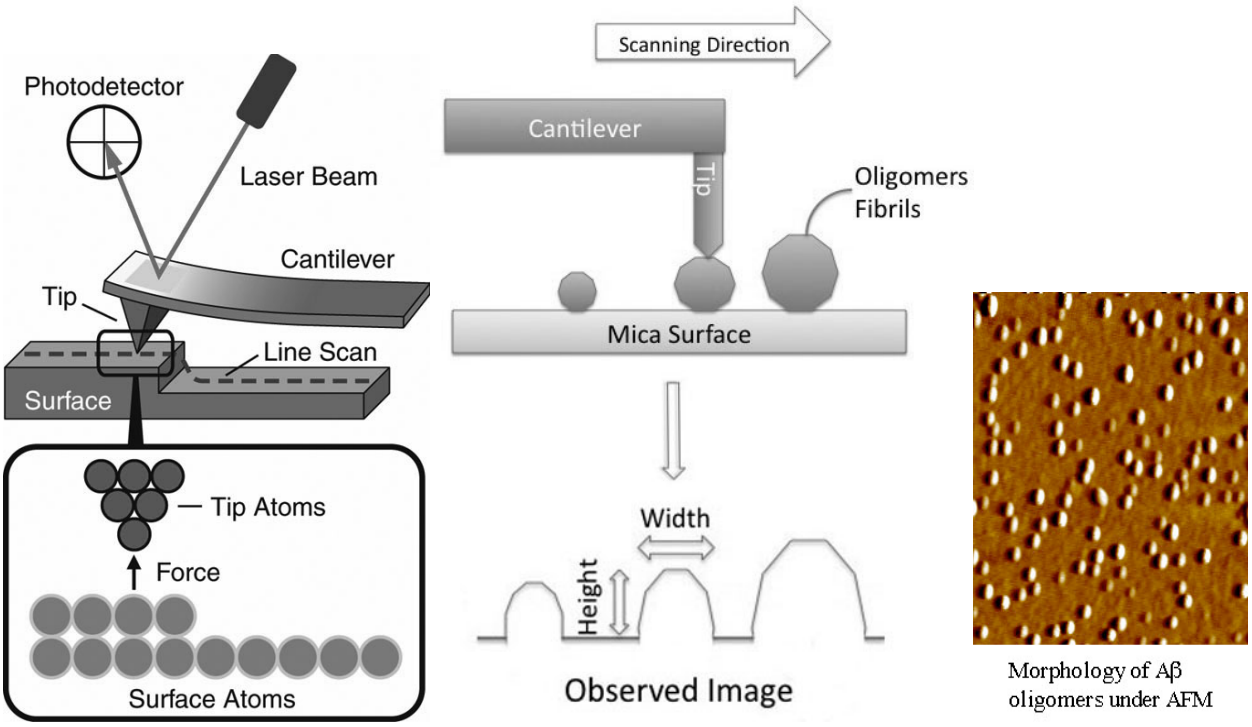

Figure 5. The principle of AFM. On the left: the instrument composition. In the middle: typical result of a single-line scan. The height of samples above surface can be accurately determined. The width is normally overestimated to some extent depending on the shape and finite size of the tip. On the right: the topography of samples, e.g. Aβ oligomers, is rastered into a three-dimensional image.

protofibrils and fibrils, their morphologies, kinetic parameters of Aβ oligomerization and fibrillogenesis, and factors affecting Aβ aggregation (Harper et al., 1997; Goldsbury et al., 1999; Kowalewski and Holtzman, 1999).

1.1.4.5 Factors Affecting Aβ Aggregation

A variety of factors, such as pH, metal ions (Cu^{2+}/Zn^{2+}), lipoproteins and cholesterol, are capable of affecting Aβ aggregation including oligomerization and fibrillogenesis (Atwood et al., 1998; Atwood et al., 2000; Harris, 2002; Kakio et al., 2002; Stanyer et al., 2002; Zhang et al., 2004).

In AD patients, metal ion homeostasis is severely impaired (Hershey et al., 1983; Basun et al., 1991; Deibel et al., 1996; Kala et al., 1996; Gonzalez et al., 1999). Senile amyloid plaques contain elevated levels of these metals (Lovell et al., 1998b). Physiological levels of Cu^{2+} and Zn^{2+} both reach 0.15 to 300 μM during synaptic transmission, and the plasma levels of Cu^{2+} and Zn^{2+} in AD patients are 19.5 μM and 10.6 μM, respectively (Nischwitz et al., 2008), which are capable of accelerating Aβ aggregation *in vitro* (Assaf and Chung, 1984; Bush et al., 1994). Under mild acidic condition (pH ~6.6), Cu^{2+} is most potent in promoting Aβ aggregation and this acidity has been found in tissues during the inflammatory process of AD patients (Atwood et al., 1998). Specific Cu^{2+} and Zn^{2+} chelators are able to reverse Aβ aggregation induced by metals (Cherny et al., 1999). In animal studies, transgenic mice overexpressing APP treated with Cu^{2+}/Zn^{2+} chelators exhibit significantly less Aβ deposition (Cherny et al., 2001; Gouras and Beal, 2001; Lee et al., 2004b). Aβ seems to play a role in copper redox cycling and produce reactive oxygen species (Dikalov et al., 1999). Based on these findings, metal chelators have been proposed as a potential preventive/therapeutic strategy for treatment of AD (Cherny et al., 2001).

Altered lipid metabolism has been implicated in AD pathogenesis. ApoE4 not only stimulates Aβ production, but also accelerates its oligomerization and fibrillogenesis both *in vitro* and *in vivo* (Kounnas et al., 1995; Holtzman et al., 2000; Fryer et al., 2003). Furthermore, it enhances Aβ cytotoxicity in cellular and mouse studies (Dolev and Michaelson, 2004; Fryer et al., 2005; Ye et al., 2005; Ji et al., 2006). On the contrary, ApoE3 is neuroprotective by sequestering Aβ and preventing its neurotoxicity (Jordan et al., 1998). ApoE has also been

proposed to play an important role in Aβ clearance *via* LRP-1 (Shibata et al., 2000). This will be discussed in detail later. Similarly to ApoE, apolipoprotein J also seems to affect Aβ aggregation, cytotoxicity and clearance (Boggs et al., 1996; Bell et al., 2007).

Cholesterol, besides affecting APP processing and Aβ production, also enhances Aβ oligomerization and fibrillogenesis either directly or indirectly (Harris, 2002). Studies using EM and AFM have shown that cholesterol and its derivatives potentiate Aβ fibrillogenesis *in vitro* by direct interactions (Yip et al., 2001; Harris, 2002). A potential indirect mechanism is through enhancing the formation of monosialoganglioside-Aβ complex (Kakio et al., 2001). Gangliosides are a group of glycosphingolipids located on the outer leaflet of mammalian plasma membranes and they are especially abundant on the neuronal cell surfaces. Monosialoganglioside is one of the major subtypes of ganglioside found in brain (Michel and Bakovic, 2007). Some species of Aβ bind to GM1-ganglioside tightly and form a complex (Yanagisawa et al., 1995). GM1-ganglioside-Aβ complex has a distinct conformation and it accelerates Aβ fibrillogenesis *in vitro* (Choo-Smith et al., 1997; Kakio et al., 2001; Kakio et al., 2002). The formation of GM1-ganglioside-Aβ complex is significantly increased in a cholesterol-rich environment suggesting cholesterol can affect Aβ aggregation indirectly (Simons and Ikonen, 1997; Kakio et al., 2001).

Aβ binds to cell membrane owing to its hydrophobicity (Datki et al., 2004). Interestingly, the density of cholesterol in plasma membrane affects the interaction between Aβ and lipid bilayers. For example, cholesterol-rich lipid bilayers exhibit lower fluidity and less affinity to Aβ, which suppresses Aβ adhesion to plasma membrane, suggesting another indirect mechanism of cholesterol affecting Aβ aggregation (Yip et al., 2001).

Hypercholesterolemia, characterized by elevated level of plasma LDL, is a risk factor for AD (Sparks, 1997). *In vitro* studies have demonstrated that LDL is capable of directly enhancing Aβ aggregation (Stanyer et al., 2004b). The potency of LDL on Aβ aggregation is dependent on its oxidative state. Oxidized LDL has greater effect than the native LDL does on Aβ polymerization (Stanyer et al., 2004a). This suggests that oxidative stress is a contributing factor to Aβ aggregation.

1.1.4.6 Aβ Cytotoxicity

Cytotoxicity of Aβ Related to its Polymerization Stage

Aβ is cytotoxic. It probably plays an important role in neurodegeneration. The cytotoxicity of Aβ is closely related to its state of polymerization. Earlier studies suggest the amyloid fibrils were cytotoxic (Yankner and Mesulam, 1991; Lorenzo and Yankner, 1994). Protofibrils were then identified and found to be more potent neurotoxins (Harper et al., 1997; Walsh et al., 1999). Further, small Aβ oligomers, particularly of $A\beta_{1-42}$, have been demonstrated to be the most cytotoxic species among all aggregated intermediates, and they are probably responsible for neurodegeneration (Walsh et al., 2002; Demuro et al., 2005; Selkoe, 2008). In mouse studies, intracranial administered oligomers were shown extremely potent at disrupting cognition and synaptic plasticity (Walsh et al., 2002; Cleary et al., 2005). Hippocampal slices shortly after exposure to oligomers lose the capability for long-term potentiation (LTP) (Lambert et al., 1998b). Some studies suggest that the senile plaques are neuroprotective by sequestering the soluble neurotoxic Aβ oligomers (Lee et al., 2004a).

Soluble Aβ oligomeric species were found in the CSF and cortex of AD patients (Pitschke et al., 1998; Kayed et al., 2003). The level of Aβ oligomers has a better correlation with dementia severity than do other Aβ species (Lue et al., 1999). Moreover, the levels of Aβ oligomers in AD brains are elevated as high as 70 fold, with an average of a 12-fold increase over matching controls (Gong et al., 2003).

Comparison of Aβ Generated *In Vivo* and *In Vitro*

Aβ oligomers used in earlier cytotoxicity studies were prepared from synthetic or cell-generated human Aβ. These oligomers are formed by homologous Aβ peptide. However, naturally generated Aβ aggregates in animal and human brains are considerably more heterogeneous in sizes (Selkoe, 2008). Synthetic or cell-derived Aβ oligomers are similar to the naturally generated Aβ oligomers in their aggregation process and cytotoxicity (Lambert et al., 1998b; Walsh et al., 2002; Cleary et al., 2005). However, there are some unresolved differences.

First, Aβ oligomers generated naturally, but not those obtained from synthetic Aβ, were found to be SDS (sodium dodecyl sulfate)-resistant (Roher et al., 1996; Enya et al., 1999; Funato et al., 1999; Lesne et al., 2006). SDS is an anionic detergent that denatures the secondary and

tertiary structures of proteins. SDS-resistant Aβ dodecamers (molecular weight ~ 56 kD) were detected in some strains of APP transgenic mice, but have not been identified in human cortical extracts (Lesne et al., 2006). Aβ conformation is related to its source and presence of cofactors. Why synthetic or cell-derived Aβ oligomers behave in a similar manner as human-derived Aβ is still unclear. Secondly, in studies using synthetic Aβ, the concentration of Aβ was usually at μM level to allow relatively rapid polymerization, whereas the assembly of Aβ *in vivo* occurs very slowly at sub-nM level (Naslund et al., 2000). Thirdly, dimers and trimers generated from nature, but not synthetic Aβ, are active at inhibiting LTP, inducing long-term depression and causing cognitive impairment (Walsh et al., 2002; Cleary et al., 2005; Selkoe, 2008). Natural Aβ dimers are cytotoxic *in vitro* (Hung et al., 2008). Therefore, further studies are required to compare the precise biochemical properties of the synaptotoxic Aβ species generated from various systems and under different conditions.

Mechanisms of Cytotoxicity

The mechanisms of Aβ cytotoxicity are complicated. Generally, the plasma membrane has been proposed to be the primary target of Aβ (Kayed et al., 2003). One potential mechanism is *via* nonspecific hydrophobic binding to the cell membrane (Datki et al., 2004), which alters membrane components and integrity. Aβ also exerts its cytotoxicity through a plasma membrane receptor-mediated process (Yan et al., 1996; Wilhelmus et al., 2007). Aβ binds to certain receptor and subsequently a vaviety of cellular pathways is activated, leading to mitochondrial dysfunction, induction of transcription factors and apoptosis. The complex mechanism of Aβ cytotoxicity suggests that different types of cells are affected by Aβ through distinct pathways. A multitude of synergic dysfunctional processes is responsible for neurodegeneration in AD. Regardless of which mechanism, the early phase of Aβ aggregation is crucial for its cytotoxicity and account for neurodegeneration. Several major hypotheses of Aβ cytotoxicity are discussed below.

<u>Disruption of Cytoplasmic Membrane</u>

Aβ disrupts the integrity of the cell membrane by its hydrophobic and electrostatic nature (Bokvist et al., 2004). In cell models, $A\beta_{1-42}$ rapidly binds to cell membranes and induces

subsequent cellular events during the first hour of treatment including tau hyperphosphorylation (Datki et al., 2004). Certain amino acid residues of Aβ peptide are crucial for its binding to plasma membrane (Barnham et al., 2003; Tickler et al., 2005). Interactions between Aβ and biological membrane components including lipids, membrane proteins and cholesterol have been discussed previously. In addition, the interaction between Aβ and Cu (II) causes membrane lipid peroxidation, which further damages the functions of membrane components (Dikalov et al., 1999; Huang et al., 1999a; Huang et al., 1999b; Bush, 2003).

Soluble Aβ oligomer itself may form a channel-like structure on plasma membrane, which is permeable to ions leading to Ca^{2+} influx and destroyed membrane potential (Arispe et al., 1993b; Arispe et al., 1993a; Kourie et al., 2001; Kagan et al., 2002). However, other studies have found that antioxidants, but not calcium channel antagonists, are capable of blocking the neurotoxic effect of Aβ on calcium homeostasis, suggesting the free radicals produced by Aβ are responsible for disrupting membrane integrity (Zhou et al., 1996). Interestingly, regardless of different amyloid sequences, oligomers of all amyloidogenic proteins increase membrane conductance but without evidence of discrete channel/pore formation or ion selectivity, suggesting a common conformation-specific mechanism of cytotoxicity (Kayed et al., 2004). These spherical oligomers increase membrane permeability and cause membrane depolarization, which is detrimental to cells, particularly neurons. Cellular pathways are also affected by the increase in membrane conductance (Mattson et al., 1993).

Membrane Receptor-mediated Cytotoxicity

Alternatively, Aβ seems to exert its cytotoxicity *via* a receptor-mediated mechanism (Lambert et al., 1998b; Wilhelmus et al., 2007). For example, LRP-1 on cerebral vasculature, notably, vascular smooth muscle and endothelial cells, plays a multifunctional role in Aβ clearance and cytotoxicity (Shibata et al., 2000; Wilhelmus et al., 2007). LRP-1 mediates Aβ endocytosis and its subsequent cytotoxicity in vascular smooth muscle cells (VSMCs), which is suppressed by LRP-1 inhibitor, receptor-associated protein (RAP) (Wilhelmus et al., 2007). RAP is a general antagonist for LDL receptor family. Moreover, Aβ as a LRP-1 ligand is able to upregulate LRP-1 expression in VSMCs (Wilhelmus et al., 2007).

The receptor for advanced glycation end products (RAGE) expressed on cerebral blood vessels and microglia mediates Aβ cytotoxicity as well (Yan et al., 1996; Cho et al., 2009).

Activation of RAGE by Aβ triggers the release of various proinflammatory factors and reactive oxygen species (Deane et al., 2003). Furthermore, RAGE activation increases intracellular expression of β-secretase and its activity, leading to increased Aβ production (Cho et al., 2009).

Mitochondrial Dysfunction

In AD brains, the mitochondrial morphology is altered as revealed by electron microscopy, and the overall numbers of mitochondria are reduced in plaque-affected areas (Hirai et al., 2001; Baloyannis et al., 2004). These findings suggest mitochondria are affected by Aβ during the development of AD.

Aβ produced in cells appears to bind to mitochondrial proteins and accumulate in mitochondria (Yan et al., 1997; Lustbader et al., 2004). Mitochondria also produce Aβ, since both APP and functional γ-secretase activity are present in mitochondria (Hansson et al., 2004; Devi et al., 2006). Mitochondria are therefore an intracellular source of Aβ during AD pathogenesis.

Intracellular Aβ directly affects mitochondrial function, but to date, there has been no evidence that extracellular Aβ plaques directly impair mitochondrial function. Activities of mitochondrial dehydrogenase, cyclo-oxygenase and tricarboxylic acid cycle enzymes are affected by Aβ in AD brains (Chagnon et al., 1995; Lustbader et al., 2004; Bubber et al., 2005). *In vitro* studies suggest that Aβ directly impairs mitochondrial calcium uptake (Kumar et al., 1994) and electron transport chain, which is crucial for energy metabolism but also produces reactive oxygen species (ROS) (Parks et al., 2001; Casley et al., 2002; Crouch et al., 2005). In addition to electron transport chain inhibition, direct binding of Aβ to mitochondria leads to a decrease in mitochondrial membrane potential and respiration rates, mitochondria swelling and cytochrome-c release, therefore causing cell death (Kim et al., 2002; Keil et al., 2004; Aleardi et al., 2005).

Inhibition of Synaptic Transmission

LTP plays an important role in neuroplasticity. Aβ oligomers potently inhibit LTP in mice (Walsh et al., 2002; Cleary et al., 2005; Selkoe, 2008). If Aβ oligomerization is blocked by certain inhibitors, *e.g.* hydroxyanaline derivatives, the LTP reduction is prevented (Walsh et al.,

2005). A recent study showed that Aβ dimers obtained from the CSF of AD patients are capable of inhibiting LTP in mice, which is blocked by Aβ antibodies (Klyubin et al., 2008).

The mechanisms of Aβ inhibiting LTP seems to involve the nicotinic acetylcholine receptors (Itoh et al., 1999; Dineley et al., 2001). However, other studies suggest that muscarinic acetylcholine receptors and several signaling pathways are responsible for this effect (Wang et al., 2004a). Aβ oligomers also downregulate N-methyl-D-aspartic acid receptors (Lacor et al., 2007). An alternative mechanism is the interaction between Aβ and metal ions produces ROS (Bush, 2003). At the synaptic cleft the levels of metal ions including Cu^{2+} and Zn^{2+}, reach as high as 300 μM during synaptic transmission (Assaf and Chung, 1984; Frederickson et al., 2000). ROS subsequently disrupts synaptic transmission.

Aβ oligomers are potent at disrupting synaptic activity in a rather complex manner depending upon Aβ concentration, types of neurons and neurotransmitters, and a number of other local factors.

1.1.4.7 Impairment of Aβ Degradation and Clearance

Aβ accumulation results from the imbalance between Aβ production and clearance. Current transgenic animal models of AD are based on gene mutations involving APP, presenilin 1 or ApoE. These models overproduce Aβ and mimic its accumulation in AD. However, to date over 90% of AD patients have no apparent genetic links, and in most cases the development of senile plaques is not a result of Aβ overproduction. Instead, Aβ accumulation in late-onset AD appears to be caused by impaired degradation or clearance of Aβ from the CNS (Iwata et al., 2000; Sagare et al., 2007).

There are two major mechanisms by which Aβ is eliminated from the brain, namely, proteolytic degradation and receptor-mediated transcytosis. Several intracellular proteases, such as neprilysin, plasmin, and angiotensin-converting enzyme, are involved in Aβ degradation (Hu et al., 2001; Iwata et al., 2001b). In mouse models of aging and AD, loss of neprilysin expression causes an increase in Aβ accumulation (Farris et al., 2007). The insulin-degrading enzyme (IDE/insulysin) exhibits dual effects on Aβ. In the extracellular compartment, IDE hydrolyzes only secreted Aβ monomers, but not oligomers or advanced aggregates (Walsh et al., 2002). Inside the cells, IDE enhances APP and Aβ trafficking to the plasma membrane (Vekrellis et al.,

2000; Gasparini et al., 2001). Deficiency of this proteolytic enzyme system during aging contributes to Aβ accumulation and subsequent plaque formation in AD (Caccamo et al., 2005; Farris et al., 2007).

It was hypothesized that the major mechanism of Aβ clearance is dependent on output from the CNS into the blood circulation (Hyman et al., 2000; Rosenberg, 2000). Aβ can be transported from the interstitial fluid bulk flow into the CSF, which accounts for 10% to 15% of the total Aβ output (Silverberg et al., 2003). The main clearance route of Aβ is transcytosis through the blood-brain barrier (BBB) *via* a receptor-mediated process into the bloodstream (Shibata et al., 2000; DeMattos et al., 2002; Deane et al., 2004; Sagare et al., 2007).

Two receptors on the cerebral vasculature, notably, LRP-1 and RAGE, are known for regulating Aβ homeostasis in the CNS. LRP-1 facilitates Aβ efflux from the brain into the blood by directly binding Aβ monomers on the ablumenal side of cerebral blood vessels and then excreting it into the blood (Deane et al., 2004). LRP-1 ligands such as α2M and ApoE also influence Aβ transcytosis (Shibata et al., 2000; Ito et al., 2007). α2M is a large tetrameric protein and functions as an irreversible pan-proteinase inhibitor and a transporter of small protein molecules including cytokines and growth factors. It facilitates endocytosis of Aβ monomers *via* LRP-1, *i.e.* by forming a transient complex with Aβ (α2M:Aβ ratio: 1:1 to 1:8) (Du et al., 1997; Hughes et al., 1998). However, α2M and Aβ also aggregate and form larger complexes (molecular ratio: >1:10) which cannot be endocytosed by vascular LRP-1 (Narita et al., 1997; Ito et al., 2007). As for ApoE, different isoforms of ApoE exert different effects on Aβ transcytosis. ApoE4 slows down its transcytosis process whereas ApoE2/3 facilitates Aβ clearance *via* LRP-1 (Deane et al., 2008). Similar to α2M, ApoE4 also forms large complexes with Aβ and enhance its aggregation (Fryer et al., 2003; Gunzburg et al., 2007; Ito et al., 2007).

RAGE, on the other hand, mediates the influx of peripheral Aβ from blood circulation into the CNS (Deane et al., 2003). Blood seems to be a chronic and stable source of soluble Aβ for the brain (Chow et al., 2007). Endothelial RAGE binds to various forms of Aβ in the blood and mediates its transcytosis into the CNS. Subsequent cellular signaling pathways are activated, releasing proinflammatory cytokines, ROS and endothelin-1, a cerebral blood flow (CBF) suppressor (Deane et al., 2003). These effects of RAGE contribute to Aβ neurotoxicity (Yan et al., 1996; Lue et al., 2001a). Moreover, RAGE expression is upregulated by its ligands such as

Aβ, AGEs and proinflammatory factors (Yan et al., 2000). The mechanism by which vascular LRP and RAGE on cerebral blood vessels regulate Aβ homeostasis in the CNS is illustrated in Figure 6. In addition to RAGE, ApoJ and ApoE4 seem to facilitate the plasma-derived Aβ transport into the CNS (Zlokovic, 1996; Martel et al., 1997). In mice, the transport of ApoJ-Aβ complexes through BBB is mediated by LRP-2. However, in humans, ApoJ is not a major carrier for Aβ transport (Sagare et al., 2007), and its role in AD pathology is unclear.

In most AD cases, a large portion of the Aβ deposits are on the outer surface of the cerebral blood vessels. The mechanism is not fully understood. Cerebrovascular dysfunction seems to contribute to cognitive impairment and neurodegeneration in AD (Grammas et al., 2002; Dede et al., 2007). It has been proposed that neurovascular dysfunction leads to impaired Aβ clearance *via* LRP-1 and enhanced Aβ influx by RAGE through cerebral blood vessels, which represents the main cause of Aβ accumulation in AD (Zlokovic, 2005). Emerging evidence supports this hypothesis. For example, LRP-1 and its ligands, including ApoE and α2M, have been detected in senile plaques (Rebeck et al., 1995; Arelin et al., 2002), and altered LRP-1 and RAGE expression are observed in post-mortem AD brains (Lue et al., 2001a; Jeynes and Provias, 2008). Increased RAGE expression is associated with Aβ plaques in AD brains (Yan et al., 1996). In mouse models, Aβ deposition increases RAGE expression by several folds in affected areas which results in downstream neuronal dysfunction (Zlokovic, 2004; Herring et al., 2008). Furthermore, people with lower LPR-1 levels exhibit increased incidence of AD (Kang et al., 2000). Polymorphisms of LRP and α2M genes are also associated with AD (Kang et al., 1997; Blacker et al., 1998; Ma et al., 2002).

In brief, as the cerebrovascular function deteriorates with aging, vascular diseases and AD, the balance between LRP-1 and RAGE on cerebral blood vessels becomes changed. This leads to the accumulation of Aβ on the cerebral vasculature to form CAA and to activate subsequent cascades including neuroinflammation, brain hypoperfusion, cerebrovascular regression and neuronal degeneration (Jeynes and Provias, 2008). Indeed, inhibition of RAGE-Aβ interaction reduces neuroinflammation, stabilizes cerebral blood vessels and restores the resting CBF (Deane et al., 2003). Therefore, the RAGE-Aβ interaction may be an important therapeutic target for the treatment of AD.

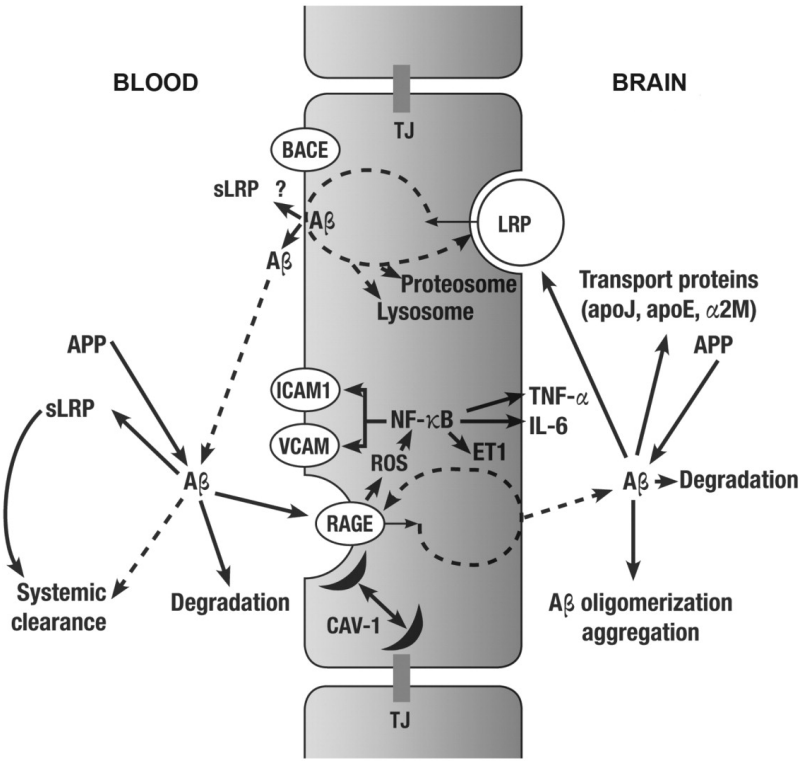

Figure 6. Transport of Aβ through blood-brain barrier regulated by LRP-1 and RAGE (Zlokovic, 2008a). LRP-1 on cell surface at ablumenal membrane binds to various forms of Aβ and mediates its transcytosis from the brain into blood circulation. LRP ligands including ApoE, ApoJ and α2M form complexes with Aβ and facilitate its clearance. RAGE on the luminal side of cerebral blood vessels binds to peripheral Aβ circulating in blood and mediates its influx into the CNS. After activated by Aβ or other ligands including inflammatory factors and AGEs, RAGE activates a number of cellular pathways releasing ROS and proinflammatory factors.

1.1.5 Carbonyl and Oxidative Stress in Relationship to AD

1.1.5.1 Reactive Aldehydes in AD Pathology

Age-related oxidative stress has been proposed to contribute to the development of neurodegenerative diseases including Parkinson's disease and AD (Gorman et al., 1996; Gonzalez-Fraguela et al., 1999; Mancuso et al., 2006). There are several markers for oxidative stress, such as reactive aldehydes produced from lipid peroxidation (LPO), notably, 4-hydroxy-2-nonenal (HNE) and malondialdehyde (MDA) (Esterbauer et al., 1991). Basal peroxidation is significantly elevated in AD brains (Subbarao et al., 1990). Higher levels of MDA were found in AD brains compared to those of healthy brains, especially in the cortex area (Subbarao et al., 1990; Palmer and Burns, 1994). In rats, levels of HNE and MDA increase with aging (Draper et al., 1995). Elevated activities of antioxidant enzymes such as superoxide dismutase and glutathione peroxidase were observed in AD brains (Pappolla et al., 1992; Lovell et al., 1995). However, other studies found significantly decreased superoxide dismutase activity in AD brains (Chen et al., 1994).

Accumulated oxidative damage to cellular macromolecules is a major event during cellular aging. The cytotoxic effects of reactive aldehydes are summarized in Figure 7. Aldehydes are able to modify proteins covalently (Smith et al., 1995). The mechanisms of how aldehydes modify proteins are not fully understood. It is known that aldehydes preferably react with the ε amino group on lysine, the imadazole nitrogen on histidine and the sulfhydryl group on cysteine (Esterbauer et al., 1991; Uchida and Stadtman, 1992). Using anti-HNE and anti-MDA antibodies, immunohistological studies revealed that proteins adducts with HNE and MDA significantly are increased in the senile plaques of AD patients (Montine et al., 1997; Sayre et al., 1997; Dei et al., 2002). The HNE-protein adducts are detected mostly in the neuronal cytoplasm or associated with NFT but not with neuritic plaques (Montine et al., 1997), whereas MDA is colocalized with both tau protein and senile plaques (Dei et al., 2002). HNE covalently modifies the lysine residues of Aβ and accelerates its aggregation *in vitro* (Zhang et al., 2004). Mass spectrometry and Western blot analyses also revealed that cortex proteins in AD brains are modified by aldehydes produced from LPO (Pamplona et al., 2005).

HNE and MDA react with a variety of biological macromolecules including plasma membrane proteins and organelles and alter their chemical nature and biological functions. A

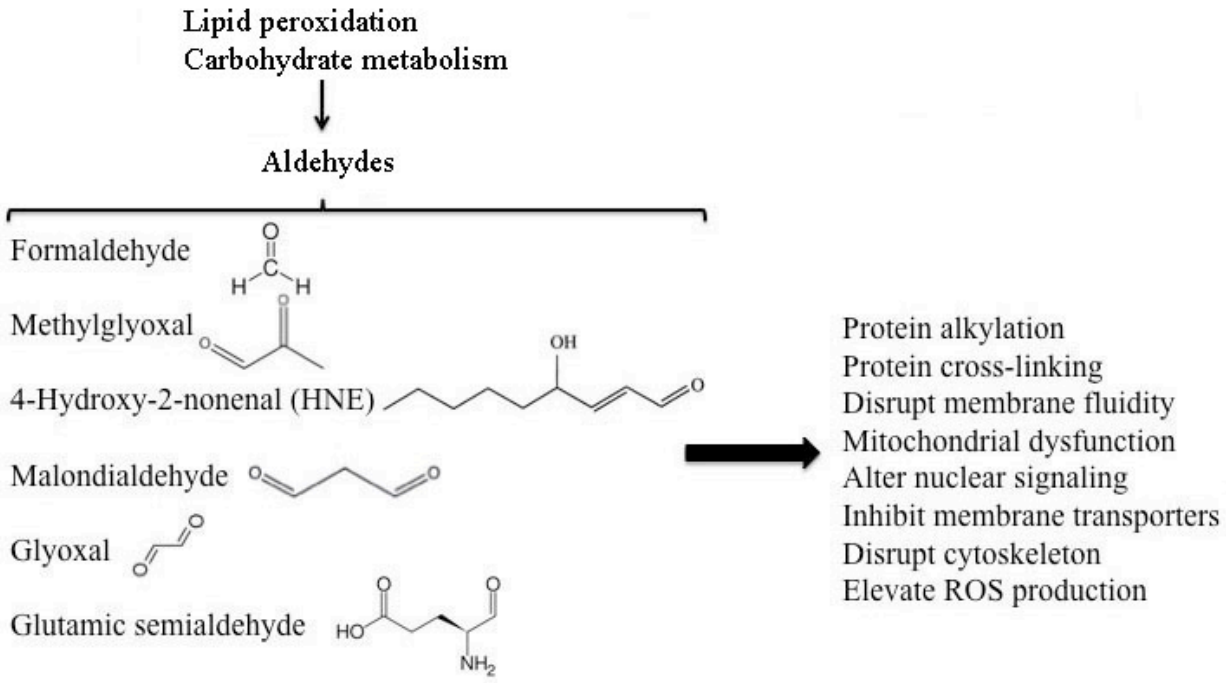

Figure 7. Structures of aldehydes and their toxic effects. Macromolecules such as lipids, carbohydrates and proteins, readily react with reactive oxygen species (ROS). Their structures are modified leading to impaired biological functions. In this process, a number of reactive aldehydes are produced, which further exacerbate oxidative damage to additional biological molecules.

variety of signaling cascades are activated, leading to cytoskeletal disruption, glutamate toxicity and mitochondrial dysfunction (Mattson et al., 1997; Neely et al., 1999; Picklo et al., 1999; Lauderback et al., 2001).

1.1.5.2 Advanced Glycation End Products in AD

Advanced glycation end products (AGEs) are the products of a chain chemical reaction during glucose metabolism. Increased production of AGEs is associated with aging and the vascular complications of diabetes (Brownlee, 2005). The levels of are elevated by about 70% in the CSF of AD patients (Shuvaev et al., 2001). The concentration of methylglyoxal in CSF from AD patients is also significantly increased compared to the matching control populations (Kuhla et al., 2005). The senile plaques from AD patients contain significantly higher levels of AGE adducts which also colocalize with NFT (Vitek et al., 1994; Yan et al., 1994). Interestingly, both Aβ and AGEs are ligands for RAGE. Aβ seems to upregulate microglial RAGE and potentiate the harmful effects of AGEs (Lue et al., 2001a).

The process of AGE formation is rather complicated. Sugars are reduced by reacting with proteins and forming Schiff bases, and subsequently subject to Amadori rearrangement (isomerization of the N-glyocoside of an aldose or the glycosylamine to 1-amino-1-deoxy-ketose) (Booth et al., 1997). A variety of toxic compounds, the Amadori products, are produced during the process. The oxidation of sugar during glycolysis produces reactive products as well (*e.g.* methylglyoxal), and they also form adducts with proteins (Thornalley et al., 1999; Wang et al., 2004b; Wang et al., 2005). The reaction pathways are summarized in Figure 8.

1.1.5.3 Impairment of Metal Ions Homeostasis in AD

Impairment of metal ion homeostasis is implicated in AD (Deibel et al., 1996). Ion is capable of enhancing Aβ aggregation (Bush et al., 1994). It also plays a significant role in the production of ROS which cause oxidation of sugars, proteins, lipids and other cellular macromolecules. Hydroxyl radicals are generated from hydrogen peroxide in the presence of Fe^{2+} *via* Fenton reactions. Cell and rat studies have shown that ion and Aβ synergistically potentiate their cytotoxicity (Dikalov et al., 1999; Huang et al., 1999b; Rottkamp et al., 2001).

Cu (II) binds to the histidine residues on both monomeric and aggregated Aβ (Curtain et al., 2001). This interaction reduces Cu (II) to Cu (I) and produces hydrogen peroxide as a by-product

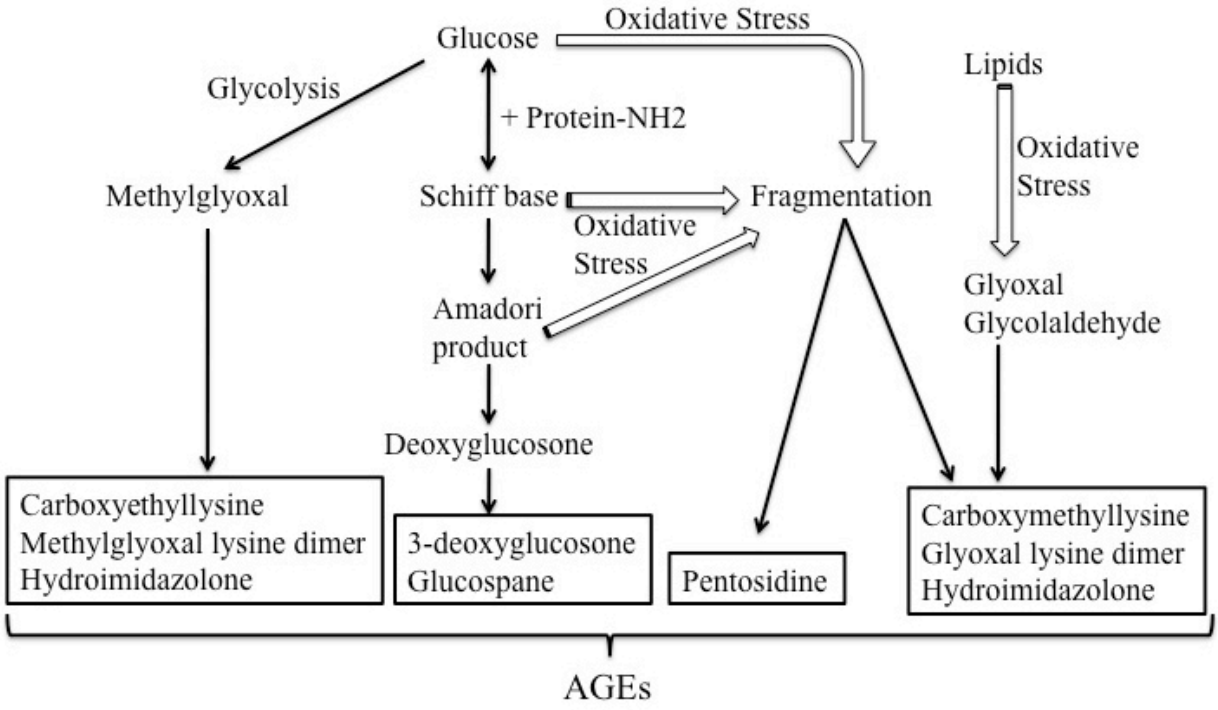

Figure 8. Formation of AGEs through various pathways (Monnier, 2003). Glucose reacts with the amino groups of proteins to form Schiff bases, followed by Amadori rearrangement. Amadori products further form deoxyglucosone, 3-deoxyglucosone lysine dimer and glucospane. ROS produced from oxidative stress react with glucose and lipids forming a variety of AGEs. Glycolysis produces methylglyoxal and also other AGEs.

(Opazo et al., 2002). Hydrogen peroxide is a reactive chemical that can diffuse through cell membrane. It further reacts with Aβ-Cu (I) producing hydroxyl radical (OH·) to oxidize lipids and proteins. Therefore, the interaction between Cu (II) and Aβ causes membrane lipid peroxidation, which damages the functions of membrane components (Dikalov et al., 1999; Huang et al., 1999a; Huang et al., 1999b; Bush, 2003). OH· has also been shown capable of reacting with Aβ peptide and promoting its aggregation (Atwood et al., 2004).

1.1.5.4 Oxidative Stress Induced by Aβ

Aβ directly induces oxidative stress and causes cytotoxicity. For instance, Aβ binds to the endothelial cells on rat aorta and generates excessive superoxide radicals, leading to oxidative damage to the vasculature (Thomas et al., 1996). Aβ oligomers and protofibrils trigger glutamate release from glial cells and cause excitotoxicity to adjacent neurons. Overactivation of glutamate N-methyl-D-aspartic acid receptors is well known to elevate intracellular Ca^{2+} levels, which activates neuronal nitric oxide synthase. Indeed, Aβ increases intracellular Ca^{2+} levels (Zhou et al., 1996) with decreased glutathione levels in astrocytes (Abramov et al., 2003). Excessive nitric oxide reacts with superoxide anion produced from Aβ to form even more reactive species (ONOO-) leading to further oxidative and nitrosative stress (Bossy-Wetzel et al., 2004).

In AD patients, mitochondrial DNA damage is detected in amyloid plaque affected areas and cerebral microvessels (Mecocci et al., 1994; Aliev et al., 2002). Aβ inhibits mitochondrial electron transport chain. Inhibition of electron transport chain is a mechanism of generating ROS in the cell. Therefore, Aβ also indirectly increases oxidative stress by affecting mitochondrial functions supported by *in vitro* studies (Behl et al., 1994; Huang et al., 1999b; Varadarajan et al., 2001).

1.1.5.5 Deficiency of Carbonyl Clearance in AD

The toxic carbonyl compounds produced during oxidative stress are scavenged by various cellular defense mechanisms. An imbalance between carbonyl production and clearance has been proposed to play a central role in aging and in the pathogenesis of neurodegenerative diseases (Picklo et al., 2002). For instance, aldehyde dehydrogenases oxidize aldehydes to carboxylic acids. They catalyze the catabolism of HNE using NAD+ as a cofactor. A subtype of the enzyme, aldehyde dehydrogenase-2, is elevated in senile plaques (Picklo et al., 2001). Moreover, Oriental

populations who lack aldehyde dehydrogenase-2 activity due to gene mutation have an increased risk of developing AD (Kamino et al., 2000).

Another major mechanism of carbonyl scavenging is through the conjunction of aldehydes, lipid peroxides and hydroperoxides with glutathione, catalyzed by glutathione transferases (Alin et al., 1985). Glutathione transferase activity is decreased in AD patients (Lovell et al., 1998a). In cell studies, neurons depleted of glutathione are more susceptible to Aβ-Cu cytotoxicity, suggesting the importance of glutathione in free radical scavenging (White et al., 1999).

In summary, carbonyl and oxidative stress contribute to various aspects of the pathology of AD such as Aβ aggregation and its cytotoxicity, ion homeostasis, vascular damage and neurodegeneration. These findings have provided therapeutic implications for AD, for example, clinical trials of antioxidants (Marlatt et al., 2008).

1.1.6 Inflammation and AD

Inflammation in the CNS is implicated in the pathogenesis of AD (Rogers et al., 1996; Halliday et al., 2000). In AD patients, inflammatory factors are elevated (Eikelenboom et al., 2008). Neuroinflammation can be stimulated by Aβ aggregates including oligomers, protofibrils and fibrils. Aβ deposits turn into a nidus for innate inflammatory responses, particularly in the cortex area (Akiyama et al., 2000; Griffin, 2006). These inflammatory responses are carried out by microglia. Upon activation, microglia migrate to inflammatory sites, secrete a variety of inflammatory factors and scavenge damaged tissue and misfolded proteins (Bales et al., 2000). The inflammatory mediators secreted by activated microglia include interleukin-1β and -6, tumor necrosis factor-α and macrophage inflammatory protein-1α (Lue et al., 2001b). In AD, most of the senile plaques are densely associated with activated microglia (Luber-Narod and Rogers, 1988; Rogers et al., 1988).

Interestingly, Aβ aggregates selectively attract and activate microglia, but not leukocyte or monocyte (Wekerle, 2002). This selectivity seems to result from that some receptors on microglia, *i.e.* the macrophage scavenger receptors, formyl chemotactic receptors and RAGE, are highly sensitive to Aβ and bind Aβ as a ligand (Yan et al., 1996; Lorton et al., 2000; El Khoury et al., 2003). The expression of RAGE on microglia is significantly increased in AD brains and anti-RAGE antibody is capable of inhibiting microglial chemotactic responses (Lue et al., 2001a).

In addition to triggering release of inflammatory mediators, Aβ aggregates also activate the complement system of inflammatory responses, notably, complement component 1q (C1q) and membrane attack complex. The complement system facilitates scavenger cell targeting and lysis. The colocalization of Aβ and C1q along with other complement factors have been observed in AD brains (Rogers et al., 1992). In AD, Aβ deposits bind to and activate C1q, which triggers the subsequent cascade of reactions to draw microglia to Aβ deposits (Rogers et al., 1992; Bradt et al., 1998). The activation of cerebral inflammation system is beneficial of scavenging neurotoxic Aβ and preventing neuronal toxicity. However, overactivation of the complement system by Aβ would destroy healthy bystander cells, which causes elimination of functional neurons and astrocytes (Daly and Kotwal, 1998; Shen et al., 1998). In a triple transgenic mouse model, increased neuroinflammation and Aβ accumulation have a synergic effect on neuronal apoptosis (Xiang et al., 2002).

Overactivation of neuroinflammation explains why some anti-inflammatory drugs show beneficial effects in AD patients. Large-scale epidemiological studies showed that the prevalence of AD is significantly reduced in patients with arthritis or leprosy, who take anti-inflammatory drugs for treatment (Breitner, 1996; McGeer et al., 1996). Chronic use of non-steroidal anti-inflammatory drugs (NSAIDs) has been found to exhibit beneficial effects on AD patients and reduce AD incidence (in t' Veld et al., 2001; Zandi et al., 2002; Etminan et al., 2003; Vlad et al., 2008). The effect appears to be due to the anti-inflammatory properties of NSAIDs that suppress the destructive effects of overactivated inflammatory factors (Breitner and Zandi, 2001). However, there are conflicting reports showing that NSAIDs have no significant therapeutic effects on AD (Fourrier et al., 1996). Moreover, new NSAIDs, namely, celecoxib and naproxen, did not show preventive or therapeutic effects on AD patients who had no apparent chronic inflammatory diseases. Naproxen even exacerbates the cognitive impairment (Martin et al., 2008). Whether both NSAIDs and inflammatory settings are required for the beneficial effects, or whether inflammation is the natural defense mechanism of the CNS and NSAIDs are accelerating the development of AD, remains unsolved. Nevertheless, the deposition of Aβ remains the primary pathological hallmark and the trigger of various cascade events. Inflammation may be the resulting defense system induction by Aβ aggregation.

1.1.7 AD and Vascular Diseases

AD is associated with vascular diseases and they share common pathologies (de la Torre, 2002a). Metabolic syndrome, which includes symptoms such as obesity, hypercholesterolemia, diabetes, hypertension and atherosclerosis, is associated with higher incidence and accelerated progression of AD (Voisin et al., 2003; Luchsinger et al., 2005; Mielke et al., 2007; Mills et al., 2007; Razay et al., 2007).

1.1.7.1 AD and Cerebrovascular Disorders

Neurovascular dysfunction is a common feature in neurodegenerative diseases (Iadecola, 2004). Morphological changes of blood vessels during aging and AD have been observed (Scheibel, 1987; Hashimura et al., 1991; Yamashita et al., 1991). Initially, the endothelial cells of cerebral capillaries and the single layer of the smooth muscle cells in arterioles are degenerated. These abnormalities lead to irregular shapes of cerebral blood vessels. The cerebrovascular dysregulation will ultimately lead to chronic impairment of CBF, glucose transport, receptor expression and signaling cascades (Kalaria and Harik, 1989; Grammas et al., 1995; Marcus and Freedman, 1997). Based on autopsy studies, 70% of definite AD patients show coexistent cerebrovascular disorders (Kalaria, 2002). Common cerebrovascular disorders in aged or AD brains include CAA, atherosclerosis and microinfarcts.

CAA is predominantly found in small cerebral vessels such as leptomeningeal and neocortical vessels, especially in the penetrating arterioles of the cortex, and is less distributed in cerebellar cortex (Yamada et al., 1987). Clinical data suggest that the extent of CAA is associated with severity of cognitive impairment (Pfeifer et al., 2002). Soluble Aβ, particularly $A\beta_{1\text{-}40}$, is vasoactive and causes vasoconstriction, CBF reduction as well as other cerebrovascular abnormalities (Iadecola, 2003; Paris et al., 2003). Soluble Aβ causes degeneration of endothelial cells and VSMCs *via* production of ROS and proinflammatory factors (Davis-Salinas et al., 1995; Iadecola, 2003). CAA was shown to further exacerbate these abnormalities caused by soluble Aβ in mice (Christie et al., 2001). The mechanism of how Aβ induces vessel dysfunction is complicated and far less clear. The process of CAA formation and its effects on cerebral blood vessels is shown in Figure 9.

The large arteries in AD brains normally do not develop CAA as observed in the cerebral microvessels. Large arteries particularly in the striatum, deep white matter and leptomeninges,

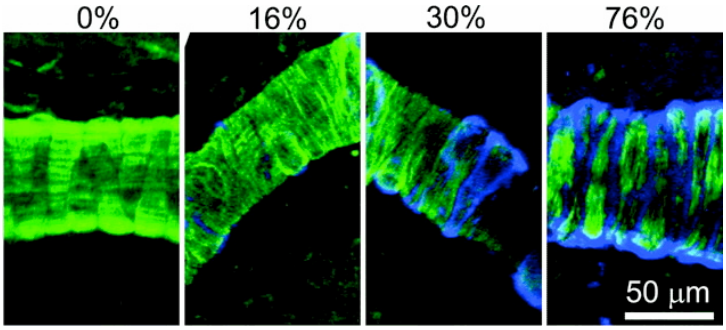

Figure 9. CAA-induced pathological changes on cerebral blood vessels (Zipfel et al., 2009). Using confocal microscopy, the amyloid deposition and vascular smooth muscle cells (VSMCs) in leptomeningeal vessels of Tg2576 mice (12- to 15-month-old) were stained blue and green, respectively. In vessel segments without CAA (Aβ coverage 0%), VSMCs were closely attached in parallel. In vessel segments with CAA, the extent of structural disruption and VSMC loss of blood vessel is associated with increased deposition of Aβ (16%, 30% and 76%). During mild CAA stage (Aβ coverage <20%), neither vascular wall was disrupted nor VSMCs were lost. In moderate CAA stage (20% to 40% of Aβ coverage), disruption of VSMC arrangement appeared but without significant loss of VSMCs. In advanced CAA (Aβ coverage >40%), both severe disruption of VSMC arrangement and VSMC loss were detected.

are frequently affected by atherosclerosis (Skoog et al., 1999; Casserly and Topol, 2004). The extent of cerebral atherosclerosis and CAA is correlated with the severity of dementia (Thal et al., 2003). Atherosclerosis results from hypercholesterolemia, oxidative stress and inflammation, which are also among the important contributing factors to AD pathology (Steinberg, 2002). It is hypothesized that atherosclerosis in extracranial and intracranial vessels causes brain hypoperfusion and discrete brain microinfarction. Chronic malnutrition of the CNS leads to brain hypotrophy, which eventually causes vascular dementia and/or AD (Hofman et al., 1997; de la Torre, 2002b; Roher et al., 2003). Alternatively, the development of atherosclerosis and AD seems to be independent but convergent (Casserly and Topol, 2004).

Cerebral ischemic lesions causing damage of prefrontal subcortical areas are associated with a 20-fold increased risk of AD (Riekse et al., 2004). These ischemic lesions are characterized by lacunae and microinfarcts. 20 to 40% demented AD individuals experience "silent" strokes which result in numerous cortical microinfarctions and white matter lesions (Snowdon et al., 1997; Heyman et al., 1998; Kalaria, 2003; Vermeer et al., 2003; Roman and Royall, 2004). Subcortical ischemic lesions, microinfarcts and demyelination are important contributing factors of cognitive deficits in aging and AD (Pantoni et al., 1999; Kalmijn et al., 2000; Kovari et al., 2004).

1.1.7.2 AD and Obesity

Obesity has been implicated as a risk factor for AD (Gustafson et al., 2003). It is associated with poorer cognitive functions (Elias et al., 2003). Hormonal abnormality, hyperleptinemia and inflammatory responses in obesity are associated with obesity linking to cognitive decline (Bjorntorp and Rosmond, 2000; Li et al., 2002a; Yaffe et al., 2003). The concurrence of obesity and hypertension further impairs cognitive performance (Waldstein and Katzel, 2006).

1.1.7.3 AD and Hyperlipidemia

Hyperlipidemia is associated with increased risk of late-onset dementia (Notkola et al., 1998; Kalmijn et al., 2000; Kivipelto et al., 2001; Whitmer et al., 2005). Drugs that lower LDL-cholesterol levels are protective against cognitive impairment (Jick et al., 2000). High density lipoprotein is the major carrier of cholesterol in the brain and plays a protective role in the development of dementia. Decreased levels of High density lipoprotein-cholesterol cause

defective cholesterol release to neurons, which leads to formation of NFT and senile plaques (Bonarek et al., 2000; Michikawa, 2003).

1.1.7.4 AD and Diabetes

In clinical studies, diabetes is consistently found to be a strong risk factor for cognitive impairment, vascular dementia and AD (Ott et al., 1999; Yaffe et al., 2004; Whitmer et al., 2005). The Rotterdam study found that elderly patients with diabetes mellitus (DM) have about a double chance to develop AD compared to nondiabetic control population (Ott et al., 1999). A causal relationship between diabetes and late-onset AD has even been proposed (Craft, 2006).

In diabetes, insulin resistance and subsequent hyperinsulinaemia increase the risk of AD by accelerating memory decline and cognitive impairment (Watson and Craft, 2003; Luchsinger et al., 2004). Insulin seems to play an important role in metabolism of Aβ and tau (Ho et al., 2004; de la Monte and Wands, 2005). The insulin-degrading enzyme (IDE) breaks down extracellular Aβ and this process is competitively inhibited by insulin (Qiu et al., 1998). Insulin also stimulates the secretion of Aβ and promote tau hyperphosphorylation in diabetes (Gasparini et al., 2001). Therefore, elevated levels of insulin in insulin-resistant brains with diabetes cause reduced Aβ degradation, enhanced Aβ secretion and subsequently increased formation of plaques and tangles. On the other hand, deficiency of insulin is also associated with cognitive impairment based on rat studies, probably by decreasing the expression of insulin-like growth factors and causing apoptosis in the CNS (Li et al., 2002b).

Hyperglycemia in diabetes leads to increased production of AGEs, which plays an important role in oxidative stress related to AD pathology. Chronic hyperglycemia disrupts cerebral capillaries and leads to brain ischemia (Mankovsky et al., 1996). Interestingly, hemoglobin glycosylation is negatively correlated with cognitive function (Kanaya et al., 2004). Other diabetic complications such as hypertension, hyperlipidimia and stroke are associated with cognitive dysfunction related to AD as previously described (in 1.1.7.2).

1.1.7.5 AD and Hypertension

Hypertension is a strong risk factor for AD and related dementia (Skoog et al., 1996; Qiu et al., 2005; Foroughan et al., 2008). For example, patients with systolic blood pressure greater than 160 mm Hg have 4-fold higher incidence in developing dementia in their later life time

compared to people with systolic blood pressure of 110 to 139 mm Hg (Launer et al., 2000). Anti-hypertensive drugs reduce the incidence of AD by up to 70% (Hajjar et al., 2005; Khachaturian et al., 2006). The contribution of hypertension to the development of AD is *via* a complicated mechanism.

First, hypertension is usually associated with other factors or pathological conditions including hyperlipidimia, obesity and type 2 DM that are risk factors for AD (Luchsinger et al., 2005). Therefore, hypertension is the common link among these conditions and they potentiate each other.

Secondly, midlife hypertension is associated with an increased formation of neuritic plaques and NFT in AD patients (Petrovitch et al., 2000). Hypertension in elderly with normal cognitive functions causes reduced regional CBF, which is associated with cerebrovascular diseases such as AD (Dai et al., 2008). BBB dysfunction has been proposed to be the major contributor to AD pathology (Hashimura et al., 1991; Shah and Mooradian, 1997; Deane et al., 2003; Zlokovic, 2008b). Hypertension contributes to BBB dysfunction by disrupting cerebrovascular integrity, causing cerebrovascular diseases and atrophy such as subcortical white matter lesions, cerebral microinfarctions ("silent" strokes) and atherosclerosis in cerebral arteries, and remodeling microvasculature (Moossy, 1993; van Dijk et al., 2004; Struijs et al., 2005).

Thirdly, peripheral Aβ circulating in the blood causes hypertension. Overactivation of the rennin-angiotensin system leading to elevated blood pressure was observed during AD development (Savaskan et al., 2001). Plasma Aβ is capable of inducing vasoconstriction and elevating blood pressure in rats (Suo et al., 1998; Arendash et al., 1999).

In summary, various vascular risk factors during midlife predispose the development of vascular dementia and/or AD in late life. It has been proposed that such pathological vascular conditions lead to cerebral hypoperfusion, which consequently causes an energy crisis in richly perfused CNS areas such as the limbic system. Chronic CBF reduction and energy deficits trigger a series of downstream events, such as mitochondrial dysfunction, oxidative stress, inflammatory responses and transport impairment. Indeed, hypoxia associated with reduced CBF downregulates LRP-1 expression on cerebral vessels and impair Aβ clearance (Bell et al., 2009). As a result, senile plaques and tangles form (de la Torre, 2006; Fillit et al., 2008; Milionis et al., 2008). AD dementia develops when the degree of neurodegeneration passes a certain threshold. Vascular conditions play a causal role in the development of AD as summarized in Figure 10.

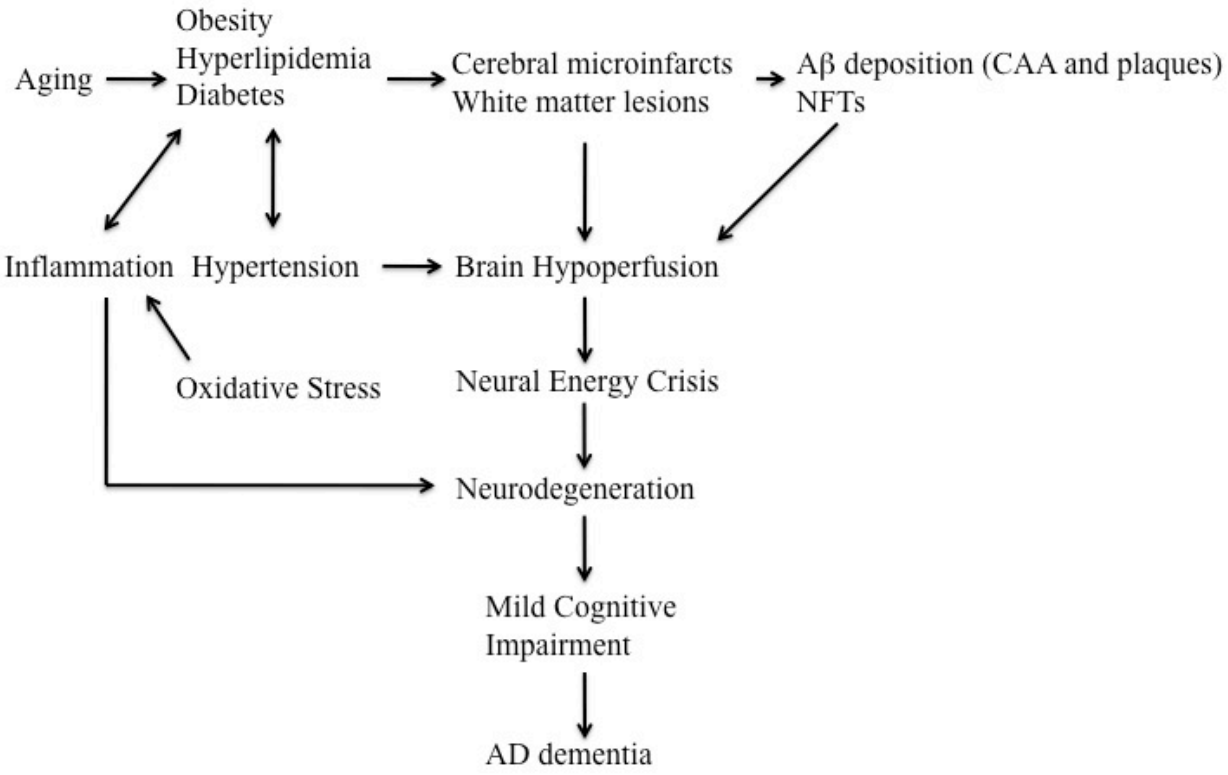

Figure 10. The involvement of vascular factors in the development of AD. During aging, vascular function deteriorates, which causes cerebral microinfarcts and white matter lesions leading to brain hypoperfusion. Chronically, it causes neural energy crisis and neurodegeneration. AD and vascular dementia appear, when the neural and vascular degeneration passes certain threshold.

AD is recognized as a chronic cerebral vascular disease due to the importance of cerebrovasculature in regulating Aβ homeostasis in the CNS. This is similar to the pathology of other vascular diseases (Zlokovic, 2008b). Effectively managing these vascular risk factors in early/midlife seems to be a preventive strategy for late-onset cognitive impairment and dementia (Marlatt et al., 2008; Pasinetti and Eberstein, 2008).

1.2 Semicarbazide-Sensitive Amine Oxidase

1.2.1 Classification of Amine Oxidases

According to the cofactors, amine oxidases (AOs) are classified into two categories, namely, the flavin adenine dinucleotide (FAD)- and 2, 4, 5-trihydroxyphenylalanine-quinone (TPQ)-containing enzymes. FAD-containing enzymes including monoamine oxidase A (MAO-A), MAO-B and polyamine oxidases are expressed intracellularly (Shih et al., 1999). TPQ-containing enzymes include lysyl oxidase, diamine oxidases, plasma membrane and soluble AOs (Klinman and Mu, 1994; Klinman, 1996; Lyles, 1996). These later enzymes are sensitive to semicarbazide (Tabor et al., 1954).

MAOs are well-known for catabolizing amine neurotransmitters (Youdim, 1989; Sherry et al., 1990), and have been extensively studied for their involvement in neuropsychiatric disorders (Aghajanian et al., 1970; Gottfries et al., 1974; Murphy and Wyatt, 1975) and neurodegenerative diseases (Steventon et al., 1990; Sparks et al., 1991). TPQ-containing diamine oxidase uses histamine, putrescine and cadaverine as substrates. It is an intracellular enzyme mainly synthesized in placenta, kidney and intestine (Buffoni, 1966; Robinson-White et al., 1985). The other type of TPQ-containing enzyme, semicarbazide-sensitive amine oxidase (SSAO), is found dissolved in the blood and in deposits on the surface of cells. SSAO is also called amine oxidase copper-containing-3. This enzyme deaminates small aliphatic amines, such as methylamine. SSAO is inhibited by semicarbazide which binds to its catalytic cofactor, the TPQ residue (Janes and Klinman, 1995; Houen, 1999). SSAO are not inhibited by classic MAO inhibitors (Callingham et al., 1995; Lyles, 1996).

1.2.2 Genes, Localization and Structure of SSAO

1.2.2.1 Genes and Localization of SSAO

In mammals, two genes encoding SSAO have been identified on chromosome 17 (Zhang and McIntire, 1996; Imamura et al., 1997). The amine oxidase copper-containing-3 gene encodes SSAO expression in most tissues. The other gene encodes a form of SSAO that seems to only exist in retina which has about 64% sequence identity to the SSAO in other mammalian tissues (Imamura et al., 1997). Its physiological functions in retina are unclear.

Mammalian SSAO presents in either a membrane-bound form or a soluble form in the cytoplasm. The membrane-bound SSAO is expressed on the outer surface of endothelial cells, smooth muscle cells and adipocytes (Callingham et al., 1995; Boomsma et al., 2000a). It is a transmembrane type II protein with a short (4 amino acids) N-terminal tail in the cytoplasm (Smith et al., 1998). The expression of SSAO differs markedly among tissues and species (Lyles, 1996). In the CNS, SSAO is not found on/in neurons or glial cells, but only on large arteries, microvessels and capillaries of cerebral vasculature (Zuo and Yu, 1994; Castillo et al., 1999; Jiang et al., 2008).

The source of plasma SSAO is not fully clarified. The N-terminal sequence of plasma SSAO is identical to the membrane distal sequence of the membrane-bound SSAO (Kurkijarvi et al., 1998; Boomsma et al., 2005a). Therefore, it is probably derived from the proteolytic cleavage of membrane-bound SSAO in liver and adipose tissue (Abella et al., 2004). Also, vascular injury increases SSAO activity and causes "shedding" of membrane-bound SSAO from endothelium and smooth muscles into the blood stream (Boomsma et al., 2005a).

1.2.2.2 Structure of SSAO

SSAO is a homodimeric copper glycoprotein with a molecular weight from 180 to 200 kD (with each subunit 90 to 100 kD) (Lyles, 1996). Its primary sequence has been identified (Zhang and McIntire, 1996; Smith et al., 1998). X-ray diffraction revealed that the tertiary structure of SSAO contains four domains and has a mushroom-like shape (Parsons et al., 1995; Jakobsson et al., 2005). Its catalytic domain is located in the extracellular compartment, which makes SSAO unique compared to other AOs (Salminen et al., 1998). The active site is buried in a 400-amino-acid-long C-terminal β-sandwich domain. This domain is involved in SSAO dimerization. At the active site, most SSAOs possess a conserved motif, namely, Asn-TPQ-Asp/Glu-Tyr (Salminen et al., 1998). Cu (II) and TPQ cofactor are essential for SSAO activity (Cai et al., 1997; McGuirl and Dooley, 1999). The copper atom is coordinated by three histidines. His-X-His motif is about 50 residues C-terminal from the TPQ cofactor and another His is 20 to 30 residues N-terminal from the TPQ motif (Salminen et al., 1998). The structures of inactive and active forms of SSAO differ in the geometry of copper coordination as well as TPQ position in the active centre. The Asp motif, around 100 residues N-terminal from TPQ, is also important for SSAO activity. The conserved motifs of SSAO are shown Figure 11.

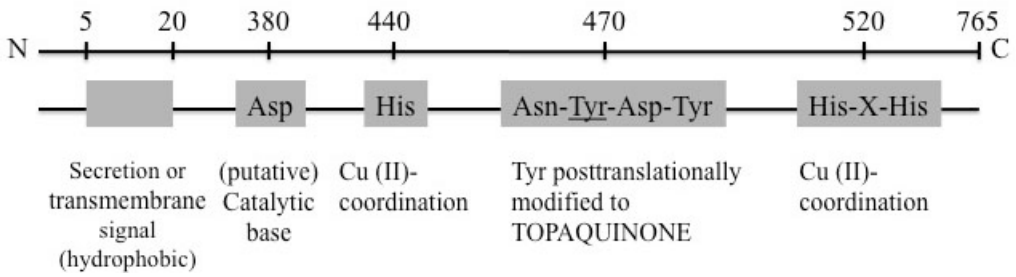

Figure 11. Structural motifs of the active site on SSAO. Histidine (440) and His-X-His coordinate Cu (II). A conserved motif, Asn-TPQ-Asp/Glu-Tyr exists in most SSAOs.

SSAOs from various species and organs are considerably different in their accessibility to the active-site for substrates (McGuirl and Dooley, 1999). Glycosylation of SSAO also varies depending on the sources of SSAO (Holt et al., 1998). Such variations are responsible for the distinct selectivity of substrates and sensitivity to inhibitors among SSAOs from various tissues and species.

1.2.2.3 Endogenous Substrates for SSAO

SSAO deaminates various primary amines. In the presence of oxygen and water, SSAO converts amines into aldehydes and produces hydrogen peroxide and ammonia as follows:

$$RCH_2NH_2+O_2+H_2O \rightarrow RCHO+NH_3+H_2O_2$$

The reaction proceeds in two steps. First, the TPQ cofactor of SSAO is reduced by its substrates and corresponding aldehydes are generated simultaneously. In this step, SSAO and its substrates undergo a sequence of transitions during which a transient covalent Schiff base is formed between them (Dooley et al., 1991). In step two, the reduced TPQ cofactor is oxidized back to its original state, producing hydrogen peroxide and ammonia.

The primary known endogenous substrates of SSAO are methylamine and aminoacetone (Precious et al., 1988; Yu, 1990; Lyles and Chalmers, 1992; Lyles, 1995). Interestingly, human SSAO exhibits none, or very little activity, towards dopamine and histamine, but has high Km values towards phenylethylamine and tyramine (Young et al., 1982; Lizcano et al., 1991; Lyles, 1995). Non-endogenous substrates include allylamine, benzylamine, mescaline and primaquine (Elliott et al., 1989; Strolin Benedetti and Tipton, 1998). Aliphatic amines are SSAO substrates as well (Yu, 1990).

Methylamine and aminoacetone are deaminated by SSAO to generate formaldehyde and methylglyoxal, respectively (Precious et al., 1988; Lyles and McDougall, 1989; Lyles and Chalmers, 1992). Methylamine exists in blood, tissues and urine (Asatoor and Kerr, 1961; Yu and Dyck, 1998). Endogenous methylamine is produced from metabolic pathways of several molecules including adrenaline, creatine/creatinine and choline (Schayer et al., 1952; Zeisel et al., 1983; Yu et al., 1997; Yu and Deng, 2000). The concentration of methylamine in human blood is normally around 1 to 5 μM. In plasma of uremia patients, methylamine level is increased to 10 to 20 μM (Asatoor and Kerr, 1961; Baba et al., 1984). In rats, SSAO inhibitor is able to increase methylamine concentration in urine, suggesting that SSAO is a major enzyme

metabolizing methylamine *in vivo* (Lyles and McDougall, 1989; Yu and Zuo, 1997). Endogenous aminoacetone is derived from glycine and threonine (Bird et al., 1984). Similar to methylamine, it is mainly metabolized by SSAO (Lyles and Chalmers, 1992). Recently, levels of methylamine and aminoacetone in tissues have been reported (Xiao and Yu, 2009).

1.2.3 Roles in Physiological Function

SSAO has been known for several decades. Since the discovery of its endogenous substrates a few years ago, several hypotheses regarding its roles in physiological function have been proposed.

1.2.3.1 SSAO and Glucose Uptake

SSAO is abundant in adipose tissue and accounts for 1% of total membrane proteins of adipocytes (Morris et al., 1997; Moldes et al., 1999). In preadipocytes, SSAO expression is minimal but is upregulated in differentiated adipocytes (Fontana et al., 2001). SSAO substrates, *i.e.* methylamine and aminoacetone, increase glucose uptake in adipocytes by several folds and this effect is blocked by SSAO inhibitors (Enrique-Tarancon et al., 1998; Carpene et al., 2001; Fontana et al., 2001; Carpene et al., 2006). This insulin-like effect of SSAO substrates is not limited to adipocytes, but was also observed in VSMCs (El Hadri et al., 2002). In SSAO-knockout mice, SSAO substrates do not have an insulin-like effect, suggesting that SSAO activity is responsible for mediating glucose uptake (Bour et al., 2007a). SSAO substrates seems to exhibit some beneficial effects on diabetic conditions (Iglesias-Osma et al., 2005). Interestingly, SSAO activity in obese dogs is significantly increased (Wanecq et al., 2006).

The involvement of SSAO activity in mediating glucose uptake suggests the products from SSAO-catalyzed reactions are responsible for this effect. Hydrogen peroxide is generated from SSAO-catalyzed reactions and catalase abolishes the effect of SSAO substrates on glucose uptake (Enrique-Tarancon et al., 1998; Enrique-Tarancon et al., 2000). It suggests that hydrogen peroxide is responsible for the insulin-like effect. Indeed, hydrogen peroxide at low concentrations functions as a signaling molecule by regulating transcription factors (Finkel, 1998; Kunsch and Medford, 1999). Moreover, hydrogen peroxide is known to mimic the effect of insulin by translocating the GLUT4 glucose transporter from intracellular vesicles onto the plasma membrane. In addition, SSAO is colocalized with GLUT4 vesicles (Fontana et al., 2001).

These findings support the role of hydrogen peroxide from SSAO-mediated reactions in regulating glucose uptake.

1.2.3.2 SSAO and Blood Pressure

Abundance of SSAO in the vascular system has triggered some interests whether SSAO is related to blood pressure. Methylamine induces vessel relaxation *via* a nitric oxide independent mechanism in isolated human blood vessels, which is blocked by SSAO inhibitor. Formaldehyde and hydrogen peroxide have similar effect to that of methylamine. It suggests that products from deamination of methylamine mediated by SSAO are responsible for vessel relaxation (Conklin et al., 2004). However, inhibition of SSAO was also found to cause vasodilatation. For instance, hydralazine, a drug previously used for the treatment of hypertension, inhibits SSAO activity (Vidrio, 2003). These studies suggest that SSAO is able to modulate blood pressure. Moreover, the effect of SSAO-catalyzed reactions on blood pressure may be dependent on the enzyme activity, levels of substrates, signaling pathways activated on vasculature, and perhaps other factors in the vicinity.

1.2.3.3 SSAO and Development of Vasculature

During embryogenesis (Salmi and Jalkanen, 2006), and throughout the early development of vasculature (Valente et al., 2008), SSAO is highly expressed on VSMCs. In rats, inhibition of SSAO leads to altered elastin architecture within the aortic media characterized by uncontrolled proliferation of smooth muscle cells (Langford et al., 1999). Decreased SSAO activity is associated with increased disorganization of elastic lamellae with reduced thickness (Sibon et al., 2008). The properties of blood vessels are also impaired including less strength and higher stiffness. Interestingly, in idiopathic annuloaortic ectasia disease, SSAO expression is significantly downregulated in affected area where there is reduction in elastic lamellar thickness as well (Sibon et al., 2004).

In mice overexpressing SSAO in VSMCs, the aortic elastic lamellae become abnormally straight and unfolded. Elastic fibers are irregularly arranged and form tangled webs between the intercalating elastic laminae (Gokturk et al., 2003). These abnormalities reduce artery elasticity and impair vessel ability in regulating blood pressure.

These studies suggest that SSAO-catalyzed reactions play an important role in deposition of extracellular matrix and maintenance of vascular smooth muscles. Vascular SSAO appears to crosslink elastin/collagen monomers with other basement membrane components (Langford et al., 2002). Aldehydes produced from SSAO-mediated deaminations crosslink vascular structural proteins. For example, formaldehyde produced from deamination of methylamine modifies and crosslinks proteins (Gubisne-Haberle et al., 2004). In addition to aldehydes, hydrogen peroxide produced on the vascular surface from SSAO-mediated deaminations regulates cell proliferation and adhesive properties of both endothelium and smooth muscles (Rao and Berk, 1992; de Bono and Yang, 1995; Li et al., 1997; Yasuda et al., 1999; Stone and Collins, 2002).

1.2.3.4 SSAO as an Endothelial Adhesion Molecule

SSAO was discovered independently as vascular adhesion molecule-1 (VAP-1). VAP-1 and SSAO have identical sequence at cDNA level (Smith et al., 1998). SSAO/VAP-1 on the surface of endothelium contributes to the leukocyte extravasation cascade (Salmi et al., 1998; Lalor et al., 2002; Bonder et al., 2005; Koskinen et al., 2007). Leukocyte extravasation from blood circulation into tissues is crucial for immune homeostasis and inflammatory responses. Under normal conditions, leukocytes flowing in the blood stream reversibly adhere to and roll on the endothelium of vasculature. Upon elicitation of inflammation, SSAO stored in intracellular granules is recruited to the luminal plasma membrane of endothelial cells, probably triggered by inflammatory mediators (Jaakkola et al., 2000). Studies using specific SSAO inhibitors or mutant forms of SSAO lacking the catalytic site have found that SSAO activity is important for leukocyte extravasation, particularly in the rolling phase and the subsequent transmigration step (Tohka et al., 2001). This effect of SSAO/VAP-1 is selective to certain types of leukocyte (Salmi et al., 1997).

The mechanisms of interaction between SSAO and leukocytes have been proposed. SSAO-mediated amine deaminations on leukocyte surface is important for leukocyte adhesion, because both inhibition of SSAO activity and addition of SSAO substrates abolish leukocyte adhesion and rolling (Salmi et al., 2001). Therefore, the lymphoid surface-bound amines such as NH_2-groups on side chains of amino acids and amino sugars rather than soluble SSAO substrates, namely, methylamine and aminoacetone, are responsible for SSAO-mediated leukocyte

adhesion. A transient link is formed between the enzyme and the cell after the initial sialic acid-dependent adhesion. However, to date such a surface-bound amine has not been identified.

In summary, SSAO activity regulates leukocyte trafficking in the peripheral system (Marttila-Ichihara et al., 2006), and small-molecule inhibitors of SSAO suppress leukocyte extravasation to sites of inappropriate inflammation. Therefore, SSAO is a potential novel target for treatment of various chronic inflammatory diseases (Salter-Cid et al., 2005; Xu et al., 2006; Smith and Vainio, 2007; Noda et al., 2008b; O'Rourke et al., 2008).

In the CNS, there are few leukocytes present under normal conditions, but in the presence of infection or injury, leukocytes enter the CNS by three routes. The first route is the blood-choroid plexus-CSF route. In healthy individuals there are about 3, 000 leukocytes per milliliter of CSF (Engelhardt et al., 2001; Kivisakk et al., 2003). The second pathway is leukocytes from blood extravagate through postcapillary venules at the brain pial surface into the subarachnoid space (Lister and Hickey, 2006). Thirdly, leukocytes continue to enter the Virchow-Robin perivascular spaces (Walther et al., 2001), which appear to be the important sites for lymphocytic interactions with antigen-expressing cells (Man et al., 2007). The role of SSAO, which is located at this compartment, on leukocyte trafficking into the CNS has not been addressed and needs to be clarified.

1.2.3.5 Plasma SSAO and Diseases

The functions of plasma/soluble SSAO are less understood. Similar to the membrane-bound form, plasma SSAO facilitates leukocyte adhesion to endothelial cells, probably by inducing signaling pathways or mediators in leukocytes (Kurkijarvi et al., 1998). Plasma SSAO activities have been measured in a variety of pathological disorders/diseases, which are summarized in Table 1.

1.2.4 SSAO and Vascular Disorders

1.2.4.1 SSAO and Heart Disease

High plasma SSAO activity is a risk factor for the progression of heart disease (Boomsma et al., 1997). Plasma SSAO activity increases with the severity of congestive heart failure. It was proposed that the toxic products generated from SSAO-catalyzed deaminations cause endothelial dysfunction and damage, which is observed in various vascular disorders

Table 1. SSAO activity in various diseases

Pathological Conditions	**Increased SSAO activity**	**Decreased SSAO activity**	**Unchanged SSAO activity**	**References**
Alzheimer's disease	Cerebral vasculature, plasma			(Ferrer et al., 2002; Jiang et al., 2008)
Congestive heart failure	Plasma			(Boomsma et al., 1997; Boomsma et al., 2000b)
Cardiac disease	Plasma			(Boomsma et al., 2000a)
Diabetes (types 1 and 2)	Plasma (human, rat and sheep), rat kidney	Rat aorta	Rat aorta, lung and pancreas	(Boomsma et al., 1995; Lyles, 1996; Meszaros et al., 1999b; Gronvall-Nordquist et al., 2001; Boomsma et al., 2005a; Somfai et al., 2006; Nunes et al., 2008)
Diabetic retinopathy	Plasma			(Garpenstrand et al., 1999b; Gronvall-Nordquist et al., 2001)
Diabetic atherosclerosis	Plasma			(Meszaros et al., 1999a; Karadi et al., 2002)
Hypertension	Rat plasma		Plasma, aorta	(Lyles, 1996; Wang et al., 2005)
Inflammatory liver disease	Plasma			(Kurkijarvi et al., 1998; Kurkijarvi et al., 2000; Lalor et al., 2007)
Kidney transplant rejection and kidney disease	Plasma			(Kurkijarvi et al., 2001; Lin et al., 2008)
Stroke	Plasma	Cerebral vasculature	Plasma	(Garpenstrand et al., 1999a; Airas et al., 2008)
Burns		Plasma		(Lyles, 1996)
Cancer (solid tumor in breast)		Tumor tissue (rat)		(Lizcano et al., 1991)
Cancer (breast)		Plasma		(Lyles, 1996)
Cancer (lung)		Plasma		(Garpenstrand et al., 2004)
Obesity	Plasma, rat and mouse adipose			(Weiss et al., 2003; Yu et al., 2004; Prevot et al., 2007)

(Boomsma et al., 1997). Moreover, heart failure patients with an elevated plasma SSAO activity have an increased mortality, and SSAO activity is an independent prognostic marker for chronic heart disease (Boomsma et al., 2000b).

1.2.4.2 SSAO and Diabetes Mellitus

Plasma SSAO activity is increased in both type 1 and 2 DM (Nilsson et al., 1968; Boomsma et al., 1995; Gronvall-Nordquist et al., 2001; Monnier, 2003; Boomsma et al., 2005b; Nunes et al., 2008). Therefore, elevated plasma SSAO activity has been considered as a potential biological marker for diabetes (Nunes et al., 2008). In the presence of obesity, hypertension, macrovascular (carotid stenosis) and microvascular (proliferative retinopathy) complications, plasma SSAO activity is further elevated (1.5 to 2 folds) compared to control populations (Meszaros et al., 1999b; Gronvall-Nordquist et al., 2001; Boomsma et al., 2005b). In diabetic mice and rats, plasma SSAO activity is significantly elevated with altered activities of tissue-bound SSAO (Gokturk et al., 2004; Somfai et al., 2006).

The increased production of reactive aldehydes by elevated SSAO activity is proposed to contribute to diabetic complications (Yu and Zuo, 1993). For instance, in a mouse model of diabetes, inhibition of SSAO reduces oxidative damage to blood vessels, which is characterized by reduced malondialdehyde excretion and atherosclerotic lesions (Yu et al., 2002). Formaldehyde produced from methylamine deamination is involved in diabetic pathology (Yu and Zuo, 1993, 1996; Yu et al., 2002; Kazachkov et al., 2007). In addition, increased AGEs formation is involved in vascular complications in diabetes (Yamagishi et al., 2005). Methylglyoxal generated from aminoacetone deamination, which is catalyzed by SSAO, contributes to AGEs formation and subsequent vascular complications of diabetes (Mathys et al., 2002). Moreover, methylglyoxal directly modifies insulin molecule and impairs its function in regulating glucose uptake (Jia et al., 2006).

1.2.4.3 SSAO and Atherosclerosis

In atherosclerosis patients, plasma SSAO activity is significantly increased (Meszaros et al., 1999a; Karadi et al., 2002). Plasma SSAO activity is also correlated with various risk factors for atherosclerosis such as body mass index, hemoglobin A1c and cholesterol (Meszaros et al.,

1999b). Therefore, elevated plasma SSAO activity seems to be a potential marker for atherosclerosis.

In rodents, mice strains that are more vulnerable to atherosclerosis, for example, C57BL/6 mice (Paigen et al., 1985; Paigen et al., 1990), express significantly higher SSAO activity compared to other strains (Yu and Deng, 1998). Rabbits, known for their high vulnerability to atherosclerosis, also possess very high SSAO activity (Boomsma et al., 2000a). Based on these findings, SSAO is involved in the development of atherosclerosis.

1.2.4.4 SSAO and Stroke

Plasma SSAO activity is significantly increased in patients after acute ischemic stroke, but membrane-bound SSAO expression on cerebral vasculature after a stroke is significantly diminished in the ipsilateral hemisphere compared to contralateral hemisphere and in control brains (Airas et al., 2008). It is known that the post-stroke events are normally more destructive than the stroke process itself. Leukocyte extravasation to the affected areas can exacerbate the tissue damage. In rats, leukocyte infiltration after ischemic stroke is significantly reduced by SSAO inhibitor, suggesting SSAO-mediated leukocyte trafficking plays an important role in this process (Xu et al., 2006).

1.2.4.5 SSAO and Obesity

Plasma SSAO activity is significantly increased in obese people (Weiss et al., 2003). Adipose tissue expresses SSAO at high levels, which is involved in regulating glucose uptake and lipolysis. Interestingly, during differentiation of human adipocytes, SSAO activity is significantly increased, supporting its role in adipogenesis (Bour et al., 2007b). Adipose SSAO seems to be associated with the development of obesity (Morin et al., 2001). Inhibition of SSAO is able to reduce fat deposition in obese rodents (Yu et al., 2004; Carpene et al., 2007; Prevot et al., 2007; Carpene et al., 2008).

1.2.4.6 SSAO and Inflammation

SSAO is involved in the inflammatory process by facilitating leukocyte trafficking. Upregulation of SSAO has been detected in some inflammatory conditions. For example, in human and mouse lungs, SSAO expression is increased during inflammation (Singh et al., 2003).

In mice with pulmonary inflammation, blocking SSAO activity reduces the number of inflammatory cells in bronchoalveolar lavage (Yu et al., 2006). In inflammatory bowl disease and in dermatoses, the expression of vascular SSAO is significantly increased (Salmi et al., 1993; Salter-Cid et al., 2005). In multiple sclerosis patients with ongoing inflammatory activity, plasma SSAO activity was found to be significantly elevated (Airas et al., 2006). SSAO is also significantly increased in the skin of patients with psoriasis, lichen ruber planus and allergic lesions, and SSAO antibodies are able to reduce lymphocyte adhesion by up to 60% (Arvilommi et al., 1996).

In humans, plasma SSAO activity is elevated in chronic inflammatory liver disease and in alcoholic hepatitis (Kurkijarvi et al., 1998; Kurkijarvi et al., 2000; Lalor et al., 2007). The difference in the concentration of SSAO in portal and hepatic veins suggests that the elevated plasma SSAO is caused by shedding from hepatic vascular bed. SSAO plays an important role in leukocyte recruitment through hepatic sinusoidal endothelium (Lalor et al., 2002; Bonder et al., 2005). In a mouse hepatitis model, SSAO inhibitors significantly attenuate inflammatory responses (Bonder et al., 2005). A similar effect has been observed in a rat model of liver transplantation (Martelius et al., 2004).

A variety of inflammatory mediators upregulates SSAO, notably, interleukins 1 and 4, interferon-γ and tumor necrosis factor-α (Arvilommi et al., 1997; Merinen et al., 2005). Both SSAO antibodies and specific inhibitors in these models are able to attenuate the inflammatory responses, which suggests potential therapeutic benefits for inflammatory diseases (Kirton et al., 2005; Merinen et al., 2005; Salter-Cid et al., 2005; Xu et al., 2006; Noda et al., 2008a).

1.2.4.7 SSAO and AD

In the CNS, SSAO is exclusively localized on cerebral blood vessels (Zuo and Yu, 1994; Jiang et al., 2008), and it is colocalized with perivascular Aβ deposition in AD brains (Ferrer et al., 2002; Unzeta et al., 2007; Jiang et al., 2008). Plasma SSAO activity has been found significantly increased in AD patients (del Mar Hernandez et al., 2005). However, little is known on the mechanism of Aβ-SSAO colocalization and upregulation in AD.

1.2.5 SSAO as a Pharmacological Target

Antibodies or small-molecule inhibitors of SSAO inhibit inflammatory responses in conditions such as arthritis, peritonitis and liver allograft rejection in rats and mice (Martelius et al., 2004; Merinen et al., 2005; Marttila-Ichihara et al., 2006). A murine monoclonal anti-SSAO IgM antibody, vepalimomab, has been evaluated and showed therapeutic effects in three Phase I clinical trials for treatment of dermatitis (Vainio et al., 2005). Interestingly, SSAO is abundant in retina (Zuo and Yu, 1994). SSAO inhibitor has been shown to suppress endotoxin-induced uveitis (Noda et al., 2008a).

Inhibiting SSAO activity also reduces the production of toxic metabolites and thus attenuate vascular damages such as retinopathy and nephropathy associated with diabetes, hypertension, atherosclerosis and other vascular diseases (Dunkel et al., 2008).

The mechanism of how plasma activity and tissue expression of SSAO are altered under pathological conditions is unclear. Increased SSAO expression may be a compensatory upregulation by other factors or its own substrates. Elevated SSAO activity or expression produces more cytotoxic chemicals causing more damage to the vasculature. This process forms a chronic and accumulative vicious cycle that contributes to the development of a variety of chronic vascular and inflammatory diseases. Therefore, SSAO could be a very important therapeutic target.

2. HYPOTHESES

In spite of some controversy, Aβ remains at the center of interest regarding the pathology of AD (Selkoe, 2008). Products resulting from the aggregation of Aβ, oligomers in particular, are neurotoxic and responsible for the neurodegeneration in AD (Cleary et al., 2005; Shankar et al., 2008). Perivascular Aβ deposition (Pfeifer et al., 2002; Fryer et al., 2003) and cerebral vascular damage such as atherosclerosis and cerebral microinfarcts have been observed in AD brains (Luchsinger et al., 2005). Impairment of cerebral vasculature and Aβ clearance *via* vascular LRP-1 has been speculated (Zlokovic, 2004). Oxidative stress and inflammation are also implicated in AD pathology (Hirai et al., 2001; Griffin, 2006).

SSAO is involved in a variety of vascular disorders, probably by producing toxic products that act on blood vessels (section 1.2.4). Plasma SSAO activity was found to be significantly increased in AD patients (del Mar Hernandez et al., 2005). In AD brains, SSAO is colocalized with perivascular Aβ deposition (Ferrer et al., 2002; Unzeta et al., 2007; Jiang et al., 2008). SSAO is up-regulated in response to inflammation (Merinen et al., 2005).

The potential involvement of cerebral vascular SSAO in the pathology of AD has been previously proposed (Yu, 2001). An extended version of the model is illustrated in Figure 12. In the present study, we hypothesize that:

(1) Reactive aldehydes produced from SSAO-mediated deamination (formaldehyde and methylglyoxal) and oxidative stress (malondialdehyde and HNE) crosslink Aβ and enhance its oligomerization and fibrillogenesis. These aldehydes also crosslink Aβ with other proteins to form large complexes;
(2) Increased production of Aβ oligomers by aldehydes exerts more cytotoxicity to neuronal cells and cerebral vasculature, accelerating neural and vascular degeneration;
(3) Toxic products from SSAO-catalyzed reactions damage the cerebral vasculature and impair its functions. For instance, aldehydes exert *in situ* modification of vascular LRP-1 and impair Aβ clearance. Vascular damage in the brain will release the membrane-bound SSAO into blood circulation;

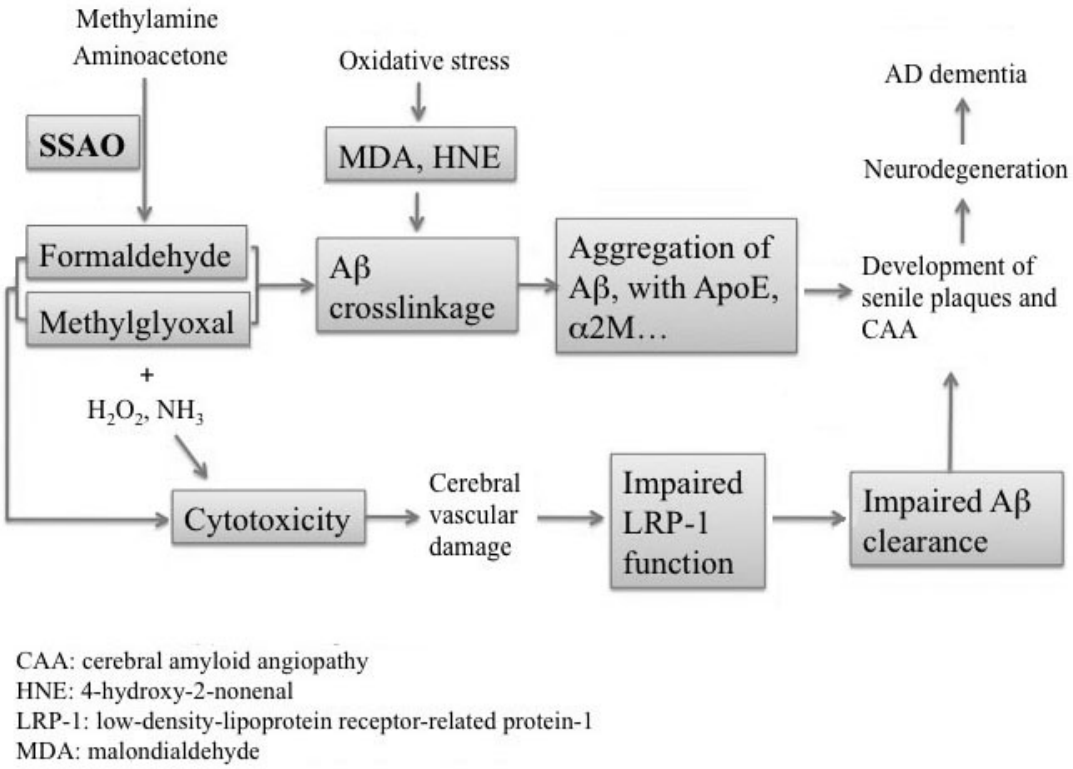

Figure 12. Hypothesis concerning the involvement of cerebral SSAO-mediated deamination in AD pathology. SSAO-catalyzed deamination produces reactive aldehydes, hydrogen peroxide and ammonia. Endogenous aldehydes react with Aβ and crosslink Aβ or with other proteins. Toxic products generated by SSAO damage cerebral blood vessels including LRP-1 function. Aβ clearance is therefore impaired. These effects of aldehydes contribute to Aβ accumulation in a chronic and accumulative manner, which eventually lead to AD.

(4) Chronically, enhanced Aβ aggregation, impaired clearance and increased influx lead to the accumulation of Aβ in the CNS. Formation of senile and perivascular plaques will be increased by aldehydes.

3. OBJECTIVES

(1) To investigate the potential effects of endogenous aldehydes, such as formaldehyde, methylglyoxal, malondialdehyde and HNE, on Aβ β-sheet formation, oligomerization, fibrillogenesis as well as crosslinking Aβ with other proteins and forming large complexes. Formaldehyde is produced from methylamine *via* SSAO-mediated deamination and lipid peroxidation (LPO). Methylglyoxal is derived from aminoacetone through SSAO, LPO and glycolysis. Malondialdehyde and HNE are products of LPO which are considered as markers for oxidative stress. The mechanism of how aldehydes react and crosslink Aβ peptide will be investigated.

(2) To test whether aldehyde-modified Aβ oligomers exhibit altered cytotoxicity: neuroblastoma SH-SY5Y cells will be employed to assess the effect of aldehyde-modified Aβ oligomers on cell death and apoptosis.

(3) To test whether SSAO-produced aldehydes can affect Aβ clearance *via* LRP-1 associated to VSMCs.

The ultimate goal of the investigation is to uncover the potential involvement of cerebrovascular SSAO-mediated reactions in Aβ misfolding and clearance and to delineate the mechanism of CAA formation in AD.

4. METHODOLOGIES

4.1 Part I: Effects of Endogenous Aldehydes on Aβ β-sheet Formation, Oligomerization and Fibrillogenesis In Vitro

4.1.1 Materials

$A\beta_{1-40}$ and A11 anti-Aβ-oligomer antibody were purchased from BioSource (Camarillo, CA, USA). 1, 1, 1, 3, 3, 3-Hexafluoro-2-propanol (HFIP), methylglyoxal, Tris-base, Tween-20, sodium chloride (NaCl) and anti-rabbit IgG were obtained from Sigma-Aldrich (St. Louis, MO, USA). Formaldehyde, malondialdehyde and HNE were obtained from BDH Inc. (Toronto, ON, Canada), Fluke (Bucks, Switzerland) and Axis (Portland, OR, USA), respectively. Ninety-six-well microfluor black plates were purchased from Dynex Technologies Inc. (Chantilly, VA, USA). [^{14}C]-Benzylamine, clorgyline, (-)-deprenyl, toluene, ethyl acetate ACS scintillation cocktail were purchased from Amersham Radiolabeled Chemicals Inc. (St. Louis, MO, USA). MDL-72974A ((E)-2-(4-fluorophenethyl)-3-fluoroallylamine) was a gift from Marion-Merrell-Dow Inc. (Cincinnati, OH, USA). Amersham enzymatic chemiluminescence (ECL) blotting detection reagents were purchased from GE Healthcare (Buckinghamshire, UK).

4.1.2 Animals

Transgenic mice (mTIEhVAP-1) overexpressing human SSAO were created and provide by Dr Stolen. Briefely, transgenic mice were created with a mouse tie-1 promoter to drive the expression of human SSAO/VAP-1 specifically on endothelial cells (Stolen et al., 2004). Homozygous and nontransgenic lines were derived from heterozygous intercrosses, and were routinely checked by PCR (polymerase chain reaction) to ensure the expression of SSAO gene.

Rodents were housed with free access to food and water on a 12-h light/dark cycle (lights on at 6 a.m.) at a temperature of 19 to 20° C. The animal studies were in strict accordance with guidelines established by the Canadian Council on Animal Care and were approved by the University of Saskatchewan Animal Care Committee.

4.1.3 Preparation of Monomeric $A\beta_{1-40}$

To ensure the purity of $A\beta_{1-40}$ monomers ("seed-free" Aβ), the solution of the peptide was pretreated immediately before each experiment. $A\beta_{1-40}$ was dissolved in 100% HFIP (1 mg/mL) and incubated in a water bath sonicator at 4º C for 2 h. The HFIP was removed under a gentle stream of nitrogen or Aβ was lyophilized (freeze-dried) using a Savant SpeedVac SVC100H vacuum concentrator from Thermo Scientific (Waltham, MA, USA). The treated $A\beta_{1-40}$ crystals were dissolved in nanopure water. The preparation of Aβ monomers free of oligomers was confirmed by dot-blot tests using A11 specific anti-Aβ-oligomer antibody. The final Aβ concentration was determined using Bradford protein assay from Bio-Rad Laboratories (Hercules, CA, USA).

4.1.4 Interactions of Aβ with Endogenous Aldehydes

Freshly prepared seed-free $A\beta_{1-40}$ (200 μM) was incubated for 2 h to up to 7 days in a sterile environment, in the presence or absence of various concentrations (ranging from 1 μM to 10 mM) of formaldehyde, methylglyoxal, malondialdehyde or HNE in phosphate-buffered saline (PBS) (pH 7.4, 20 mM). The incubation was carried out at 37º C without shaking or re-pipetting. For AFM imaging experiments, to overcome the interference of salt crystallization from PBS buffer, ammonia/formic acid (20 mM, pH 7.4) volatile buffer was used.

4.1.5 Isolation of Membrane-Bound SSAO from Transgenic Mice

Small intestines of mTIEhVAP-1 mice are rich in SSAO and were used for the preparation of SSAO. 1.5 mL of PBS was added to each 50 mg of tissue in a 12 X 75 mm glass culture tube (VWR International, Mississauga, ON, Canada) on ice. The tissue was then homogenized for 20 seconds by a polytron homogenizer (Kinematica GMBH, Luzern, Switzerland). Repeat the homogenization twice with one minute cooling down at intervals. The homogenate was then centrifuged at 900 g for 10 min. The supernatant was further ultracentrifuged at 100,000 g for 30 min (Beckman, Fullerton, CA, USA). The supernatant was discarded and the pellet was resuspended. The last centrifugation was repeated and the pellet which contained SSAO was collected. All centrifugation procedures were carried out at 4º C.

4.1.6 SSAO Activity Assay

SSAO activity was assessed by a radioisotope-enzymatic procedure using ^{14}C-labeled benzylamine as the substrate. Briefly, 50 μL of SSAO enzyme preparations were incubated with clorgyline (1 μM) and (-)-deprenyl (1 μM) at 37° C for 20 min to inhibit MAO activities. Aliquots of the enzyme preparation were then incubated with 50 μL of [^{14}C]-benzylamine (0.4 mM cold benzylamine and 50 nCi of ^{14}C) in 200 μL phosphate buffer (0.1 M, pH 7.4) at 37° C for 30 min. 250 μL of 2 M citric acid was added to terminate the enzyme reaction. The oxidized products were extracted in 1 mL of toluene: ethyl acetate (1:1, v/v). After centrifugation at 2,000 g for 10 min, 600 μL of the upper layer was transferred into a counting vial containing 10 mL of ACS scintillation cocktail. Radioactivity was measured in a Beckman LS-7500 liquid scintillation counter (Fullerton, CA, USA). Sample protein concentrations were determined by Bradford assay. SSAO activity is calculated based on the following formula, where Blank was 50 μL of phosphate buffer instead of SSAO preparation and Standard was 50 μL of [^{14}C]-benzylamine (0.4 mM cold benzylamine and 50 nCi of ^{14}C-benzylamine) in ACS scintillation cocktail.

$$\text{SSAO activity (nmol/mg protein/min)} = \frac{\text{Total amount of benzylamine: } 50\ \mu l * 4 * 10^{-4}\ M * \dfrac{DPM_{sample} - DPM_{blank}}{DPM_{standard} - DPM_{blank}}}{600\ \mu l/1000\ \mu l * 90\% * 30\ min * \text{Protein concentration} * 50\ \mu l}$$

(Extraction ratio; Pippetting error; Reaction time; Sample protein amount)

$$= \frac{(DPM_{sample} - DPM_{blank}) * 1.235}{(DPM_{standard} - DPM_{blank}) * \text{Protein amount}}$$

4.1.7 Structural Analysis

4.1.7.1 Thioflavin-T Fluorometry for Detection of Aβ β-Sheets Formation

Thioflavin T (ThT) fluorescence assays reveal the early stage of $A\beta_{1-40}$ aggregation, namely, β-sheet formation (Naiki et al., 1989; Naiki and Nakakuki, 1996). $A\beta_{1-40}$ (200 μM) was incubated with various concentrations of aldehydes at 37° C. At designated time points, Aβ samples were diluted in glycine-NaOH buffer (50 mM, pH 9.0, 2 mM ThT) with a final

concentration at 2 μM. Aliquots (200 μL) of the reaction solution were transferred to black microfluor plates and their fluorescence was measured. Fluorescence (excitation wavelength of 450 nm and emission wavelength of 482 nm) was measured using a SpectraMax GeminiXS fluorescence reader from Molecular Devices (Sunnyvale, CA, USA).

4.1.7.2 Circular Dichroism Spectroscopy for Measurement of Aβ Secondary Structures

$A\beta_{1-40}$ (200 μM) was incubated with various concentrations of aldehydes at 37° C. CD spectra were measured at desired time points (from 2 h to 48 h) at room temperature in a 0.1-cm cell optical path length cuvette (Hellma, 106-OS) using a PiStar-180 spectrometer (Applied Photophysics, Surrey, UK). The sample solutions were scanned from 260 to 190 nm in 0.5-nm steps at a scan rate of 10 nm per min and with 4 nm bandwidth. CD spectra of the PBS buffer containing the appropriate aldehydes were obtained and subtracted from the protein solutions. Percentages of protein secondary structures were calculated using CD Spectra Deconvolution (CDNN) software (v 2.1) (Bohm et al., 1992).

4.1.7.3 Dynamic Light Scattering Analysis: Distribution of Aβ Molecular Sizes

$A\beta_{1-40}$ (200 μM) was incubated with various concentrations of aldehydes at 37° C. A time course of DLS measurements were conducted using an 824.8-nm (55 mW) Anodisk with a fixed catering angle of 90º with a Dyna-Pro 99 MS800 instrument (Protein Solutions, Lakewood, NJ, USA) at 25º C. Protein solutions were filtered through a 0.2-μm Anodisk filter, and placed in a 12-μL cuvette (b = 1.5 nm). Data acquisition time was 5 s and S/N Threshold was set at 2. The count rates (signal intensity), which are proportional to the amount of photons reflected from the sample solution, were assessed at various time points after incubation. The size distributions were analyzed by Dynamic V5.26.60 (Protein Solutions, Lakewood, NJ, USA).

4.1.7.4 Atomic Force Microscopy Imaging of Aβ Aggregates

For AFM imaging under ambient conditions, aliquots (1 μL) of the formaldehyde/methylglyoxal-incubated Aβ in a volatile buffer as described above were dropped on freshly cleaved mica (Structure Probe Inc., West Chester, PA, USA) for 1 min until dry. Aβ incubated with malondialdehyde and HNE were also imaged but under wet conditions, where 10-

μL aliquots were placed onto freshly cleaved mica in a sample well for 2 min, and subsequently imaged in 250 μL PBS (20 mM, pH 7.4).

AFM measurements were carried out on a Pico-SPM (Molecular Imaging Inc., Tempe, AZ, USA) with an AFM M-scanner operating in alternating-contact mode. Type I alternating-contact mode levers from Molecular Imaging were used and their specifications include a force constant of approximately 1.2 to 5.5 N/m, and a resonant frequency of approximately 60 to 90 kHz under ambient conditions. All measurements were taken with the ratio of the set-point oscillation amplitude to free air oscillation amplitude of 0.80. In addition, all measurements were performed with the instrument mounted in a vibration isolation system.

The scan rate was 1 to 2 lines/s (256 pixels per line) for all images. At least five positions on the mica were randomly chosen for scanning and imaging each sample. Each image was conducted in two opposite directions simultaneously and the final image was averaged. Size distribution within the scanning area, and the final three-dimensional image, were calculated and generated by software from Visual SPM Molecular Imaging Inc. (Tempe, AZ, USA).

4.1.7.5 Dot-Blot Assay of Aβ Oligomers

In order to quantify the effect of aldehydes on Aβ oligomerization and to ensure a seed-free monomeric Aβ preparation for the experiments, a dot-blot assay using a specific anti-Aβ-oligomer antibody, A11, was used. $A\beta_{1\text{-}40}$ (200 μM) was incubated with various aldehydes (100 μM each) at 37° C for certain time periods. A 2 μL aliquot of each sample was spotted onto the nitrocellulose membrane and air dried. The membrane was blocked in 1X tris buffered saline (TBS) buffer containing 5% non-fat dry milk at 4º C overnight with gentle shaking. The membrane was then incubated with A11 anti-Aβ-oligomer antibody (1 μg/mL in TBS with 5% non-fat dry milk) at room temperature for 1 h and washed in TBST (Tween-20: 0.5% in 1X TBS buffer) for 10 min by 3 repeats with gentle shaking. Then the membrane was incubated with anti-rabbit secondary antibody (dilution factor: 1:16,000 in TBS with 5% non-fat dry milk) for 1 h, washed as in the previous step, and revealed with Amersham ECL solution by a developing machine.

10X TBS buffer was prepared by dissolving 24.2 g Tris base and 80 g NaCl in 1 L of nanopure water. pH was adjusted to 7.6 with hydrochloric acid (HCl).

4.2 Part II: Effect of Formaldehyde-induced Crosslinkage on the Cytotoxicity of Aβ Oligomers

4.2.1 Materials

Acetic acid, boric acid, bovine serum albumin (BSA), 3-[(3-cholamidopropyl)dimethylammonio]-1-propanesulfonate (CHAPS), citric acid, dithiothreitol, 9-fluorenylmethyl chloroformate (FMOC-Cl), glycerol, 4-(2-Hydroxyethyl)piperazine-1-ethanesulfonic acid-N-(2-Hydroxyethyl)piperazine-N′-(2-ethanesulfonic acid) (HEPES), HCl, isopropanol, lactic acid, MTT (3-[4, 5-dimethylthiazol-2-yl]-2, 5-diphenyl-tetrazolium bromide), nicotinamide adenine dinucleotide (NAD+), phosphoric acid, ribonuclease A, sodium acetate, sodium tetrahydridoborate ($NaBH_4$) tetramethylammonium chloride (TMA), thyroglobulin, Tris-HCl and Ttriton-X100 were purchased from Sigma–Aldrich (St. Louis, MO, USA). Ethylenediaminetetraacetic acid (EDTA), high performance liquid chromatography (HPLC)-grade acetonitrile, methanol, hexane and hydrochloric acid were obtained from EMD Merck (Darmstadt, Germany).

SH-SY5Y neuroblastoma cell line was purchased from American Type Culture Collection (ATCC, Manassas, VA, USA). Dulbecco's Modified Eagle's Medium (DMEM, D6429) and trypsin EDTA solution were purchased from Sigma (Okaville, ON, Canada). Fetal bovine serum (FBS) was obtained from Gibco (Carlsbad, CA, USA). $A\beta_{1-42}$ was purchased from BioSource (Camarillo, CA, USA). Protease inhibitor cocktail tablets were purchased from Roche (Indianapolis, IN, USA). Caspase-3 substrate, DEVE-pNA, was purchased from Biomol (Plymouth Meeting, PA, USA). Bradford reagent was obtained from Bio-Rad Laboratories (Hercules, CA, USA).

4.2.2 Identification of Interaction Sites of Aβ with Formaldehyde

Seed-free $A\beta_{1-40}$ (200 μM) was dissolved in PBS (20 mM, pH 7.4) (see Section 4.1.3) and incubated in various concentrations of formaldehyde at 37º C for 24 h. After incubation, Aβ aggregates were further incubated with or without sodium borohydride (10 mM) for 24 h to convert the Schiff bases into covalent bonds. Aβ aggregates were then subjected to Western blot for Aβ analysis.

To identify the reaction sites, similarly, seed-free $A\beta_{1-40}$ (200 μM in PBS) was incubated in the presence or absence of formaldehyde (10 μM) at 37º C for 48 h followed by incubating with

$NaBH_4$ (10 mM) for 24 h. The aggregates were then hydrolyzed by HCl (6 N) at 110º C for 24 h. FMOC derivatization and HPLC procedures were conducted as previously described (Kazachkov and Yu, 2005). Briefly, one mL of hydrolyzed Aβ sample was diluted with 500 μL potassium-borate buffer (0.8 M, pH 10) and vortexed for one minute. One mL of FMOC-Cl reagent solution (10 mM in acetonitrile) was then added to the buffered samples and vigorously vortexed. The derivatization reaction was terminated by extraction in 5.0 mL hexane to remove excess FMOC-Cl reagent, FMOC-OH from FMOC-Cl and acetonitrile. The upper layer was discarded and the extraction procedure was repeated twice. The solution was neutralized by adding 0.1 mL 20% (v/v) acetic acid. Aliquots (250 μL) were injected into the HPLC for amino acid detection.

The HPLC experiments were conducted with a Shimadzu solvent delivery module (LC-10 ADvp), a Shimadzu auto injector (SIL-10ADvp), a Shimadzu DGU-14A degasser, a Shimadzu SPD-10AvpUV-VIS detector with Bio-Rad UV monitor (model 1305), and a Beckman Ultrasphere IP reversed phase HPLC column (ID 4.6mm×250 mm; particle size 5 μm; C-18). A modified tertiary gradient system was adopted from previous method for amino acids detection (Ahmed et al., 1997). The elution gradient of mobile phase is graphically shown in Figure 13. The flow rate was set constant at 1.4 mL/min. UV absorbance was measured at 265 nm. All the procedures above were carried out at room temperature.

4.2.3 Isolation of Aβ Oligomers by Size Exclusion Chromatography

Seed-free $A\beta_{1-42}$ was prepared by pretreatment with HFIP similarly as that for $A\beta_{1-40}$. $A\beta_{1-42}$ monomers (1 mg/mL in PBS) were then incubated in the presence or absence of formaldehyde (10 mM) at 37º C for 12 h. A ProSphereTM size exclusion column (125 HR 4 μ m from Alltech) was used to separate Aβ oligomers from monomers and dimers based on their molecular sizes. The HPLC system was described in Part I. The mobile phase was 0.3 M NaCl, 0.05 M phosphate, pH 7.0 and a constant flow at 1 mL/min was employed. The Aβ peptides and its aggregated forms were spectrophotometrically detected at 280 nm. The eluent fractions of peaks were collected and placed on ice immediately. The collected Aβ oligomers were concentrated by a Savant SpeedVac SVC100H vacuum concentrator (ThermoScientific, Waltham, MA, USA) for 1 h. The concentrations of Aβ oligomers and monomers were determined by Bradford assay.

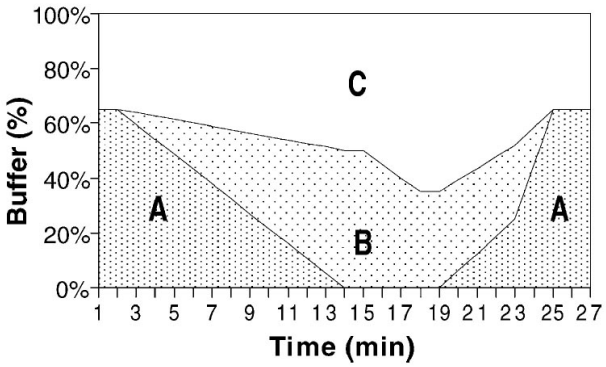

Figure 13. The elution gradient of mobile phase of FMOC-HPLC (Kazachkov and Yu, 2005). Solvent A was 20 mM citric acid with 5 mM TMA, adjusted to pH 2.85 with 20 mM sodium acetate. Solvent B was 80% (v/v) of 20 mM sodium acetate solution and 20% (v/v) methanol with 5 mM TMA adjusted to pH 4.5 by concentrated phosphoric acid. Solvent C was acetonitrile (100%).

4.2.4 Cytotoxic Effect of Aβ Monomers and Oligomers on Neuroblastoma SH-SY5Y Cells

SH-SY5Y cells were cultured in DMEM containing 10% (v/v) of FBS. The cells were seeded at a density of 2 X 10^5 cells/mL and grown at 37º C in a 5% CO_2 atmosphere until confluence. The medium was changed about every 48 h and the cells were subcultured every 3 to 4 days. Cells of passages 5 to 20 were used for Aβ cytotoxicity studies. The toxic effects of both Aβ monomers and oligomers were tested at various concentrations.

SH-SY5Y cells were seeded from dishes into 96-well plates at a density of 2 X 10^4 cells/well. The plates were then incubated for 48 h to allow cells to attach and grow to 90% confluence. DMEM media containing FBS (10%) was refreshed and various concentrations of native or formaldehyde-modified $A\beta_{1-42}$ oligomers isolated from SEC were added to cultures and incubated for 3 to 24 h. MTT, LDH (lactate dehydrogenase) and caspase-3 assays were used for measurement of cell viability.

4.2.5 Cytotoxicity Assays

4.2.5.1 MTT Assay

10X MTT stock solution (5 mg/mL) was prepared by dissolving MTT in DMEM or PBS (pH 7.2) and filtering through a 0.2-μm Acrodisc syringe filter. Stock solution was stored at -20º C. The working MTT solution was prepared by diluting one volume of MTT stock solution in 9 volumes of DMEM containing 1% FBS. MTT solvent was composed of 0.1 N HCl and 10% (v/v) Triton-X100 in isopropanol.

The media supernatant was carefully removed from each well, and 50 μL of MTT reagent solution was added. After incubation for 4 h at 37º C, 100 μL of MTT solvent was added and thoroughly mixed to dissolve the MTT formazan crystals. The optical density (OD) of each well in the plates was immediately read at 570 nm using a SpectraMax microplate reader. The blank was without cells but contained MTT solution and solvent. The average OD values of control group (without Aβ treatment) were set to 100% of cell viability and other groups treated with Aβ were normalized accordingly.

4.2.5.2 LDH Assay

Cytoplasmic LDH was determined spectrophotometrically based on the conversion of lactic acid to pyruvic acid in the presence of NAD+. After treatment with Aβ, cells of each well were

collected by trypsin digestion, centrifuged at 500 g for 5 min and resuspended in 200 μL Hank's balanced salts solution (HBSS). The samples were then subjected to freezing and thawing twice to release the cytoplasmic LDH. The cell lysates were centrifuged at 10,000 g for 3 min in a microcentrifuge (Beckman Coulter, Fullerton, CA USA) to remove the cellular debris. A 50 μL aliquot of supernatant was transferred to a 96-well plate and 50 μL of NAD+ (1 mg/mL in 0.05 M sodium pyrophosphate, pH 9.0) was added to each well. The reaction was initiated by adding 100 μL of lactic acid (1% in 0.05 M sodium pyrophosphate, pH 9.0). The sample OD was read at 340 nm by a SpectraMax microplate reader within 1 h of starting reaction. Protein concentrations were determined by Bradford assay. The blank was NAD+ and lactic acid solutions without cells. Specific LDH activity (μmol/mg protein/min) was estimated as follows. The standard was 0.1 mmol of pyruvic acid in 0.05 M sodium pyrophosphate, pH 9.0. Relative cell viability/death was calculated similarly as described in MTT assay.

$$\text{LDH activity } (\mu\text{mol/min/mg protein}) = \frac{\text{Total lactic acid amount} \left(\frac{1\text{ mg}}{90\text{ g/mol}}\right) * \left(\frac{OD340_{sample} - OD340_{blank}}{OD340_{standard} - OD340_{blank}}\right)}{\text{Reaction time (min)} * \text{Protein concentration} * 50\ \mu\text{l}}$$

4.2.5.3 Caspase-3 Assay

After Aβ treatment for desired time periods, cells were collected and cell numbers were counted using a hemocytometer. It is important for the assay that at least 2 X 10^6 cells are present in each sample. The cells were centrifuged at 500 g for 5 min, resuspended in 50 μL of chilled cell lysis buffer (25 mM Tris, 1 mM EDTA, 1% Triton-X100, 10% glycerol, pH 7.5 with protease inhibitor cocktail) and incubated on ice for 10 min. Cell lysates were centrifuged in a microcentrifuge at 10,000 g for 3 min. The supernatants were transferred into new microcentrifuge tubes on ice. 50 μL of 2X reaction buffer/dithiothreitol mix (100 mM HEPES, pH 7.4, 200 mM NaCl, 0.2% CHAPS, 2 mM EDTA, 20% glycerol and 20 mM dithiothreitol) was added to 50 μL of supernatant. 5 μL of Ac-Asp-Glu-Val-Asp-p-nitroaniline (DEVD-pNA, 1 mM), a caspase-3 substrate from Biomol (Plymouth Meeting, PA, USA), was added to each sample with a final concentration of 50 μM. The samples were then incubated at 37º C (Fisher Scientific, Hampton, NH, USA) for 1 h or up to 3 h at maximum. After incubation, the sample OD was read at 405 nm by a SpectraMax microplate reader. Protein concentrations were

determined by Bradford assay. In each experiment, the average OD value of control group (without Aβ treatment) was set to 100% of caspase-3 activity and other groups were normalized accordingly and adjusted by protein concentrations.

4.3 Part III: Effect of SSAO-Catalyzed Deamination on α2M Uptake via VSMC LRP-1

4.3.1 Materials

Acetone was purchased from EMD Merck (Darmstadt, Germany). α2M, ammonium persulfate, collagenase (type II), nystatin, penicillin/streptomycin, trypan blue, anti-goat, anti-mouse and anti-rat IgGs were purchased from Sigma (St. Louis, MO, USA). Collagenase inhibitor I (Z-PDLDA-NHOH) and mouse anti-human LRP (5A6) antibody were purchased from Calbiochem (EMD Biosciences, La Jolla, CA USA). Rabbit anti-α-actin antibody was obtained from Abcam Inc. (Cambridge, MA, USA). Rat anti-mouse SSAO antibody was customized by Biotie Therapies (Turku, Finland). Goat anti-human α2M antibody was obtained from GeneTex Inc. (Irvine, CA, USA). Mouse anti-human Aβ antibody was purchased from Santa Cruz Biotechnology (Santa Cruz, CA, USA). Acrylamide (30%), nitrocellulose membrane, TEMED, Western blot set were purchased from Bio-Rad Laboratories (Hercules, CA, USA). SeeBlue Plus2 prestained standard for Western blot was purchased from Invitrogen Inc. (Carlsbad, CA, USA). Amersham ECL Western blot blotting detection reagents were purchased from GE Healthcare (Buckinghamshire, UK). MDL-72974A ((E)-2-(4-fluorophenethyl)-3-fluoroallylamine) was provided by Marion-Merrell-Dow Inc. (Cincinnati, OH, USA).

4.3.2 Immunohistochemistry of LRP-1 and SSAO on Blood Vessels and VSMC Primary Culture

Fresh human umbilical cords were collected and arteries were cut into 20 μm thick frozen sections at -27º C using a Shandon cryostat from Fisher Scientific (Pittsburgh, PA, USA). The sections were then fixed in acetone for 8 min. After fixation, the slices were air dried for 30 min and an ImmEdge pen (Vector Laboratories Inc., Burlingame, CA, USA) was used to define the edge of slices. The slices were rinsed in PBS for 5 min, then incubated in 0.3% H_2O_2 for 20 to 30 min and PBS again for 5 min repeated for 3 times. The slices were then incubated in 2.5% (v/v) goat serum (Vector Laboratories Inc.) for 1 h. Anti-LRP-1 or anti-SSAO antibody (dilution factor: 1:500 in PBS) was added and incubated at 4º C overnight. After incubation, the slices

were warmed up to room temperature for 30 min and rinsed in PBS for 5 min for 3 times. Secondary antibody (anti-mouse 2nd antibody for LRP-1 staining; anti-rat 2nd antibody for SSAO staining; dilution factor: 1:200 in PBS) was added and incubated for 1 h and rinsed as previously described. Finally, streptavidin-horseradish peroxidase (1:200) was added to sample slides and incubated for 1 h. Slides were rinsed in PBS as above.

The sections were then incubated with peroxidase substrate, namely, DAB Kit (Vector Laboratories Inc., Burlingame, CA, USA). The development of color was monitored under a microscope. These sections were then dehydrated by rinsing in a gradient concentration of ethanol: 70% for 30 s, 90% for 1 min, 95% for 1 min, 100% for 1 min and 100% for 2 min, and immersed in xyline for 3 times by 1 min, 2 min and 2 to 3 min. 2 to 3 drops of resin were dropped on the sections. Sections were covered tightly by glass coverslips (VWR, West Chester, PA, USA) with air bubbles removed, dried overnight and stored at room temperature.

The immunohistochemical images were examined under an Olympus microscope and photographed using a SpotRT Slider CCD camera (Diagnostic Instruments Inc., Sterling Heights, MI, USA) mounted on an Olympus BH2-RFCA microscope (Olympus Optical Co. Ltd, Tokyo, Japan).

4.3.3 Activation of α2M

α2M needs to be activated in order to bind to LRP-1 (Qiu et al., 1999). Its activation was carried out by incubating equal volume of α2M (4 mg/mL) and methylamine (0.4M in 0.1 M Tris-HCl, pH 8) for 2 h at room temperature. Unbound methylamine was removed by ultrafiltration-centrifugation in a 10 K NMWL Millipore centrifuge tube (Billerica, MA, USA) for 5 min with 3 repeats. The final concentration of activated α2M was determined by Bradford method.

4.3.4 Effect of Formaldehyde on Binding of Aβ with α2M or ApoE4

Aβ requires α2M or ApoE4 as a carrier in transporting *via* LRP-1. They further form large complexes. Seed-free Aβ (50 μM) was incubated with various concentrations of formaldehyde ranging from 1 μM to 1 mM in the presence or absence of activated α2M (1 mg/mL). The incubation was conducted in PBS (20 mM, pH 7.4) at 37º C for 24 h. After incubation, the

samples were mixed with equal volume of 2X electrophoresis loading buffer, denatured in boiling water bath for 5 min and subjected to Western blot analysis of Aβ-α2M complex.

To reveal the effect of formaldehyde on the interaction between Aβ and ApoE4, Aβ monomers (100 μM) and ApoE (100 μM) were incubated in the presence or absence of formaldehyde (1 mM) at 37º C for 24 h. The samples were subjected to AFM imaging as described in Part I.

4.3.5 Preparation of Primary Mouse Aortic VSMC Culture

SSAO transgenic mTIEhVAP-1 mice (about 8 weeks old) overexpressing human SSAO were euthanized and aortas were collected. According to earlier studies (Ray et al., 2001), each aorta (about 2 to 3 cm long) was perfused with 3 mL of Fungizone solution (2.4% v/v of nystatin in PBS). The aortas were then rinsed in DMEM with 1% penicillin/streptomycin and cut into fine pieces. The aorta pieces were digested by type II collagenase (1.4 mg/mL in DMEM) in a 12-well plate (Falcon, Becton Dickinson Labware, Franklin Lakes, NJ, USA). The plate was incubated at 37º C (Fisher Scientific, Pittsburgh, PA, USA) for 4 h. The progress of digestion was monitored under a microscope hourly until most tissue chunks disappeared. All the above procedures were carried out under a sterile condition in a biological cabinet.

After the digestion was completed, the smooth muscle and endothelial cells were collected by centrifugation at 500 g for 5 min. Cell pellets were resuspended in DMEM containing 10% FBS and 1% penicillin/streptomycin, and cultured in a 12-well plate at 37º C in a 5% CO_2 atmosphere. On Day 6 of culturing, cells were treated with FBS-free DMEM media for 48 h to reduce the number of endothelial cells. The purified VSMCs were subcultured into T25 flasks (Falcon, Becton Dickinson Labware, Franklin Lakes, NJ, USA).

Primary VSMCs were then cultured in DMEM containing 10% (v/v) of FBS. The cells were seeded at a density of 2 X 10^5 cells/mL and grown at 37º C in a 5% CO_2 atmosphere until confluence. The medium was changed about every 48 h and the cells were subcultured every 3 to 4 days.

4.3.6 Isolation of VSMCs from Mouse Aorta for *Ex Vivo* Studies

Freshly isolated VSMCs from transgenic mouse aorta were used for the studies of α2M uptake *via* LRP-1. mTIEhVAP-1 mice were euthanized and aortas were collected. Aortas were

cut into fine pieces in DMEM containing 10% FBS and then incubated with type II collagenase (1.4 mg/mL in DMEM). These aortas were immersed in 1 mL of collagenase solution. The digestion was conducted at 37º C in a water bath incubator (Precision Scientific) with constant slow shaking for 1 to 2 h. After most gross vessel tissue pieces had disintegrated, larger chunks of tissue were removed by mesh filtration (Tyler 100) and tissue suspension was centrifuged at 1,000 g for 5 min. The supernatant was discarded and the cell pellet was resuspended in DMEM with 10% FBS.

Cell viability was quickly determined using trypan blue staining procedure. Trypan blue solution (0.8 mM in PBS) was stored at room temperature. VSMCs were mixed 1:1 with trypan blue solution and observed under an Olympus microscope. Dead cells stain blue, whereas live cells exclude trypan blue and appear as bright dots under a microscope. Viable cells were counted on a hemocytometer within 30 min.

4.3.7 Isolation of Microvessels from Rat Brains

Rats were euthanized with CO_2. Meninges were carefully separated from freshly dissected brains. The brain tissues were then homogenized in 10 volumes of chilled HBSS containing 1% BSA and 10 mM HEPES at pH 7.4 using a glass homogenizer. Ten upward and downward strokes were applied during the homogenization. The homogenates were centrifuged at 1,500 g for 15 min. The supernatant was discarded and the pellet was resuspended in HBSS and centrifuged at 1,000 g for 10 min. The pellet was resuspended again in 10 mL of cold sucrose (0.25 M, pH 7.0) and layered over 1.0 to 1.5 M sucrose gradient and centrifuged at 58,000 g for 30 min. The pellet containing microvessels was checked under a microscope.

For measurement of SSAO activity, both meninges and microvessel preparations were homogenized by a polytron in 0.05 M phosphate butter. For isolation of VSMCs, the meninges and microvessels were digested in type II collagenase as in isolation of aortic VSMCs procedures described previously.

4.3.8 Uptake of α2M by VSMCs *via* LRP-1

4.3.8.1 Determination of Incubation Conditions

VSMCs (200 μL each in Eppendorf tubes) were incubated with various concentrations of activated α2M ranging from 0.1 to 100 nM at 37º C for 2 h. After the incubation, VSMCs were

collected by centrifugation at 1,000 g for 5 min and resuspended in 200 μL of DMEM with 10% FBS. The centrifugation and resuspending steps were repeated twice to remove the unbound and loosely membrane-bound α2M. After three washes, the cell pellets were incubated in lysis buffer (25 mM Tris, 1 mM EDTA, 1% Triton X-100, 10% glycerol, pH 7.5 with protease inhibitor cocktail) for 1 h on ice with occasional vortexing. The lysates were centrifuged at 10,000 g for 3 min and the supernatant was collected. Protein concentrations of the supernatant were determined by Bradford assay. Aliquots of each sample were mixed with 2X loading buffer and denatured in boiling water bath for 5 min. The samples were subjected to Western blot analysis of α2M.

10 nM of α2M was used for time course study (uptake time from 30 min to 4 h). Lactoferrin, a competitive LRP-1 substrate, was included to substantiate that α2M uptake by isolated VSMCs was *via* LRP-1 transporter.

4.3.8.2 Effect of Formaldehyde on α2M Uptake

Aortic VSMCs (200 μL each in DMEM with 10% FBS) were incubated with formaldehyde (concentration from 1 μM to 1 mM) for 1 h. Excess formaldehyde was removed by centrifugation at 1,000g for 5 min. The supernatant was discarded and cell pellets were resuspended in 200 μL of DMEM containing 10% FBS. Activated α2M was then added to make a final concentration of 10 nM and the samples were incubated at 37º C in a water bath for 2 h. After the incubation, the samples were washed three times, lysed and subjected to Western blot analysis of α2M. In the subsequent time-course experiment, 10 μM of formaldehyde was used for treatment of VSMCs and incubated for 10 to 90 min. Formaldehyde was removed by centrifugation at each designated time period. These treated cells were used for determination of α2M (10 nM) uptake assessed by Western blot method as described above.

4.3.8.3 Effect of SSAO-mediated Deamination of Methylamine on α2M Uptake

Both control and SSAO-blocked (pre-incubation with SSAO inhibitor, MDL-72974A, 1 μM for 10 min) aortic VSMCs were incubated in various concentrations of methylamine (10 μM to 1 mM) for 1 h prior to addition of the activated α2M. The assessment of α2M uptake was conducted as described above. In the subsequent time-course experiment, 0.5 mM of

methylamine was used for treatment of VSMCs and incubated for 30 min to 2 h. These treated cells were used for α2M uptake as described above. In this experiment, the concentration of α2M was increased to 20 nM. Other procedures were the same as described above.

4.3.8.4 Effect of SSAO-mediated Deamination of Methylamine on Aβ Uptake

Collagenase was used in isolation of VSMCs. In order to test whether residual collagenase can degrade Aβ, Aβ (200 μM) was incubated with various concentrations of type II collagenase from 0.01 to 1 mg/mL in PBS (20 mM, pH 7.4) at 37º C for 2 h. After incubation, samples were subjected to Western blot for Aβ analysis. Consequently, Aβ (100 μM) was incubated with type II collagenase (0.01 mg/mL) in the presence of various concentrations of collagenase inhibitor I (Z-PDLDA-NHOH, 0.1 to 1 mg/mL) at 37º C for 2 h and then subjected to Western blot.

This study included 2 experiments: (1) Aβ (10 μM) uptake with activated α2M (20 nM) as a carrier and (2) Aβ (10 μM) alone. Collagenase inhibitor I (25 mg/mL in 100% ethanol) was added to VSMCs to make a final concentration of 1 mg/mL. Similarly, MDL-72974A (1 μM) was used to block SSAO-mediated deamination by 10 min pretreatment. Various concentrations of methylamine (from 10 μM to 1 mM) were then added to each sample and incubated for 1 h. Activated α2M and Aβ monomers were added to VSMCs and incubated for another 2 h. After washing and lysis, the samples were subjected to Western blot for Aβ and α2M measurements as previously described.

4.3.8.5 Comparison of Native and Formaldehyde-modified α2M: Uptake by VSMCs

Finally, the direct effect of formaldehyde on α2M function was assessed. Prior to incubation with VSMC suspension, the activated α2M was treated with various concentrations of formaldehyde for 2 h. Excess formaldehyde was removed by Millipore centrifugal tube (Billerica, MA, USA). Formaldehyde-treated α2M was then added to VSMCs and incubated for 2 h, followed by washing and lysis for Western blot.

4.3.9 Western Blot

Mini-PROTEAN Tetra electrophoresis system and Mini Trans-Blot Cell from Bio-Rad Laboratories (Hercules, CA, USA) were used for electrophoresis and blotting in Western blot. A

7.5 X 10 cm, 0.75 mm-thick and 15-well gel of 10% acrylamide was used to identify α2M and Aβ. Resolving gel was prepared by mixing 5 mL 30% acrylamide, 3.75 mL 4X Tris-HCl/SDS (pH 8.8), 6.25 mL DD H_2O, 75 μL 10% (w/v) ammonium persulfate and 25 μL TEMED. 4X Tris-HCl/SDS was prepared by dissolving 18.45 g of Tris-HCl, 77 g of Tris base and 2 g of SDS in 500 mL of DD water with pH adjusted to 8.8. Stacking gel was prepared by mixing 0.65 mL 30% acrylamide, 1.25 mL 4X Tris base/SDS (pH 6.8), 3.05 mL DD H_2O, 25 μL 10% ammonium persulfate and 10 μL TEMED. 4X Tris base/SDS was prepared by dissolving 30 g of Tris base and 2 g of SDS in 500 mL of DD water with pH adjusted to 6.8. Running buffer contained 25 mM Tris base, 0.2 M glycine and 0.1% SDS. Transfer buffer contained 25 mM Tris base, 0.2 M glycine and 15% (v/v) methanol. Electrophoresis was conducted at constant voltage of 120 v for 1 to 1.5 h. After the separation, the gel was immersed in transfer buffer at 4º C for 30 min. The bands were then transferred to a nitrocellulose membrane. The transfer was set at constant current of 230 mA for 1.5 to 2 h on ice with stirring.

The transferred membrane was blocked using 5% (w/v) skimmed milk in TBS buffer for 1 h and incubated with first antibody (dilution factor for anti-α2M: 1:2,000; for anti-Aβ: 1:500; for actin: 1:5,000) in 5% milk TBS for 1 h at room temperature (or overnight at 4º C). After the first antibody incubation, the membrane was washed for 10 min by TBST (0.5% Tween-20) for 3 times. The secondary antibody (dilution factors: anti-goat for α2M: 1:8,000; anti-mouse for Aβ and actin: 1:8,000) in 5% milk TBS was added and incubated for another hour at room temperature. The membrane was washed for 10 min in TBST for 3 times. All the incubation and washing steps were carried out on a VWR micro plate shaker (West Chester, PA, USA). The membrane was then immediately exposed in Amersham ECL solution from GE Healthcare (Buckinghamshire, UK) by a developing machine.

4.3.10 Western Blot Data Analysis

The exposed films of Western blot were scanned by a UMAX scanner. The image software, Umax VistaScan, was set in transmissive mode. Scanned images were analyzed by ImageJ from the National Institutes of Health. The total amount of signal of a band was calculated by band area divided by its average grey scale. Actin was used as a housekeeping reference protein. The ratio of α2M: actin or Aβ: actin from control was set to 100% and experimental groups were normalized accordingly in each experiment.

4.4 Statistics

The results were assessed using one-way analysis of variance followed by multiple comparisons (Newman-Keuls). The null hypothesis used for all analyses was that the factor has no influence on the measured variable and significance was accepted at > 95% confidence level.

5. RESULTS

5.1 Part I: Aldehydes Enhance Aβ Aggregation

5.1.1 Effect of Aldehydes on Aβ β-sheet Formation Assessed by Thioflavin T Fluorometry

ThT does not exhibit fluorescence on its own. It reacts with β-sheet structure of proteins and produce fluorescence. The intensity of fluorescence represents the amount of β-sheet content (Naiki et al., 1989; Naiki and Nakakuki, 1996). As can be seen in Figure 14a, b and c, ThT fluorometry revealed that formaldehyde, methylglyoxal and malondialdehyde significantly enhance β-sheet formation. HNE (Figure 14d) exhibits relatively small but also significant increase under the same experimental conditions. The increase was in a time- and concentration-dependent manner. The most prominent effect of these aldehydes was detected at 48 h of incubation except for HNE. After prolonged incubation, namely, around Day 5, the fluorescence intensity reached a plateau and began to decline slightly thereafter. This phenomenon is consistent with results from other laboratories. β-sheet formation takes place predominantly in the early phase of Aβ aggregation. In the more advanced stages, β-sheets are no longer detectable with ThT (Liu et al., 2004; Stanyer et al., 2004a).

Subsequent experiments demonstrated the effect of formaldehyde produced *via* methylamine deamination catalyzed by SSAO. As shown in Figure 15, methylamine, in the presence of SSAO, enhances β-sheet formation of $A\beta_{1\text{-}40}$, even though the enzyme preparation quenched the fluorescence. Methylamine alone was insufficient to affect the β-sheet formation of $A\beta_{1\text{-}40}$. Separate experiments showed that hydrogen peroxide and ammonia, which are produced from SSAO-catalyzed reactions, do not have significant effects on Aβ1-40 β-sheet formation (data not shown). SSAO inhibitor, MDL-72974A, significantly blocked the effect of methylamine, suggesting that the deaminated product, formaldehyde is responsible for enhancing $A\beta_{1\text{-}40}$ β-sheet formation.

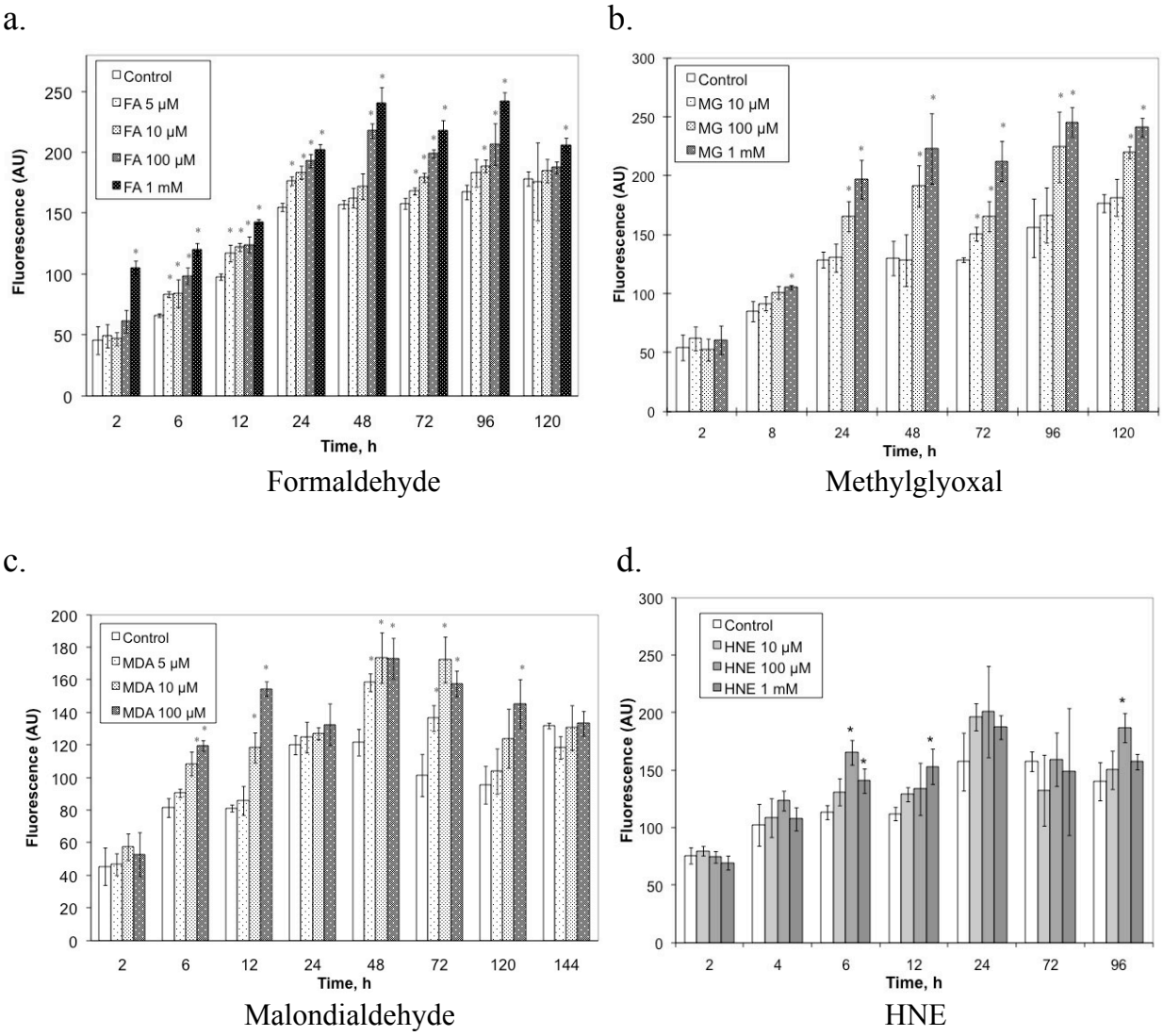

Figure 14. Effect of formaldehyde (FA), methylglyoxal (MG), malondialdehyde (MDA) and HNE on the kinetics of $A\beta_{1-40}$ β-sheet formation assessed by ThT fluorometry. $A\beta_{1-40}$ (200 µM) was incubated in the presence or absence of various concentrations of formaldehyde (a), methylglyoxal (b), malondialdehyde (c) and HNE (d) for a period of up to 6 days in a sterile environment. The fluorescence was measured at various time points. The measurements were carried out in 200 µL reaction solution (2 mM ThT in 50 mM glycine-NaOH buffer, pH 9.0) containing Aβ (2 µM). λex = 450 nm, λem = 482 nm. The background fluorescence was subtracted. Data represent means ± SD (n=3) of a representative experiment out of three. *$p < 0.05$, compared to corresponding control values.

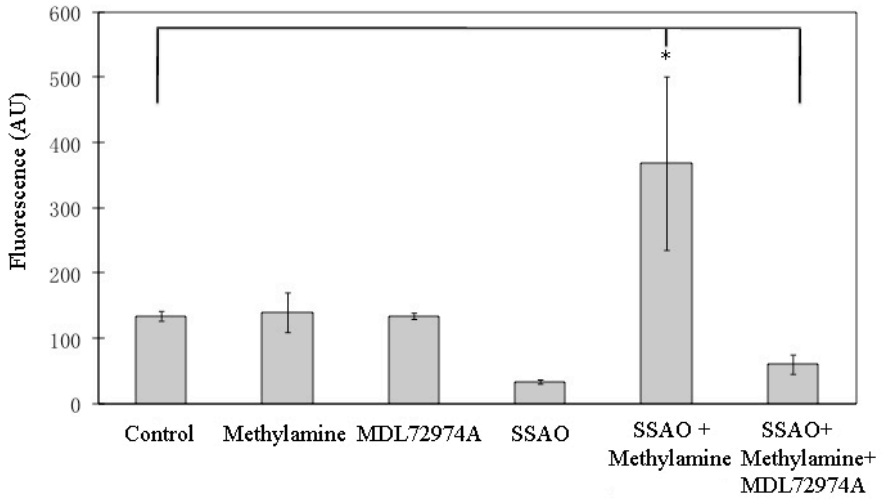

Figure 15. Effect of formaldehyde, derived from SSAO-catalyzed deamination of methylamine, on Aβ β-sheet formation assessed by ThT fluorometry. $A\beta_{1-40}$ (200 μM) was incubated with methylamine (1 mM), SSAO (specific activity: 1.3 nmol/min/mg protein), in the presence or absence of MDL-72974A (10 μM) for 48 h. Data represent mean (n=3) ± SD of a representative experiment out of three. *$p<0.05$, compared to corresponding control values.

5.1.2 Analysis of Aβ Secondary Structures by CD Spectroscopy

CD spectra provide information not only on β-sheets but also on α-helix and random coils in a protein solution. There are several advantages of this technique. First, it can monitor the kinetic process of Aβ aggregation over time. Secondly, the samples can be repeatedly measured at various time points, thereby reducing inaccuracy caused by changing samples. Also, the percentages of various secondary structures in a protein solution can be calculated from CD spectrum, providing more information on the dynamics of Aβ aggregation.

As can be seen in Figure 16, formaldehyde affected the CD spectra of Aβ in a concentration- and time-dependent manner. In Figure 16b, the negative peak at 200 nm of the control group (representing a mixture of α-helices and random coils) was gradually shifted to around 218 nm (the characteristic peak of β-sheet structure) in response to increasing formaldehyde concentration after 12 h. Figure 16c and d demonstrated that formaldehyde reduced the amplitude of the negative peak, suggesting increased β-sheet content. As seen in Figure 16d, methylglyoxal, malondialdehyde and formaldehyde (10 μM each) enhanced Aβ β-sheet formation after 24 h of incubation, whereas HNE had no significant effect on Aβ CD spectra. Aldehydes themselves exhibited no effect on spectrum background. CDNN software (CD Spectra Deconvolution v 2.1, Martin-Luther University Halle-Wittenberg) was used to calculate the percentage of each secondary structure in each sample.

CD spectroscopy results are consistent with the observations from ThT fluorometry. Formaldehyde, methylglyoxal and malondialdehyde are capable of facilitating the transition of α-helices and random coils in Aβ monomers into β-sheet structure in a concentration- and time-dependent manner. HNE in comparison with other aldehydes exerts limited but still significant effect on Aβ β-sheet formation.

5.1.3 Molecular Assembly of Aβ Assessed by DLS

ThT fluorometry and CD spectroscopy reveal the secondary structures of Aβ. These methods do not directly examine the molecular sizes of Aβ polymers. Followed DLS data can provide useful information regarding the distribution of molecular sizes of polymerized $A\beta_{1\text{-}40}$ in solution. As can be seen in Figure 17, aldehydes clearly induced shifts of the molecular sizes to the larger side, particularly in the early phases of polymerization. After incubation for 24 h,

a. 2 h of incubation

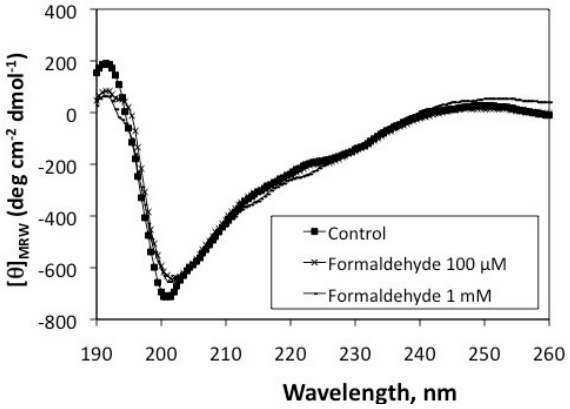

	random coil	α-helix	β-sheet
Control	55%	42%	3%
FA 100 µM	53%	46%	1%
FA 1 mM	51%	48%	1%

b. 12 h of incubation

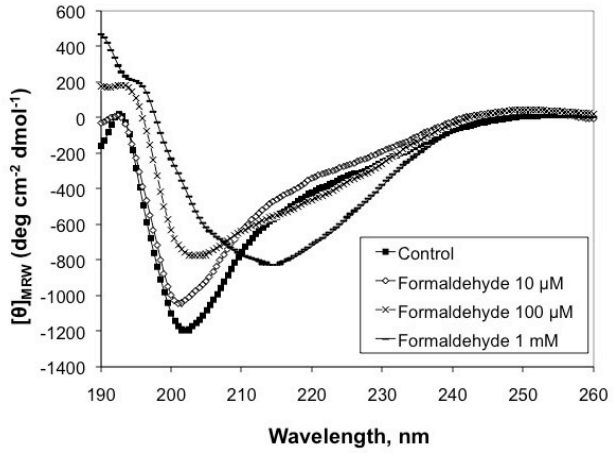

	random coil	α-helix	β-sheet
Control	28%	60%	12%
FA 10 µM	25%	60%	15%
FA 100 µM	25%	50%	25%
FA 1 mM	25%	40%	35%

c. 48 h of incubation

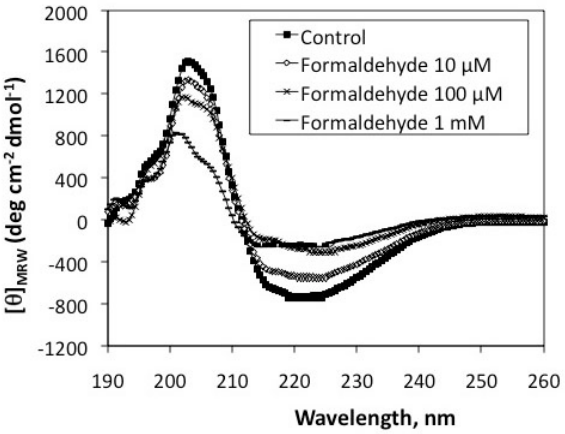

	random coil	α-helix	β-sheet
Control	30%	27%	43%
FA 10 µM	33%	25%	42%
FA 100 µM	20%	20%	60%
FA 1 mM	20%	20%	60%

d. 24 h of incubation

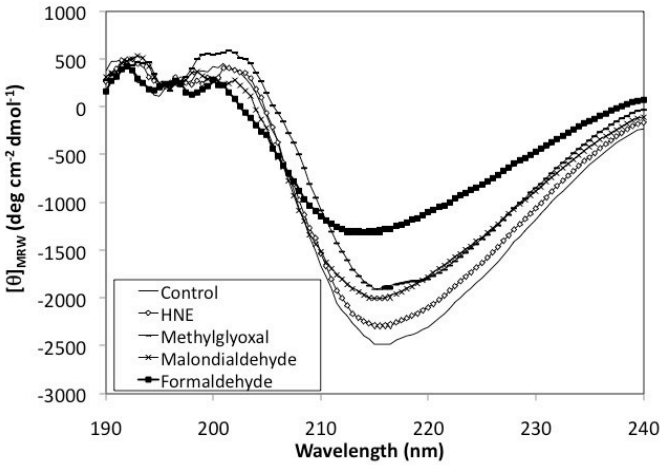

	random coil	α-helix	β-sheet
Control	30%	43%	27%
HNE	33%	40%	27%
MDA	33%	36%	31%
MG	30%	36%	34%
FA	30%	30%	40%

Figure 16. Effect of aldehydes on Aβ CD spectrum. Aβ (200 μM) was incubated with various concentrations of formaldehyde for 2 h (a), 12 h (b), and 48 h (c), or with formaldehyde, methylglyoxal, malondialdehyde and HNE (10 μM each) for 24 h (d) in microcentrifuge tubes at room temperature (20º C) without stirring. Samples were degassed before measurement. Each sample was measured five times and an average was obtained. Corresponding backgrounds with respect to each aldehyde in PBS were subtracted for final plotting and comparison. $\theta_{[MRW]}$ = mean residue weight ellipticity. The percentages of each secondary structure were calculated by CDNN software (CD Spectra Deconvolution v 2.1).

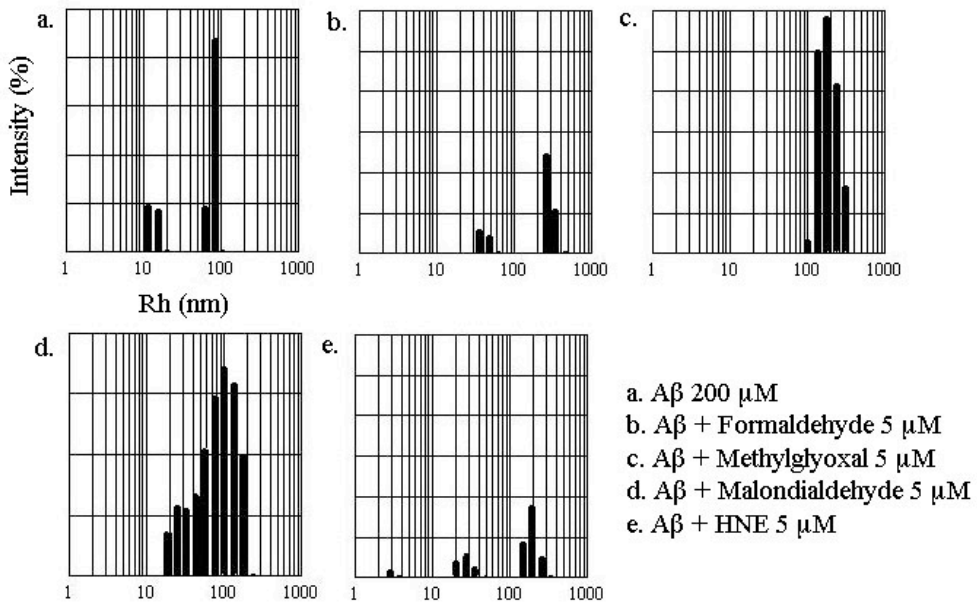

Figure 17. Effect of aldehydes on the size distribution of $A\beta_{1-40}$ assessed by DLS. Aβ (200 μM) was incubated alone (a) or with 5 μM of formaldehyde (b), methylglyoxal (c), malondialdehyde (d) and HNE (e). The incubation was carried out at 37º C in 20 mM PBS (pH 7.4) for 24 h without stirring. The total number of deflected photons by each sample was normalized as 100% intensity. Aggregated Aβ accounts for the majority of the scattering intensities. Rh distribution in each sample was calculated individually. The magnitudes of intensity among different samples were therefore not comparable. The scattering intensity from the buffer (Rh < 0.2 nm) is not shown.

native Aβ formed mainly two populations, namely, oligomers with hydrodynamic radius (Rh) around 10 nm and protofibrils about 100 nm in length. In the presence of formaldehyde, the Rh increased to around 50 nm and 200 nm. Methylglyoxal treated Aβ was composed of a mixed population with Rh from 150 to 500 nm. Similarly, malondialdehyde and HNE were also capable of increasing molecular sizes of Aβ aggregates. It is important to note that the Rh calculated in DLS measurements is not the actual diameter or length of Aβ species. The volume of H_2O molecules surrounding Aβ aggregates also contributes to the Rh values Therefore, Rh is a reflective indicator of the real molecular size.

In DLS, the numbers of photons deflected per second by particles in solution are converted into electrical signals for detection, which is known as count rate. During a measurement, the average count rate reflects the general molecular size of particles in the solution. The higher the count rate, the larger the particles present in the solution (Chayen et al., 2004). As shown in Figure 18, all aldehydes significantly increased the count rate of Aβ in comparison with the native Aβ, suggesting that aldehydes increased the average size of Aβ aggregates. Among the aldehydes, malondialdehyde was most potent in increasing Aβ sizes.

For DLS analysis, significantly lower concentrations of aldehydes were applied. The DLS results are consistent with earlier observations from ThT fluorometry and CD spectroscopy, namely, that Aβ formed significantly more and larger aggregates in the presence of endogenous aldehydes.

The above results have demonstrated that aldehydes are capable of inducing and accelerating Aβ aggregation at the initial phase. Whether aldehydes can affect Aβ aggregation in the more advanced stages is unclear. To study this, auto-assembly of Aβ for 48 h to form protofibrils were used before treatment. Aldehydes were then added to these 2-day aged Aβ solutions and further incubated for additional time periods. As can be seen in Figure 19, although the count rate of Aβ had reached a plateau after 48-h preincubation, formaldehyde further increased the count rate in a concentration-dependent manner, and remained throughout the prolonged incubation. This suggests that formaldehyde, and probably other aldehydes, are able to enhance Aβ aggregation from the initial stage of β-sheet formation to the advanced stage of fibrillogenesis. It is important to note that there is a limitation to the DLS assay, namely, that particles of 1 micron or larger are no longer suitable for the DLS analysis. Therefore, the effect of aldehydes on further aggregation

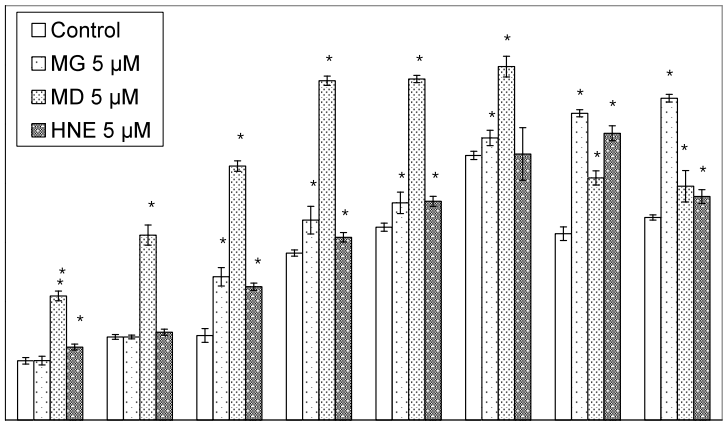

Figure 18. Effect of aldehydes on DLS count rate of Aβ polymerization. $A\beta_{1\text{-}40}$ (200 μM) was incubated in the presence or absence of various aldehydes (5 μM) for desired time periods at 37º C in PBS buffer (20 mM, pH 7.4) without stirring. Count rates of PBS and aldehydes were subtracted from corresponding Aβ count rate for comparison. Data represent means ± SD (n=3) of a representative experiment out of three. *$p < 0.05$, compared to corresponding control values.

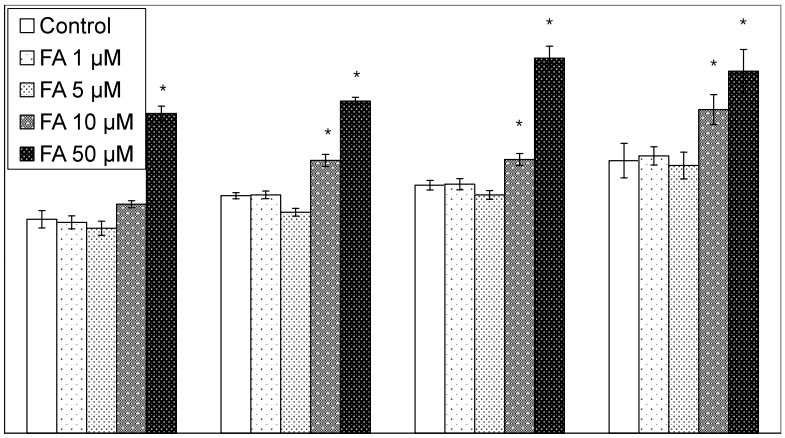

Figure 19. Effect of formaldehyde on aggregation of aged-Aβ assessed by DLS count rate. Aβ were preaggregated alone for 48 h at 37º C in PBS (20 mM, pH 7.4). Formaldehyde was added at a final concentration of 1, 5, 10 and 50 μM, and further incubated for up to 48 h. Data represent the means ± SD (n=3) of a representative experiment out of three. *$p < 0.05$, compared to corresponding control values.

of Aβ are not applicable using DLS.

5.1.4 AFM Imaging of Aβ Aggregation

The above spectrophotometric techniques revealed the effects of aldehydes on the conformation and molecular sizes of $A\beta_{1-40}$ aggregates. AFM was employed to examine the morphological appearance of the $A\beta_{1-40}$ oligomers, protofibrils and fibrils following incubation with aldehydes. At zero time, freshly prepared Aβ monomers did not form any detectable images (data not shown). As revealed by AFM "dry" method in Figure 20, during 7-day incubation, both native and formaldehyde-treated Aβ formed polymer species including oligomers (started to form in approximately 6 h), protofibrils (between 24 to 48 h) and fibrils (after 7 d). Formaldehyde significantly increased the production of oligomers and protofibrils. It also increased the sizes of $A\beta_{1-40}$ oligomers. The average diameter of native $A\beta_{1-40}$ oligomers, based on the heights of the oligomers following AFM scans, was about 4 to 5 nm. The sizes were increased to 6–7 nm in the presence of formaldehyde after 6-h incubation. The number of protofibrils was also significantly increased by formaldehyde. Formaldehyde did not affect the average height (about 4 nm) or length (about 50 nm) of protofibrils.

Similarly, methylglyoxal was capable of accelerating the rate of Aβ aggregation and increasing the sizes of $A\beta_{1-40}$ oligomers and protofibrils. Figure 21a shows the effect of methylglyoxal on $A\beta_{1-40}$ oligomerization in a three-dimensional presentation. After 6 h incubation (Figure 21b), the average diameters of $A\beta_{1-40}$ oligomers, based on the heights, were about 5 nm for the native and 7–8 nm for the methylglyoxal-treated $A\beta_{1-40}$. After prolonged incubation (48 h), the average sizes increased to 10 nm and 20 nm for native and the methylglyoxal-treated $A\beta_{1-40}$, respectively (Figure 21d).

HNE and malondialdehyde by themselves would crystallize at dryness and therefore the "dry" AFM scan is not suitable. A wet AFM method was adopted in which Aβ aggregates were imaged in PBS solution. The appearances of Aβ aggregates between the dry and wet methods were different. The sharpness of the images was decreased in wet method, resulted from the interface between Aβ and water molecules. After 12-h aggregation, both native and HNE/malondialdehyde-treated Aβ formed a mixture of oligomers and protofibrils. It is evident that at this time point, oligomers started to assemble into protofibrils with beaded structures.

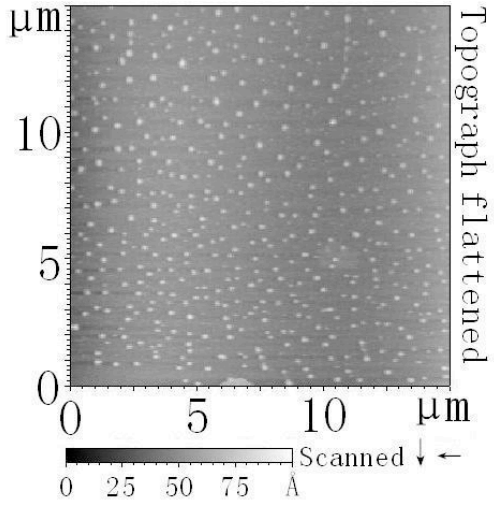

Control (6 h)

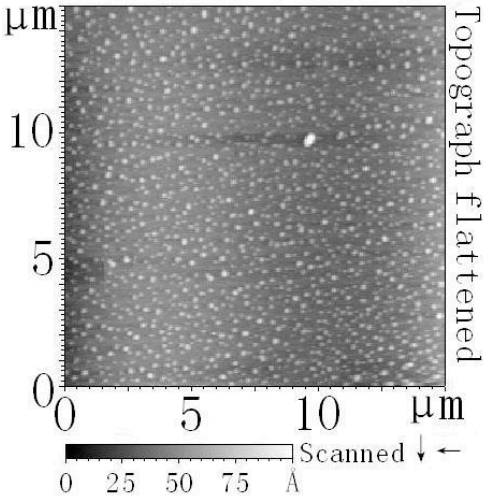

Formaldehyde (6 h)

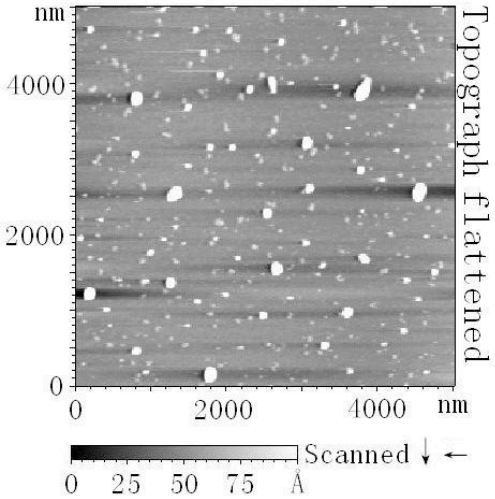

Control (12 h)

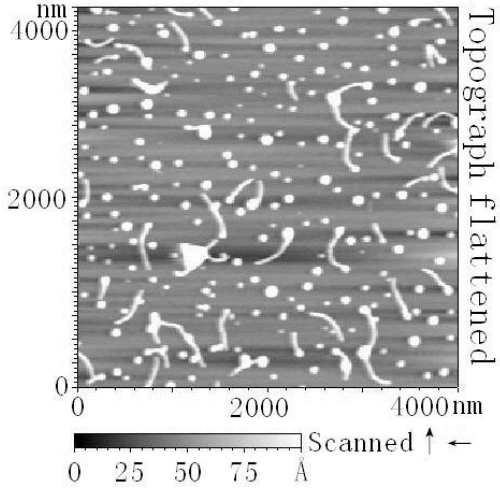

Formaldehyde (12 h)

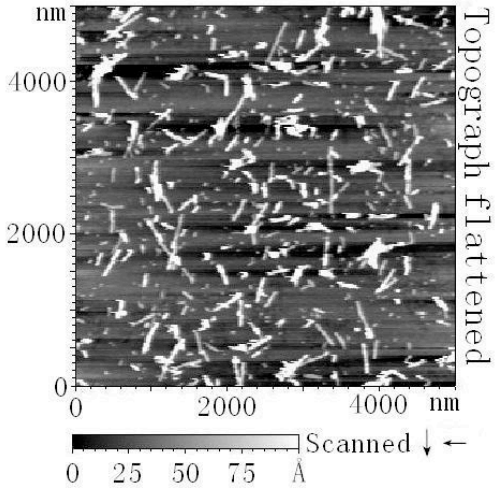

Control (24 h)

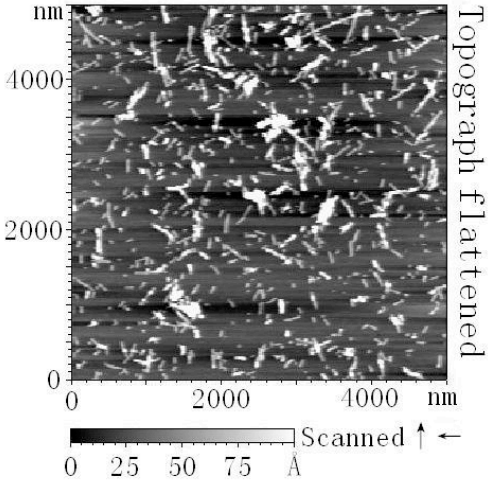

Formaldehyde (24 h)

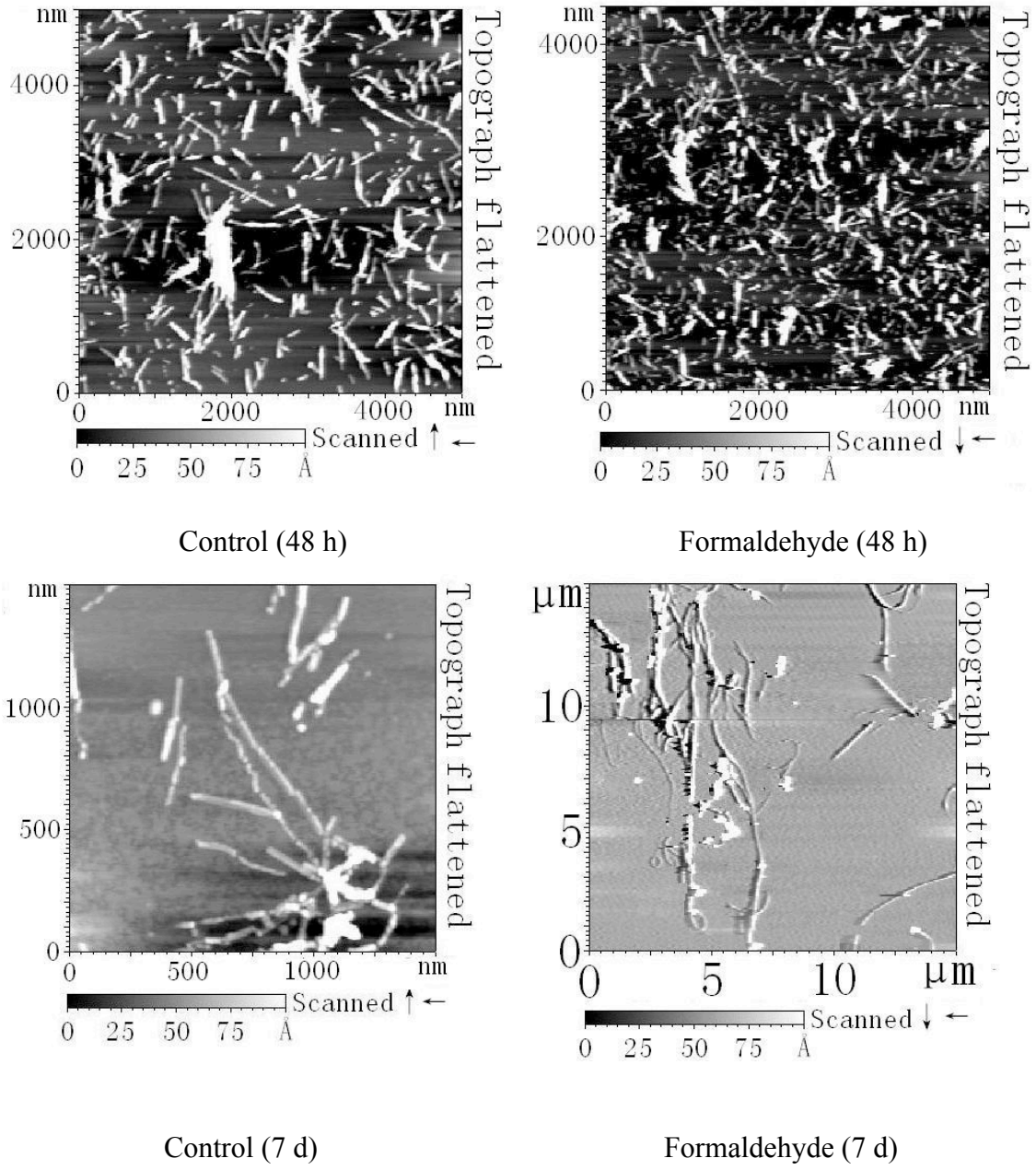

Figure 20. The effect of formaldehyde on $A\beta_{1-40}$ aggregation using AFM imaging. Aβ (200 μM) was incubated in the absence or presence of formaldehyde (10 mM) for up to 7 days. At each time point during incubation, aliquots of samples were diluted 100 times before imaging. One μL of diluted sample was dropped, dried and imaged on freshly cleaved mica sheet. Five positions on the sample area were randomly picked for each sample.

a.

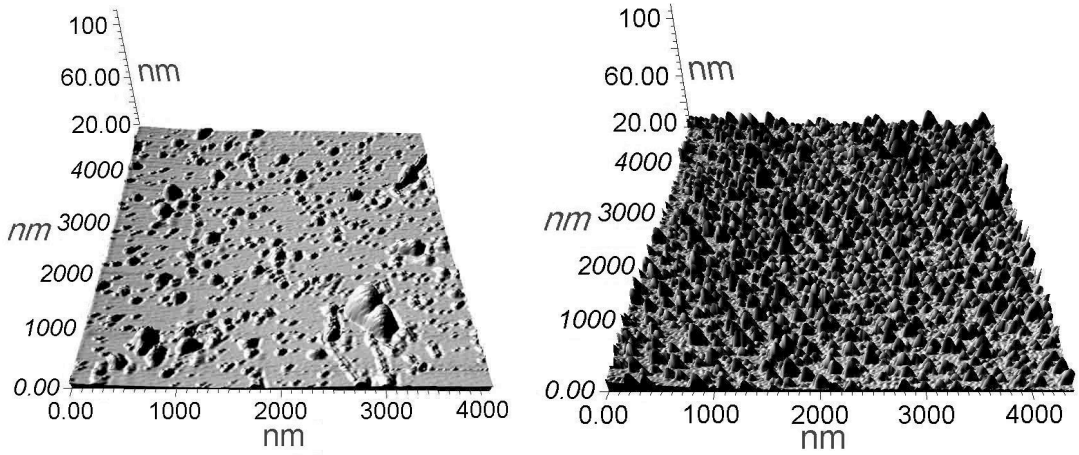

b.

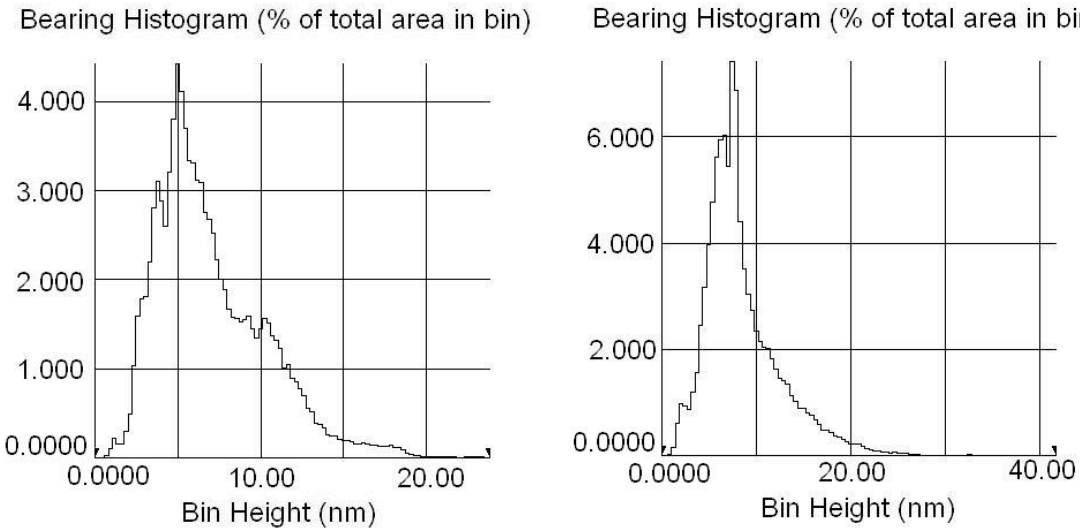

Control (6 h)

Methylglyoxal (10 μM) (6 h)

c.

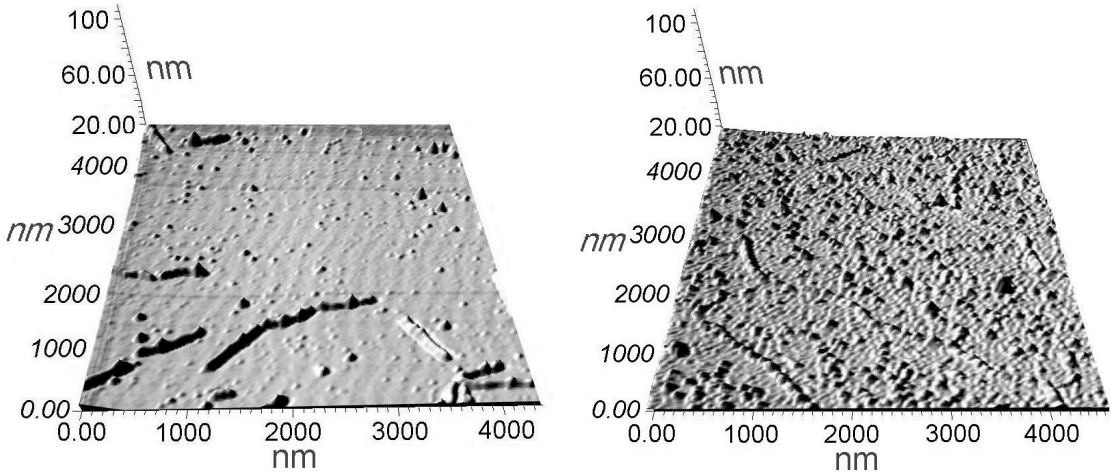

d.

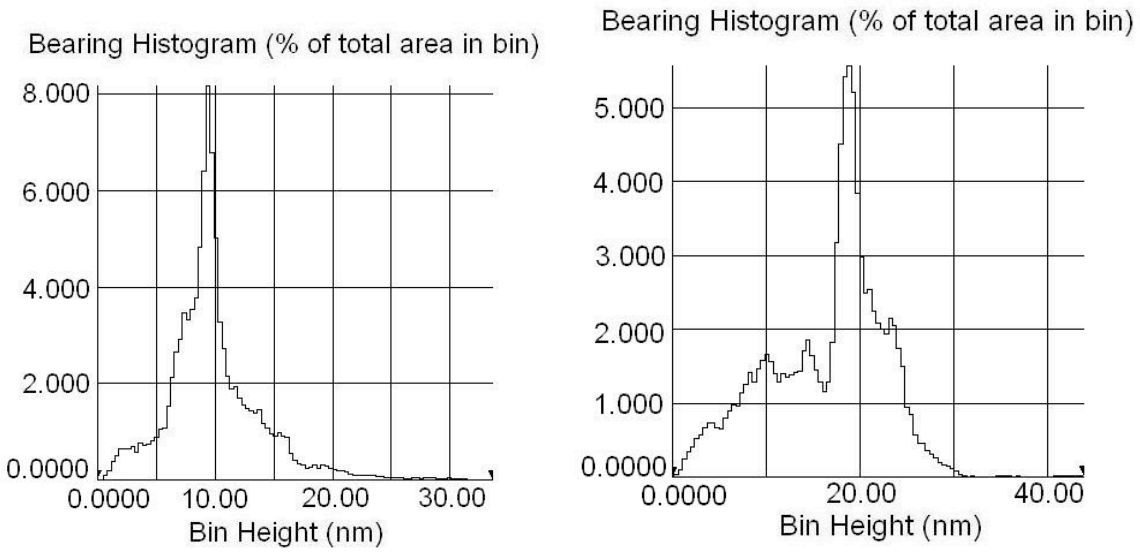

Control (48 h)

Methylglyoxal (10 μM) (48 h)

Figure 21. The effect of methylglyoxal on $A\beta_{1\text{-}40}$ aggregation demonstrated in three-demensional images and height distribution of AFM. Aβ (200 μM) was incubated in the absence or presence of methylglyoxal (10 μM). After 6-h and 48-h incubation, aliquots of samples were diluted 100 times before imaging. One μL diluted sample was imaged on freshly cleaved mica sheet. Five positions on a sample area were randomly picked for each sample. a: 6-h incubation; c: 48-h incubation. The height (diameter) distribution (b, d) was calculated by PicoSPM imaging software and shown under each morphology image.

Similarly, HNE and malondialdehyde increased the sizes of Aβ oligomers. The effect on the rate of aggregation was less pronounced in comparison with those induced by formaldehyde and methylglyoxal (Figure 22). This result is consistent with the results seen in ThT fluorometry and CD spectroscopy.

5.1.5 Detection of Aβ Oligomers by Dot-Blot Assay

An oligomer-specific antibody (A11) of Aβ has been developed for identification of neurotoxic oligomers (Kayed et al., 2003). Neither monomers nor advanced aggregates of Aβ (protofibrils and fibrils) are recognized by A11 antibody. In the present study, it was employed to ensure seed-free preparation of Aβ for all experiments and to investigate the effects of aldehydes on Aβ oligomerization. $A\beta_{1\text{-}40}$ was incubated in the presence or absence of aldehydes as described previously. Figure 23 shows that freshly prepared $A\beta_{1\text{-}40}$ by HFIP was completely not recognized by A11 antibody, suggesting a seed-free preparation. After 6 h of incubation, oligomers were formed. Formaldehyde, methylglyoxal and malondialdehyde enhanced the formation of oligomers (Figure 23). With prolonged aggregation, namely, after 24 h, the positive staining diminished, suggesting the formation of protofibrils. Malondialdehyde also increased the amount of Aβ oligomers in a concentration-dependent manner (Figure 23c). Results of dot-blot assay are also consistent with findings of previous experiments. In addition, the maximal amount of $A\beta_{1\text{-}40}$ oligomers was observed at 6-h incubation, in agreement with AFM studies.

a.

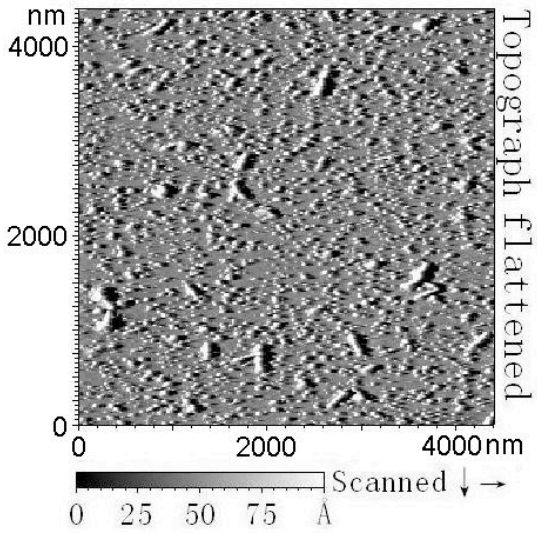

Control (12 h)

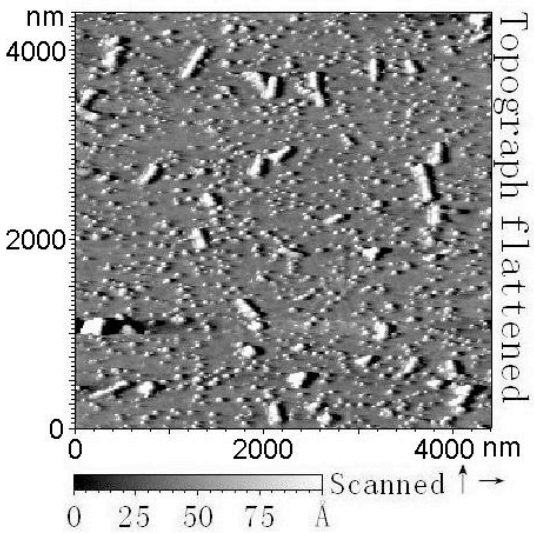

HNE (10 μM) (12 h)

b.

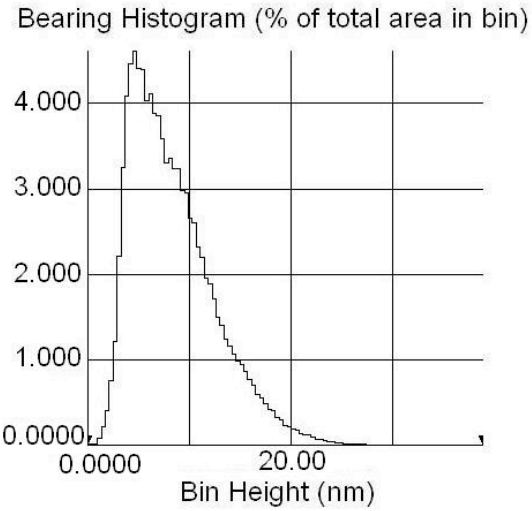

Control (12 h)

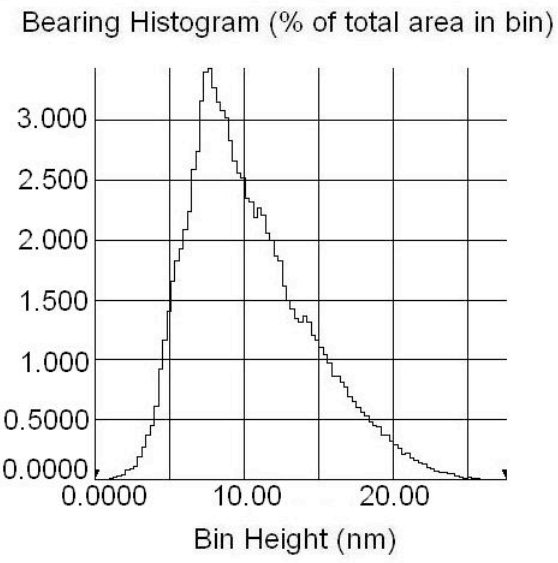

HNE (10 μM) (12 h)

c.

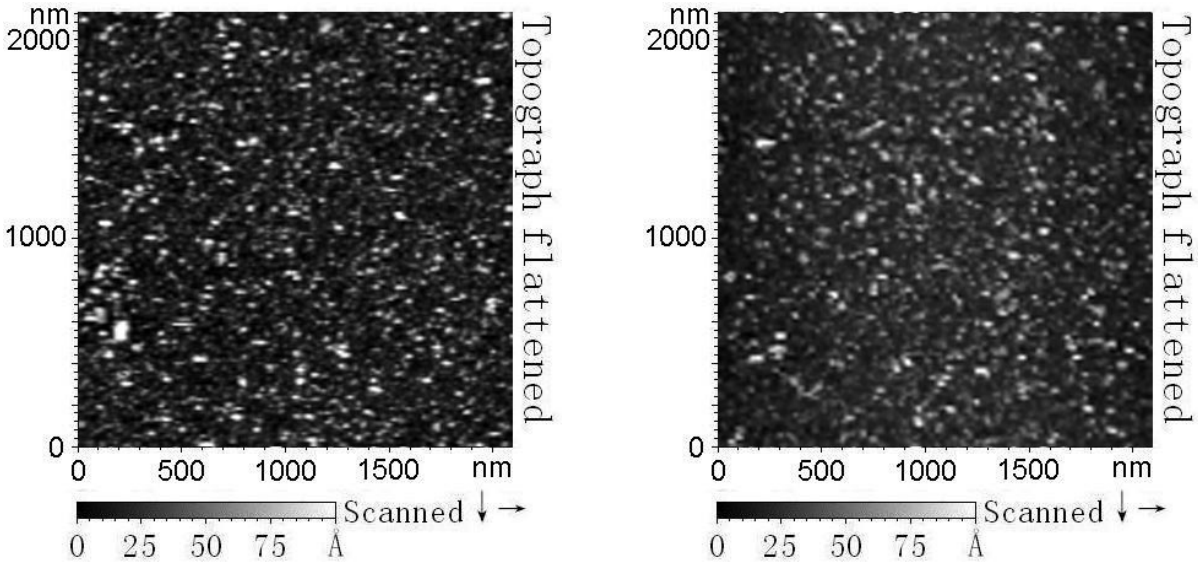

Control (12 h) Malondialdehyde (10 μM) (12 h)

d.

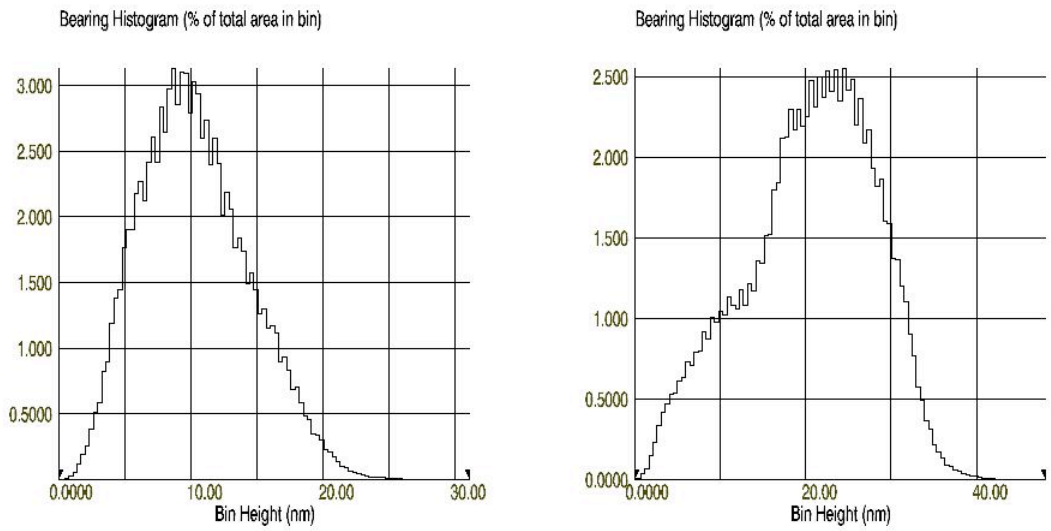

Control (12 h) Malondialdehyde (10 μM) (12 h)

Figure 22. Effect of HNE and malondialdehyde on $A\beta_{1-40}$ aggregation using the wet method of AFM imaging. $A\beta_{1-40}$ (200 μM) was incubated in the absence or presence of HNE (a) or malondialdehyde (c) (10 μM) for 12 h. Aliquots of samples were imaged in PBS buffer. Size (height) distribution (b, d) was statistically calculated by PicoSPM imaging software and shown under each morphology image.

a.

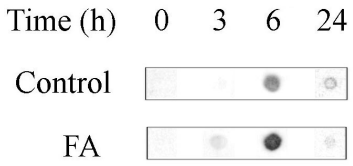

b.

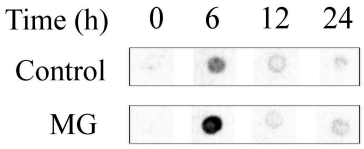

c.

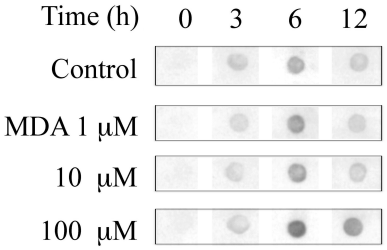

Figure 23. Effect of aldehydes on $A\beta_{1-40}$ oligomerization assessed by dot-blot assay. Seed-free $A\beta_{1-40}$ (200 μM) was incubated with formaldehyde (a) and methylglyoxal (b) (both 100 μM) for various time periods. Malondialdehyde of various concentrations (c) were incubated with $A\beta_{1-40}$ (200 μM) for up to 12 h. Aliquots were dropped on a nitrocellulose membrane after desired incubation periods and assessed immunochemically using A11 oligomer-specific antibody of Aβ.

5.2 Part II: Mechanism of Interaction between Formaldehyde and Aβ; Relevance to Aβ Cytotoxicity Study

5.2.1 Detection of N-Methyl-Lysine by FMOC-HPLC

Aldehydes preferably react with the free amino groups of lysine and arginine residues. $A\beta_{1-40}$ has 2 lysine (Lys 16 and Lys 28) residues and 1 arginine (Arg 5) residue. To confirm such an interaction, Aβ was incubated with or without formaldehyde. The aggregates were then treated with or without $NaBH_4$ to convert the non-covalent bonds into covalent. As can be seen in Figure 24, in presence of $NaBH_4$, the amount of SDS-resistant Aβ aggregates was increased in a formaldehyde-concentration dependent manner. This suggests that formaldehyde crosslinked Aβ, and that $NaBH_4$ converted the Schiff bases to covalent bonds. The $NaBH_4$-stabilized formaldehyde-Aβ adducts were hydrolyzed and the formaldehyde-modified amino acid residues were analyzed by HPLC. As shown in Figure 25, the amount of lysine residues in the hydrolysates of the formaldehyde-Aβ adducts was reduced in comparison to native Aβ. A new N-methyl-lysine peak (confirmed by N-methyl-lysine internal standard) was detected only in the hydrolysates of the formaldehyde-Aβ adducts. This is clear evidence that formaldehyde interacts with and modifies the lysine residues of Aβ. In addition to lysine, other residues on Aβ including glutamate (peak 1) and arginine (peak 2) have also been reduced by formaldehyde, indicating that formaldehyde also crosslinks Aβ by reacting with multiple residues, although the corresponding adducts were not detected in the present chromatography system.

5.2.2 Isolation of Aβ Oligomers by Size Exclusion Chromatography

Aldehydes are capable of modifying $A\beta_{1-40}$ oligomers by increasing their sizes (see Part I). However, $A\beta_{1-40}$ oligomers exert less cytotoxicity in comparison to $A\beta_{1-42}$. $A\beta_{1-42}$ oligomers are the most cytotoxic species among all aggregation intermediates and have been proposed to be responsible for neurodegeneration in AD (Klein et al., 2004; Lacor et al., 2007). Therefore, in order to investigate whether aldehydes can alter the cytotoxicity of other Aβ oligomers, $A\beta_{1-42}$ oligomers were used in addition to $A\beta_{1-40}$ oligomers.

We confirmed that formaldehyde has a similar effect on $A\beta_{1-42}$ aggregation as it does on $A\beta_{1-40}$. As can be seen in Figure 26, ThT fluorometry revealed that formaldehyde increased

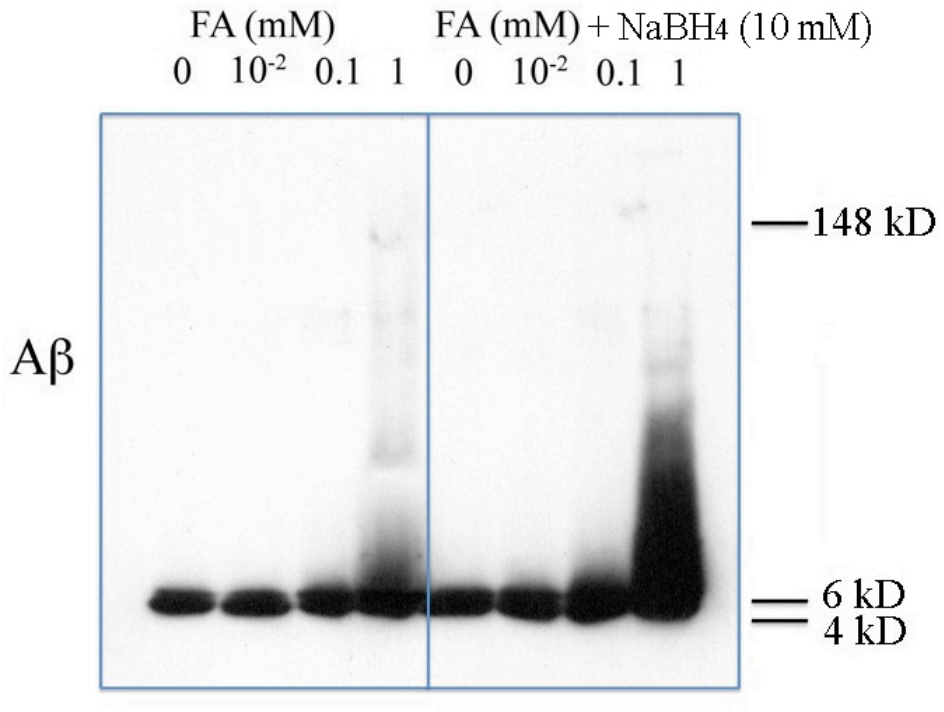

Figure 24. The effect of formaldehyde on Aβ aggregation revealed by Western blot. Aβ (100 μM) was incubated with various concentrations of formaldehyde at 37º C for 24 h. The aggregates were further incubated with or without $NaBH_4$ (10 mM) for 24 h to stabilize Schiff bases covalently. Western blot was used for analysis of Aβ aggregates. The Aβ antibodies used in these experiments recognize all forms of $A\beta_{1\text{-}40}$, but are not oligomer-specific as A11 antibody used in dot-blot.

a.

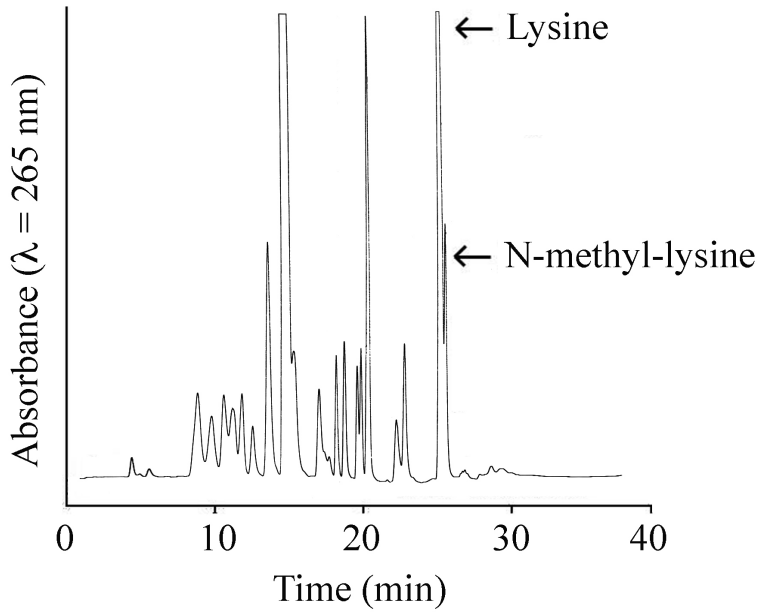

b.

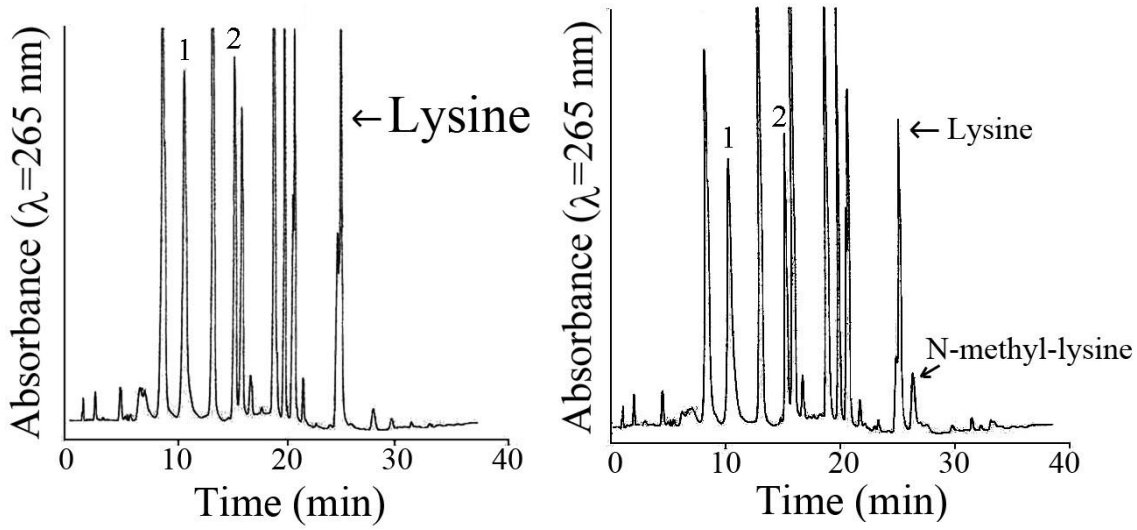

Figure 25. Detection of N-methyl-lysine in formaldehyde-induced $A\beta_{1-40}$ aggregates by FMOC-HPLC. $A\beta_{1-40}$ (200 μM) was incubated in the absence or presence of formaldehyde (10 μM) for 48 h. (a) Amino acid standards including lysine and N-methyl-lysine. (b) Left: $A\beta_{1-40}$ alone and arrow indicates the lysine peak; right: formaldehyde-induced $A\beta_{1-40}$ and arrows indicate the lysine and N-methyl-lysine peaks. Other altered peaks of residues are marked as 1 for glutamate and 2 for arginine.

a.

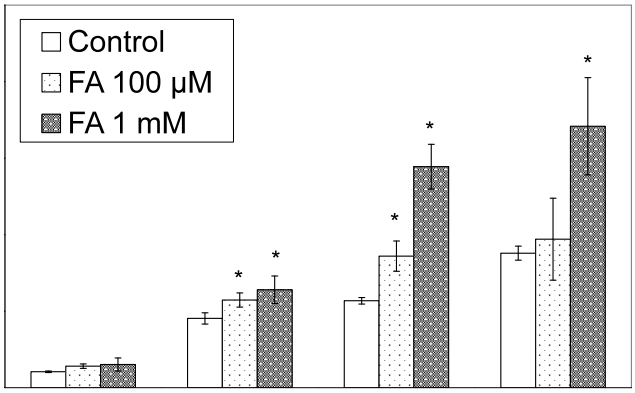

b.

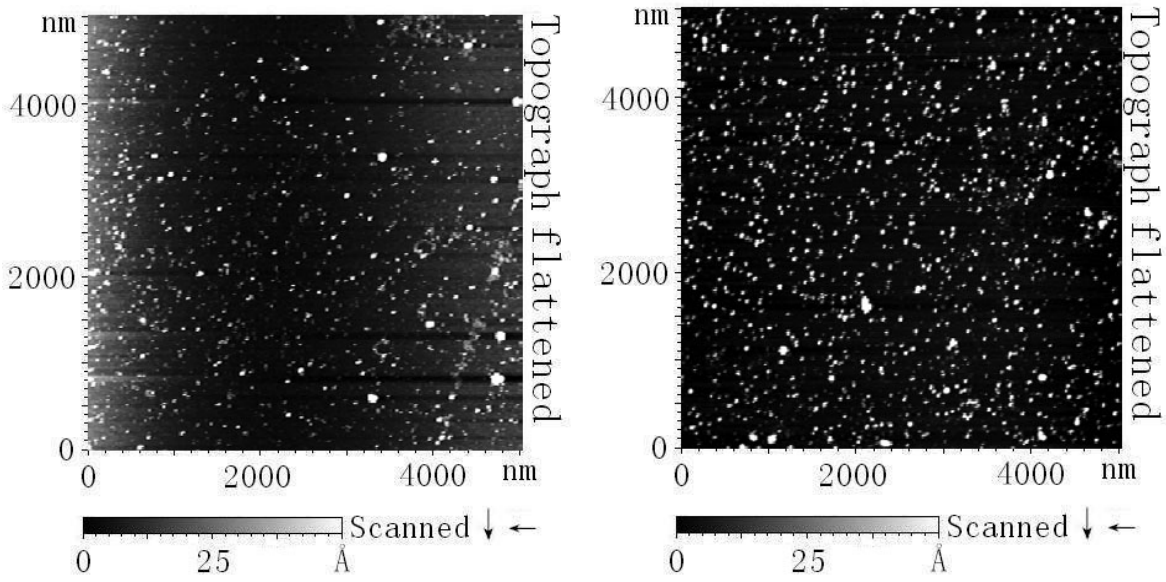

Control FA 100 μM

Figure 26. The effect of formaldehyde on $A\beta_{1-42}$ aggregation revealed by ThT fluoremetry and AFM imaging. Similar to studies on $A\beta_{1-40}$, $A\beta_{1-42}$ (1 mg/mL) was incubated with various concentrations of formaldehyde at 37º C for desired time periods. (a) ThT fluorometry was used to measure β-sheet formation. Data represent the means ± SD (n=3) of a representative experiment out of three. *$p < 0.05$, compared to corresponding control values. (b) Morphology of $A\beta_{1-42}$ oligomers was imaged by AFM at 12 h of incubation.

$A\beta_{1-42}$ β-sheet formation in a time- and concentration-dependent manner. The morphologies of $A\beta_{1-42}$ oligomers as revealed by AFM were similar to those of $A\beta_{1-40}$ with an average diameter of 4 nm, which was also increased by formaldehyde treatment. In the following cytotoxicity experiments, $A\beta_{1-42}$ was incubated with formaldehyde to produce aldehyde-modified Aβ oligomers. Based on studies in Part I, $A\beta_{1-40}$ forms most oligomeric species at 6 h of aggregation followed by protofibril formation. However, $A\beta_{1-42}$ behaved differently from $A\beta_{1-40}$ by forming most oligomers at 12 h of aggregation. Confirmed by AFM, after 12 h of aggregation under the same incubation conditions as for $A\beta_{1-40}$, $A\beta_{1-42}$ predominantly formed oligomers with negligible protofibrils.

To study whether formaldehyde can alter $A\beta_{1-42}$ cytotoxicity, the native and formaldehyde-induced Aβ oligomers were isolated using size exclusion chromatography (SEC). SEC is capable of separating molecules based on their molecular sizes. An SEC column of pore size 125 Å, which is suitable for separating proteins of molecular weights from 5 kD to 150 kD, was used for separation of amyloid oligomers. Therefore, $A\beta_{1-42}$ (1 mg/mL) was incubated in the presence or absence of formaldehyde (10 mM) for 12 h and then subjected to (SEC) for separation. As shown in Figure 27, after 12 h of incubation at 37º C, in both native and formaldehyde-induced Aβ aggregate three prominent protein peaks appeared with retention time of 6 min (peak 1), 12 min (peak 2) and 13 min (peak 3). According to the elution retention time of the marker proteins, peak 1 represented a mixture of $A\beta_{1-42}$ oligomers with molecular weights ranging from 30 kD to ~100 kD (pentamer to 20'mers). Peak 2 represented $A\beta_{1-42}$ dimers (8 to 9 kD) and peak 3 was the $A\beta_{1-42}$ monomer (~5 kD). Formaldehyde induced a five-fold increase in oligomer amount along with consumption of $A\beta_{1-42}$ monomers. Peak 1 and peak 3 were collected and concentrated using a protein concentrator (ThermoScientific, Waltham, MA, USA). The excess formaldehyde was removed during SEC separation. For subsequent cytotoxicity studies, equal amount of $A\beta_{1-42}$ was used to treat cells adjusted by protein concentrations.

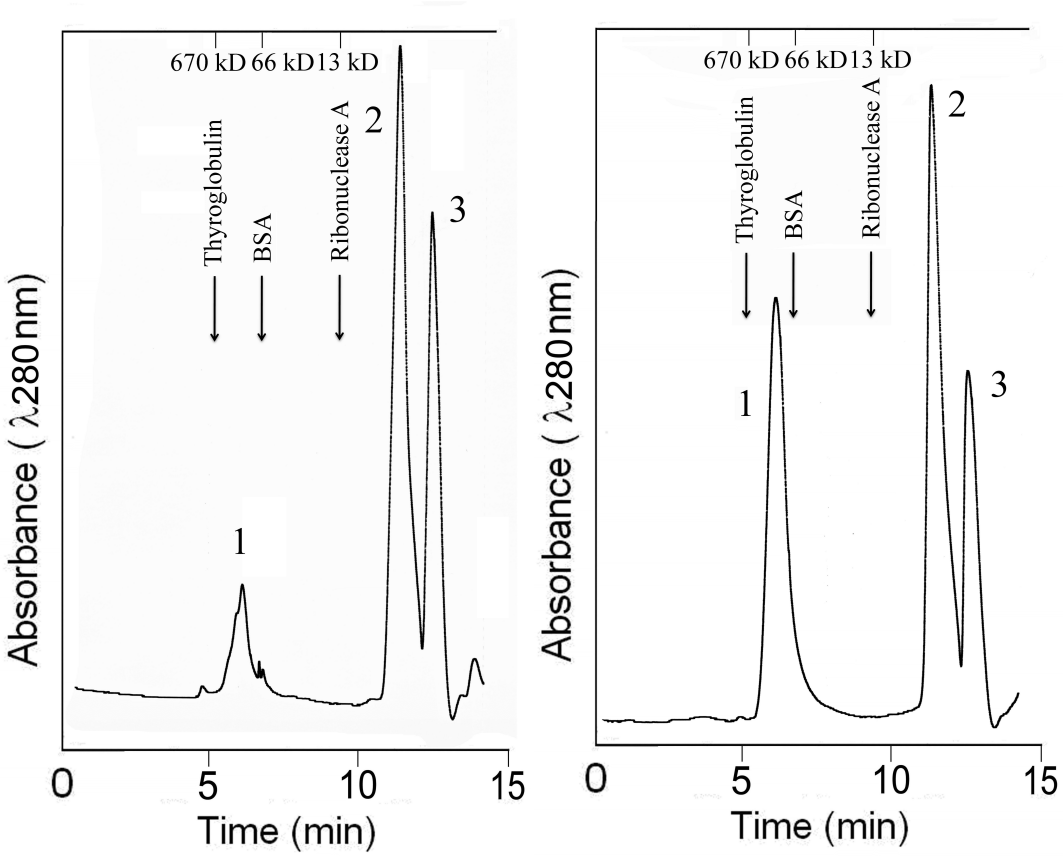

Figure 27. Isolation of Aβ oligomers by SEC. $A\beta_{1-42}$ was incubated in the presence or absence formaldehyde (10 mM in PBS) at 37º C for 12 h and then subjected to SEC column (4 μm from Alltech). The mobile phase was 0.3 M NaCl, 0.05 M phosphate, pH 7.0. The flow rate was constant at 1 mL/min. Marker proteins were thyroglobulin (670 kD), BSA (66 kD) and ribonuclease A (13 kD). A function of molecular weight with retention time was derived based on marker proteins. $A\beta_{1-42}$ oligomers and monomers were detected at 280 nm. Calculated from the molecular weight-retention time function, peak 1 represents a mixture of oligomeric species with molecular weights from 30 to 100 kD (Aβ pentamers to 20'mers). Peak 2 represents $A\beta_{1-42}$ dimers and peak 3 is the monomers.

5.2.3 Comparison of Cytotoxic Effects of Native and Formaldehyde-induced $A\beta_{1-42}$ Oligomers on SH-SY5Y Cells

5.2.3.1 Cell Viability Assessed by MTT Assay

The MTT assay measures the activity of mitochondrial reductase, which reflects the cell viability. Reductase converts MTT into a purple formazan. As can be seen in Figure 28, 5 nM of native Aβ oligomers caused about 10% cell death after 24 h of treatment, whereas 5 nM of formaldehyde-induced oligomers caused 15% to 25% cell death. The magnitude of cytotoxicity caused by 5 nM of Aβ oligomers on this cell line was consistent with results reported by other groups (Klein et al., 2004). The quantity difference of cell death between native and formaldehyde-induced Aβ oligomers was marginal, but significant and reproducible in individual experiment.

5.2.3.2 Cell Death Induced by Aβ Oligomers Assessed by LDH Assay

LDH is a group of cytoplasmic enzymes that interconvert pyruvate and lactate in the presence of NADH or NAD+. Aβ oligomers result in aberration of cytoplasmic integrity and then release of LDH into culture medium. Therefore, LDH activity is widely used as another indicator for cell viability.

After Aβ oligomers were concentrated in a concentrator, higher concentrations (up to 50 nM) of Aβ were achieved. Various dilutions of Aβ oligomers were then applied to the SH-SY5Y cells. As shown in Figure 29, Aβ oligomers exerted cytotoxicity in a concentration-dependent manner. There was no significant difference in cytotoxicity between native and formaldehyde-induced Aβ oligomers. However, the mean level of cell death caused by formaldehyde-induced Aβ oligomers was slightly higher, which was consistent with the results from MTT assay.

5.2.3.3 Measurement of Caspase-3 Activity during Aβ Oligomer-induced Apoptosis

MTT and LDH assays require a relative long treatment period (24 h) of Aβ to the cells. Based on the previous aggregation studies, Aβ has already formed protofibrils after 24-h incubation. Therefore, to examine the oligomer-induced cell death would be complicated, since the oligomers begin to form less cytotoxic protofibrils during treatment, and thus interfere with results interpretation. Aβ oligomers activate a variety of signaling pathways prior to cell death

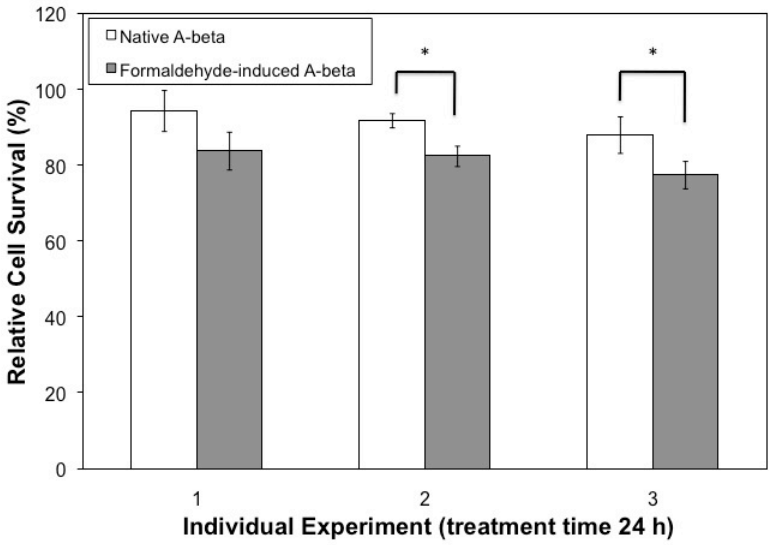

Figure 28. Comparison of cytotoxicity from native and formaldehyde-induced Aβ oligomers to SH-SY5Y cells assessed by MTT assay. Aβ oligomers (5 nM) isolated from size exclusion chromatography were added to SH-SY5Y cells and incubated for 24 h. MTT assay was described in Methodologies section. Data represent means (n=6) ± SD of three individual experiment. *$p < 0.05$, compared to corresponding control values.

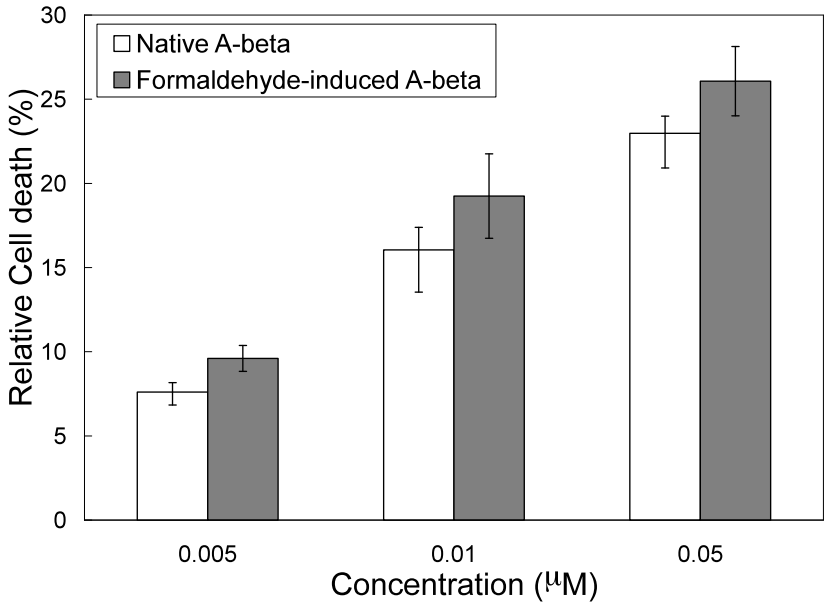

Figure 29. The cytotoxicity of native and formaldehyde-induced Aβ oligomers to SH-SY5Y cells assessed by LDH assay. Aβ oligomers isolated from SEC were concentrated in a Savant SVC100H vacuum concentrator (Thermo Scientific) for 1 h. SH-SY5Y cells were treated with various concentrations of Aβ oligomers for 24 h. LDH assay was described in Methodologies section. Graph represents means (n=6) ± SD of a representative experiment out of three.

(Lambert et al., 1998b; Walsh et al., 2002; Datki et al., 2004; Ronicke et al., 2008). In particular, Aβ oligomers induce apoptosis *via* a caspase-3 activity-dependent mechanism (Yang et al., 1998; Su et al., 2000; Eckert et al., 2001; St John, 2007; Paulsson et al., 2008). Based on these findings, it is useful to study the early cellular responses to examine the effect of aldehydes on Aβ cytotoxicity instead of comparing the final stage of Aβ effect, namely, cell death. In the following studies, caspase-3 activities were measured to test whether the apoptotic effects caused by native and formaldehyde-modified oligomers are different.

To validate this method, SH-SY5Y cells were first treated with hydrogen peroxide, which is well-known exhibiting apoptotic effect. As can be seen in Figure 30, hydrogen peroxide induced caspase-3 activity in a concentration-dependent manner. Figure 31 shows the effects of Aβ oligomers on caspase-3 activity in SH-SY5Y cells after incubation for 3 h (a), 12 h (b) and 24 h (c). A group of cells was separately treated with hydrogen peroxide as the positive control. After 3 h of treatment, neither native nor formaldehyde-induced oligomers induced changes in caspase-3 activity compared to the control. After 12 h of incubation, both native and formaldehyde-induced oligomers significantly increased caspase-3 activity in a concentration-dependent manner. Formaldehyde-induced Aβ oligomers caused a significantly higher caspase-3 activity than that by native oligomers after 12 h treatment, but not after shorter (3 h) or prolonged (24 h) treatment. This difference in caspase-3 activity induced by native and formaldehyde-induced oligomer was also in a concentration-dependent manner as shown in Figure 31b. Neither native nor formaldehyde-modified Aβ monomers exhibited any significant effect on caspase-3 activity throughout all treatment periods.

The data suggest that Aβ oligomers induce an early induction of caspase-3 activity (beginning from 3 h of treatment), which diminishes over time. The results were consistent with the MTT and LDH experiments, namely, formaldehyde modification slightly increased the cytotoxicity of Aβ oligomers by approximately 25%.

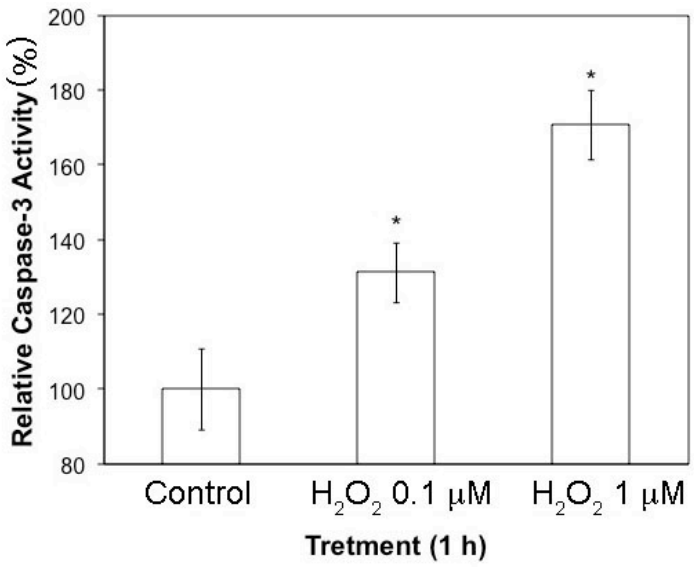

Figure 30. Induction of caspase-3 activity by hydrogen peroxide in SH-SY5Y cells. The cells were treated with various concentrations of hydrogen peroxide for 1 h followed by caspase-3 activity assay. Graph represents means (n=6) ± SD of a representative experiment out of three. *$p < 0.05$, compared to corresponding control values.

a.

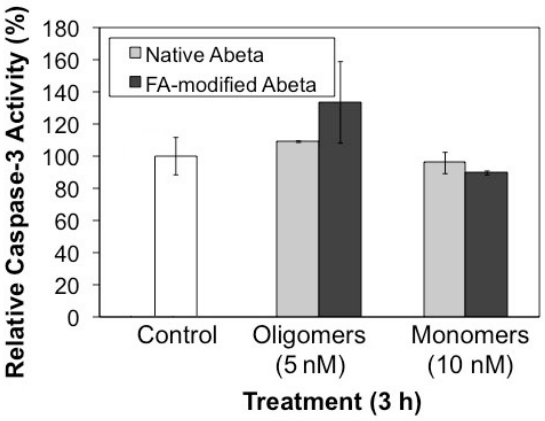

b.

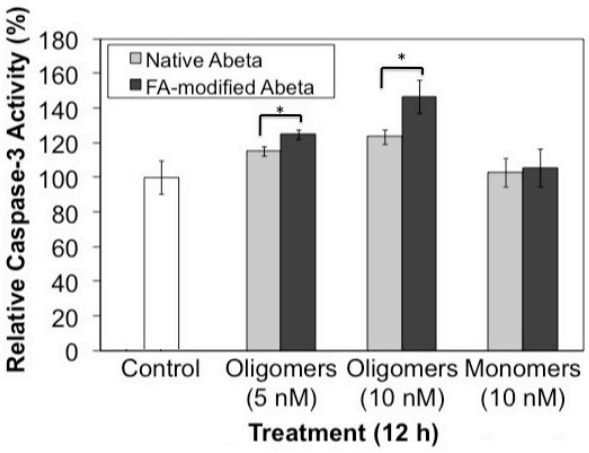

c.

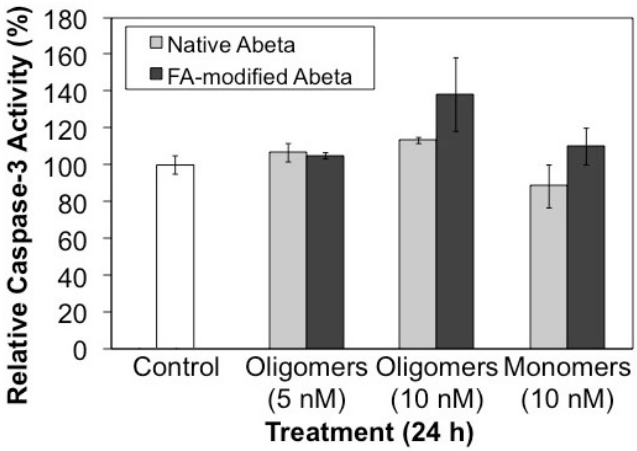

Figure 31. The effect of native and formaldehyde-modified Aβ on caspase-3 activity during apoptosis of SH-SY5Y cells. Aβ oligomers and monomers isolated from SEC were concentrated and used to treat SH-SY5Y cells for various time periods as indicated in panel a., b., c. Graph represents means (n=6) ± SD of a representative experiment out of three. *$p < 0.05$, compared to corresponding control values.

5.3 Part III: Effect of Formaldehyde Derived from SSAO-catalyzed Deamination on LRP-1-mediated Transport

5.3.1 Expression of Both SSAO and LRP-1 on Human Umbilical Blood Vessels

VSMCs and endothelial cells of the cerebral vasculature play a crucial role in Aβ clearance. In these cells, both SSAO and LRP-1 are localized on the outer surface of plasma membrane. In order to investigate whether SSAO affects LRP-1 function, VSMCs were freshly prepared from human umbilical arteries. The expression of SSAO and LRP-1 on these blood vessels was demonstrated. As shown in Figure 32, immunostaining of artery cross-sections reveals that both SSAO and LRP-1 are richly expressed on blood vessel walls. Thus, VSMCs can be a good *in vitro* model for studying the potential interactions between SSAO and LRP-1.

Transgenic mouse aorta was subsequently used as a source for VSMCs primary culture. LRP-1 and SSAO were stained after cell growth was established and stabilized. Figure 33 shows that LRP-1 is highly expressed on the cell membrane and concentrated in intracellular granules at Day-4 culture. In contrast to LRP-1, SSAO expression was very weak and its activity of this cell culture was hardly detectable. VSMC specific α-actin was also stained to confirm the cell type.

It is known that SSAO is not expressed by VSMCs in primary subcultures. The reason is unclear. Neither is SSAO expressed in any endothelial or smooth muscle cell lines. Growth factors, cytokines and bile salts were used to stimulate SSAO expression on endothelial cell culture from various sources, but without success (Lalor et al., 2002). hSSAO gene has been transfected to VSMC cell line (Sole et al., 2007). However, the specific SSAO activity in this cell line is still much lower compared to tissues and the sub-cellular localization of transfected SSAO has not been determined.

VSMCs could lose their phenotype after subculture including SSAO expression, which may be restored by stimulating its differentiation. A variety of culture conditions was tested in order to restore SSAO expression in VSMCs culture. Serum deprivation from culture medium can induce cell differentiation. VSMC cell line was therefore incubated in various concentrations of FBS (0%, 2%, 5%, 10% and 15%) for 12 h to 24 h. Various types of DMEM culture medium were also tested to induce SSAO activity. Yet, SSAO activity was not induced. Sphingosine 1-phosphate, an intermediate product during sphingolipids degradation, was found to stimulate VSMC differentiation by activating multiple signaling pathways (Lockman et al., 2004). VSMCs

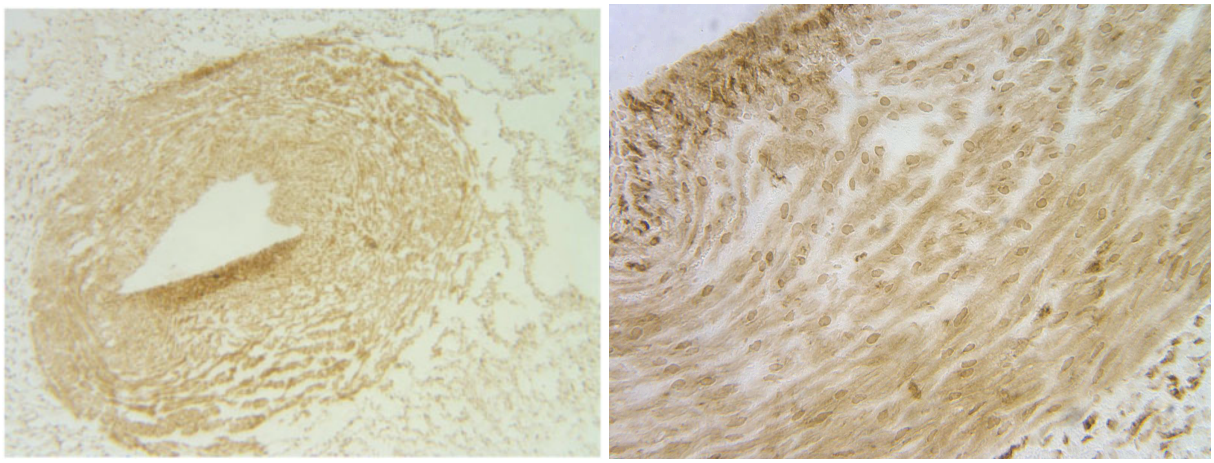

LRP-1 40X 200X

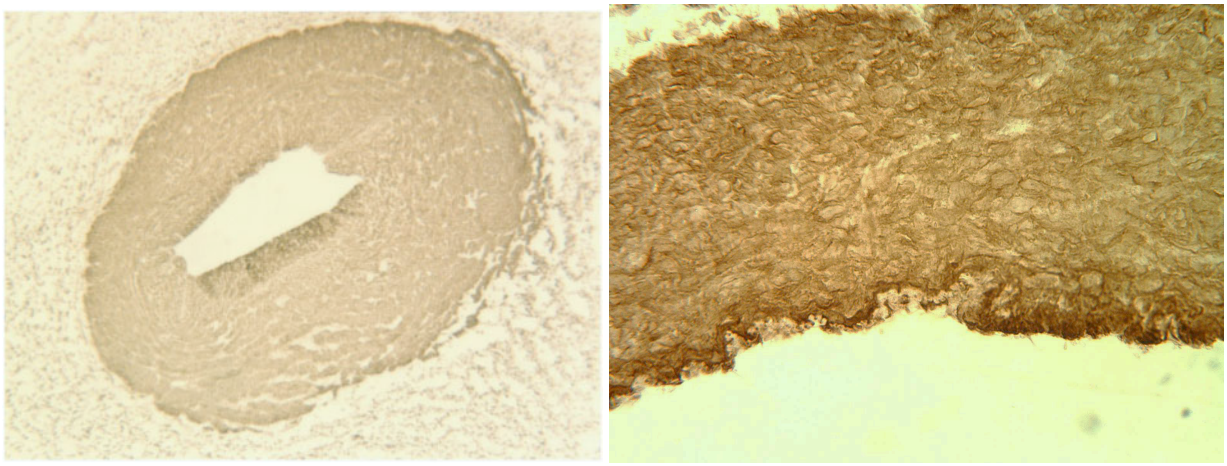

SSAO 40X 200X

Figure 32. Immunostaining of LRP-1 and SSAO on cross-sections of human umbilical arteries. Human umbilical arteries were cut into sections (20 μm in thickness) at -27º C in a cryostat. Consecutive sections were stained for LRP-1 and SSAO, respectively. Upper: LRP-1 staining under magnitude 40X and 200X; lower: SSAO staining under magnitude 40X and 200X.

a.

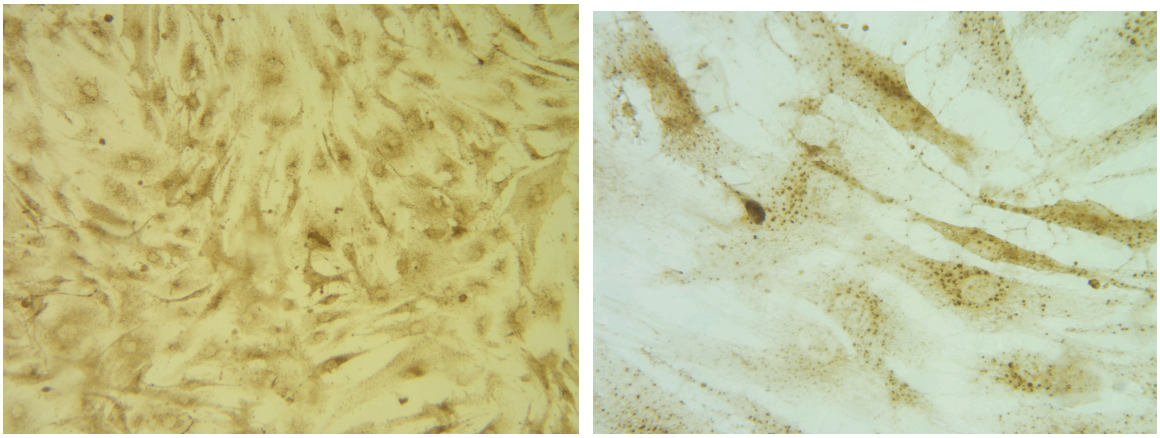

LRP-1 staining 100X 400X

b. c.

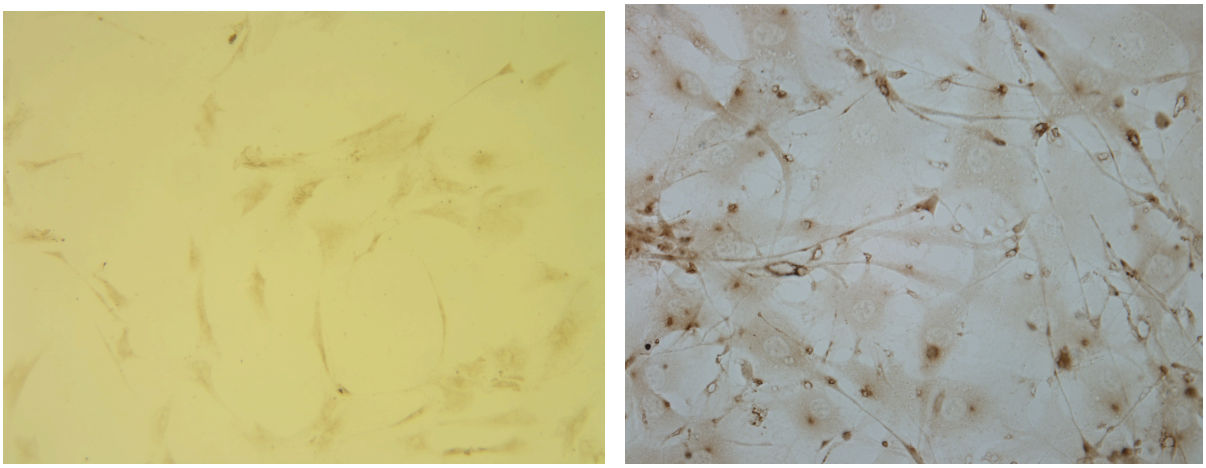

SSAO staining 100X α-actin staining 200X

Figure 33. Immunostaining of LRP-1 and SSAO on primary culture of VSMCs. VSMCs were isolated from mice aorta after digestion by type II collagenase. The cells were cultured in DMEM with 10% FBS. Immunostaining of LRP-1 (a), SSAO (b), and VSMC specific α-actin (c), were carried out at day 4 after cell culture was established and stabilized.

were therefore incubated in sphingosine 1-phosphate (1 μM) for 24 h, but such a treatment also failed to induce SSAO expression. Another study reported a dramatic increase in SSAO expression and activity by VSMCs after 10-day culture under serum-free DMEM/F-12 Ham plus transferrin (50 μg/mL), ascorbate (0.2 mM) and insulin (1 μM) (El Hadri et al., 2002). However, this observation was not reproduced in the present study.

Due to the unavailability of cultured cell line simultaneously expressing both LRP-1 and SSAO, freshly isolated VSMCs from transgenic mouse aorta were used for studying the potential effect of SSAO-mediated reactions on LRP-1 function.

5.3.2 SSAO Activity of Isolated VSMCs

The results from previous immunohistochemical staining demonstrated that human umbilical arteries possess very high SSAO expression. SSAO with associated to all blood vessels including cerebral microvessels. Therefore, human umbilical arteries, mouse aorta, rat aorta, meninges and cerebral microvessels were collected, and their SSAO activities were measured and compared using radioisotope-labeled substrate (data not shown). With both high specific and total SSAO activity, mouse aortic VSMCs were chosen for subsequent experiments.

During the digestion process by collagenase, the total number of the dissociated cells from mouse aorta, and their viability, were monitored routinely. Figure 34a shows that the cell number reached a maximum after 1 to 2 h of digestion. Prolonged digestion dramatically reduced the cell number, probably due to proteolysis of cell membrane by collagenase. Cell viability measured by trypan blue indicates that most isolated cells were viable for at least 6 h as shown in Figure 34b.

Interestingly, collagenase was found to inactivate SSAO activity and also to release the enzyme from the cell surface, *i.e.* shedding effect. After digestion by type II collagenase for 1 h, VSMCs were collected by centrifugation. SSAO activities of the cell pellets, supernatant, remaining tissue chunks and aorta without collagenase digestion were measured. As shown in Figure 34c, cells digested from aorta had the highest specific activity suggesting relatively purified and concentrated preparation of cells, whereas its total SSAO activity was the lowest due to limited cell quantity. In the supernatant however substantial SSAO activity was detected, suggesting membrane-bound SSAO was cleaved by collagenase during digestion. For the subsequent α2M transport experiments, the process of VSMCs isolation by collagenase digestion was all completed within 2 h.

a.

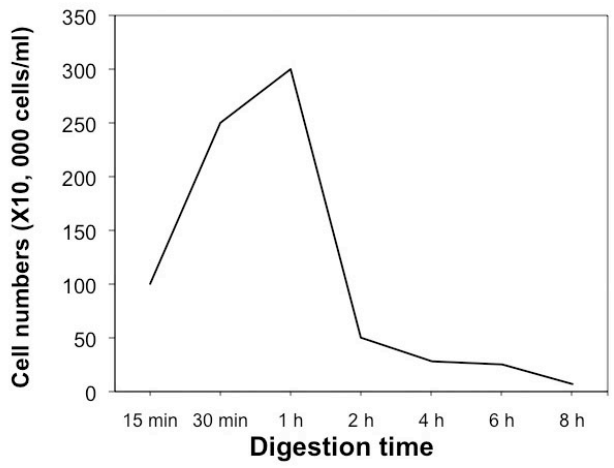

b.

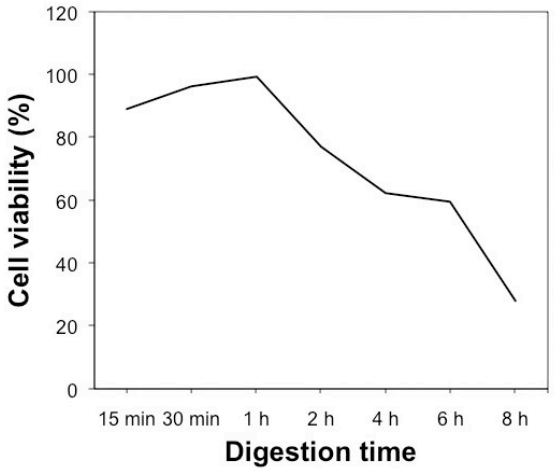

c.

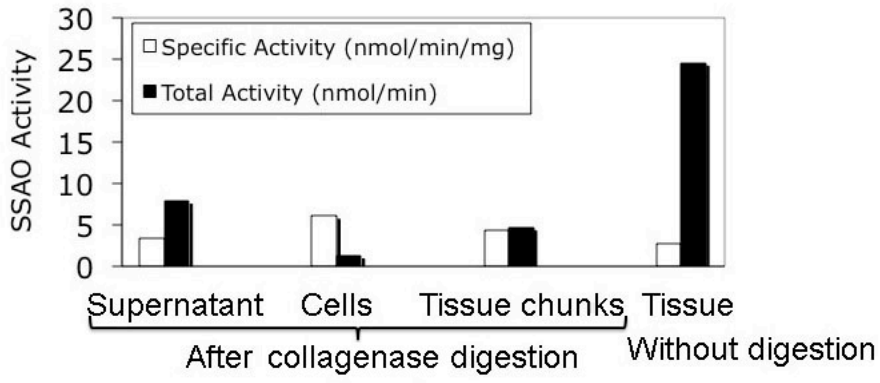

Figure 34. Isolation of mouse aortic VSMCs by collagenase digestion. (a) During the digestion process, the total number of cells digested off aorta was monitored. (b) Cell viability was assessed by Trypan blue using a hemocytometer under a microscope. (c) After digestion for 1 h, SSAO activities of the supernatant, cell pellets, remaining tissue chunks and aorta without digestion were measured and compared. Data represent one typical experiment.

5.3.3 α2M Uptake by VSMCs *via* LRP-1

LRP-1, a multifunctional cell surface receptor, is responsible for Aβ transcytosis. Its substrates such as α2M facilitate this process. In the present study, α2M uptake by isolated VSMCs was used as an indicator for LRP-1 function.

α2M needs to be "activated" first before it can be recognized by LRP-1. *In vivo*, α2M is activated by proteinase cleavage to induce a conformational change in its tetramer. This activation traps proteinase in the α2M tetramer, after which proteinase activity is inhibited. It also makes α2M a competent ligand for LRP-1 (Bjork et al., 1985; Moestrup and Gliemann, 1991). *In vitro*, activation of α2M is achieved by incubation with a high concentration of methylamine, which causes similar conformational changes as proteinase does (Bjork and Fish, 1982; Gonias et al., 1982; Strickland et al., 1984).

The experimental conditions for the transport of activated α2M by the isolated VSMCs were determined. Also, it is necessary to confirm that α2M uptake by isolated VSMCs is specifically mediated by LRP-1 function. The isolated VSMCs were incubated with activated α2M (0.1 to 100 nM) for 2 h. As can be seen in Figure 35a, α2M uptake was increased in a concentration-dependent manner. VSMCs were then incubated in 20 nM of α2M for various time periods (from 30 min to 4 h). Figure 35b shows that α2M uptake level reached the maximum after 2 h of incubation. Prolonged incubation caused a decrease in α2M uptake level. This was probably due to decreased cell viability, because aortic VSMCs were viable within 3 h after isolation as previously observed. Based on these results, the uptake conditions for the subsequent experiments were kept as 20 nM of activated α2M and 2 h of incubation period with VSMCs.

To date, drugs that inhibit LRP-1 are not available. In the present study, lactoferrin, a competitive LRP-1 substrate, was used to substantiate that in isolated VSMCs, α2M binds to LRP-1. Figure 35c shows that in the presence of lactoferrin, the level of α2M uptake was significantly reduced in a lactoferrin-concentration-dependent manner, confirming that α2M uptake in this model was mediated by LRP-1 function. Activation of α2M by methylamine was essential for its uptake. As shown in Figure 35d, uptake of the native α2M by VSMCs was dramatically increased after activation. The non-activated α2M detected by Western blot results from nonspecific binding of α2M to cell membrane.

a.

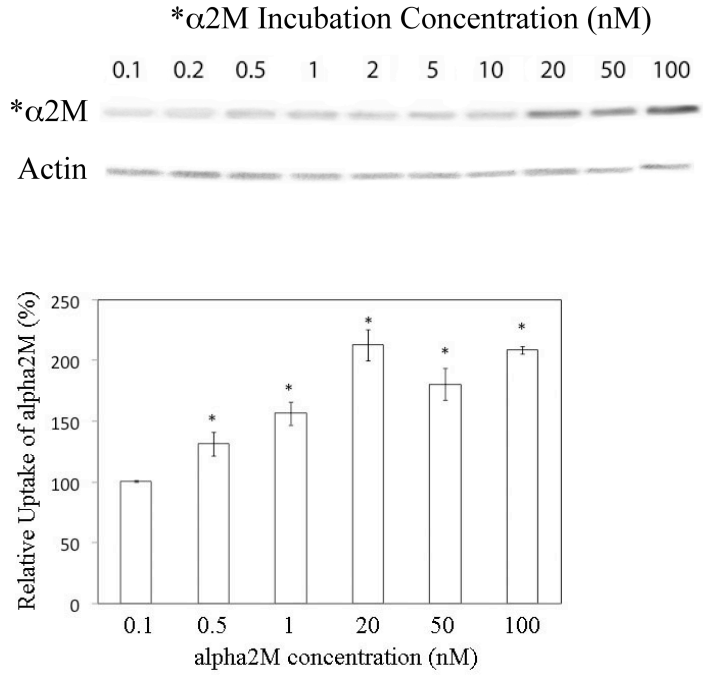
*α2M Incubation Concentration (nM)
0.1 0.2 0.5 1 2 5 10 20 50 100
*α2M
Actin
Relative Uptake of alpha2M (%)
250
200
150
100
50
0
0.1 0.5 1 20 50 100
alpha2M concentration (nM)

b.

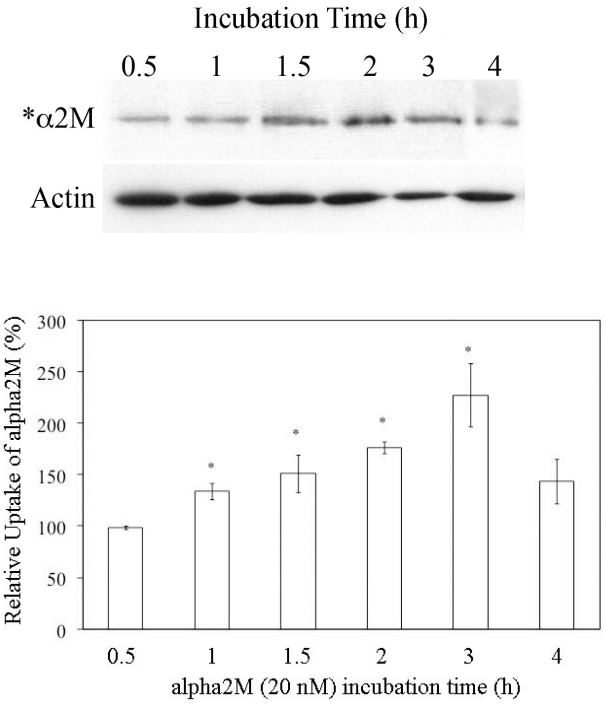
Incubation Time (h)
0.5 1 1.5 2 3 4
*α2M
Actin
Relative Uptake of alpha2M (%)
300
250
200
150
100
50
0
0.5 1 1.5 2 3 4
alpha2M (20 nM) incubation time (h)

c.

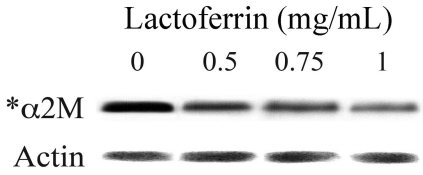

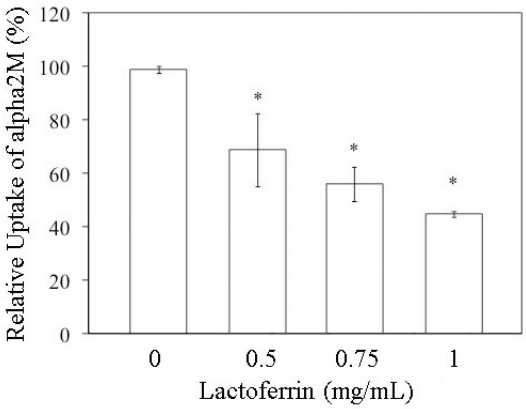

d.

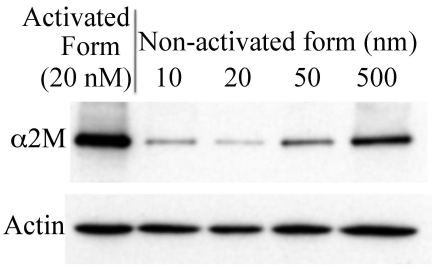

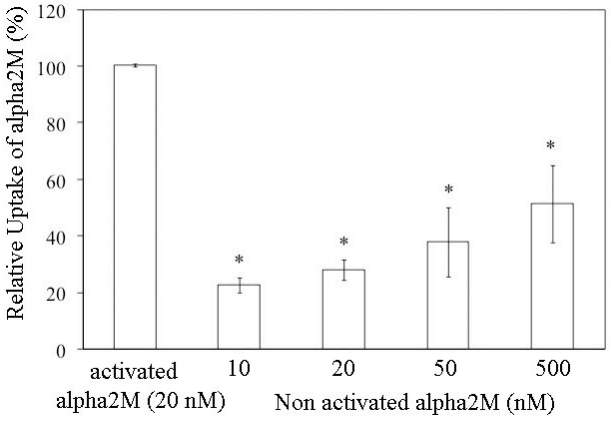

Figure 35. The uptake of α2M by isolated VSMCs measured by Western blot. (a) VSMCs were incubated with activated α2M (*α2M) at concentrations from 0.1 to 100 nM for 2 h. (b) VSMCs were incubated with 20 nM of *α2M for various time periods (0.5 to 4 h). (c) VSMCs were incubated with *α2M (20 nM) for 2 h in the presence of lactoferrin, an LRP-1 substrate, as a competitive inhibitor. (d) α2M was activated by incubating with methylamine (0.2 M) for 2 h at room temperature. Activated α2M (20 nM) and native form of α2M (10 to 500 nM) were compared for their uptake by VSMCs. The amount of α2M and actin were calculated by multiplying band area and band grayscale, determined by ImageJ software from the National Institutes of Health. The α2M: actin ratio of control was converted to 100% and the other groups were normalized to corresponding control. Data represent mean (n=3) ± SD of a representative experiment out of three. *$p < 0.05$, compared to corresponding control values.

In brief, the above experiments confirmed that in this model, isolated VSMCs bind and take up α2M that has been activated by methylamine *via* LRP-1. The experimental conditions including α2M concentration and incubation time with VSMCs were determined and used for subsequent experiments.

5.3.4 Effect of Formaldehyde on VSMC LRP-1

Both LRP-1 and SSAO are richly expressed on the VSMC surface. Therefore, reactive aldehydes such as formaldehyde generated *via* deamination of methylamine could interact with the adjacent LRP-1 and thus affect its function. For the first several experiments, freshly isolated VSMCs were directly treated with series of concentrations of formaldehyde for 1 h prior to the addition of α2M. As shown in Figure 36a, the uptake of α2M was significantly reduced by formaldehyde in a concentration-dependent manner. This reduction was aggravated by prolonged treatment period. Figure 36b shows that 10 μM of formaldehyde began to reduce α2M uptake level after 30 min of treatment and exerted the maximal effect after 90 min. In these experiments, cell viability was monitored by trypan blue and formaldehyde of all concentrations did not affect cell viability within 90 min of treatment.

Hydrogen peroxide is another toxic product from SSAO-mediated deaminations. Its potential effect on α2M uptake *via* LRP-1 was also assessed. As shown in Figure 36c, VSMCs were treated with various concentrations of hydrogen peroxide in parallel with formaldehyde treatment. Hydrogen peroxide did not substantially affect the uptake of α2M as formaldehyde did.

5.3.5 Effect of SSAO-mediated Deamination of Methylamine on VSMC LRP-1

To study the effect of SSAO-mediated deamination on LRP-1, freshly isolated VSMCs were incubated with various concentrations of methylamine for 2 h before addition of α2M, instead of direct treatment with formaldehyde. Figure 37a shows that methylamine reduced the uptake of α2M at higher concentrations. MDL72974A, a selective SSAO inhibitor, attenuated such an effect. The effect of methylamine was increased with prolonged incubation time and was also alleviated by SSAO inhibitor as seen in Figure 37b. The results indicate that formaldehyde produced from SSAO-catalyzed deamination of methylamine is responsible for impairing LRP-1 function.

a.

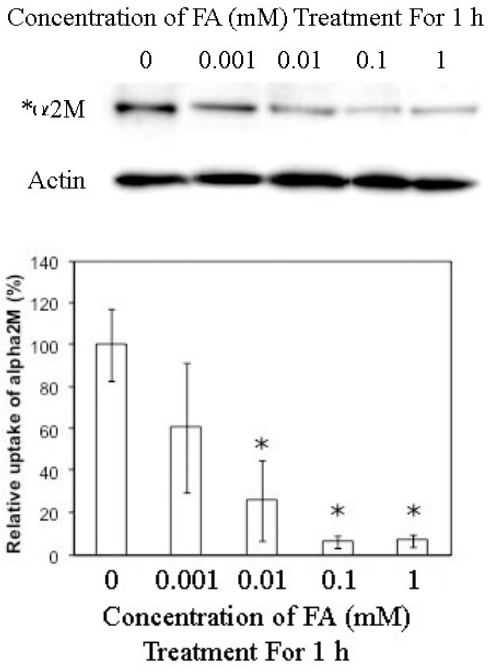

b.

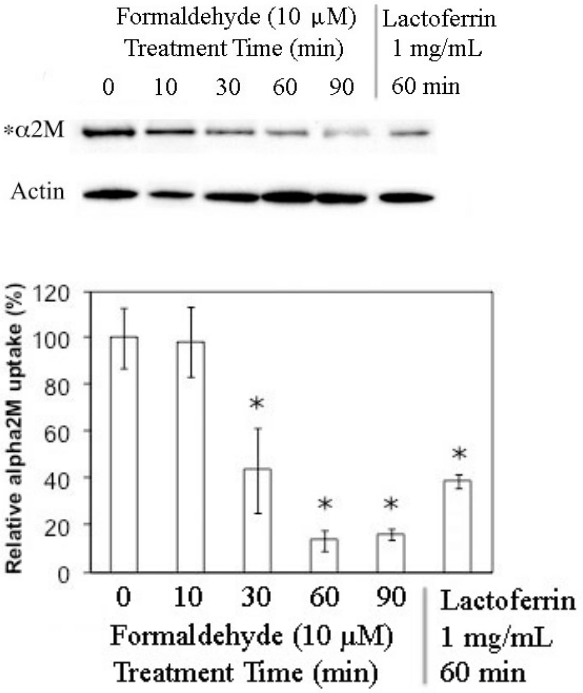

c.

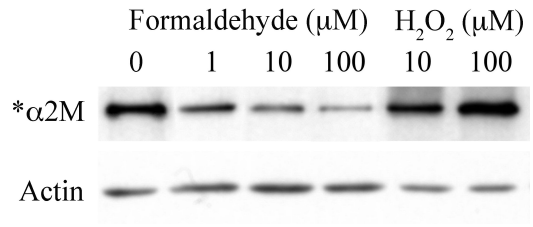

Figure 36. The effect of formaldehyde on α2M uptake by VSMCs. (a) VSMCs were treated with a gradient concentration (1 μM to 1 mM) of formaldehyde for 1 h prior to addition of α2M. (b) VSMCs were treated with 10 μM of formaldehyde for various time periods (10 to 90 min). The amount of α2M and actin were calculated by multiplying band area and band grayscale, determined by ImageJ software from the National Institutes of Health. The α2M: actin ratio of control was converted to 100% and the other groups were normalized to corresponding control. Data represent mean (n=3) ± SD of a representative experiment out of three. *$p < 0.05$, compared to corresponding control values. (c) VSMCs were treated with H_2O_2 before incubating with α2M.

a.

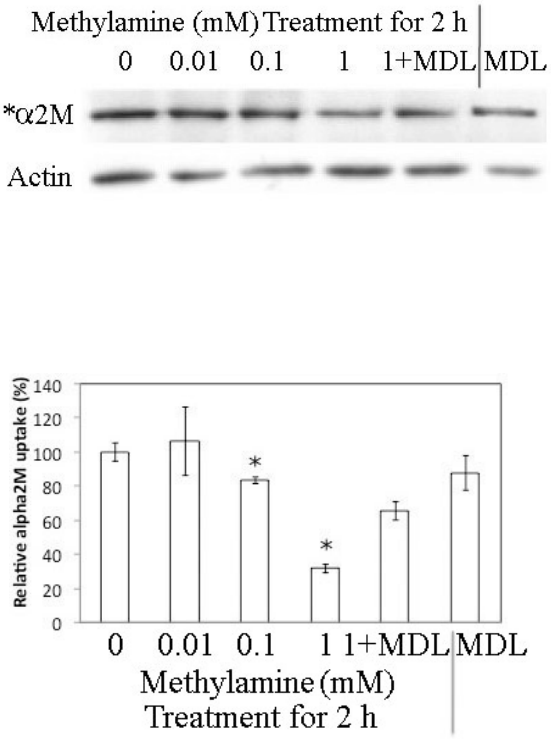

b.

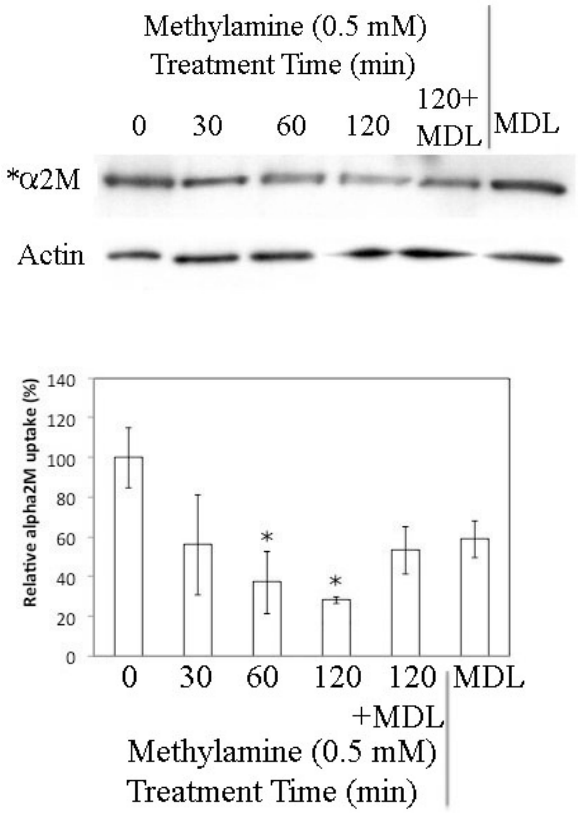

Figure 37. Effect of SSAO-mediated deamination of methylamine on α2M uptake by VSMCs. (a) VSMCs were incubated with a series of concentration of methylamine (10 μM to 1 mM) for 2 h in the presence of absence of SSAO inhibitor. (b) VSMCs were incubated with methylamine (0.5 mM) for different time periods (30 to 120 min) in the presence or absence of SSAO inhibitor. SSAO inhibitor (1 μM), MDL72974A, was incubated with VSMCs for 10 min before addition of methylamine. The α2M: actin ratio of control was converted to 100% and the other groups were normalized. Data represent mean (n=3) ± SD of a representative experiment out of three. *$p < 0.05$, compared to corresponding control values.

In order to investigate whether SSAO on cerebral VSMCs has a similar effect on LRP-1 function as was observed in aortic tissue, VSMCs of rat meninges and cerebral microvessels were isolated and used for α2M uptake. As can be seen in Figure 38, methylamine (100 μM) was capable of reducing the α2M uptake by about 30% and SSAO inhibition by MDL72974A reversed this effect, suggesting that in the brain, aldehydes produced from cerebral SSAO-mediated deamination are potentially harmful to LRP-1 on brain blood vessels.

The above studies on α2M uptake indicate that LRP-1 function is impaired by formaldehyde produced from SSAO-mediated deamination. In order to substantiate whether methylamine deamination also affects Aβ endocytosis *via* LRP-1, isolated VSMCs, treated with methylamine, were incubated with Aβ monomers in the presence or absence of α2M. In preliminary experiments, Western blot did not detect any Aβ associated with the cells. Aβ was not detected in the media either. This puzzling observation was subsequently solved. Collagenase has been used for the isolation of VSMCs. Although most of the excess collagenase was removed by centrifugation and resuspending the cells, a trace amount of collagenase could remain in the cell suspension. To test whether residual collagenase was responsible for proteolysis of Aβ, Aβ was incubated with various dilutions of type II collagenase at 37º C for 2 h and subjected to Western blot for Aβ analysis. As shown in Figure 39a, indeed, type II collagenase was highly potent in digesting Aβ. To overcome this technical problem, a collagenase inhibitor (Z-PDLDA-NHOH from Calbiochem, EMD Biosciences, La Jolla, CA USA) was included. Figure 39b shows that the recovery of Aβ was significantly increased in the presence of collagenase inhibitor in a concentration-dependent manner. It is very interesting to note that Aβ proteolysis by collagenase has not been reported previously.

VSMCs were then incubated with Aβ monomers together with collagenase inhibitor (1 mg/mL) and various concentrations of methylamine in the presence or absence of α2M. As can be seen in Figure 40, consistent with earlier experiments, methylamine at higher concentrations significantly reduced α2M uptake level and SSAO inhibitor, MDL72974A, reversed this effect. In both groups, *i.e.* with and without α2M, formaldehyde derived from methylamine increased Aβ aggregation by forming more smeared bands in a concentration-dependent manner, which was reversed by SSAO inhibitor. Therefore, SSAO-mediated deamination exerts independent effects on α2M and Aβ, namely, reducing α2M uptake by VSMCs and increasing Aβ

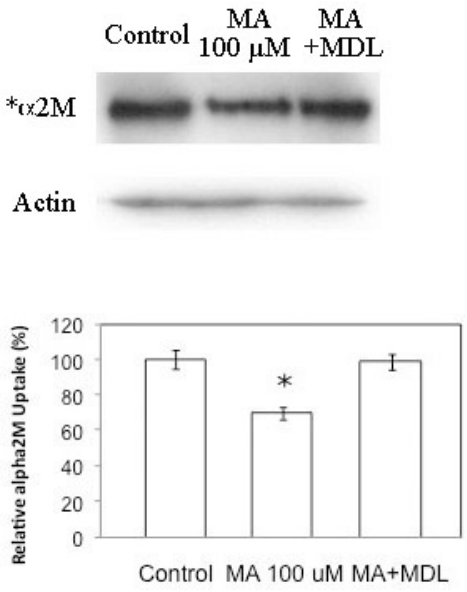

Figure 38. Effect of SSAO-mediated deamination of methylamine on α2M uptake by cerebral VSMCs. Cerebral VSMC suspensions were obtained from combined fractions of rat meninges and microvessels. VSMCs were treated with 100 μM of methylamine for 1 h in the presence or absence of SSAO inhibitor (1 μM). SSAO inhibitor, MDL72974A, was incubated with VSMCs for 10 min before methylamine treatment. 20 nM of activated α2M was then added to the cell suspensions and further incubated for 2 h. The α2M: actin ratio of control was converted to 100% and the other groups were normalized to control. Data represent mean (n=3) ± SD of a representative experiment out of three. *$p < 0.05$, compared to corresponding control values.

a.

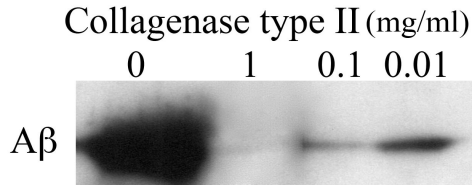

b.

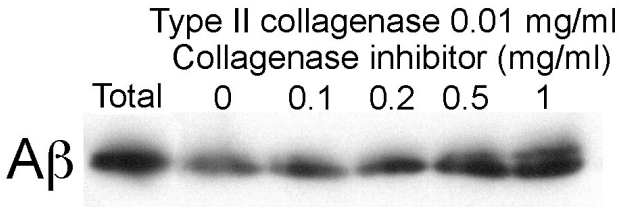

Figure 39. Degradation of Aβ by type II collagenase. (a) Aβ (200 μM) was incubated with various concentrations (0.01 to 1 mg/mL) of type II collagenase at 37º C for 2 h. (b) Aβ (100 μM) was incubated with type II collagenase (0.01 mg/mL) in the presence of various concentrations of collagenase inhibitor (0.1 to 1 mg/mL of Z-PDLDA-NHOH from Calbiochem, EMD Biosciences, La Jolla, CA USA) at 37º C for 2 h.

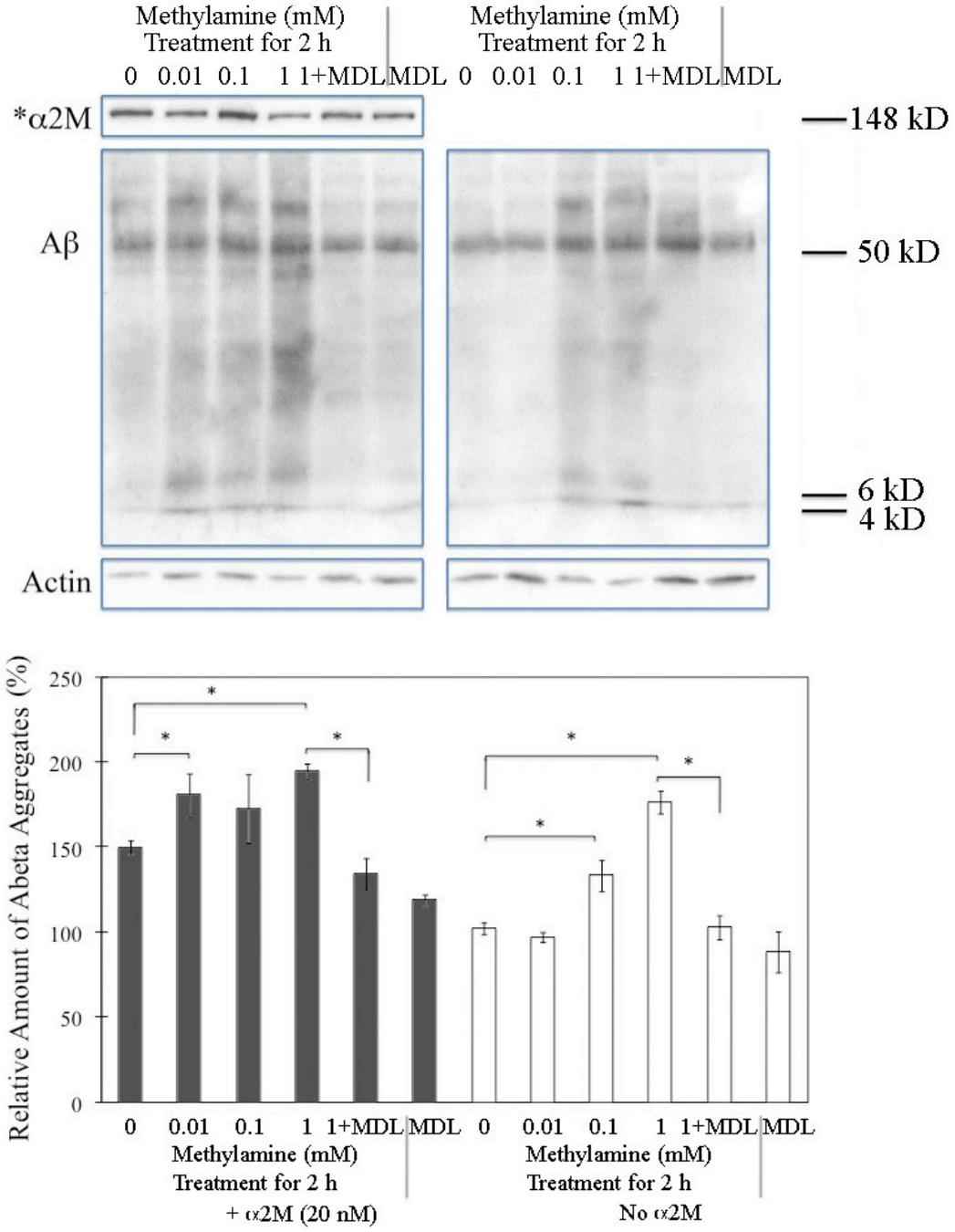

Figure 40. Effect of SSAO-mediated deamination of methylamine on α2M and Aβ uptake by isolated VSMCs. The experiments were designed into 2 groups. One group of VSMCs (left panel) was incubated with Aβ (10 μM) and α2M (20 nM) for 2 h for uptake. The other group (right panel) was incubated with Aβ (10 μM) only for 2 h. Prior to addition of Aβ and α2M, both groups were treated with a series of concentration of methylamine for 1 h in the presence or

absence of SSAO inhibitor, MDL72974A. The amount of α2M and actin were calculated by multiplying band area and band grayscale, determined by ImageJ software from the National Institutes of Health. The α2M: actin ratio of control (without α2M or methylamine treatment) was converted to 100% and the other groups were normalized to corresponding control. Data represent mean (n=3) ± SD of a representative experiment out of three. *$p < 0.05$, compared to corresponding control values.

aggregation.

α2M facilitates Aβ transcytosis *in vivo* (Shibata et al., 2000). Aβ also binds to LRP-1 directly without a carrier (Deane et al., 2004). In this experiment, the level of Aβ detected in VSMCs was not directly affected by α2M. Whether α2M can facilitate Aβ endocytosis in this model requires further investigation. Interestingly, α2M enhanced Aβ aggregation by forming more smeared bands on the Western blot, especially in the presence of methylamine. Collagenase inhibitor itself does not affect Aβ aggregation. This suggests that formaldehyde derived from methylamine enhances Aβ aggregation with α2M.

5.3.6 Effect of Formaldehyde on α2M and Its Uptake by VSMCs

Formaldehyde reacts with a variety of proteins indiscriminately. It was questioned whether formaldehyde might also directly interact with α2M, thus modify its configuration, affect its binding to LRP-1, and disrupt the endocytosis of α2M. Activated α2M was treated with formaldehyde prior to incubation with VSMC suspensions for uptake. As shown in Figure 41, pretreatment of formaldehyde to α2M did not cause any change in α2M uptake level, suggesting that formaldehyde does not affect the structure, or at least the binding site of α2M to LRP-1. The reduction of α2M uptake by VSMCs results from formaldehyde reacting with LRP-1 and impairing its function.

In brief, LRP-1 has been shown to be very sensitive to formaldehyde. Formaldehyde derived from deamination of methylamine decreases α2M uptake by VSMCs. Elevated SSAO activity on VSMCs or increased availability of its substrates, or both, potentially impairs the function of vascular LRP-1 and affect the transcytosis of its ligands including α2M and Aβ.

5.3.7 Effect of Formaldehyde on the Complex Formation between Aβ with α2M or ApoE

Aβ and α2M or ApoE form large complexes, which can no longer be eliminated *via* LRP-1 (Ito et al., 2007). We demonstrated that aldehydes crosslink Aβ peptides and enhance their aggregation. It is interesting to know whether aldehydes can crosslink Aβ with α2M or ApoE to form large complexes.

Aβ was incubated with α2M in the presence or absence of various concentrations of

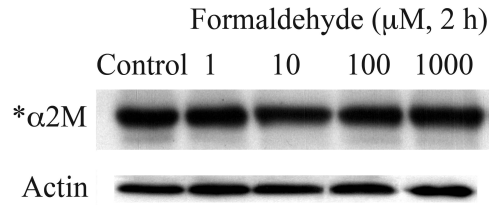

Figure 41. Uptake of native and formaldehyde-modified α2M by isolated VSMCs. Activated α2M was pre-treated with various concentrations of formaldehyde for 2 h. Excess formaldehyde was then removed by an ultracentrifugation filter tube. Native and formaldehyde-modified α2M were incubated with isolated VSMCs as previous described.

formaldehyde for 24 h. As can be seen in Figure 42, formaldehyde induced the formation of large SDS-resistant aggregates of Aβ in the presence of α2M, whereas in the absence of α2M, ormaldehyde did not promote the production of such large aggregates. Formaldehyde-induced Aβ aggregates without α2M were blocked in the presence of SDS used in Western blot. Formaldehyde also induced smeared bands of α2M on Western blot to higher molecular weights in a concentration-dependent manner, suggesting that α2M was crosslinked with Aβ by formaldehyde. Our data suggest that indeed, formaldehyde and probably other aldehydes are quite capable of crosslinking Aβ with α2M to form complexes that cannot be endocytosed into cells.

Subsequent experiment demonstrated the crosslinkage between ApoE and Aβ. Similar to Aβ, ApoE by itself also aggregates into different forms including octamers and even larger oligomers. The aggregation was revealed by AFM. Parallel arrays of short fibrils were formed by ApoE itself (Figure 43a). Formaldehyde significantly enhanced the self-aggregation of ApoE. Figure 43b shows that the aggregation of Aβ was enhanced by formaldehyde. When ApoE and Aβ were incubated together, a population of ApoE-Aβ complexes with larger molecular sizes was formed (Figure 43c). The morphologies and density of these complexes were not significantly affected by formaldehyde. However, formaldehyde increased the sizes of these complexes by significantly shifting their size distribution shown in the bearing histogram.

In brief, we have provided evidence that formaldehyde not only induces Aβ oligomerization and fibrillogenesis, but also enhances the formation of protein complexes composed of Aβ and α2M and ApoE.

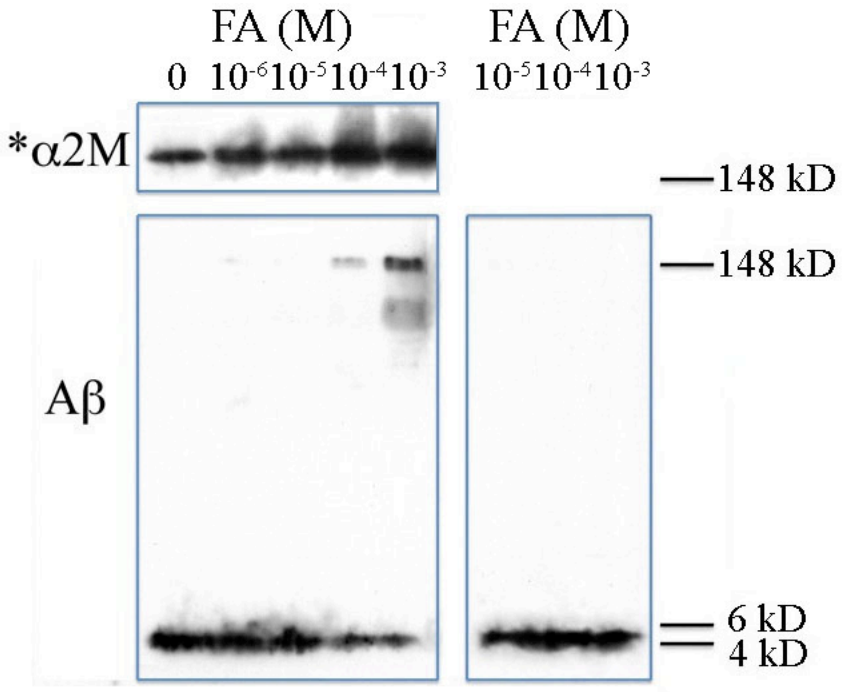

Figure 42. Effect of formaldehyde on the formation of aggregated complexes between α2M and Aβ, revealed by Western blot. Left panel: activated α2M (1.5 μM) and Aβ (50 μM) were together treated with various concentrations of formaldehyde (1 μM to 1 mM) for 24 h. Right panel: Aβ (50 μM) alone was incubated with formaldehyde (100 μM to 1 mM) for 24 h.

a.

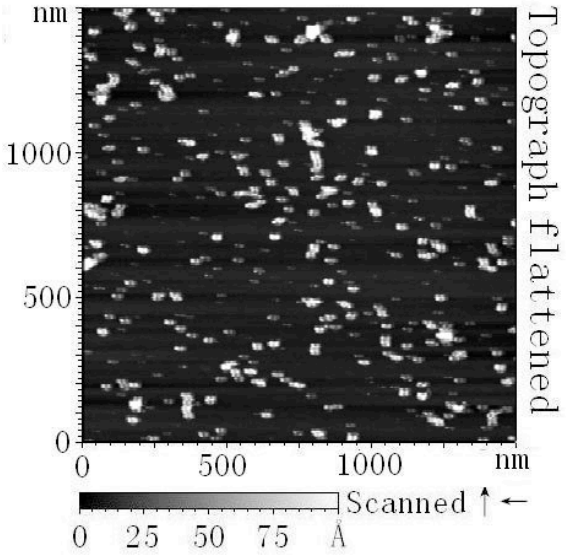

ApoE4

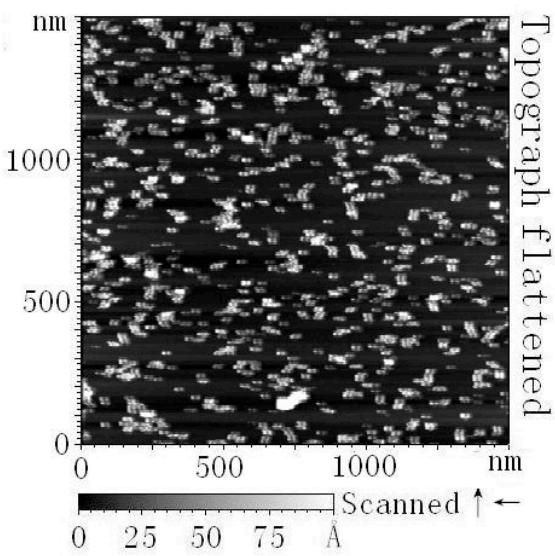

ApoE4 + Formaldehyde

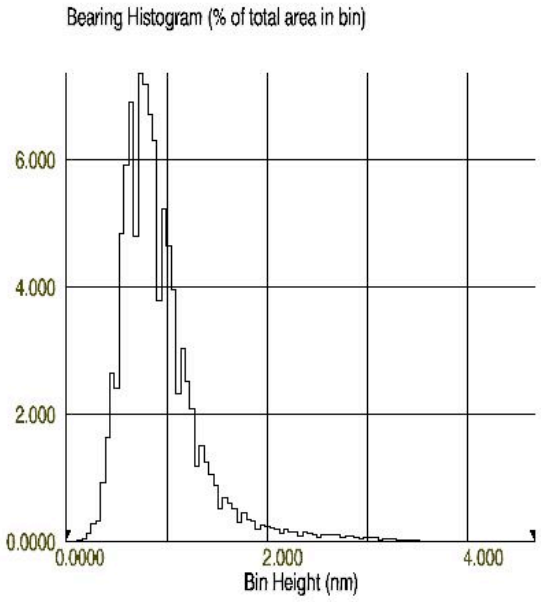

ApoE4

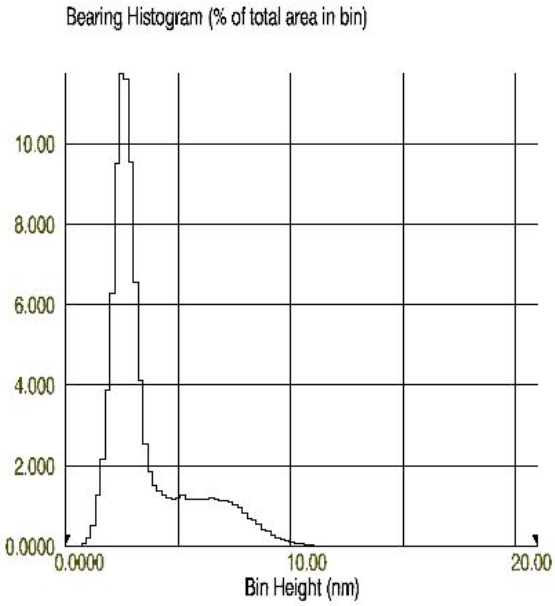

ApoE4 + Formaldehyde

b.

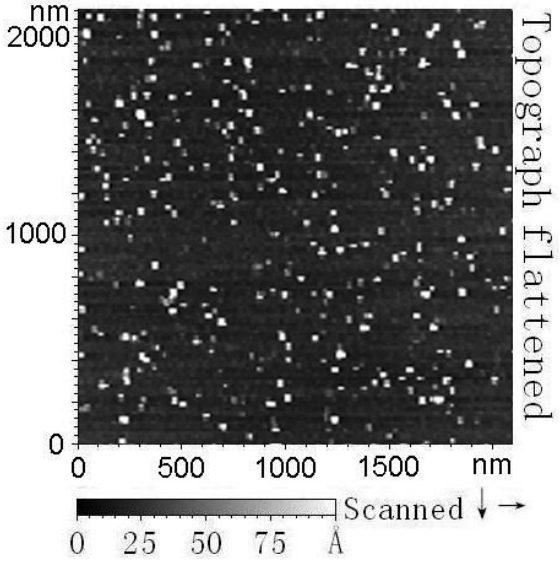

Aβ

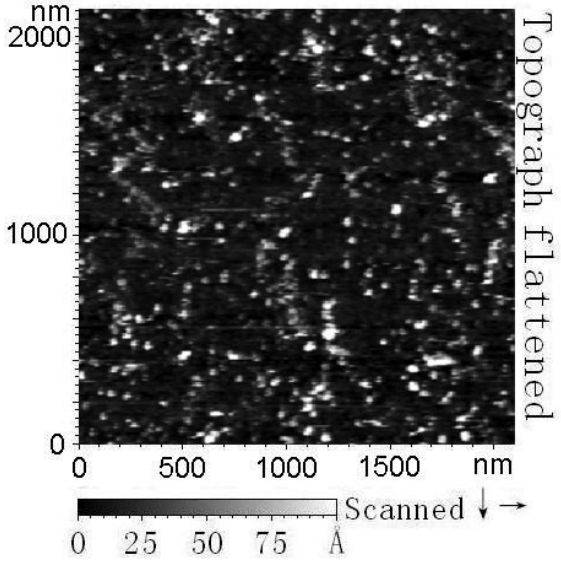

Aβ + Formaldehyde

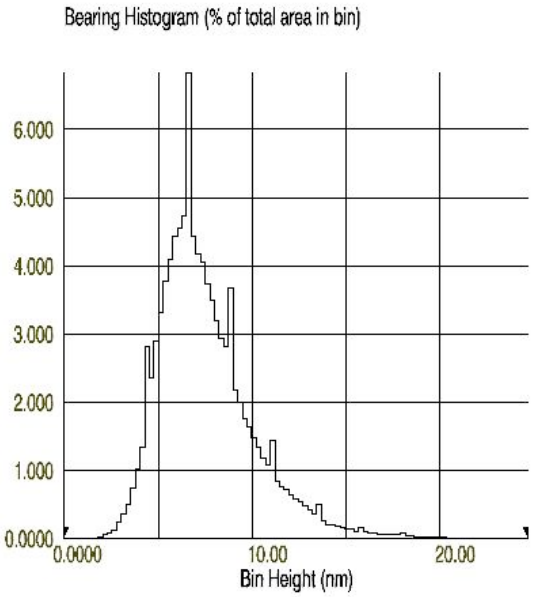

Aβ

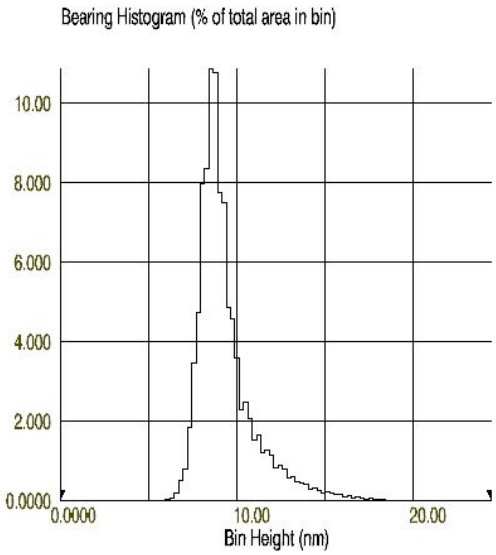

Aβ + Formaldehyde

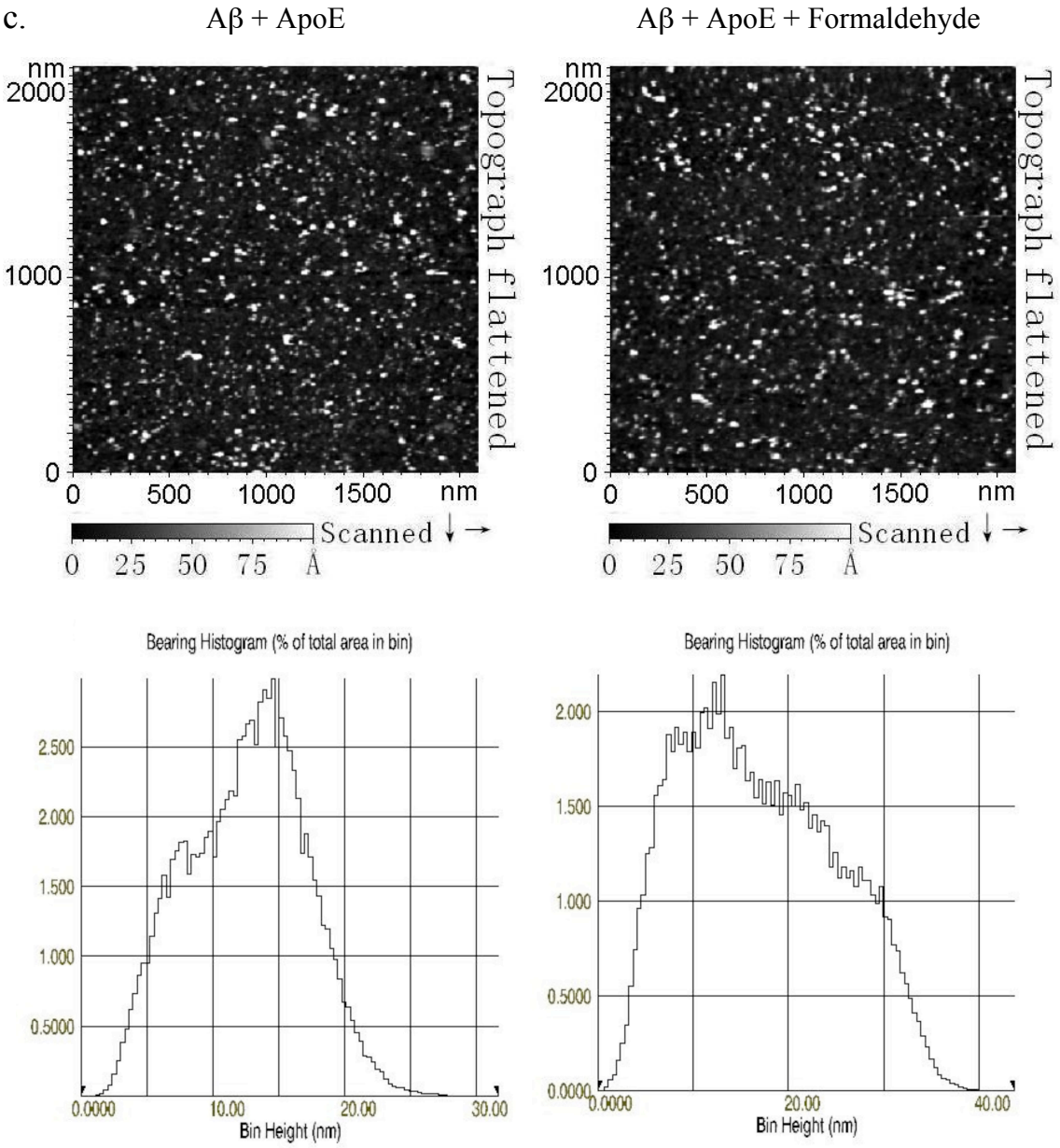

Figure 43. Effect of formaldehyde on Aβ-ApoE4 complex formation. (a) ApoE4 (100 μM) alone and (b) Aβ (100 μM) alone were individually incubated in the presence or absence of formaldehyde (1 mM) at 37º C for 24 h. (c) ApoE4 (100 μM) and Aβ (100 μM) were incubated together in the presence or absence of formaldehyde (1 mM) at 37º C for 24 h. After incubation, samples were observed under AFM using wet method as previously described. Bearing histograms show the distribution and shift sizes of aggregates sizes. The height (diameter) distribution of ApoE, Aβ and ApoE-Aβ complexes was calculated by software from Visual SPM Molecular Imaging Inc (Tempe, AZ, USA) and shown under each morphology image.

6. DISCUSSIONS

6.1 Overall Rationale

6.1.1 Endogenous Aldehydes and Aβ Aggregation

Aβ remains at the center of attention regarding pathology of Alzheimer's disease (Selkoe, 2008). Cytotoxic oligomers of Aβ, especially pentamers to 16'mers of $A\beta_{1-42}$, are responsible for cerebrovascular damage and neurodegeneration (Huang et al., 2000; Walsh et al., 2002; Gong et al., 2003). Yet, overproduction of Aβ in AD brains is rare. The accumulation of Aβ in most cases is a result of its enhanced oligomerization and impaired clearance.

Aldehydes produced from oxidative deamination, LPO and other sources including methylglyoxal, malondialdehyde and HNE, are elevated in AD patients. Some of these aldehydes were also found to be bound to senile plaques (reviewed in Section 1.1.5). However, whether elevated aldehyde levels could be involved in Aβ aggregation such as oligomerization and fibrillogenesis, cytotoxicity and clearance has not been studied.

The compartments, where endogenous aldehydes are produced, are crucial for their potential interactions with Aβ. Intracellular aldehydes would be quickly metabolized by cellular defense system, for example, aldehyde dehydrogenase (in the presence of NAD cofactor), before reacting with and denaturing other biological macromolecules. On the vascular surface aldehydes derived from SSAO-mediated reactions (formaldehyde and methylglyoxal) or from membrane lipid peroxidation (malondialdehyde and HNE) would not be readily metabolized due to absence of scavenging enzymes. Aβ is produced on and secreted from the cytoplasmic membranes. These aldehydes would have sufficient time and chance to crosslink Aβ and other adjacent proteins. Lysine and arginine residues of proteins are the primary targets for aldehydes. Indeed, modified lysine by methylglyoxal has been found to be increased during aging (Ahmed et al., 1997).

In the brain SSAO is exclusively associated with cerebral blood vessels (Zuo and Yu, 1994). This is the location, where Aβ clearance takes place as well as Aβ accumulates and forms CAA in AD (Alonzo et al., 1998; Shibata et al., 2000). Colocalization of cerebral vascular SSAO and perivascular Aβ deposition in AD brains has been observed (Unzeta et al., 2007; Jiang et al., 2008).

Based on these findings, it is reasonable to postulate that aldehydes produced in vicinity of Aβ react with Aβ, modify its structure and enhance its aggregation by inducing protein crosslinkage. Their interaction occurs in a chronic and accumulative manner, which contributes to Aβ accumulation and plaque formation, leading to increased neurotoxicity.

6.1.2 Endogenous Aldehydes and Aβ Clearance

Amyloid tends depositions around cerebral blood vessels have been detected in most AD cases (Yamada et al., 1987; Ellis et al., 1996). Aβ is eliminated from the CNS into blood circulation *via* cerebrovascular LRP-1 (Shibata et al., 2000). It has been proposed that aging, vascular disorders and AD cause dysfunction of cerebrovascular components including LRP-1, which impairs Aβ clearance and lead to perivascular Aβ accumulation (Zlokovic, 2005, 2008b). Indeed, impaired function and reduced expression of LRP-1 have been observed in AD brains (Jeynes and Provias, 2008). However, the mechanism is unclear.

In the CNS, SSAO and LRP-1 are both richly expressed on the cell surface of cerebral vasculature (Zuo and Yu, 1994; Shibata et al., 2000). Vascular SSAO catalyzes the production of cytotoxic aldehydes, hydrogen peroxide and ammonia in the extracellular compartment (Yu and Zuo, 1996). These toxic products are not readily scavenged and exert oxidative damage of the blood vessels. Increased plasma SSAO activity was found to be associated with a number of vascular disorders including AD (reviewed in 1.2.3.5). We found that products derived from cerebral SSAO-mediated reactions inactivate the adjacent LRP-1. This finding has provided a novel mechanism of the chronic Aβ accumulation around blood vessel and formation of CAA.

6.1.3 Methylglyoxal and Aβ Influx *via* RAGE

Aβ is also produced in the peripheral system (Li et al., 1999). Peripheral Aβ peptides can be transported from blood circulation into the brain *via* RAGE on the cerebral blood vessels (Deane et al., 2003). RAGE expression was upregulated during aging and in AD patients (Yan et al., 2000; Lue et al., 2001a; Simm et al., 2004; Jeynes and Provias, 2008; Cho et al., 2009). Methylglyoxal produced from glycolysis and SSAO-mediated deamination of aminoacetone contributes to AGEs formation (Thornalley et al., 1999; Mathys et al., 2002). Therefore, it is reasonable to speculate increased production of methylglyoxal contributes to AGEs formation and upregulate RAGE expression, enhancing Aβ influx into the CNS.

In summary, the effects of aldehydes produced from SSAO-mediated reactions and other sources on Aβ β-sheet formation, oligomerization and fibrillogenesis, oligomer cytotoxicity and clearance collectively contribute to Aβ accumulation in the brain, particularly the formation of CAA. The process is schematically illustrated in Figure 44. The potential role of cerebral vascular SSAO in Aβ aggregation and clearance explains why a large portion of amyloid is associated with brain blood vessels in AD. Moreover, hydrogen peroxide and ammonia from SSAO-catalyzed reactions are toxic and cause further oxidative damage to the cerebral vasculature, which could contribute to the development of AD. Vascular damage could release the membrane-bound SSAO into blood circulation. This explains why plasma SSAO activity in AD patients was elevated (del Mar Hernandez et al., 2005). SSAO is upregulated in response to inflammatory factors and tissue damage. Formaldehyde produced from SSAO-catalyzed reactions induces inflammation and further upregulates SSAO activity. The increased production of toxic products causes more damage and inflammation, therefore creating a vicious cycle that chronically and accumulatively leads to neurodegeneration and onset of dementia.

6.2 Effects of Endogenous Aldehydes on Aβ Aggregation

6.2.1 Enhancing the Rate of Aβ Oligomerization and Increasing Sizes of Aβ Oligomers

Folding of proteins to form functional tertiary configurations is an essential biochemical process. The amino acid sequence and environmental factors determine how proteins fold (Anfinsen, 1973). In AD, Aβ peptides not only fold but also aggregate with themselves and subsequently with other proteins. Although it is unclear whether this process is physiological or a metabolic accident, the aggregation products such as Aβ oligomers (5–16'mers) are toxic towards neurons (Lambert et al., 1998b; Parks et al., 2001; Demuro et al., 2005) and further aggregation leads to formation of senile plaques (Iwatsubo et al., 1994). Aβ oligomers are capable of inhibiting LTP that is crucial for memory formation (Walsh et al., 2002; Cleary et al., 2005). It is therefore considered a process of protein misfolding. Protein misfoldings have been found to associate with a variety of disorders (reviewed in section 1.1.4.3).

A lot of factors affect Aβ aggregation. For instance, ApoE4 enhances Aβ polymerization and subsequently deposit in Aβ plaques (Holtzman et al., 2000; Arelin et al., 2002). Reactive carbonyl metabolites, for example, aldehydes generated from cholesterol ozonolysis during inflammation, have been shown capable of modifying Aβ peptide covalently and accelerating

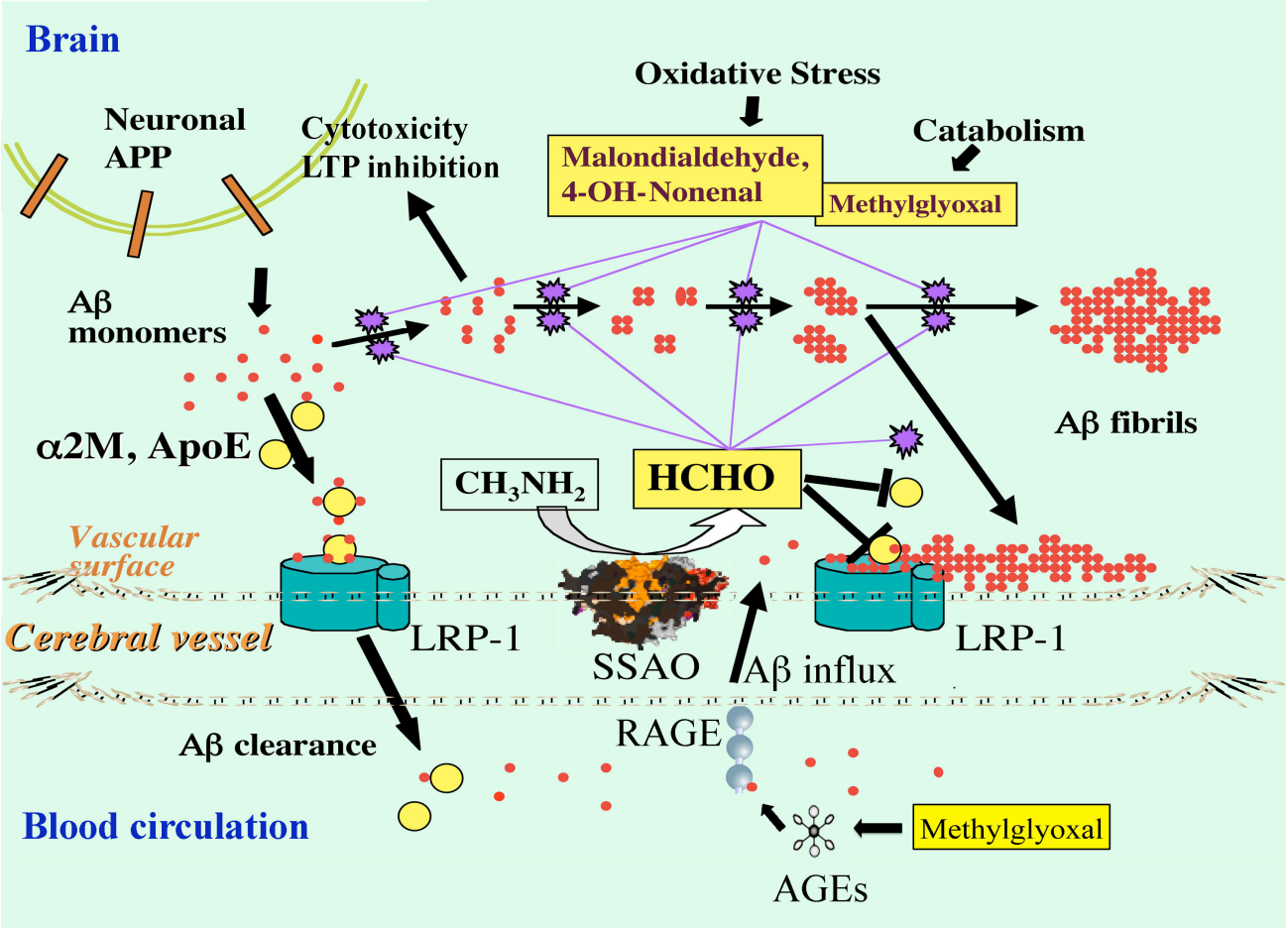

Figure 44. The potential involvement of SSAO-mediated deaminations in Aβ oligomerization and fibrillogenesis, cytotoxicity and clearance; implications to CAA (unpublished, modified from Dr. Yu with permission). Endogenous aldehydes produced from various sources react with Aβ and enhance its aggregation. Increased production of Aβ oligomers leads to more LTP inhibition and cytotoxicity. Formaldehyde and methylglyoxal produced from vascular SSAO could exert in situ modification on LRP-1 and impair its function. Aβ clearance is subsequently damaged. Methylglyoxal increases AGEs formation, upregulate RAGE expression and cause more peripheral Aβ influx into the CNS. These pathways collectively increase Aβ accumulation in the brain, accelerating the progression of AD.

Aβ aggregation (Wentworth et al., 2003; Zhang et al., 2004). Endogenous aldehydes including formaldehyde, methylglyoxal, malondialdehyde and HNE, are derived from various processes, such as oxidative deamination, LPO and hyperglycemia-induced glycolysis. These reactions are all known risk factors for AD (Dei et al., 2002; Ferrer et al., 2002; de la Monte and Wands, 2005; Pamplona et al., 2005).

The present study revealed the effects of endogenous aldehydes on Aβ aggregation *in vitro*. The concentrations of Aβ and aldehyde have become a limiting factor to study their interactions. In order to assess the aggregation process in a relatively short period of time, the concentration of Aβ was from 50 to 200 μM and aldehyde concentrations ranged from 1 μM to 10 mM. These concentrations seem to be much higher than reported *in vivo* levels of aldehydes (1 to 10 μM) (Cighetti et al., 1999; Kuhla et al., 2005) and Aβ (~nM) (Haass et al., 1992). However, the distribution of Aβ is very uneven. The *in situ* concentrations, *i.e.* on the cell surface, could be much higher than the circulatory levels such as in the CSF and blood. Formaldehyde and methylglyoxal are extremely reactive. Under *in vivo* situation, the interaction between these aldehydes and Aβ takes place over a very long period of time. The reaction is chronic and accumulative. It will achieve the same end results as of the acute *in vitro* experimental situation.

We applied a variety of structural techniques including ThT-T fluorometry, CD spectrometry, DLS and AFM imaging to reveal the potential effects of aldehydes on various stages of Aβ aggregation.

In ThT fluorometry and CD spectroscopy the effect of aldehydes on Aβ β-sheet formation diminished over time. This is due to that these methods are unable to detect the β-sheets conformation in advanced Aβ assembly. After prolonged incubation (Figure 14 and 20), advanced aggregates such as Aβ protofibrils and fibrils, begin to form. Notably, in Figure 14 a, b and c, after 120 h of incubation, the β-sheet amount of control group detected by ThT varied among experiments. It suggests that a large amount of fibrils have been formed, which made ThT unable to detect β-sheet accurately. This observation (Figure 16c) is consistent with other studies (Liu et al., 2004; Stanyer et al., 2004b). One study using CD spectroscopy reported that the amplitudes of negative peaks representing β-sheet structure were all close to zero after prolonged incubation (Stanyer et al., 2004b). A drawback of ThT and CD methods is they cannot provide information on the sizes of Aβ aggregates.

To study the effect of aldehydes on the sizes of Aβ aggregates, DLS technique was applied. The molecular-size distributions of Aβ particles in solution were analyzed. Interestingly, formaldehyde and malondialdehyde exhibited similar effect on β-sheet formation in ThT assay. Malondialdehyde appeared to be more effective distinctly from other aldehydes, as shown in the DLS experiment (Figure 17). Such an effect suggests that in addition to increasing β-sheet formation, malondialdehyde is more potent at enhancing Aβ intermolecular interactions. This observation is also consistent with an earlier report on protein crosslinking property of malondialdehyde and HNE (Esterbauer et al., 1991). DLS analysis is designed for measuring globular proteins and it is suitable for analyzing Aβ oligomerization.

Similar to ThT fluorometry, the count rates of Aβ reached a plateau after 48 h of aggregation, when protofibrils began to form. However, the mechanism of assessment of aggregation by DLS is different. DLS monitors the Brownian motion of particles by measuring photon deflection. Fibril-shaped molecules would cause large variations in the number of scattered and detected photons. In this case, the values of measurement will be considered as errors and rejected by the instrument. Therefore, DLS is only suitable for analyzing globular Aβ oligomers. During Aβ aggregation, when the number of oligomers increases, they start to assemble into protofibrils. In this stage, the number of photons scattered by oligomers will be stable, leading to a plateau in count rate.

AFM imaging has been applied in studying morphologies of various biological molecules. Compared to the traditional EM, it has some advantages. AFM is capable of providing a true three-dimensional surface profile. In AFM, there is no special treatment procedure for samples as required in EM that may alter their structures. AFM can work in an ambient or liquid environment, whereas EM requires to be operated in a vacuum environment. However, EM can observe an area on the order of millimeters with a depth of field on the order of millimeters. AFM can only scan a maximum view area of 100 μm by 100 μm with a maximum height of several microns.

In the present studies, AFM imaging not only revealed the effects of aldehydes on the morphologies of oligomers, protofibrils and fibrils, but also estimated their reaction rates and sizes of the aggregates based on the surface heights in the scans. In the initial AFM experiments, prior to imaging, Aβ in PBS buffer was dropped on a mica surface for up to 2 minutes to allow adhesion. The mica surface was then rinsed with nanopure water to remove the buffer salts and

obtain a relatively even distribution of Aβ. However, as Aβ oligomers are water soluble, rinsing the mica piece with water would remove the majority of adhered oligomers, which would prevent the observation of Aβ aggregates. Omitting the rinsing step causes crystallization of buffer salts that interferes with the AFM scan. This difficulty was overcome by replacing PBS buffer with a volatile buffer (ammonia/formic acid) and bringing samples to dryness without rinsing. The formaldehyde- and methylglyoxal-modified Aβ were observed under ambient condition (known as dry method). Subsequently, a wet AFM method was applied for examination of the effects of malondialdehyde and HNE because these aldehydes were in salt form and thus would form crystals at dryness. Aldehydes were found not only increase the number but also the size of the oligomers (by about 1 to 2 nm in diameter shown in Figure 20 and 21). The increase in oligomer diameters may result from addition of carbon atoms after conjugation with the aldehyde or increase in the number of monomers aggregated into each oligomer. Aldehydes could even alter the forms of aggregation. How aldehydes modify the tertiary structure of Aβ aggregates needs other technology.

In general, formaldehyde, methylglyoxal and malondialdehyde exhibit similar effects on Aβ oligomerization and fibrillogenesis (Chen et al., 2006). The effect of HNE is somewhat limited under present experimental conditions. The longer aliphatic chain of HNE may hinder its kinetic property of interacting with proteins. Such a relative weak effect of HNE on Aβ oligomerization agrees with an earlier report (Stanyer et al., 2002). Other studies found that HNE is capable of modifying and increasing Aβ hydrophobicity to turn it more prone to aggregation (Qahwash et al., 2007; Liu et al., 2008). HNE was also found to enhance the formation of Aβ protofibrils (Siegel et al., 2007). In these studies, the conditions of interaction between HNE and Aβ were different including incubation time, concentration and pH.

6.2.2 Potential Mechanisms of Aldehyde-Aβ Interactions

Formaldehyde generated *via* SSAO-mediated deamination of methylamine was shown to crosslink with proteins *in vivo* (Yu and Zuo, 1996). Lysine and arginine residues are the primary targets of Aβ for formaldehyde (Gubisne-Haberle et al., 2004). Such an interaction is illustrated in Figure 45. Another mechanism of reaction is by a two-step reaction (Esterbauer et al., 1991; Kalasz, 2003):

$$\text{Lysine-NH}_2 + \text{HCHO} \Leftrightarrow \text{Lysine-NH-CH}_2\text{-OH}$$

$$\text{Lysine-NH-CH}_2\text{-OH} + \text{HCHO} \Leftrightarrow \text{Lysine-NH-CH}_3 + \text{HCOOH}$$

Either pathway will add a methyl group to the free ε-amino group on lysine to form N-methyl-lysine.

Aβ peptide possesses two lysine (Lys16 and Lys28) residues and one arginine (Arg5) residue and therefore readily interacts with aldehydes. We confirmed that lysine residues of Aβ are subject to interaction with formaldehyde by detection of N-methyl-lysine using HPLC (Chen et al., 2007). Between Lys16 and Lys28 is a lipophilic domain (recall the importance of residues 17 to 21 in Aβ aggregation) and it interacts and folds with another lipophilic domain at the N-terminus of Aβ (Petkova et al., 2002). Modification of the lysine residues by aldehydes would alter the lipophilicity and flexibility of the lipophilic domain of Aβ in favor of stabilizing the folding. Subsequently, it may form intermolecular methylene bridges and stabilize the aggregation products. The potential mechanism of interaction between Aβ and aldehydes is illustrated in Figure 46.

Although formaldehyde preferably reacts with lysine residue, depending on the ambient conditions, it also interacts with other amino acid residues of proteins in a much more complex manner (Metz et al., 2004). In fact, the FMOC-HPLC experiments showed that in the formaldehyde-induced Aβ aggregates, not only the lysine residue was modified, but also several other amino acids were affected including glutamate and arginine suggesting a complicated mechanism of reaction.

Information on concentrations of aldehydes and Aβ in the brain is limited. Highly reactive aldehydes produced would immediately react with adjacent molecules. The assessment of free aldehydes in tissues does not directly reflect the concentrations at the compartments of their generation. The local concentrations of these aldehydes, such as on the cell surface of vascular endothelial and smooth muscle cells, could be much higher. Nevertheless, the concentration of methylglyoxal in the CSF from AD patients is 20 to 40 μM, compared to 10 to 15 μM in the control population (Kuhla et al., 2005). The concentration of formaldehyde in human blood is 2 to 3 mg/L (67 to 100 μM) according to World Health Organization. Methylamine in blood is normally at 1 to 5 μM and 10 to 20 μM in uremic human plasma (Wingender, 1983; Baba et al., 1984). It is unclear how much circulatory formaldehyde is derived from deamination of methylamine in the blood. Concentrations of malondialdehyde and HNE are as high as 1.3 μM

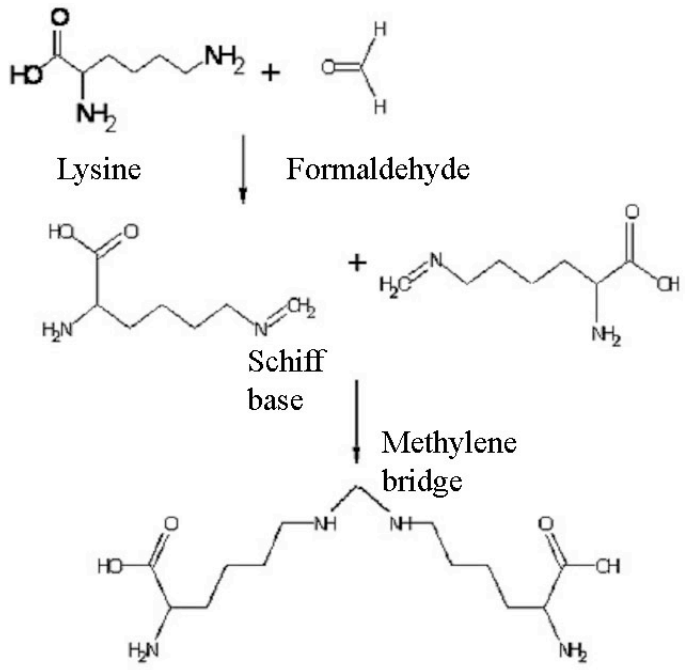

Figure 45. Mechanism of reaction between formaldehyde and lysine. Formaldehyde and the ε-amino group of lysine form a Schiff base. Under physiological conditions, Schiff bases are not stable and when they are close to each other, two Schiff bases form a methylene bridge. As a consequence, two lysines groups are crosslinked, which induces both intra- and intermolecular crosslinkage.

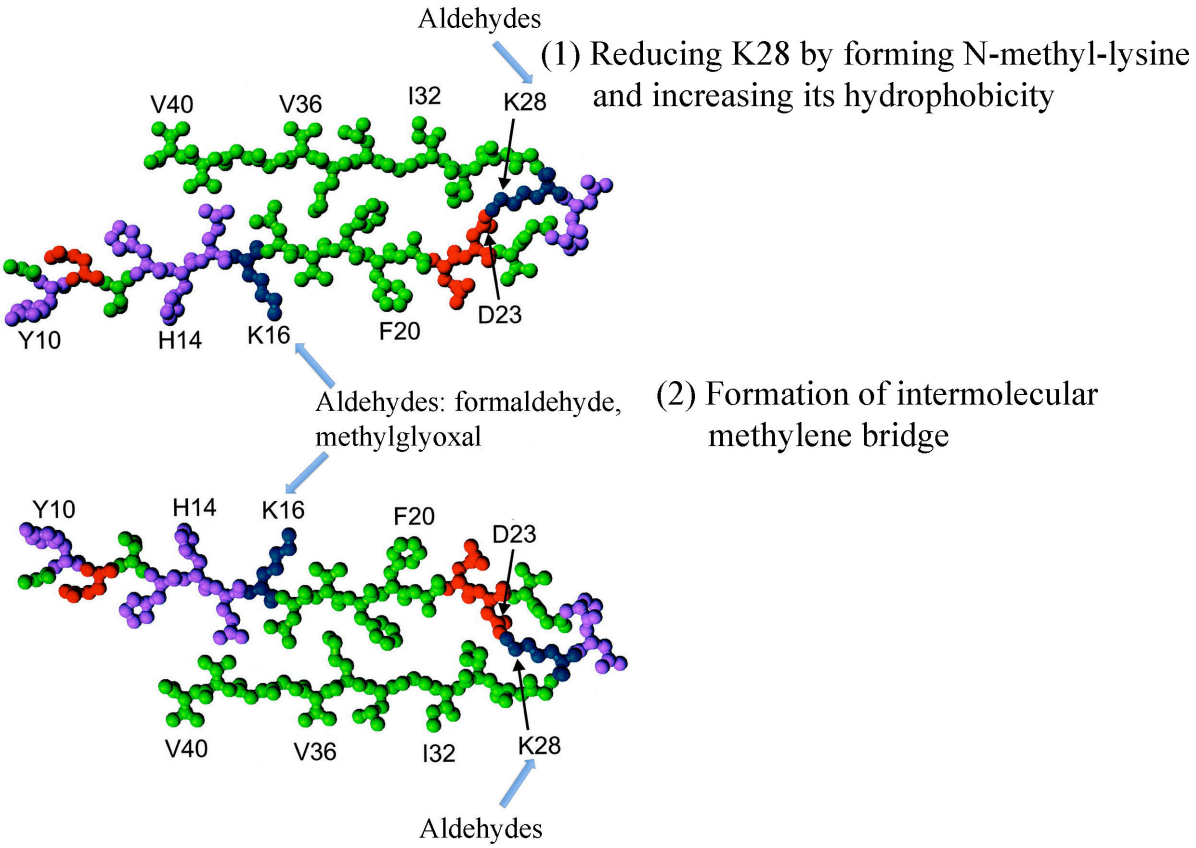

Figure 46. Potential mechanisms of Aβ crosslinkage by aldehydes based on solid NMR experiment (Petkova et al., 2002). Aldehydes preferably react with the lysine residues on Aβ peptides. One mechanism is that aldehydes modify the lysine residue to form N-methyl-lysine and increase Aβ hydrophobicity. Another mechanism is that aldehydes react with lysine residues on Aβ and form intermolecular methylene bridges, after which Aβ peptides are crosslinked. Both mechanisms enhance Aβ aggregation.

and 100 μM, respectively (Benedetti et al., 1984; Cighetti et al., 1999). As for Aβ, its level in the CSF is normally at 1 nM (Haass et al., 1992). However, Aβ distribution in the brain is probably vastly uneven. The cell membrane surface may possess much higher concentration of Aβ since it is subject to translocation and clearance.

The concentrations of endogenous aldehydes *in vivo*, which are generated *via* deamination of short chain aliphatic amines, lipid peroxidation and glucose metabolism, are likely insufficient to cause massive protein crosslinkage or acute cytotoxicity. However, the interaction of aldehydes with proteins, especially structural proteins, is in a chronic, irreversible and accumulative manner following a pseudo first-order kinetic mode. Indeed, protein misfolding and subsequent formation of plaques, *i.e.* amyloidosis, is a very slow and chronic process as seen in many chronic disorders including type 2 diabetes and AD.

6.3 Effect of Aldehyde Modification on Aβ Cytotoxicity

Research on Aβ cytotoxicity has evolved from plaques, fibrils and protofibrils to oligomers (Lorenzo and Yankner, 1994; Harper et al., 1999; Bitan et al., 2001). Aβ oligomers (5 to 16'mer) induce LTP inhibition and subsequent neurodegeneration (Lambert et al., 1998b; Walsh et al., 2002). More recently, Aβ dimers and trimers, seem to be the very first toxic intermediates during Aβ aggregation (Hung et al., 2008; Selkoe, 2008). It is therefore interesting to delineate whether aldehyde may alter the cytotoxicity of Aβ oligomers.

Aldehydes are able to modify Aβ structure and increase the average size of Aβ oligomers probably resulting from addition of extra carbons (Chen et al., 2006). The cell survival assays (MTT and LDH assays) indicated that the formaldehyde-induced oligomers are slightly but significantly more (~10%) cytotoxic compared to the untreated Aβ oligomers. By measuring apoptosis, formaldehyde-modified oligomers triggered an increase (~20%) in caspase-3 activity compared to the native oligomers in SH-SY5Y cells. AFM, dot-blot assay and SEC experiments have demonstrated that formaldehyde increased the production of oligomers for about 5 folds. Moreover, with formaldehyde-induced oligomers being more cytotoxic (10 to 20%), the final total cytotoxicity of Aβ would be significantly increased after interactions with aldehydes. It remains to be investigated whether/how endogenous aldehydes could affect the oligomers of Aβ under physiological or pathological conditions. The reaction between Aβ and aldehydes may not

be as dramatic and rapid; yet, increased aldehydes levels provide a constant stressful and toxic condition in favor of a slow but accumulative oligomerization process over a very long period of time. Such a chronic accumulative cytotoxicity could lead to gradual damage of cerebrovasculature as well as neurodegeneration, which consists with the slow progression of AD.

A potential mechanism of Aβ cytotoxicity was proposed, namely, Aβ binds to cell membrane by its hydrophobicity and exert nonspecific toxicity by increasing membrane conductance/permeability (Klunk et al., 1999; Kayed et al., 2003; Datki et al., 2004; Kayed et al., 2004). Indeed, HNE is capable of modifying Aβ structure on specific sites and increasing its lipophilicity and affinity to cell membrane (Qahwash et al., 2007; Liu et al., 2008). There is another aspect towards cytotoxicity of Aβ, namely, it is a receptor-dependent process. In SH-SY5Y cells, LRP-1 (Fabrizi et al., 2001; Wilhelmus et al., 2007) and RAGE (Yan et al., 1996) were claimed involved in mediating Aβ cytotoxicity. SH-SY5Y cells normally express a low level of RAGE which is significantly upregulated by Aβ treatment for 24 h (Cho et al., 2009). In the present study, SH-SY5Y cells were treated with Aβ for up to 24 h. Therefore, it is possible that Aβ oligomers upregulated RAGE expression during the experiments.

It is important to note that, in the present study the cells were treated with oligomers for a period from 3 to 24 h before cell survival assays. The oligomers would probably continuously aggregate during this treatment period of time. Based on results shown in Figure 14 and 20, from 12 h on the oligomers already start to form protofibrils. The cytotoxicity measured by the assays could be caused by the mixture of oligomers and less cytotoxic protofibrils. However, the concentrations of Aβ oligomers used for treatment of the cells (5 to 50 nM) were much lower than those concentrations used in the aggregation study (100 to 200 μM). It is possible that the Aβ oligomerization process would be slower at such low concentrations.

6.4 The Role of Vascular Surface SSAO on LRP-1 Function

6.4.1 LRP-1 and SSAO on Cerebral Vasculature

The cerebral capillaries are surrounded by pericytes which belong to VSMC lineage (Allt and Lawrenson, 2001). VSMCs contribute to the stability of cerebral microvessels by regulating matrix deposition (Armulik et al., 2005). VSMCs also regulate angiogenesis and microvascular permeability (Dore-Duffy and LaManna, 2007). In AD patients, the total length of cerebral

capillaries, microvascular densities and diameters are reduced (Bailey et al., 2004). This regression reduces the transport of energy, nutrients, and potential neurotoxins across BBB. Subcortical ischemic lesions and microinfarcts are important contributors to cognitive deficits in aging and AD (Pantoni et al., 1999; Kalmijn et al., 2000; Kovari et al., 2004). Therefore, AD is recognized as a cerebral vascular disease and it shares many common risk factors with other vascular disorders/diseases such as atherosclerosis (Casserly and Topol, 2004).

SSAO contributes to a number of vascular disorders such as atherosclerosis and stroke, which is attenuated by SSAO inhibitor (Yu and Deng, 1998; Meszaros et al., 1999a; Conklin et al., 2004; Kazachkov et al., 2007; Airas et al., 2008). In the CNS, SSAO is expressed exclusively on cerebral VSMCs and endothelial cells, producing toxic aldehydes from primary amines to cause damage to brain blood vessels. Therefore, chronic accumulative carbonyl stress and oxidative damage due to increased SSAO-mediated reactions may impair cerebrovascular functions, cause vascular disorders in the brain and increase the risk of AD.

The accumulation of Aβ in AD brains results from impaired Aβ clearance from the CNS. Cerebrovascular LRP-1 plays a crucial role in Aβ efflux from the CNS into the blood circulation (Shibata et al., 2000). The cause of LRP-1 impairment in AD is unclear. It has been proposed that cerebral vasculature dysfunction is responsible for LRP-1 dysfunction (Zlokovic, 2004). We have obtained some evidence that cerebral VSMC LRP-1, as the mediator of Aβ clearance, is affected by SSAO-catalyzed deaminations. LRP-1 is the largest member of the LDL receptor family, with 31 repeats of ligand-binding domains (Nykjaer and Willnow, 2002). These binding domains and the interactions with co-receptors are responsible for its wide range of ligands (May et al., 2007). The structure of LRP-1 is illustrated in Figure 47. Aldehydes produced from SSAO impair nearby LRP-1, probably by modifying its long extracellular domains. The binding sites on LRP-1 for its substrates, including α2M, ApoE, and Aβ, can be altered by aldehydes.

6.4.2 Experiment Model

In order to study the potential effect of SSAO-catalyzed reactions on LRP-1 function, a cell model expressing both SSAO and LRP-1 is required. Unfortunately, primary culture of VSMCs does not express SSAO after subculture. The exact cause is still unclear. It may result from matrix metalloproteinase cleavage, collagenase or trypsin shedding from membrane during digestion and subculture, lack of posttranslational modification of the enzyme, *i.e.*

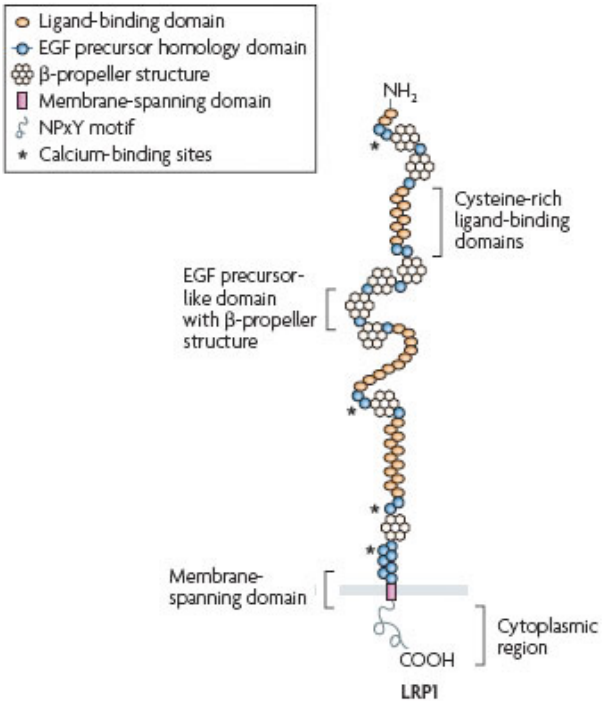

Figure 47. The structure of LRP-1 (Jeon and Blacklow, 2005; Wasan et al., 2008). EGF: epidermal growth factor. The β-propeller structure is composed of Tyr-Trp-Thr-Asp. The cytosolic NPxY motif is responsible for signal transduction. The asterisks indicate the regions stabilized by calcium binding.

incorporation of cofactors TPQ or Cu (II), altered environment triggering signaling pathways that suppress SSAO expression, or lack of contact with the basement membrane compartment that may be required for SSAO expression. Although LRP-1 is expressed, primary culture and cells missing of SSAO cannot be applied for the present investigation.

In the present study, freshly isolated aortic and meningeal VSMCs were used. These cells possess both active SSAO and LRP-1. α2M is a well-known substrate for LRP-1 (Shibata et al., 2000). Its uptake was used as an indicator for LRP-1 function. Methylamine significantly reduces α2M uptake in both aortic and meningeal VSMCs. Selective SSAO inhibitor blocks such reduction. During the time period of uptake experiments, the cell viability was not affected by either formaldehyde or methylamine under the concentrations used. The reduction in α2M uptake was therefore not due to decreased cell viability. Formaldehyde but not hydrogen peroxide exhibited similar effects as of methylamine. The results suggest that aldehydes produced from SSAO-catalyzed reactions are responsible for reduced α2M uptake and thus they impair LRP-1 function. It seems reasonable to conclude that aldehydes generated *via* SSAO-mediated deaminations inactivate adjacent LRP-1 on the cell membranes. It changes the configuration of LRP-1 and affects α2M recognition and binding.

6.4.3 Mechanisms of Aβ Uptake by Isolated VSMCs

α2M is able to facilitate Aβ uptake *via* LRP-1 (Shibata et al., 2000). VSMCs, which express both SSAO and LRP-1, are a useful model for studying the effects SSAO-mediated reactions on LRP-1 function and on Aβ endocytosis. Logically, the amount of Aβ endocytosis *via* VSMCs is proportional to α2M uptake level. Although deamination of methylamine has been shown to reduce α2M uptake by VSMC LRP-1, it did not reduce Aβ uptake. In this model, the level of Aβ in VSMCs was not directly correlated to α2M level (Figure 39). The mechanism is currently unclear.

This model has been complicated by the facts, that first, LRP-1 is very sensitive to formaldehyde (see section 5.3.4). It modifies the α2M binding site on LRP-1 and thus affect α2M uptake *via* VSMCs. There are conflicting reports regarding whether Aβ absolutely needs α2M as a carrier protein for LRP-1 (Shibata et al., 2000; Deane et al., 2004; Ito et al., 2007;

Wilhelmus et al., 2007). LRP-1 could possess different binding sites for α2M and Aβ, therefore Aβ could bind to LRP-1 independently (without α2M as a carrier).

Secondly, Aβ binds to cell membrane nonspecifically *via* hydrophobic interaction (Datki et al., 2004). In our experiments, although after incubation the cells were repeatedly washed and centrifuged to remove the loosely membrane-bound Aβ, it did not rule out the possibility that trace amount of Aβ was still associated with the cell surface. Using isolated VSMCs as a model to study Aβ endocytosis, the amount of Aβ measured by Western blot was the sum of uptaken Aβ *via* LRP-1 and the membrane-bound Aβ attached on the cell surface. It is difficult to differentiate between the intracellular Aβ and non-specific membrane-bound Aβ.

Thirdly, formaldehyde derived from methylamine may increase Aβ oligomerization and its hydrophobicity. This would be in favor of Aβ deposition on the cell membrane. The results seem to suggest that in the presence of α2M, formaldehyde increases Aβ aggregation even more. α2M seems to facilitate Aβ aggregation instead of endocytosis in this system. It is therefore difficult to determine the precise role of aldehyde on Aβ endocytosis.

Moreover, the type II collagenase used for isolation of VSMCs is potent at degrading Aβ. Residual collagenase activity digests most Aβ in 2 h during experiments. In later experiments a collagenase inhibitor (Z-PDLDA-NHOH from Calbiochem, EMD Biosciences, La Jolla, CA USA) was included along with Aβ. The recovery of Aβ was improved, but a large portion of Aβ was still degraded by the residual collagenase activity. Therefore, it is difficult to determine how much Aβ was actually available for VSMCs to uptake. The observation that type II collagenase is potent at degrading Aβ is novel. It seems worthy of checking other types of collagenases in hydrolyzing Aβ. Currently, only IDE (insulin-degrading enzyme) and neprilysin were reported to be involved in proteolysis of Aβ (Iwata et al., 2001b; Walsh et al., 2002). The finding also raises a general technical concern, namely, it should be cautious using collagenase in cell culture technology, to ensure that it does not affect the experiment.

Interestingly, Aβ peptides were found to upregulate LRP-1 expression in VSMCs after incubation for 3 days (Wilhelmus et al., 2007). In the present model, such an LRP-1 upregulation was unlikely, since the incubation time of the VSMCs with Aβ was only 2 h. LRP-1 level was assessed in the experiments and there was no significant change after Aβ treatment.

In brief, increased production of formaldehyde derived from deamination of methylamine on the VSMC surface impairs LRP-1 function. Formaldehyde may alter the configuration of the α2M binding site on LRP-1 and reduce its uptake as well as the associated transport of Aβ. Formaldehyde simultaneously enhances Aβ aggregation and increases its deposition on cell membrane. SSAO inhibitor is able to attenuate such effects. Under the present experimental conditions, the measurement of Aβ endocytosis *via* LRP-1 may be interfered by Aβ oligomerization and its binding to cell membrane. More investigations are required to clarify the mechanism of effects of formaldehyde on Aβ endocytosis by VSMCs.

6.4.4 Effects of Aldehydes on Aβ-α2M/ApoE Complexes Formation

α2M or ApoE serves as a carrier for Aβ, form complexes and function as LRP-1 ligands (Shibata et al., 2000; Bell et al., 2007; Deane et al., 2008). They are extended to aggregate and to form larger complexes, which can no longer be taken up by LRP-1 and cleared through BBB (Hughes et al., 1998; Moir et al., 1999; Ito et al., 2007). Subsequently, these complexes may deposit on cerebral vasculature and continue aggregation with Aβ as well as other molecules. This process eventually leads to typical CAA pathology (Ito et al., 2007). However, this has not sufficiently explained why Aβ and α2M or ApoE4 do not deposit on other types of cells in the brain. LRP-1 is widely distributed in the brain, including neurons and glia (Bu et al., 2006). In the present study, formaldehyde was found to crosslink Aβ with α2M or ApoE and enhance the formation of large aggregates. It suggests that aldehydes produced by VSMC SSAO play an important role in Aβ oligomerization and crosslinkage with other proteins adjacent to brain blood vessels. The unique localization of SSAO, *i.e.* only on the cerebral vasculature in the CNS, is particular interesting. It explains why Aβ deposition is often seen to be associated with blood vessels in vascular dementia and AD.

7. CONCLUSIONS

7.1 Summary of Major Findings

(1) Endogenous aldehydes generated from various sources including formaldehyde, methylglyoxal, malondialdehyde and HNE are capable of interacting with Aβ and increasing the rates of Aβ aggregation;

(2) Aldehydes affect every stage of Aβ polymerization including β-sheet formation, oligomerization and fibrillogenesis in a time- and concentration-dependent manner;

(3) Aldehydes are also capable of modifying the structure of Aβ peptide and increasing the sizes of Aβ oligomers *in vitro*;

(4) The primary target of aldehyde interaction is the lysine and/or arginine residues on Aβ peptides that forms Schiff bases. The Schiff bases react with each other to form stable intermolecular methylene bridges crosslinking Aβ molecules. Aldehydes also react with other amino acid residues of Aβ molecule leading to more complicated interactions;

(5) Aldehydes also crosslink Aβ with other proteins such as ApoE and α2M, to form large protein complexes. These large complexes cannot be eliminated from the CNS through cerebral vasculature, leading to formation of perivascular Aβ deposits and senile plaques;

(6) Formaldehyde-modified Aβ oligomers become slightly more cytotoxic compared to those of native Aβ;

(7) Formaldehyde substantially increases the rate of formation of Aβ oligomers. Therefore, the final total cytotoxicity would be significantly increased by aldehydes, suggesting the role of aldehydes in Aβ induced neurovascular damage and neurodegeneration;

(8) Aldehydes produced on the membrane surface, *i.e.* from cerebral vascular SSAO-catalyzed reactions or LPO, impair adjacent LRP-1 function. The endocytosis of its ligands, *i.e.* α2M and Aβ, is subsequently reduced. Specific SSAO inhibitors reverse such an effect by aldehydes;

(9) Since α2M is an Aβ carrier *via* LRP-1, the transcytosis of Aβ is affected by SSAO-mediated reactions. SSAO may contribute to the impairment of Aβ clearance *via* vascular LRP-1, which leads to deposits of Aβ in the brain;

(10) Type II collagenase is quite potent in degrading Aβ. This novel finding is implicated in the role of collagenase to Aβ degradation, and to other technical remark in cell culture studies on Aβ.

7.2 Future Directions of the Research

7.2.1 Effects of Aldehydes on Protein Misfolding

The present study has demonstrated that aldehydes are capable of enhancing Aβ aggregation *in vitro*. However, whether aldehydes can react with Aβ and enhance its aggregation *in vivo* remains to be substantiated. Malondialdehyde and HNE have been detected in senile plaques of AD brains by immunohistology studies (Montine et al., 1997; Sayre et al., 1997; Dei et al., 2002), which strongly supports the hypothesis that reactive aldehydes modify Aβ peptides, enhance their aggregation and contribute to plaque formation. To date there has been no reports demonstrating whether formaldehyde or methylglyoxal is associated with senile plaques in AD, although anti-methylglyoxal antibody is available now commercially.

Formaldehyde and methylglyoxal can be produced by SSAO-mediated deaminations. Transgenic mouse strain overexpressing human SSAO on the endothelium and/or VSMCs would be useful. In the future, this mouse strain can be crossed with the APP/PS1 transgenic mice, which are widely used for mimicking Aβ accumulation in AD. Using these SSAO/APP/PS1 triple transgenic mice, and with help of specific SSAO inhibitors, the role of SSAO-mediated deaminations in Aβ deposition, especially on the cerebral vasculature, may provide evidence on whether formaldehyde or methylglyoxal is involved in Aβ amyloidosis *in vivo*.

In addition to Aβ, a number of proteins (tau, islet amyloid polypeptide, α-synuclein, polyglutamine, human insulin and prion peptide) can lead to amyloidosis and are associated with a variety of diseases, such as type 2 diabetes, Down's syndrome, Parkinson's disease, Huntington's disease and Creutzfeldt-Jakob disease (Merlini and Bellotti, 2003; Cleary et al., 2005; Kovacs and Budka, 2008; Ono et al., 2008). The protein misfolding mechanisms of amyloidogenic peptides appear to be very similar (Kayed et al., 2003). HNE modifiess and affect

a variety of peptides including Aβ, tau and α-synuclein (Perez et al., 2000; Qin et al., 2007; Siegel et al., 2007). It is therefore of great interest to know whether endogenous aldehydes also affect amyloidosis of other peptides in general.

7.2.2 Effects of Aldehydes on Aβ Cytotoxicity

The mechanism of how Aβ oligomers induce cytotoxicity has not been fully established. Two popular mechanisms, namely, nonspecific hydrophobic binding of Aβ oligomers to cell membrane which affects membrane integrity, or binding of Aβ oligomers to LRP-1/RAGE receptors which triggers apoptotic pathways were proposed (Datki et al., 2004; Wilhelmus et al., 2007). It would be interesting to test whether the aldehyde-modified Aβ oligomers can affect these pathways.

Aβ oligomers isolated from AD brains including dimer, trimer and tetramer, were recently found to be potent in inhibiting LTP *in vivo* (Klyubin et al., 2008; Shankar et al., 2008). LTP inhibition is the early event of Aβ effects responsible for cognitive impairment in AD pathogenesis (Walsh et al., 2002; Klyubin et al., 2008; Selkoe, 2008). It is therefore interesting to know whether aldehydes alter the potency of Aβ oligomers in inhibiting LTP or inducing long-term depression.

7.2.3 Effects of Aldehydes on Aβ Clearance

An *in vivo* mouse model has been currently employed to assess Aβ clearance. Either ^{125}I-labeled or native Aβ was stereotaxically injected into certain brain areas including cortex, hippocampus and caudate putamen followed by quantitative measurement of peripheral radioactivity or by enzyme-linked immunosorbent assays (Shibata et al., 2000; Deane et al., 2004; Bell et al., 2007; Deane et al., 2008). The levels of peripheral Aβ and Aβ remaining in the CNS can be measured, and thus the rate of transcytosis through BBB can be determined. Aβ is cleared from the CNS into blood circulation. The turnover is very fast ($t_{1/2}$ = ~30 min) (Shibata et al., 2000). $A\beta_{1-42}$ can be cleared faster than $A\beta_{1-40}$, which was interpreted as why $A\beta_{1-40}$ tends to accumulate around cerebral vasculature to form CAA (Deane et al., 2004; Ito et al., 2007). *In vivo* investigations using Aβ stereotaxic injections in SSAO transgenic mice will provide important information on the involvement of SSAO-mediated reactions in Aβ transcytosis. It

would be possible to increase SSAO-mediated deamination, *i.e.* with administration of methylamine or using transgenic mice overexpressing SSAO. Also SSAO can be blocked by using specific SSAO inhibitors.

7.3 Significance and Clinical Implication

The present study is closely related to vascular dementia, AD, and perhaps other disease. The results have provided a link between elevated levels of aldehydes and amyloid aggregation observed in AD, by demonstrating that endogenous aldehydes from SSAO-mediated deaminations and other sources affect Aβ aggregation, cytotoxicity, and clearance. Such effects contribute to the formation of amyloid plaques, particularly CAA, in vascular dementia and in most cases of AD. The increase in Aβ aggregation leads to the production of more toxic oligomers causing neurodegeneration and vascular damage.

If the current hypothesis is further substantiated, SSAO would be an important new therapeutic target for the treatment of AD. Reagents that scavenge aldehydes may be beneficial in slowing down Aβ aggregation and the formation of perivascular plaques.

8. REFERENCES

Abella A, Garcia-Vicente S, Viguerie N, Ros-Baro A, Camps M, Palacin M, Zorzano A, Marti L (2004) Adipocytes release a soluble form of VAP-1/SSAO by a metalloprotease-dependent process and in a regulated manner. Diabetologia 47:429-438.

Abramov AY, Canevari L, Duchen MR (2003) Changes in intracellular calcium and glutathione in astrocytes as the primary mechanism of amyloid neurotoxicity. J Neurosci 23:5088-5095.

Aghajanian GK, Graham AW, Sheard MH (1970) Serotonin-containing neurons in brain: depression of firing by monoamine oxidase inhibitors. Science 169:1100-1102.

Ahmed MU, Brinkmann Frye E, Degenhardt TP, Thorpe SR, Baynes JW (1997) N-epsilon-(carboxyethyl)lysine, a product of the chemical modification of proteins by methylglyoxal, increases with age in human lens proteins. Biochem J 324 (Pt 2):565-570.

Airas L, Mikkola J, Vainio JM, Elovaara I, Smith DJ (2006) Elevated serum soluble vascular adhesion protein-1 (VAP-1) in patients with active relapsing remitting multiple sclerosis. J Neuroimmunol 177:132-135.

Airas L, Lindsberg PJ, Karjalainen-Lindsberg ML, Mononen I, Kotisaari K, Smith DJ, Jalkanen S (2008) Vascular adhesion protein-1 in human ischaemic stroke. Neuropathol Appl Neurobiol 34:394-402.

Akiyama H, Barger S, Barnum S, Bradt B, Bauer J, Cole GM, Cooper NR, Eikelenboom P, Emmerling M, Fiebich BL, Finch CE, Frautschy S, Griffin WS, Hampel H, Hull M, Landreth G, Lue L, Mrak R, Mackenzie IR, McGeer PL, O'Banion MK, Pachter J, Pasinetti G, Plata-Salaman C, Rogers J, Rydel R, Shen Y, Streit W, Strohmeyer R, Tooyoma I, Van Muiswinkel FL, Veerhuis R, Walker D, Webster S, Wegrzyniak B, Wenk G, Wyss-Coray T (2000) Inflammation and Alzheimer's disease. Neurobiol Aging 21:383-421.

Aleardi AM, Benard G, Augereau O, Malgat M, Talbot JC, Mazat JP, Letellier T, Dachary-Prigent J, Solaini GC, Rossignol R (2005) Gradual alteration of mitochondrial structure and function by beta-amyloids: importance of membrane viscosity changes, energy deprivation, reactive oxygen species production, and cytochrome c release. J Bioenerg Biomembr 37:207-225.

Aliev G, Seyidova D, Neal ML, Shi J, Lamb BT, Siedlak SL, Vinters HV, Head E, Perry G, Lamanna JC, Friedland RP, Cotman CW (2002) Atherosclerotic lesions and mitochondria DNA deletions in brain microvessels as a central target for the development of human AD and AD-like pathology in aged transgenic mice. Ann N Y Acad Sci 977:45-64.

Alin P, Danielson UH, Mannervik B (1985) 4-Hydroxyalk-2-enals are substrates for glutathione transferase. FEBS Lett 179:267-270.

Allt G, Lawrenson JG (2001) Pericytes: cell biology and pathology. Cells Tissues Organs 169:1-11.

Alonzo NC, Hyman BT, Rebeck GW, Greenberg SM (1998) Progression of cerebral amyloid angiopathy: accumulation of amyloid-beta40 in affected vessels. J Neuropathol Exp Neurol 57:353-359.

Alzheimer A (1906) Über einen eigenartigen schweren Erkrankungsprozeí der Hirnrinde. Neurol Centralbl (Leipz) 25:1134.

Anfinsen CB (1973) Principles that govern the folding of protein chains. Science 181:223-230.

Arelin K, Kinoshita A, Whelan CM, Irizarry MC, Rebeck GW, Strickland DK, Hyman BT (2002) LRP and senile plaques in Alzheimer's disease: colocalization with apolipoprotein E and with activated astrocytes. Brain Res Mol Brain Res 104:38-46.

Arendash GW, Su GC, Crawford FC, Bjugstad KB, Mullan M (1999) Intravascular beta-amyloid infusion increases blood pressure: implications for a vasoactive role of beta-amyloid in the pathogenesis of Alzheimer's disease. Neurosci Lett 268:17-20.

Arispe N, Rojas E, Pollard HB (1993a) Alzheimer disease amyloid beta protein forms calcium channels in bilayer membranes: blockade by tromethamine and aluminum. Proc Natl Acad Sci U S A 90:567-571.

Arispe N, Pollard HB, Rojas E (1993b) Giant multilevel cation channels formed by Alzheimer disease amyloid beta-protein [A beta P-(1-40)] in bilayer membranes. Proc Natl Acad Sci U S A 90:10573-10577.

Armulik A, Abramsson A, Betsholtz C (2005) Endothelial/pericyte interactions. Circ Res 97:512-523.

Arvilommi AM, Salmi M, Jalkanen S (1997) Organ-selective regulation of vascular adhesion protein-1 expression in man. Eur J Immunol 27:1794-1800.

Arvilommi AM, Salmi M, Kalimo K, Jalkanen S (1996) Lymphocyte binding to vascular endothelium in inflamed skin revisited: a central role for vascular adhesion protein-1 (VAP-1). Eur J Immunol 26:825-833.

Asami-Odaka A, Ishibashi Y, Kikuchi T, Kitada C, Suzuki N (1995) Long amyloid beta-protein secreted from wild-type human neuroblastoma IMR-32 cells. Biochemistry 34:10272-10278.

Asatoor AM, Kerr DN (1961) Amines in blood and urine in relation to liver disease. Clin Chim Acta 6:149-156.

Assaf SY, Chung SH (1984) Release of endogenous Zn2+ from brain tissue during activity. Nature 308:734-736.

Atwood CS, Scarpa RC, Huang X, Moir RD, Jones WD, Fairlie DP, Tanzi RE, Bush AI (2000) Characterization of copper interactions with alzheimer amyloid beta peptides: identification of an attomolar-affinity copper binding site on amyloid beta1-42. J Neurochem 75:1219-1233.

Atwood CS, Moir RD, Huang X, Scarpa RC, Bacarra NM, Romano DM, Hartshorn MA, Tanzi RE, Bush AI (1998) Dramatic aggregation of Alzheimer abeta by Cu(II) is induced by conditions representing physiological acidosis. J Biol Chem 273:12817-12826.

Atwood CS, Perry G, Zeng H, Kato Y, Jones WD, Ling KQ, Huang X, Moir RD, Wang D, Sayre LM, Smith MA, Chen SG, Bush AI (2004) Copper mediates dityrosine cross-linking of Alzheimer's amyloid-beta. Biochemistry 43:560-568.

Baba S, Watanabe Y, Gejyo F, Arakawa M (1984) High-performance liquid chromatographic determination of serum aliphatic amines in chronic renal failure. Clin Chim Acta 136:49-56.

Bailey TL, Rivara CB, Rocher AB, Hof PR (2004) The nature and effects of cortical microvascular pathology in aging and Alzheimer's disease. Neurol Res 26:573-578.

Balbach JJ, Ishii Y, Antzutkin ON, Leapman RD, Rizzo NW, Dyda F, Reed J, Tycko R (2000) Amyloid fibril formation by A beta 16-22, a seven-residue fragment of the Alzheimer's beta-amyloid peptide, and structural characterization by solid state NMR. Biochemistry 39:13748-13759.

Bales KR, Du Y, Holtzman D, Cordell B, Paul SM (2000) Neuroinflammation and Alzheimer's disease: critical roles for cytokine/Abeta-induced glial activation, NF-kappaB, and apolipoprotein E. Neurobiol Aging 21:427-432; discussion 451-423.

Baloyannis SJ, Costa V, Michmizos D (2004) Mitochondrial alterations in Alzheimer's disease. Am J Alzheimers Dis Other Demen 19:89-93.

Barnham KJ, Ciccotosto GD, Tickler AK, Ali FE, Smith DG, Williamson NA, Lam YH, Carrington D, Tew D, Kocak G, Volitakis I, Separovic F, Barrow CJ, Wade JD, Masters CL, Cherny RA, Curtain CC, Bush AI, Cappai R (2003) Neurotoxic, redox-competent Alzheimer's beta-amyloid is released from lipid membrane by methionine oxidation. J Biol Chem 278:42959-42965.

Basun H, Forssell LG, Wetterberg L, Winblad B (1991) Metals and trace elements in plasma and cerebrospinal fluid in normal aging and Alzheimer's disease. J Neural Transm Park Dis Dement Sect 3:231-258.

Baum L, Chen L, Ng HK, Chan YS, Mak YT, Woo J, Chiu HF, Pang CP (1998) Low density lipoprotein receptor related protein gene exon 3 polymorphism association with Alzheimer's disease in Chinese. Neurosci Lett 247:33-36.

Behl C, Davis JB, Lesley R, Schubert D (1994) Hydrogen peroxide mediates amyloid beta protein toxicity. Cell 77:817-827.

Bell RD, Sagare AP, Friedman AE, Bedi GS, Holtzman DM, Deane R, Zlokovic BV (2007) Transport pathways for clearance of human Alzheimer's amyloid beta-peptide and apolipoproteins E and J in the mouse central nervous system. J Cereb Blood Flow Metab 27:909-918.

Bell RD, Deane R, Chow N, Long X, Sagare A, Singh I, Streb JW, Guo H, Rubio A, Van Nostrand W, Miano JM, Zlokovic BV (2009) SRF and myocardin regulate LRP-mediated amyloid-beta clearance in brain vascular cells. Nat Cell Biol 11:143-153.

Benedetti A, Comporti M, Fulceri R, Esterbauer H (1984) Cytotoxic aldehydes originating from the peroxidation of liver microsomal lipids. Identification of 4,5-dihydroxydecenal. Biochim Biophys Acta 792:172-181.

Berezovska O, Jack C, McLean P, Aster JC, Hicks C, Xia W, Wolfe MS, Kimberly WT, Weinmaster G, Selkoe DJ, Hyman BT (2000) Aspartate mutations in presenilin and gamma-secretase inhibitors both impair notch1 proteolysis and nuclear translocation with relative preservation of notch1 signaling. J Neurochem 75:583-593.

Bertram L, Tanzi RE (2004) The current status of Alzheimer's disease genetics: what do we tell the patients? Pharmacol Res 50:385-396.

Bertram L, Tanzi RE (2008) Thirty years of Alzheimer's disease genetics: the implications of systematic meta-analyses. Nat Rev Neurosci 9:768-778.

Bertram L, McQueen MB, Mullin K, Blacker D, Tanzi RE (2007) Systematic meta-analyses of Alzheimer disease genetic association studies: the AlzGene database. Nat Genet 39:17-23.

Bird MI, Nunn PB, Lord LA (1984) Formation of glycine and aminoacetone from L-threonine by rat liver mitochondria. Biochim Biophys Acta 802:229-236.

Bitan G, Lomakin A, Teplow DB (2001) Amyloid beta-protein oligomerization: prenucleation interactions revealed by photo-induced cross-linking of unmodified proteins. J Biol Chem 276:35176-35184.

Bitan G, Kirkitadze MD, Lomakin A, Vollers SS, Benedek GB, Teplow DB (2003) Amyloid beta -protein (Abeta) assembly: Abeta 40 and Abeta 42 oligomerize through distinct pathways. Proc Natl Acad Sci U S A 100:330-335.

Bjork I, Fish WW (1982) Evidence for similar conformational changes in alpha 2-macroglobulin on reaction with primary amines or proteolytic enzymes. Biochem J 207:347-356.

Bjork I, Lindblom T, Lindahl P (1985) Changes of the proteinase binding properties and conformation of bovine alpha 2-macroglobulin on cleavage of the thio ester bonds by methylamine. Biochemistry 24:2653-2660.

Bjorntorp P, Rosmond R (2000) Neuroendocrine abnormalities in visceral obesity. Int J Obes Relat Metab Disord 24 Suppl 2:S80-85.

Blacker D, Wilcox MA, Laird NM, Rodes L, Horvath SM, Go RC, Perry R, Watson B, Jr., Bassett SS, McInnis MG, Albert MS, Hyman BT, Tanzi RE (1998) Alpha-2 macroglobulin is genetically associated with Alzheimer disease. Nat Genet 19:357-360.

Bodovitz S, Klein WL (1996) Cholesterol modulates alpha-secretase cleavage of amyloid precursor protein. J Biol Chem 271:4436-4440.

Boggs LN, Fuson KS, Baez M, Churgay L, McClure D, Becker G, May PC (1996) Clusterin (Apo J) protects against in vitro amyloid-beta (1-40) neurotoxicity. J Neurochem 67:1324-1327.

Bohm G, Muhr R, Jaenicke R (1992) Quantitative analysis of protein far UV circular dichroism spectra by neural networks. Protein Eng 5:191-195.

Bokvist M, Lindstrom F, Watts A, Grobner G (2004) Two types of Alzheimer's beta-amyloid (1-40) peptide membrane interactions: aggregation preventing transmembrane anchoring versus accelerated surface fibril formation. J Mol Biol 335:1039-1049.

Bonarek M, Barberger-Gateau P, Letenneur L, Deschamps V, Iron A, Dubroca B, Dartigues JF (2000) Relationships between cholesterol, apolipoprotein E polymorphism and dementia: a cross-sectional analysis from the PAQUID study. Neuroepidemiology 19:141-148.

Bond JP, Deverin SP, Inouye H, el-Agnaf OM, Teeter MM, Kirschner DA (2003) Assemblies of Alzheimer's peptides A beta 25-35 and A beta 31-35: reverse-turn conformation and side-chain interactions revealed by X-ray diffraction. J Struct Biol 141:156-170.

Bonder CS, Norman MU, Swain MG, Zbytnuik LD, Yamanouchi J, Santamaria P, Ajuebor M, Salmi M, Jalkanen S, Kubes P (2005) Rules of recruitment for Th1 and Th2 lymphocytes in inflamed liver: a role for alpha-4 integrin and vascular adhesion protein-1. Immunity 23:153-163.

Boomsma F, Derkx FH, van den Meiracker AH, Man in 't Veld AJ, Schalekamp MA (1995) Plasma semicarbazide-sensitive amine oxidase activity is elevated in diabetes mellitus and correlates with glycosylated haemoglobin. Clin Sci (Lond) 88:675-679.

Boomsma F, van Dijk J, Bhaggoe UM, Bouhuizen AM, van den Meiracker AH (2000a) Variation in semicarbazide-sensitive amine oxidase activity in plasma and tissues of mammals. Comp Biochem Physiol C Toxicol Pharmacol 126:69-78.

Boomsma F, de Kam PJ, Tjeerdsma G, van den Meiracker AH, van Veldhuisen DJ (2000b) Plasma semicarbazide-sensitive amine oxidase (SSAO) is an independent prognostic marker for mortality in chronic heart failure. Eur Heart J 21:1859-1863.

Boomsma F, Hut H, Bagghoe U, van der Houwen A, van den Meiracker A (2005a) Semicarbazide-sensitive amine oxidase (SSAO): from cell to circulation. Med Sci Monit 11:RA122-126.

Boomsma F, van Veldhuisen DJ, de Kam PJ, Man in't Veld AJ, Mosterd A, Lie KI, Schalekamp MA (1997) Plasma semicarbazide-sensitive amine oxidase is elevated in patients with congestive heart failure. Cardiovasc Res 33:387-391.

Boomsma F, Pedersen-Bjergaard U, Agerholm-Larsen B, Hut H, Dhamrait SS, Thorsteinsson B, van den Meiracker AH (2005b) Association between plasma activities of semicarbazide-sensitive amine oxidase and angiotensin-converting enzyme in patients with type 1 diabetes mellitus. Diabetologia 48:1002-1007.

Booth AA, Khalifah RG, Todd P, Hudson BG (1997) In vitro kinetic studies of formation of antigenic advanced glycation end products (AGEs). Novel inhibition of post-Amadori glycation pathways. J Biol Chem 272:5430-5437.

Borchelt DR, Thinakaran G, Eckman CB, Lee MK, Davenport F, Ratovitsky T, Prada CM, Kim G, Seekins S, Yager D, Slunt HH, Wang R, Seeger M, Levey AI, Gandy SE, Copeland NG, Jenkins NA, Price DL, Younkin SG, Sisodia SS (1996) Familial Alzheimer's disease-linked presenilin 1 variants elevate Abeta1-42/1-40 ratio in vitro and in vivo. Neuron 17:1005-1013.

Bossy-Wetzel E, Schwarzenbacher R, Lipton SA (2004) Molecular pathways to neurodegeneration. Nat Med 10 Suppl:S2-9.

Bour S, Prevot D, Guigne C, Stolen C, Jalkanen S, Valet P, Carpene C (2007a) Semicarbazide-sensitive amine oxidase substrates fail to induce insulin-like effects in fat cells from AOC3 knockout mice. J Neural Transm 114:829-833.

Bour S, Daviaud D, Gres S, Lefort C, Prevot D, Zorzano A, Wabitsch M, Saulnier-Blache JS, Valet P, Carpene C (2007b) Adipogenesis-related increase of semicarbazide-sensitive amine oxidase and monoamine oxidase in human adipocytes. Biochimie 89:916-925.

Bradt BM, Kolb WP, Cooper NR (1998) Complement-dependent proinflammatory properties of the Alzheimer's disease beta-peptide. J Exp Med 188:431-438.

Breitner JC (1996) The role of anti-inflammatory drugs in the prevention and treatment of Alzheimer's disease. Annu Rev Med 47:401-411.

Breitner JC, Zandi PP (2001) Do nonsteroidal antiinflammatory drugs reduce the risk of Alzheimer's disease? N Engl J Med 345:1567-1568.

Brownlee M (2005) The pathobiology of diabetic complications: a unifying mechanism. Diabetes 54:1615-1625.

Bu G, Cam J, Zerbinatti C (2006) LRP in amyloid-beta production and metabolism. Ann N Y Acad Sci 1086:35-53.

Bubber P, Haroutunian V, Fisch G, Blass JP, Gibson GE (2005) Mitochondrial abnormalities in Alzheimer brain: mechanistic implications. Ann Neurol 57:695-703.

Buffoni F (1966) Histaminase and related amine oxidases. Pharmacol Rev 18:1163-1199.

Bush AI (2003) The metallobiology of Alzheimer's disease. Trends Neurosci 26:207-214.

Bush AI, Pettingell WH, Multhaup G, d Paradis M, Vonsattel JP, Gusella JF, Beyreuther K, Masters CL, Tanzi RE (1994) Rapid induction of Alzheimer A beta amyloid formation by zinc. Science 265:1464-1467.

Buttini M, Yu GQ, Shockley K, Huang Y, Jones B, Masliah E, Mallory M, Yeo T, Longo FM, Mucke L (2002) Modulation of Alzheimer-like synaptic and cholinergic deficits in transgenic mice by human apolipoprotein E depends on isoform, aging, and overexpression of amyloid beta peptides but not on plaque formation. J Neurosci 22:10539-10548.

Caccamo A, Oddo S, Sugarman MC, Akbari Y, LaFerla FM (2005) Age- and region-dependent alterations in Abeta-degrading enzymes: implications for Abeta-induced disorders. Neurobiol Aging 26:645-654.

Cai D, Williams NK, Klinman JP (1997) Effect of metal on 2,4,5-trihydroxyphenylalanine (topa) quinone biogenesis in the Hansenula polymorpha copper amine oxidase. J Biol Chem 272:19277-19281.

Callingham BA, Crosbie AE, Rous BA (1995) Some aspects of the pathophysiology of semicarbazide-sensitive amine oxidase enzymes. Prog Brain Res 106:305-321.

Capaldi AP, Radford SE (1998) Kinetic studies of beta-sheet protein folding. Curr Opin Struct Biol 8:86-92.

Carpene C, Iffiu-Soltesz Z, Bour S, Prevot D, Valet P (2007) Reduction of fat deposition by combined inhibition of monoamine oxidases and semicarbazide-sensitive amine oxidases in obese Zucker rats. Pharmacol Res 56:522-530.

Carpene C, Fontana E, Morin N, Visentin V, Prevot D, Castan I (2001) Substrates of semicarbazide-sensitive amine oxidase mimic diverse insulin effects in adipocytes. Inflamm Res 50 Suppl 2:S142-143.

Carpene C, Abello V, Iffiu-Soltesz Z, Mercier N, Feve B, Valet P (2008) Limitation of adipose tissue enlargement in rats chronically treated with semicarbazide-sensitive amine oxidase and monoamine oxidase inhibitors. Pharmacol Res 57:426-434.

Carpene C, Daviaud D, Boucher J, Bour S, Visentin V, Gres S, Duffaut C, Fontana E, Testar X, Saulnier-Blache JS, Valet P (2006) Short- and long-term insulin-like effects of monoamine oxidases and semicarbazide-sensitive amine oxidase substrates in cultured adipocytes. Metabolism 55:1397-1405.

Carrell RW, Lomas DA (1997) Conformational disease. Lancet 350:134-138.

Casley CS, Canevari L, Land JM, Clark JB, Sharpe MA (2002) Beta-amyloid inhibits integrated mitochondrial respiration and key enzyme activities. J Neurochem 80:91-100.

Casserly I, Topol E (2004) Convergence of atherosclerosis and Alzheimer's disease: inflammation, cholesterol, and misfolded proteins. Lancet 363:1139-1146.

Castillo V, Lizcano JM, Unzeta M (1999) Presence of SSAO in human and bovine meninges and microvessels. Neurobiology (Bp) 7:263-272.

Chagnon P, Betard C, Robitaille Y, Cholette A, Gauvreau D (1995) Distribution of brain cytochrome oxidase activity in various neurodegenerative diseases. Neuroreport 6:711-715.

Chayen N, Dieckmann M, Dierks K, Fromme P (2004) Size and shape determination of proteins in solution by a noninvasive depolarized dynamic light scattering instrument. Ann N Y Acad Sci 1027:20-27.

Chen K, Maley J, Yu PH (2006) Potential inplications of endogenous aldehydes in beta-amyloid misfolding, oligomerization and fibrillogenesis. J Neurochem 99:1413-1424.

Chen K, Kazachkov M, Yu PH (2007) Effect of aldehydes derived from oxidative deamination and oxidative stress on beta-amyloid aggregation; pathological implications to Alzheimer's disease. J Neural Transm 114:835-839.

Chen L, Richardson JS, Caldwell JE, Ang LC (1994) Regional brain activity of free radical defense enzymes in autopsy samples from patients with Alzheimer's disease and from nondemented controls. Int J Neurosci 75:83-90.

Cherny RA, Legg JT, McLean CA, Fairlie DP, Huang X, Atwood CS, Beyreuther K, Tanzi RE, Masters CL, Bush AI (1999) Aqueous dissolution of Alzheimer's disease Abeta amyloid deposits by biometal depletion. J Biol Chem 274:23223-23228.

Cherny RA, Atwood CS, Xilinas ME, Gray DN, Jones WD, McLean CA, Barnham KJ, Volitakis I, Fraser FW, Kim Y, Huang X, Goldstein LE, Moir RD, Lim JT, Beyreuther K, Zheng H, Tanzi RE, Masters CL, Bush AI (2001) Treatment with a copper-zinc chelator markedly and rapidly inhibits beta-amyloid accumulation in Alzheimer's disease transgenic mice. Neuron 30:665-676.

Cho HJ, Son SM, Jin SM, Hong HS, Shin DH, Kim SJ, Huh K, Mook-Jung I (2009) RAGE regulates BACE1 and A{beta} generation via NFAT1 activation in Alzheimer's disease animal model. Faseb J.

Choo-Smith LP, Garzon-Rodriguez W, Glabe CG, Surewicz WK (1997) Acceleration of amyloid fibril formation by specific binding of Abeta-(1-40) peptide to ganglioside-containing membrane vesicles. J Biol Chem 272:22987-22990.

Chow N, Bell RD, Deane R, Streb JW, Chen J, Brooks A, Van Nostrand W, Miano JM, Zlokovic BV (2007) Serum response factor and myocardin mediate arterial hypercontractility and cerebral blood flow dysregulation in Alzheimer's phenotype. Proc Natl Acad Sci U S A 104:823-828.

Christie R, Yamada M, Moskowitz M, Hyman B (2001) Structural and functional disruption of vascular smooth muscle cells in a transgenic mouse model of amyloid angiopathy. Am J Pathol 158:1065-1071.

Cighetti G, Debiasi S, Paroni R, Allevi P (1999) Free and total malondialdehyde assessment in biological matrices by gas chromatography-mass spectrometry: what is needed for an accurate detection. Anal Biochem 266:222-229.

Citron M, Diehl TS, Gordon G, Biere AL, Seubert P, Selkoe DJ (1996) Evidence that the 42- and 40-amino acid forms of amyloid beta protein are generated from the beta-amyloid precursor protein by different protease activities. Proc Natl Acad Sci U S A 93:13170-13175.

Cleary JP, Walsh DM, Hofmeister JJ, Shankar GM, Kuskowski MA, Selkoe DJ, Ashe KH (2005) Natural oligomers of the amyloid-beta protein specifically disrupt cognitive function. Nat Neurosci 8:79-84.

Conklin DJ, Cowley HR, Wiechmann RJ, Johnson GH, Trent MB, Boor PJ (2004) Vasoactive effects of methylamine in isolated human blood vessels: role of semicarbazide-sensitive amine oxidase, formaldehyde, and hydrogen peroxide. Am J Physiol Heart Circ Physiol 286:H667-676.

Corder EH, Saunders AM, Strittmatter WJ, Schmechel DE, Gaskell PC, Small GW, Roses AD, Haines JL, Pericak-Vance MA (1993) Gene dose of apolipoprotein E type 4 allele and the risk of Alzheimer's disease in late onset families. Science 261:921-923.

Corder EH, Saunders AM, Risch NJ, Strittmatter WJ, Schmechel DE, Gaskell PC, Jr., Rimmler JB, Locke PA, Conneally PM, Schmader KE, et al. (1994) Protective effect of apolipoprotein E type 2 allele for late onset Alzheimer disease. Nat Genet 7:180-184.

Craft S (2006) Insulin resistance syndrome and Alzheimer disease: pathophysiologic mechanisms and therapeutic implications. Alzheimer Dis Assoc Disord 20:298-301.

Crews L, Rockenstein E, Masliah E (2008) Biological transgenic mouse models of Alzheimer's disease. Handb Clin Neurol 89:291-301.

Crouch PJ, Blake R, Duce JA, Ciccotosto GD, Li QX, Barnham KJ, Curtain CC, Cherny RA, Cappai R, Dyrks T, Masters CL, Trounce IA (2005) Copper-dependent inhibition of human cytochrome c oxidase by a dimeric conformer of amyloid-beta1-42. J Neurosci 25:672-679.

Curtain CC, Ali F, Volitakis I, Cherny RA, Norton RS, Beyreuther K, Barrow CJ, Masters CL, Bush AI, Barnham KJ (2001) Alzheimer's disease amyloid-beta binds copper and zinc to generate an allosterically ordered membrane-penetrating structure containing superoxide dismutase-like subunits. J Biol Chem 276:20466-20473.

Dai W, Lopez OL, Carmichael OT, Becker JT, Kuller LH, Gach HM (2008) Abnormal regional cerebral blood flow in cognitively normal elderly subjects with hypertension. Stroke 39:349-354.

Daly Jt, Kotwal GJ (1998) Pro-inflammatory complement activation by the A beta peptide of Alzheimer's disease is biologically significant and can be blocked by vaccinia virus complement control protein. Neurobiol Aging 19:619-627.

Das HK, McPherson J, Bruns GA, Karathanasis SK, Breslow JL (1985) Isolation, characterization, and mapping to chromosome 19 of the human apolipoprotein E gene. J Biol Chem 260:6240-6247.

Datki Z, Papp R, Zadori D, Soos K, Fulop L, Juhasz A, Laskay G, Hetenyi C, Mihalik E, Zarandi M, Penke B (2004) In vitro model of neurotoxicity of Abeta 1-42 and neuroprotection by a pentapeptide: irreversible events during the first hour. Neurobiol Dis 17:507-515.

Davis-Salinas J, Saporito-Irwin SM, Cotman CW, Van Nostrand WE (1995) Amyloid beta-protein induces its own production in cultured degenerating cerebrovascular smooth muscle cells. J Neurochem 65:931-934.

de Bono DP, Yang WD (1995) Exposure to low concentrations of hydrogen peroxide causes delayed endothelial cell death and inhibits proliferation of surviving cells. Atherosclerosis 114:235-245.

de la Monte SM, Wands JR (2005) Review of insulin and insulin-like growth factor expression, signaling, and malfunction in the central nervous system: relevance to Alzheimer's disease. J Alzheimers Dis 7:45-61.

de la Torre JC (2002a) Vascular basis of Alzheimer's pathogenesis. Ann N Y Acad Sci 977:196-215.

de la Torre JC (2002b) Alzheimer disease as a vascular disorder: nosological evidence. Stroke 33:1152-1162.

de la Torre JC (2006) How do heart disease and stroke become risk factors for Alzheimer's disease? Neurol Res 28:637-644.

Deane R, Sagare A, Hamm K, Parisi M, Lane S, Finn MB, Holtzman DM, Zlokovic BV (2008) apoE isoform-specific disruption of amyloid beta peptide clearance from mouse brain. J Clin Invest 118:4002-4013.

Deane R, Wu Z, Sagare A, Davis J, Du Yan S, Hamm K, Xu F, Parisi M, LaRue B, Hu HW, Spijkers P, Guo H, Song X, Lenting PJ, Van Nostrand WE, Zlokovic BV (2004) LRP/amyloid beta-peptide interaction mediates differential brain efflux of Abeta isoforms. Neuron 43:333-344.

Deane R, Du Yan S, Submamaryan RK, LaRue B, Jovanovic S, Hogg E, Welch D, Manness L, Lin C, Yu J, Zhu H, Ghiso J, Frangione B, Stern A, Schmidt AM, Armstrong DL, Arnold

B, Liliensiek B, Nawroth P, Hofman F, Kindy M, Stern D, Zlokovic B (2003) RAGE mediates amyloid-beta peptide transport across the blood-brain barrier and accumulation in brain. Nat Med 9:907-913.

Dede DS, Yavuz B, Yavuz BB, Cankurtaran M, Halil M, Ulger Z, Cankurtaran ES, Aytemir K, Kabakci G, Ariogul S (2007) Assessment of endothelial function in Alzheimer's disease: is Alzheimer's disease a vascular disease? J Am Geriatr Soc 55:1613-1617.

Dei R, Takeda A, Niwa H, Li M, Nakagomi Y, Watanabe M, Inagaki T, Washimi Y, Yasuda Y, Horie K, Miyata T, Sobue G (2002) Lipid peroxidation and advanced glycation end products in the brain in normal aging and in Alzheimer's disease. Acta Neuropathol 104:113-122.

Deibel MA, Ehmann WD, Markesbery WR (1996) Copper, iron, and zinc imbalances in severely degenerated brain regions in Alzheimer's disease: possible relation to oxidative stress. J Neurol Sci 143:137-142.

del Mar Hernandez M, Esteban M, Szabo P, Boada M, Unzeta M (2005) Human plasma semicarbazide sensitive amine oxidase (SSAO), beta-amyloid protein and aging. Neurosci Lett 384:183-187.

DeMattos RB, Bales KR, Cummins DJ, Paul SM, Holtzman DM (2002) Brain to plasma amyloid-beta efflux: a measure of brain amyloid burden in a mouse model of Alzheimer's disease. Science 295:2264-2267.

Demuro A, Mina E, Kayed R, Milton SC, Parker I, Glabe CG (2005) Calcium dysregulation and membrane disruption as a ubiquitous neurotoxic mechanism of soluble amyloid oligomers. J Biol Chem 280:17294-17300.

Devi L, Prabhu BM, Galati DF, Avadhani NG, Anandatheerthavarada HK (2006) Accumulation of amyloid precursor protein in the mitochondrial import channels of human Alzheimer's disease brain is associated with mitochondrial dysfunction. J Neurosci 26:9057-9068.

Dietschy JM, Turley SD (2001) Cholesterol metabolism in the brain. Curr Opin Lipidol 12:105-112.

Dietschy JM, Turley SD (2004) Thematic review series: brain Lipids. Cholesterol metabolism in the central nervous system during early development and in the mature animal. J Lipid Res 45:1375-1397.

Dikalov SI, Vitek MP, Maples KR, Mason RP (1999) Amyloid beta peptides do not form peptide-derived free radicals spontaneously, but can enhance metal-catalyzed oxidation of hydroxylamines to nitroxides. J Biol Chem 274:9392-9399.

Dineley KT, Westerman M, Bui D, Bell K, Ashe KH, Sweatt JD (2001) Beta-amyloid activates the mitogen-activated protein kinase cascade via hippocampal alpha7 nicotinic acetylcholine receptors: In vitro and in vivo mechanisms related to Alzheimer's disease. J Neurosci 21:4125-4133.

Dolev I, Michaelson DM (2004) A nontransgenic mouse model shows inducible amyloid-beta (Abeta) peptide deposition and elucidates the role of apolipoprotein E in the amyloid cascade. Proc Natl Acad Sci U S A 101:13909-13914.

Dooley DM, McGuirl MA, Brown DE, Turowski PN, McIntire WS, Knowles PF (1991) A Cu(I)-semiquinone state in substrate-reduced amine oxidases. Nature 349:262-264.

Dore-Duffy P, LaManna JC (2007) Physiologic angiodynamics in the brain. Antioxid Redox Signal 9:1363-1371.

Dovey HF, Suomensaari-Chrysler S, Lieberburg I, Sinha S, Keim PS (1993) Cells with a familial Alzheimer's disease mutation produce authentic beta-peptide. Neuroreport 4:1039-1042.

Draper HH, Agarwal S, Nelson DE, Wee JJ, Ghoshal AK, Farber E (1995) Effects of peroxidative stress and age on the concentration of a deoxyguanosine-malondialdehyde adduct in rat DNA. Lipids 30:959-961.

Du Y, Ni B, Glinn M, Dodel RC, Bales KR, Zhang Z, Hyslop PA, Paul SM (1997) alpha2-Macroglobulin as a beta-amyloid peptide-binding plasma protein. J Neurochem 69:299-305.

Duff K, Suleman F (2004) Transgenic mouse models of Alzheimer's disease: how useful have they been for therapeutic development? Brief Funct Genomic Proteomic 3:47-59.

Dunkel P, Gelain A, Barlocco D, Haider N, Gyires K, Sperlagh B, Magyar K, Maccioni E, Fadda A, Matyus P (2008) Semicarbazide-sensitive amine oxidase/vascular adhesion protein 1: recent developments concerning substrates and inhibitors of a promising therapeutic target. Curr Med Chem 15:1827-1839.

Ebly EM, Parhad IM, Hogan DB, Fung TS (1994) Prevalence and types of dementia in the very old: results from the Canadian Study of Health and Aging. Neurology 44:1593-1600.

Eckert A, Steiner B, Marques C, Leutz S, Romig H, Haass C, Muller WE (2001) Elevated vulnerability to oxidative stress-induced cell death and activation of caspase-3 by the Swedish amyloid precursor protein mutation. J Neurosci Res 64:183-192.

Eikelenboom P, Veerhuis R, Familian A, Hoozemans JJ, van Gool WA, Rozemuller AJ (2008) Neuroinflammation in plaque and vascular beta-amyloid disorders: clinical and therapeutic implications. Neurodegener Dis 5:190-193.

El Hadri K, Moldes M, Mercier N, Andreani M, Pairault J, Feve B (2002) Semicarbazide-sensitive amine oxidase in vascular smooth muscle cells: differentiation-dependent expression and role in glucose uptake. Arterioscler Thromb Vasc Biol 22:89-94.

El Khoury JB, Moore KJ, Means TK, Leung J, Terada K, Toft M, Freeman MW, Luster AD (2003) CD36 mediates the innate host response to beta-amyloid. J Exp Med 197:1657-1666.

Elias MF, Elias PK, Sullivan LM, Wolf PA, D'Agostino RB (2003) Lower cognitive function in the presence of obesity and hypertension: the Framingham heart study. Int J Obes Relat Metab Disord 27:260-268.

Elliott J, Callingham BA, Sharman DF (1989) The influence of amine metabolizing enzymes on the pharmacology of tyramine in the isolated perfused mesenteric arterial bed of the rat. Br J Pharmacol 98:515-522.

Ellis RJ, Olichney JM, Thal LJ, Mirra SS, Morris JC, Beekly D, Heyman A (1996) Cerebral amyloid angiopathy in the brains of patients with Alzheimer's disease: the CERAD experience, Part XV. Neurology 46:1592-1596.

Engelhardt B, Wolburg-Buchholz K, Wolburg H (2001) Involvement of the choroid plexus in central nervous system inflammation. Microsc Res Tech 52:112-129.

Enrique-Tarancon G, Marti L, Morin N, Lizcano JM, Unzeta M, Sevilla L, Camps M, Palacin M, Testar X, Carpene C, Zorzano A (1998) Role of semicarbazide-sensitive amine oxidase on glucose transport and GLUT4 recruitment to the cell surface in adipose cells. J Biol Chem 273:8025-8032.

Enrique-Tarancon G, Castan I, Morin N, Marti L, Abella A, Camps M, Casamitjana R, Palacin M, Testar X, Degerman E, Carpene C, Zorzano A (2000) Substrates of semicarbazide-sensitive amine oxidase co-operate with vanadate to stimulate tyrosine phosphorylation of insulin-receptor-substrate proteins, phosphoinositide 3-kinase activity and GLUT4 translocation in adipose cells. Biochem J 350 Pt 1:171-180.

Enya M, Morishima-Kawashima M, Yoshimura M, Shinkai Y, Kusui K, Khan K, Games D, Schenk D, Sugihara S, Yamaguchi H, Ihara Y (1999) Appearance of sodium dodecyl sulfate-stable amyloid beta-protein (Abeta) dimer in the cortex during aging. Am J Pathol 154:271-279.

Esterbauer H, Schaur RJ, Zollner H (1991) Chemistry and biochemistry of 4-hydroxynonenal, malonaldehyde and related aldehydes. Free Radic Biol Med 11:81-128.

Etminan M, Gill S, Samii A (2003) Effect of non-steroidal anti-inflammatory drugs on risk of Alzheimer's disease: systematic review and meta-analysis of observational studies. Bmj 327:128.

Fabrizi C, Businaro R, Lauro GM, Fumagalli L (2001) Role of alpha2-macroglobulin in regulating amyloid beta-protein neurotoxicity: protective or detrimental factor? J Neurochem 78:406-412.

Farris W, Schutz SG, Cirrito JR, Shankar GM, Sun X, George A, Leissring MA, Walsh DM, Qiu WQ, Holtzman DM, Selkoe DJ (2007) Loss of neprilysin function promotes amyloid plaque formation and causes cerebral amyloid angiopathy. Am J Pathol 171:241-251.

Fassbender K, Simons M, Bergmann C, Stroick M, Lutjohann D, Keller P, Runz H, Kuhl S, Bertsch T, von Bergmann K, Hennerici M, Beyreuther K, Hartmann T (2001) Simvastatin strongly reduces levels of Alzheimer's disease beta -amyloid peptides Abeta 42 and Abeta 40 in vitro and in vivo. Proc Natl Acad Sci U S A 98:5856-5861.

Felsenstein KM, Hunihan LW, Roberts SB (1994) Altered cleavage and secretion of a recombinant beta-APP bearing the Swedish familial Alzheimer's disease mutation. Nat Genet 6:251-255.

Ferrer I, Lizcano JM, Hernandez M, Unzeta M (2002) Overexpression of semicarbazide sensitive amine oxidase in the cerebral blood vessels in patients with Alzheimer's disease and cerebral autosomal dominant arteriopathy with subcortical infarcts and leukoencephalopathy. Neurosci Lett 321:21-24.

Fillit H, Nash DT, Rundek T, Zuckerman A (2008) Cardiovascular risk factors and dementia. Am J Geriatr Pharmacother 6:100-118.

Finkel T (1998) Oxygen radicals and signaling. Curr Opin Cell Biol 10:248-253.

Fontana E, Boucher J, Marti L, Lizcano JM, Testar X, Zorzano A, Carpene C (2001) Amine oxidase substrates mimic several of the insulin effects on adipocyte differentiation in 3T3 F442A cells. Biochem J 356:769-777.

Foroughan M, Farahani ZG, Shariatpanahi M, Vaezinejad M, Kamerani AA, Sheikhvatan M (2008) Risk factors of Alzheimer's disease among Iranian population. Curr Alzheimer Res 5:70-72.

Fourrier A, Letenneur L, Begaud B, Dartigues JF (1996) Nonsteroidal antiinflammatory drug use and cognitive function in the elderly: inconclusive results from a population-based cohort study. J Clin Epidemiol 49:1201.

Frank EM (1994) Effect of Alzheimer's disease on communication function. J S C Med Assoc 90:417-423.

Fratiglioni L, De Ronchi D, Aguero-Torres H (1999) Worldwide prevalence and incidence of dementia. Drugs Aging 15:365-375.

Frears ER, Stephens DJ, Walters CE, Davies H, Austen BM (1999) The role of cholesterol in the biosynthesis of beta-amyloid. Neuroreport 10:1699-1705.

Frederickson CJ, Suh SW, Silva D, Frederickson CJ, Thompson RB (2000) Importance of zinc in the central nervous system: the zinc-containing neuron. J Nutr 130:1471S-1483S.

Fryer JD, Taylor JW, DeMattos RB, Bales KR, Paul SM, Parsadanian M, Holtzman DM (2003) Apolipoprotein E markedly facilitates age-dependent cerebral amyloid angiopathy and spontaneous hemorrhage in amyloid precursor protein transgenic mice. J Neurosci 23:7889-7896.

Fryer JD, Simmons K, Parsadanian M, Bales KR, Paul SM, Sullivan PM, Holtzman DM (2005) Human apolipoprotein E4 alters the amyloid-beta 40:42 ratio and promotes the formation of cerebral amyloid angiopathy in an amyloid precursor protein transgenic model. J Neurosci 25:2803-2810.

Funato H, Enya M, Yoshimura M, Morishima-Kawashima M, Ihara Y (1999) Presence of sodium dodecyl sulfate-stable amyloid beta-protein dimers in the hippocampus CA1 not exhibiting neurofibrillary tangle formation. Am J Pathol 155:23-28.

Garpenstrand H, Ekblom J, von Arbin M, Oreland L, Murray V (1999a) Plasma semicarbazide-sensitive amine oxidase in stroke. Eur Neurol 41:20-23.

Garpenstrand H, Ekblom J, Backlund LB, Oreland L, Rosenqvist U (1999b) Elevated plasma semicarbazide-sensitive amine oxidase (SSAO) activity in Type 2 diabetes mellitus complicated by retinopathy. Diabet Med 16:514-521.

Garpenstrand H, Bergqvist M, Brattstrom D, Larsson A, Oreland L, Hesselius P, Wagenius G (2004) Serum semicarbazide-sensitive amine oxidase (SSAO) activity correlates with VEGF in non-small-cell lung cancer patients. Med Oncol 21:241-250.

Gasparini L, Gouras GK, Wang R, Gross RS, Beal MF, Greengard P, Xu H (2001) Stimulation of beta-amyloid precursor protein trafficking by insulin reduces intraneuronal beta-amyloid and requires mitogen-activated protein kinase signaling. J Neurosci 21:2561-2570.

Gokturk C, Nordquist J, Sugimoto H, Forsberg-Nilsson K, Nilsson J, Oreland L (2004) Semicarbazide-sensitive amine oxidase in transgenic mice with diabetes. Biochem Biophys Res Commun 325:1013-1020.

Gokturk C, Nilsson J, Nordquist J, Kristensson M, Svensson K, Soderberg C, Israelson M, Garpenstrand H, Sjoquist M, Oreland L, Forsberg-Nilsson K (2003) Overexpression of semicarbazide-sensitive amine oxidase in smooth muscle cells leads to an abnormal structure of the aortic elastic laminas. Am J Pathol 163:1921-1928.

Goldsbury C, Kistler J, Aebi U, Arvinte T, Cooper GJ (1999) Watching amyloid fibrils grow by time-lapse atomic force microscopy. J Mol Biol 285:33-39.

Gong Y, Chang L, Viola KL, Lacor PN, Lambert MP, Finch CE, Krafft GA, Klein WL (2003) Alzheimer's disease-affected brain: presence of oligomeric A beta ligands (ADDLs) suggests a molecular basis for reversible memory loss. Proc Natl Acad Sci U S A 100:10417-10422.

Gonias SL, Reynolds JA, Pizzo SV (1982) Physical properties of human alpha 2-macroglobulin following reaction with methylamine and trypsin. Biochim Biophys Acta 705:306-314.

Gonzalez-Fraguela ME, Castellano-Benitez O, Gonzalez-Hoyuela M (1999) [Oxidative stress in neurodegeneration]. Rev Neurol 28:504-511.

Gonzalez C, Martin T, Cacho J, Brenas MT, Arroyo T, Garcia-Berrocal B, Navajo JA, Gonzalez-Buitrago JM (1999) Serum zinc, copper, insulin and lipids in Alzheimer's disease epsilon 4 apolipoprotein E allele carriers. Eur J Clin Invest 29:637-642.

Gorman AM, McGowan A, O'Neill C, Cotter T (1996) Oxidative stress and apoptosis in neurodegeneration. J Neurol Sci 139 Suppl:45-52.

Gottfries CF, Oreland L, Wiberg A, Winblad B (1974) Letter: Brain-levels of monoamine oxidase in depression. Lancet 2:360-361.
Gouras GK, Beal MF (2001) Metal chelator decreases Alzheimer beta-amyloid plaques. Neuron 30:641-642.
Grammas P, Yamada M, Zlokovic B (2002) The cerebromicrovasculature: a key player in the pathogenesis of Alzheimer's disease. J Alzheimers Dis 4:217-223.
Grammas P, Moore P, Botchlet T, Hanson-Painton O, Cooper DR, Ball MJ, Roher A (1995) Cerebral microvessels in Alzheimer's have reduced protein kinase C activity. Neurobiol Aging 16:563-569.
Griffin WS (2006) Inflammation and neurodegenerative diseases. Am J Clin Nutr 83:470S-474S.
Gronvall-Nordquist JL, Backlund LB, Garpenstrand H, Ekblom J, Landin B, Yu PH, Oreland L, Rosenqvist U (2001) Follow-up of plasma semicarbazide-sensitive amine oxidase activity and retinopathy in Type 2 diabetes mellitus. J Diabetes Complications 15:250-256.
Grundke-Iqbal I, Iqbal K, Quinlan M, Tung YC, Zaidi MS, Wisniewski HM (1986a) Microtubule-associated protein tau. A component of Alzheimer paired helical filaments. J Biol Chem 261:6084-6089.
Grundke-Iqbal I, Iqbal K, Tung YC, Quinlan M, Wisniewski HM, Binder LI (1986b) Abnormal phosphorylation of the microtubule-associated protein tau (tau) in Alzheimer cytoskeletal pathology. Proc Natl Acad Sci U S A 83:4913-4917.
Gubisne-Haberle D, Hill W, Kazachkov M, Richardson JS, Yu PH (2004) Protein cross-linkage induced by formaldehyde derived from semicarbazide-sensitive amine oxidase-mediated deamination of methylamine. J Pharmacol Exp Ther 310:1125-1132.
Gunzburg MJ, Perugini MA, Howlett GJ (2007) Structural basis for the recognition and cross-linking of amyloid fibrils by human apolipoprotein E. J Biol Chem 282:35831-35841.
Gustafson D, Rothenberg E, Blennow K, Steen B, Skoog I (2003) An 18-year follow-up of overweight and risk of Alzheimer disease. Arch Intern Med 163:1524-1528.
Haass C, Schlossmacher MG, Hung AY, Vigo-Pelfrey C, Mellon A, Ostaszewski BL, Lieberburg I, Koo EH, Schenk D, Teplow DB, et al. (1992) Amyloid beta-peptide is produced by cultured cells during normal metabolism. Nature 359:322-325.
Hajjar I, Catoe H, Sixta S, Boland R, Johnson D, Hirth V, Wieland D, Eleazer P (2005) Cross-sectional and longitudinal association between antihypertensive medications and cognitive impairment in an elderly population. J Gerontol A Biol Sci Med Sci 60:67-73.
Halliday G, Robinson SR, Shepherd C, Kril J (2000) Alzheimer's disease and inflammation: a review of cellular and therapeutic mechanisms. Clin Exp Pharmacol Physiol 27:1-8.
Hansson CA, Frykman S, Farmery MR, Tjernberg LO, Nilsberth C, Pursglove SE, Ito A, Winblad B, Cowburn RF, Thyberg J, Ankarcrona M (2004) Nicastrin, presenilin, APH-1, and PEN-2 form active gamma-secretase complexes in mitochondria. J Biol Chem 279:51654-51660.
Hardy J, Selkoe DJ (2002) The amyloid hypothesis of Alzheimer's disease: progress and problems on the road to therapeutics. Science 297:353-356.
Harper JD, Wong SS, Lieber CM, Lansbury PT (1997) Observation of metastable Abeta amyloid protofibrils by atomic force microscopy. Chem Biol 4:119-125.
Harper JD, Wong SS, Lieber CM, Lansbury PT, Jr. (1999) Assembly of A beta amyloid protofibrils: an in vitro model for a possible early event in Alzheimer's disease. Biochemistry 38:8972-8980.

Harris JR (2002) In vitro fibrillogenesis of the amyloid beta 1-42 peptide: cholesterol potentiation and aspirin inhibition. Micron 33:609-626.
Hashimura T, Kimura T, Miyakawa T (1991) Morphological changes of blood vessels in the brain with Alzheimer's disease. Jpn J Psychiatry Neurol 45:661-665.
Herring A, Yasin H, Ambree O, Sachser N, Paulus W, Keyvani K (2008) Environmental enrichment counteracts Alzheimer's neurovascular dysfunction in TgCRND8 mice. Brain Pathol 18:32-39.
Hershey CO, Hershey LA, Varnes A, Vibhakar SD, Lavin P, Strain WH (1983) Cerebrospinal fluid trace element content in dementia: clinical, radiologic, and pathologic correlations. Neurology 33:1350-1353.
Herz J (2001) The LDL receptor gene family: (un)expected signal transducers in the brain. Neuron 29:571-581.
Herz J, Bock HH (2002) Lipoprotein receptors in the nervous system. Annu Rev Biochem 71:405-434.
Heyman A, Fillenbaum GG, Welsh-Bohmer KA, Gearing M, Mirra SS, Mohs RC, Peterson BL, Pieper CF (1998) Cerebral infarcts in patients with autopsy-proven Alzheimer's disease: CERAD, part XVIII. Consortium to Establish a Registry for Alzheimer's Disease. Neurology 51:159-162.
Hirai K, Aliev G, Nunomura A, Fujioka H, Russell RL, Atwood CS, Johnson AB, Kress Y, Vinters HV, Tabaton M, Shimohama S, Cash AD, Siedlak SL, Harris PL, Jones PK, Petersen RB, Perry G, Smith MA (2001) Mitochondrial abnormalities in Alzheimer's disease. J Neurosci 21:3017-3023.
Ho L, Qin W, Pompl PN, Xiang Z, Wang J, Zhao Z, Peng Y, Cambareri G, Rocher A, Mobbs CV, Hof PR, Pasinetti GM (2004) Diet-induced insulin resistance promotes amyloidosis in a transgenic mouse model of Alzheimer's disease. Faseb J 18:902-904.
Hofman A, Ott A, Breteler MM, Bots ML, Slooter AJ, van Harskamp F, van Duijn CN, Van Broeckhoven C, Grobbee DE (1997) Atherosclerosis, apolipoprotein E, and prevalence of dementia and Alzheimer's disease in the Rotterdam Study. Lancet 349:151-154.
Holt A, Alton G, Scaman CH, Loppnow GR, Szpacenko A, Svendsen I, Palcic MM (1998) Identification of the quinone cofactor in mammalian semicarbazide-sensitive amine oxidase. Biochemistry 37:4946-4957.
Holtzman DM, Bales KR, Tenkova T, Fagan AM, Parsadanian M, Sartorius LJ, Mackey B, Olney J, McKeel D, Wozniak D, Paul SM (2000) Apolipoprotein E isoform-dependent amyloid deposition and neuritic degeneration in a mouse model of Alzheimer's disease. Proc Natl Acad Sci U S A 97:2892-2897.
Houen G (1999) Mammalian Cu-containing amine oxidases (CAOs): new methods of analysis, structural relationships, and possible functions. APMIS Suppl 96:1-46.
Hu J, Igarashi A, Kamata M, Nakagawa H (2001) Angiotensin-converting enzyme degrades Alzheimer amyloid beta-peptide (A beta); retards A beta aggregation, deposition, fibril formation; and inhibits cytotoxicity. J Biol Chem 276:47863-47868.
Huang TH, Yang DS, Plaskos NP, Go S, Yip CM, Fraser PE, Chakrabartty A (2000) Structural studies of soluble oligomers of the Alzheimer beta-amyloid peptide. J Mol Biol 297:73-87.
Huang X, Atwood CS, Hartshorn MA, Multhaup G, Goldstein LE, Scarpa RC, Cuajungco MP, Gray DN, Lim J, Moir RD, Tanzi RE, Bush AI (1999a) The A beta peptide of

Alzheimer's disease directly produces hydrogen peroxide through metal ion reduction. Biochemistry 38:7609-7616.

Huang X, Cuajungco MP, Atwood CS, Hartshorn MA, Tyndall JD, Hanson GR, Stokes KC, Leopold M, Multhaup G, Goldstein LE, Scarpa RC, Saunders AJ, Lim J, Moir RD, Glabe C, Bowden EF, Masters CL, Fairlie DP, Tanzi RE, Bush AI (1999b) Cu(II) potentiation of alzheimer abeta neurotoxicity. Correlation with cell-free hydrogen peroxide production and metal reduction. J Biol Chem 274:37111-37116.

Hughes SR, Khorkova O, Goyal S, Knaeblein J, Heroux J, Riedel NG, Sahasrabudhe S (1998) Alpha2-macroglobulin associates with beta-amyloid peptide and prevents fibril formation. Proc Natl Acad Sci U S A 95:3275-3280.

Hung LW, Ciccotosto GD, Giannakis E, Tew DJ, Perez K, Masters CL, Cappai R, Wade JD, Barnham KJ (2008) Amyloid-beta peptide (Abeta) neurotoxicity is modulated by the rate of peptide aggregation: Abeta dimers and trimers correlate with neurotoxicity. J Neurosci 28:11950-11958.

Hyman BT, Strickland D, Rebeck GW (2000) Role of the low-density lipoprotein receptor-related protein in beta-amyloid metabolism and Alzheimer disease. Arch Neurol 57:646-650.

Iadecola C (2003) Cerebrovascular effects of amyloid-beta peptides: mechanisms and implications for Alzheimer's dementia. Cell Mol Neurobiol 23:681-689.

Iadecola C (2004) Neurovascular regulation in the normal brain and in Alzheimer's disease. Nat Rev Neurosci 5:347-360.

Iglesias-Osma MC, Bour S, Garcia-Barrado MJ, Visentin V, Pastor MF, Testar X, Marti L, Enrique-Tarancon G, Valet P, Moratinos J, Carpene C (2005) Methylamine but not mafenide mimics insulin-like activity of the semicarbazide-sensitive amine oxidase-substrate benzylamine on glucose tolerance and on human adipocyte metabolism. Pharmacol Res 52:475-484.

Ikeuchi T, Dolios G, Kim SH, Wang R, Sisodia SS (2003) Familial Alzheimer disease-linked presenilin 1 variants enhance production of both Abeta 1-40 and Abeta 1-42 peptides that are only partially sensitive to a potent aspartyl protease transition state inhibitor of "gamma-secretase". J Biol Chem 278:7010-7018.

Imamura Y, Kubota R, Wang Y, Asakawa S, Kudoh J, Mashima Y, Oguchi Y, Shimizu N (1997) Human retina-specific amine oxidase (RAO): cDNA cloning, tissue expression, and chromosomal mapping. Genomics 40:277-283.

in t' Veld BA, Ruitenberg A, Hofman A, Launer LJ, van Duijn CM, Stijnen T, Breteler MM, Stricker BH (2001) Nonsteroidal antiinflammatory drugs and the risk of Alzheimer's disease. N Engl J Med 345:1515-1521.

Ito S, Ohtsuki S, Kamiie J, Nezu Y, Terasaki T (2007) Cerebral clearance of human amyloid-beta peptide (1-40) across the blood-brain barrier is reduced by self-aggregation and formation of low-density lipoprotein receptor-related protein-1 ligand complexes. J Neurochem 103:2482-2490.

Itoh A, Akaike T, Sokabe M, Nitta A, Iida R, Olariu A, Yamada K, Nabeshima T (1999) Impairments of long-term potentiation in hippocampal slices of beta-amyloid-infused rats. Eur J Pharmacol 382:167-175.

Iwata K, Eyles SJ, Lee JP (2001a) Exposing asymmetry between monomers in Alzheimer's amyloid fibrils via reductive alkylation of lysine residues. J Am Chem Soc 123:6728-6729.

Iwata N, Tsubuki S, Takaki Y, Shirotani K, Lu B, Gerard NP, Gerard C, Hama E, Lee HJ, Saido TC (2001b) Metabolic regulation of brain Abeta by neprilysin. Science 292:1550-1552.

Iwata N, Tsubuki S, Takaki Y, Watanabe K, Sekiguchi M, Hosoki E, Kawashima-Morishima M, Lee HJ, Hama E, Sekine-Aizawa Y, Saido TC (2000) Identification of the major Abeta1-42-degrading catabolic pathway in brain parenchyma: suppression leads to biochemical and pathological deposition. Nat Med 6:143-150.

Iwatsubo T, Odaka A, Suzuki N, Mizusawa H, Nukina N, Ihara Y (1994) Visualization of A beta 42(43) and A beta 40 in senile plaques with end-specific A beta monoclonals: evidence that an initially deposited species is A beta 42(43). Neuron 13:45-53.

Jaakkola K, Nikula T, Holopainen R, Vahasilta T, Matikainen MT, Laukkanen ML, Huupponen R, Halkola L, Nieminen L, Hiltunen J, Parviainen S, Clark MR, Knuuti J, Savunen T, Kaapa P, Voipio-Pulkki LM, Jalkanen S (2000) In vivo detection of vascular adhesion protein-1 in experimental inflammation. Am J Pathol 157:463-471.

Jakobsson E, Nilsson J, Ogg D, Kleywegt GJ (2005) Structure of human semicarbazide-sensitive amine oxidase/vascular adhesion protein-1. Acta Crystallogr D Biol Crystallogr 61:1550-1562.

Janes SM, Klinman JP (1995) Isolation of 2,4,5-trihydroxyphenylalanine quinone (topa quinone) from copper amine oxidases. Methods Enzymol 258:20-34.

Jeynes B, Provias J (2008) Evidence for altered LRP/RAGE expression in Alzheimer lesion pathogenesis. Curr Alzheimer Res 5:432-437.

Ji ZS, Mullendorff K, Cheng IH, Miranda RD, Huang Y, Mahley RW (2006) Reactivity of apolipoprotein E4 and amyloid beta peptide: lysosomal stability and neurodegeneration. J Biol Chem 281:2683-2692.

Jia X, Olson DJ, Ross AR, Wu L (2006) Structural and functional changes in human insulin induced by methylglyoxal. Faseb J 20:1555-1557.

Jiang ZJ, Richardson JS, Yu PH (2008) The contribution of cerebral vascular semicarbazide-sensitive amine oxidase to cerebral amyloid angiopathy in Alzheimer's disease. Neuropathol Appl Neurobiol 34:194-204.

Jick H, Zornberg GL, Jick SS, Seshadri S, Drachman DA (2000) Statins and the risk of dementia. Lancet 356:1627-1631.

Joachim CL, Duffy LK, Morris JH, Selkoe DJ (1988) Protein chemical and immunocytochemical studies of meningovascular beta-amyloid protein in Alzheimer's disease and normal aging. Brain Res 474:100-111.

Jordan J, Galindo MF, Miller RJ, Reardon CA, Getz GS, LaDu MJ (1998) Isoform-specific effect of apolipoprotein E on cell survival and beta-amyloid-induced toxicity in rat hippocampal pyramidal neuronal cultures. J Neurosci 18:195-204.

Kagan BL, Hirakura Y, Azimov R, Azimova R, Lin MC (2002) The channel hypothesis of Alzheimer's disease: current status. Peptides 23:1311-1315.

Kakio A, Nishimoto SI, Yanagisawa K, Kozutsumi Y, Matsuzaki K (2001) Cholesterol-dependent formation of GM1 ganglioside-bound amyloid beta-protein, an endogenous seed for Alzheimer amyloid. J Biol Chem 276:24985-24990.

Kakio A, Nishimoto S, Yanagisawa K, Kozutsumi Y, Matsuzaki K (2002) Interactions of amyloid beta-protein with various gangliosides in raft-like membranes: importance of GM1 ganglioside-bound form as an endogenous seed for Alzheimer amyloid. Biochemistry 41:7385-7390.

Kala SV, Hasinoff BB, Richardson JS (1996) Brain samples from Alzheimer's patients have elevated levels of loosely bound iron. Int J Neurosci 86:263-269.
Kalaria RN (2002) Small vessel disease and Alzheimer's dementia: pathological considerations. Cerebrovasc Dis 13 Suppl 2:48-52.
Kalaria RN (2003) Vascular factors in Alzheimer's disease. Int Psychogeriatr 15 Suppl 1:47-52.
Kalaria RN, Harik SI (1989) Reduced glucose transporter at the blood-brain barrier and in cerebral cortex in Alzheimer disease. J Neurochem 53:1083-1088.
Kalasz H (2003) Biological role of formaldehyde, and cycles related to methylation, demethylation, and formaldehyde production. Mini Rev Med Chem 3:175-192.
Kalmijn S, Foley D, White L, Burchfiel CM, Curb JD, Petrovitch H, Ross GW, Havlik RJ, Launer LJ (2000) Metabolic cardiovascular syndrome and risk of dementia in Japanese-American elderly men. The Honolulu-Asia aging study. Arterioscler Thromb Vasc Biol 20:2255-2260.
Kamino K, Nagasaka K, Imagawa M, Yamamoto H, Yoneda H, Ueki A, Kitamura S, Namekata K, Miki T, Ohta S (2000) Deficiency in mitochondrial aldehyde dehydrogenase increases the risk for late-onset Alzheimer's disease in the Japanese population. Biochem Biophys Res Commun 273:192-196.
Kanaya AM, Barrett-Connor E, Gildengorin G, Yaffe K (2004) Change in cognitive function by glucose tolerance status in older adults: a 4-year prospective study of the Rancho Bernardo study cohort. Arch Intern Med 164:1327-1333.
Kaneko H, Kakita A, Kasuga K, Nozaki H, Ishikawa A, Miyashita A, Kuwano R, Ito G, Iwatsubo T, Takahashi H, Nishizawa M, Onodera O, Sisodia SS, Ikeuchi T (2007) Enhanced accumulation of phosphorylated alpha-synuclein and elevated beta-amyloid 42/40 ratio caused by expression of the presenilin-1 deltaT440 mutant associated with familial Lewy body disease and variant Alzheimer's disease. J Neurosci 27:13092-13097.
Kang DE, Saitoh T, Chen X, Xia Y, Masliah E, Hansen LA, Thomas RG, Thal LJ, Katzman R (1997) Genetic association of the low-density lipoprotein receptor-related protein gene (LRP), an apolipoprotein E receptor, with late-onset Alzheimer's disease. Neurology 49:56-61.
Kang DE, Pietrzik CU, Baum L, Chevallier N, Merriam DE, Kounnas MZ, Wagner SL, Troncoso JC, Kawas CH, Katzman R, Koo EH (2000) Modulation of amyloid beta-protein clearance and Alzheimer's disease susceptibility by the LDL receptor-related protein pathway. J Clin Invest 106:1159-1166.
Karadi I, Meszaros Z, Csanyi A, Szombathy T, Hosszufalusi N, Romics L, Magyar K (2002) Serum semicarbazide-sensitive amine oxidase (SSAO) activity is an independent marker of carotid atherosclerosis. Clin Chim Acta 323:139-146.
Kayed R, Head E, Thompson JL, McIntire TM, Milton SC, Cotman CW, Glabe CG (2003) Common structure of soluble amyloid oligomers implies common mechanism of pathogenesis. Science 300:486-489.
Kayed R, Sokolov Y, Edmonds B, McIntire TM, Milton SC, Hall JE, Glabe CG (2004) Permeabilization of lipid bilayers is a common conformation-dependent activity of soluble amyloid oligomers in protein misfolding diseases. J Biol Chem 279:46363-46366.
Kazachkov M, Yu PH (2005) A novel HPLC procedure for detection and quantification of aminoacetone, a precursor of methylglyoxal, in biological samples. J Chromatogr B Analyt Technol Biomed Life Sci 824:116-122.

Kazachkov M, Chen K, Babiy S, Yu PH (2007) Evidence for in vivo scavenging by aminoguanidine of formaldehyde produced via semicarbazide-sensitive amine oxidase-mediated deamination. J Pharmacol Exp Ther 322:1201-1207.

Kehoe PG, Katzov H, Feuk L, Bennet AM, Johansson B, Wiman B, de Faire U, Cairns NJ, Wilcock GK, Brookes AJ, Blennow K, Prince JA (2003) Haplotypes extending across ACE are associated with Alzheimer's disease. Hum Mol Genet 12:859-867.

Keil U, Bonert A, Marques CA, Scherping I, Weyermann J, Strosznajder JB, Muller-Spahn F, Haass C, Czech C, Pradier L, Muller WE, Eckert A (2004) Amyloid beta-induced changes in nitric oxide production and mitochondrial activity lead to apoptosis. J Biol Chem 279:50310-50320.

Kelly JW (1998) The alternative conformations of amyloidogenic proteins and their multi-step assembly pathways. Curr Opin Struct Biol 8:101-106.

Khachaturian AS, Zandi PP, Lyketsos CG, Hayden KM, Skoog I, Norton MC, Tschanz JT, Mayer LS, Welsh-Bohmer KA, Breitner JC (2006) Antihypertensive medication use and incident Alzheimer disease: the Cache County Study. Arch Neurol 63:686-692.

Kheterpal I, Lashuel HA, Hartley DM, Walz T, Lansbury PT, Jr., Wetzel R (2003) Abeta protofibrils possess a stable core structure resistant to hydrogen exchange. Biochemistry 42:14092-14098.

Kim HS, Lee JH, Lee JP, Kim EM, Chang KA, Park CH, Jeong SJ, Wittendorp MC, Seo JH, Choi SH, Suh YH (2002) Amyloid beta peptide induces cytochrome C release from isolated mitochondria. Neuroreport 13:1989-1993.

Kinoshita A, Whelan CM, Smith CJ, Mikhailenko I, Rebeck GW, Strickland DK, Hyman BT (2001) Demonstration by fluorescence resonance energy transfer of two sites of interaction between the low-density lipoprotein receptor-related protein and the amyloid precursor protein: role of the intracellular adapter protein Fe65. J Neurosci 21:8354-8361.

Kirkitadze MD, Condron MM, Teplow DB (2001) Identification and characterization of key kinetic intermediates in amyloid beta-protein fibrillogenesis. J Mol Biol 312:1103-1119.

Kirton CM, Laukkanen ML, Nieminen A, Merinen M, Stolen CM, Armour K, Smith DJ, Salmi M, Jalkanen S, Clark MR (2005) Function-blocking antibodies to human vascular adhesion protein-1: a potential anti-inflammatory therapy. Eur J Immunol 35:3119-3130.

Kivipelto M, Helkala EL, Laakso MP, Hanninen T, Hallikainen M, Alhainen K, Soininen H, Tuomilehto J, Nissinen A (2001) Midlife vascular risk factors and Alzheimer's disease in later life: longitudinal, population based study. Bmj 322:1447-1451.

Kivisakk P, Mahad DJ, Callahan MK, Trebst C, Tucky B, Wei T, Wu L, Baekkevold ES, Lassmann H, Staugaitis SM, Campbell JJ, Ransohoff RM (2003) Human cerebrospinal fluid central memory CD4+ T cells: evidence for trafficking through choroid plexus and meninges via P-selectin. Proc Natl Acad Sci U S A 100:8389-8394.

Klein WL, Stine WB, Jr., Teplow DB (2004) Small assemblies of unmodified amyloid beta-protein are the proximate neurotoxin in Alzheimer's disease. Neurobiol Aging 25:569-580.

Klinman JP (1996) New quinocofactors in eukaryotes. J Biol Chem 271:27189-27192.

Klinman JP, Mu D (1994) Quinoenzymes in biology. Annu Rev Biochem 63:299-344.

Klunk WE, Jacob RF, Mason RP (1999) Quantifying amyloid beta-peptide (Abeta) aggregation using the Congo red-Abeta (CR-abeta) spectrophotometric assay. Anal Biochem 266:66-76.

Klyubin I, Betts V, Welzel AT, Blennow K, Zetterberg H, Wallin A, Lemere CA, Cullen WK, Peng Y, Wisniewski T, Selkoe DJ, Anwyl R, Walsh DM, Rowan MJ (2008) Amyloid beta protein dimer-containing human CSF disrupts synaptic plasticity: prevention by systemic passive immunization. J Neurosci 28:4231-4237.

Koo EH, Squazzo SL (1994) Evidence that production and release of amyloid beta-protein involves the endocytic pathway. J Biol Chem 269:17386-17389.

Koskinen K, Nevalainen S, Karikoski M, Hanninen A, Jalkanen S, Salmi M (2007) VAP-1-deficient mice display defects in mucosal immunity and antimicrobial responses: implications for antiadhesive applications. J Immunol 179:6160-6168.

Kounnas MZ, Moir RD, Rebeck GW, Bush AI, Argraves WS, Tanzi RE, Hyman BT, Strickland DK (1995) LDL receptor-related protein, a multifunctional ApoE receptor, binds secreted beta-amyloid precursor protein and mediates its degradation. Cell 82:331-340.

Kourie JI, Henry CL, Farrelly P (2001) Diversity of amyloid beta protein fragment [1-40]-formed channels. Cell Mol Neurobiol 21:255-284.

Kovacs GG, Budka H (2008) Prion diseases: from protein to cell pathology. Am J Pathol 172:555-565.

Kovari E, Gold G, Herrmann FR, Canuto A, Hof PR, Michel JP, Bouras C, Giannakopoulos P (2004) Cortical microinfarcts and demyelination significantly affect cognition in brain aging. Stroke 35:410-414.

Kowalewski T, Holtzman DM (1999) In situ atomic force microscopy study of Alzheimer's beta-amyloid peptide on different substrates: new insights into mechanism of beta-sheet formation. Proc Natl Acad Sci U S A 96:3688-3693.

Kuhla B, Luth HJ, Haferburg D, Boeck K, Arendt T, Munch G (2005) Methylglyoxal, glyoxal, and their detoxification in Alzheimer's disease. Ann N Y Acad Sci 1043:211-216.

Kumar U, Dunlop DM, Richardson JS (1994) Mitochondria from Alzheimer's fibroblasts show decreased uptake of calcium and increased sensitivity to free radicals. Life Sci 54:1855-1860.

Kunsch C, Medford RM (1999) Oxidative stress as a regulator of gene expression in the vasculature. Circ Res 85:753-766.

Kurkijarvi R, Jalkanen S, Isoniemi H, Salmi M (2001) Vascular adhesion protein-1 (VAP-1) mediates lymphocyte-endothelial interactions in chronic kidney rejection. Eur J Immunol 31:2876-2884.

Kurkijarvi R, Adams DH, Leino R, Mottonen T, Jalkanen S, Salmi M (1998) Circulating form of human vascular adhesion protein-1 (VAP-1): increased serum levels in inflammatory liver diseases. J Immunol 161:1549-1557.

Kurkijarvi R, Yegutkin GG, Gunson BK, Jalkanen S, Salmi M, Adams DH (2000) Circulating soluble vascular adhesion protein 1 accounts for the increased serum monoamine oxidase activity in chronic liver disease. Gastroenterology 119:1096-1103.

Lacor PN, Buniel MC, Furlow PW, Clemente AS, Velasco PT, Wood M, Viola KL, Klein WL (2007) Abeta oligomer-induced aberrations in synapse composition, shape, and density provide a molecular basis for loss of connectivity in Alzheimer's disease. J Neurosci 27:796-807.

Lalor PF, Edwards S, McNab G, Salmi M, Jalkanen S, Adams DH (2002) Vascular adhesion protein-1 mediates adhesion and transmigration of lymphocytes on human hepatic endothelial cells. J Immunol 169:983-992.

Lalor PF, Tuncer C, Weston C, Martin-Santos A, Smith DJ, Adams DH (2007) Vascular adhesion protein-1 as a potential therapeutic target in liver disease. Ann N Y Acad Sci 1110:485-496.

Lambert JC, Wavrant-De Vrieze F, Amouyel P, Chartier-Harlin MC (1998a) Association at LRP gene locus with sporadic late-onset Alzheimer's disease. Lancet 351:1787-1788.

Lambert MP, Barlow AK, Chromy BA, Edwards C, Freed R, Liosatos M, Morgan TE, Rozovsky I, Trommer B, Viola KL, Wals P, Zhang C, Finch CE, Krafft GA, Klein WL (1998b) Diffusible, nonfibrillar ligands derived from Abeta1-42 are potent central nervous system neurotoxins. Proc Natl Acad Sci U S A 95:6448-6453.

Langford SD, Trent MB, Boor PJ (2002) Semicarbazide-sensitive amine oxidase and extracellular matrix deposition by smooth-muscle cells. Cardiovasc Toxicol 2:141-150.

Langford SD, Trent MB, Balakumaran A, Boor PJ (1999) Developmental vasculotoxicity associated with inhibition of semicarbazide-sensitive amine oxidase. Toxicol Appl Pharmacol 155:237-244.

Lauderback CM, Hackett JM, Huang FF, Keller JN, Szweda LI, Markesbery WR, Butterfield DA (2001) The glial glutamate transporter, GLT-1, is oxidatively modified by 4-hydroxy-2-nonenal in the Alzheimer's disease brain: the role of Abeta1-42. J Neurochem 78:413-416.

Launer LJ, Ross GW, Petrovitch H, Masaki K, Foley D, White LR, Havlik RJ (2000) Midlife blood pressure and dementia: the Honolulu-Asia aging study. Neurobiol Aging 21:49-55.

Lee HG, Casadesus G, Zhu X, Takeda A, Perry G, Smith MA (2004a) Challenging the amyloid cascade hypothesis: senile plaques and amyloid-beta as protective adaptations to Alzheimer disease. Ann N Y Acad Sci 1019:1-4.

Lee JY, Friedman JE, Angel I, Kozak A, Koh JY (2004b) The lipophilic metal chelator DP-109 reduces amyloid pathology in brains of human beta-amyloid precursor protein transgenic mice. Neurobiol Aging 25:1315-1321.

Lee PL, Ho NJ, Olson R, Beutler E (1999) The effect of transferrin polymorphisms on iron metabolism. Blood Cells Mol Dis 25:374-379.

Lee VM, Balin BJ, Otvos L, Jr., Trojanowski JQ (1991) A68: a major subunit of paired helical filaments and derivatized forms of normal Tau. Science 251:675-678.

Lesne S, Koh MT, Kotilinek L, Kayed R, Glabe CG, Yang A, Gallagher M, Ashe KH (2006) A specific amyloid-beta protein assembly in the brain impairs memory. Nature 440:352-357.

Levy E, Carman MD, Fernandez-Madrid IJ, Power MD, Lieberburg I, van Duinen SG, Bots GT, Luyendijk W, Frangione B (1990) Mutation of the Alzheimer's disease amyloid gene in hereditary cerebral hemorrhage, Dutch type. Science 248:1124-1126.

Li PF, Dietz R, von Harsdorf R (1997) Differential effect of hydrogen peroxide and superoxide anion on apoptosis and proliferation of vascular smooth muscle cells. Circulation 96:3602-3609.

Li QX, Fuller SJ, Beyreuther K, Masters CL (1999) The amyloid precursor protein of Alzheimer disease in human brain and blood. J Leukoc Biol 66:567-574.

Li XL, Aou S, Oomura Y, Hori N, Fukunaga K, Hori T (2002a) Impairment of long-term potentiation and spatial memory in leptin receptor-deficient rodents. Neuroscience 113:607-615.

Li Y, Cam J, Bu G (2001) Low-density lipoprotein receptor family: endocytosis and signal transduction. Mol Neurobiol 23:53-67.

Li ZG, Zhang W, Grunberger G, Sima AA (2002b) Hippocampal neuronal apoptosis in type 1 diabetes. Brain Res 946:221-231.
Lin MS, Li HY, Wei JN, Lin CH, Smith DJ, Vainio J, Shih SR, Chen YH, Lin LC, Kao HL, Chuang LM, Chen MF (2008) Serum vascular adhesion protein-1 is higher in subjects with early stages of chronic kidney disease. Clin Biochem 41:1362-1367.
Lister KJ, Hickey MJ (2006) Immune complexes alter cerebral microvessel permeability: roles of complement and leukocyte adhesion. Am J Physiol Heart Circ Physiol 291:H694-704.
Liu L, Komatsu H, Murray IV, Axelsen PH (2008) Promotion of amyloid beta protein misfolding and fibrillogenesis by a lipid oxidation product. J Mol Biol 377:1236-1250.
Liu R, McAllister C, Lyubchenko Y, Sierks MR (2004) Residues 17-20 and 30-35 of beta-amyloid play critical roles in aggregation. J Neurosci Res 75:162-171.
Lizcano JM, Escrich E, Ribalta T, Muntane J, Unzeta M (1991) Amine oxidase activities in rat breast cancer induced experimentally with 7,12-dimethylbenz(alpha)anthracene. Biochem Pharmacol 42:263-269.
Lockman K, Hinson JS, Medlin MD, Morris D, Taylor JM, Mack CP (2004) Sphingosine 1-phosphate stimulates smooth muscle cell differentiation and proliferation by activating separate serum response factor co-factors. J Biol Chem 279:42422-42430.
Lomakin A, Chung DS, Benedek GB, Kirschner DA, Teplow DB (1996) On the nucleation and growth of amyloid beta-protein fibrils: detection of nuclei and quantitation of rate constants. Proc Natl Acad Sci U S A 93:1125-1129.
Lorenzo A, Yankner BA (1994) Beta-amyloid neurotoxicity requires fibril formation and is inhibited by congo red. Proc Natl Acad Sci U S A 91:12243-12247.
Lorton D, Schaller J, Lala A, De Nardin E (2000) Chemotactic-like receptors and Abeta peptide induced responses in Alzheimer's disease. Neurobiol Aging 21:463-473.
Lovell MA, Xie C, Markesbery WR (1998a) Decreased glutathione transferase activity in brain and ventricular fluid in Alzheimer's disease. Neurology 51:1562-1566.
Lovell MA, Ehmann WD, Butler SM, Markesbery WR (1995) Elevated thiobarbituric acid-reactive substances and antioxidant enzyme activity in the brain in Alzheimer's disease. Neurology 45:1594-1601.
Lovell MA, Robertson JD, Teesdale WJ, Campbell JL, Markesbery WR (1998b) Copper, iron and zinc in Alzheimer's disease senile plaques. J Neurol Sci 158:47-52.
Luber-Narod J, Rogers J (1988) Immune system associated antigens expressed by cells of the human central nervous system. Neurosci Lett 94:17-22.
Luchsinger JA, Tang MX, Shea S, Mayeux R (2004) Hyperinsulinemia and risk of Alzheimer disease. Neurology 63:1187-1192.
Luchsinger JA, Reitz C, Honig LS, Tang MX, Shea S, Mayeux R (2005) Aggregation of vascular risk factors and risk of incident Alzheimer disease. Neurology 65:545-551.
Lue LF, Walker DG, Brachova L, Beach TG, Rogers J, Schmidt AM, Stern DM, Yan SD (2001a) Involvement of microglial receptor for advanced glycation endproducts (RAGE) in Alzheimer's disease: identification of a cellular activation mechanism. Exp Neurol 171:29-45.
Lue LF, Kuo YM, Roher AE, Brachova L, Shen Y, Sue L, Beach T, Kurth JH, Rydel RE, Rogers J (1999) Soluble amyloid beta peptide concentration as a predictor of synaptic change in Alzheimer's disease. Am J Pathol 155:853-862.

Lue LF, Rydel R, Brigham EF, Yang LB, Hampel H, Murphy GM, Jr., Brachova L, Yan SD, Walker DG, Shen Y, Rogers J (2001b) Inflammatory repertoire of Alzheimer's disease and nondemented elderly microglia in vitro. Glia 35:72-79.

Lustbader JW, Cirilli M, Lin C, Xu HW, Takuma K, Wang N, Caspersen C, Chen X, Pollak S, Chaney M, Trinchese F, Liu S, Gunn-Moore F, Lue LF, Walker DG, Kuppusamy P, Zewier ZL, Arancio O, Stern D, Yan SS, Wu H (2004) ABAD directly links Abeta to mitochondrial toxicity in Alzheimer's disease. Science 304:448-452.

Lyles GA (1995) Substrate-specificity of mammalian tissue-bound semicarbazide-sensitive amine oxidase. Prog Brain Res 106:293-303.

Lyles GA (1996) Mammalian plasma and tissue-bound semicarbazide-sensitive amine oxidases: biochemical, pharmacological and toxicological aspects. Int J Biochem Cell Biol 28:259-274.

Lyles GA, McDougall SA (1989) The enhanced daily excretion of urinary methylamine in rats treated with semicarbazide or hydralazine may be related to the inhibition of semicarbazide-sensitive amine oxidase activities. J Pharm Pharmacol 41:97-100.

Lyles GA, Chalmers J (1992) The metabolism of aminoacetone to methylglyoxal by semicarbazide-sensitive amine oxidase in human umbilical artery. Biochem Pharmacol 43:1409-1414.

Ma B, Nussinov R (2002) Stabilities and conformations of Alzheimer's beta -amyloid peptide oligomers (Abeta 16-22, Abeta 16-35, and Abeta 10-35): Sequence effects. Proc Natl Acad Sci U S A 99:14126-14131.

Ma SL, Ng HK, Baum L, Pang JC, Chiu HF, Woo J, Tang NL, Lam LC (2002) Low-density lipoprotein receptor-related protein 8 (apolipoprotein E receptor 2) gene polymorphisms in Alzheimer's disease. Neurosci Lett 332:216-218.

Makin OS, Serpell LC (2005) Structures for amyloid fibrils. Febs J 272:5950-5961.

Man S, Ubogu EE, Ransohoff RM (2007) Inflammatory cell migration into the central nervous system: a few new twists on an old tale. Brain Pathol 17:243-250.

Mancuso M, Coppede F, Migliore L, Siciliano G, Murri L (2006) Mitochondrial dysfunction, oxidative stress and neurodegeneration. J Alzheimers Dis 10:59-73.

Mandybur TI (1975) The incidence of cerebral amyloid angiopathy in Alzheimer's disease. Neurology 25:120-126.

Mandybur TI, Chuirazzi CC (1990) Astrocytes and the plaques of Alzheimer's disease. Neurology 40:635-639.

Mankovsky BN, Metzger BE, Molitch ME, Biller J (1996) Cerebrovascular disorders in patients with diabetes mellitus. J Diabetes Complications 10:228-242.

Marcus DL, Freedman ML (1997) Decreased brain glucose metabolism in microvessels from patients with Alzheimer's disease. Ann N Y Acad Sci 826:248-253.

Marjanska M, Curran GL, Wengenack TM, Henry PG, Bliss RL, Poduslo JF, Jack CR, Jr., Ugurbil K, Garwood M (2005) Monitoring disease progression in transgenic mouse models of Alzheimer's disease with proton magnetic resonance spectroscopy. Proc Natl Acad Sci U S A 102:11906-11910.

Marlatt MW, Lucassen PJ, Perry G, Smith MA, Zhu X (2008) Alzheimer's disease: cerebrovascular dysfunction, oxidative stress, and advanced clinical therapies. J Alzheimers Dis 15:199-210.

Martel CL, Mackic JB, Matsubara E, Governale S, Miguel C, Miao W, McComb JG, Frangione B, Ghiso J, Zlokovic BV (1997) Isoform-specific effects of apolipoproteins E2, E3, and

E4 on cerebral capillary sequestration and blood-brain barrier transport of circulating Alzheimer's amyloid beta. J Neurochem 69:1995-2004.
Martelius T, Salaspuro V, Salmi M, Krogerus L, Hockerstedt K, Jalkanen S, Lautenschlager I (2004) Blockade of vascular adhesion protein-1 inhibits lymphocyte infiltration in rat liver allograft rejection. Am J Pathol 165:1993-2001.
Martin BK, Szekely C, Brandt J, Piantadosi S, Breitner JC, Craft S, Evans D, Green R, Mullan M (2008) Cognitive function over time in the Alzheimer's Disease Anti-inflammatory Prevention Trial (ADAPT): results of a randomized, controlled trial of naproxen and celecoxib. Arch Neurol 65:896-905.
Marttila-Ichihara F, Smith DJ, Stolen C, Yegutkin GG, Elima K, Mercier N, Kiviranta R, Pihlavisto M, Alaranta S, Pentikainen U, Pentikainen O, Fulop F, Jalkanen S, Salmi M (2006) Vascular amine oxidases are needed for leukocyte extravasation into inflamed joints in vivo. Arthritis Rheum 54:2852-2862.
Masinovsky B, Urdal D, Gallatin WM (1990) IL-4 acts synergistically with IL-1 beta to promote lymphocyte adhesion to microvascular endothelium by induction of vascular cell adhesion molecule-1. J Immunol 145:2886-2895.
Mathys KC, Ponnampalam SN, Padival S, Nagaraj RH (2002) Semicarbazide-sensitive amine oxidase in aortic smooth muscle cells mediates synthesis of a methylglyoxal-AGE: implications for vascular complications in diabetes. Biochem Biophys Res Commun 297:863-869.
Mattson MP, Fu W, Waeg G, Uchida K (1997) 4-Hydroxynonenal, a product of lipid peroxidation, inhibits dephosphorylation of the microtubule-associated protein tau. Neuroreport 8:2275-2281.
Mattson MP, Cheng B, Culwell AR, Esch FS, Lieberburg I, Rydel RE (1993) Evidence for excitoprotective and intraneuronal calcium-regulating roles for secreted forms of the beta-amyloid precursor protein. Neuron 10:243-254.
May P, Woldt E, Matz RL, Boucher P (2007) The LDL receptor-related protein (LRP) family: an old family of proteins with new physiological functions. Ann Med 39:219-228.
McGeer PL, Schulzer M, McGeer EG (1996) Arthritis and anti-inflammatory agents as possible protective factors for Alzheimer's disease: a review of 17 epidemiologic studies. Neurology 47:425-432.
McGuirl MA, Dooley DM (1999) Copper-containing oxidases. Curr Opin Chem Biol 3:138-144.
Mecocci P, MacGarvey U, Beal MF (1994) Oxidative damage to mitochondrial DNA is increased in Alzheimer's disease. Ann Neurol 36:747-751.
Merinen M, Irjala H, Salmi M, Jaakkola I, Hanninen A, Jalkanen S (2005) Vascular adhesion protein-1 is involved in both acute and chronic inflammation in the mouse. Am J Pathol 166:793-800.
Merlini G, Bellotti V (2003) Molecular mechanisms of amyloidosis. N Engl J Med 349:583-596.
Meszaros Z, Karadi I, Csanyi A, Szombathy T, Romics L, Magyar K (1999a) Determination of human serum semicarbazide-sensitive amine oxidase activity: a possible clinical marker of atherosclerosis. Eur J Drug Metab Pharmacokinet 24:299-302.
Meszaros Z, Szombathy T, Raimondi L, Karadi I, Romics L, Magyar K (1999b) Elevated serum semicarbazide-sensitive amine oxidase activity in non-insulin-dependent diabetes mellitus: correlation with body mass index and serum triglyceride. Metabolism 48:113-117.

Metz B, Kersten GF, Hoogerhout P, Brugghe HF, Timmermans HA, de Jong A, Meiring H, ten Hove J, Hennink WE, Crommelin DJ, Jiskoot W (2004) Identification of formaldehyde-induced modifications in proteins: reactions with model peptides. J Biol Chem 279:6235-6243.

Michel V, Bakovic M (2007) Lipid rafts in health and disease. Biol Cell 99:129-140.

Michikawa M (2003) Cholesterol paradox: is high total or low HDL cholesterol level a risk for Alzheimer's disease? J Neurosci Res 72:141-146.

Mielke MM, Rosenberg PB, Tschanz J, Cook L, Corcoran C, Hayden KM, Norton M, Rabins PV, Green RC, Welsh-Bohmer KA, Breitner JC, Munger R, Lyketsos CG (2007) Vascular factors predict rate of progression in Alzheimer disease. Neurology 69:1850-1858.

Milionis HJ, Florentin M, Giannopoulos S (2008) Metabolic syndrome and Alzheimer's disease: a link to a vascular hypothesis? CNS Spectr 13:606-613.

Mills S, Cain J, Purandare N, Jackson A (2007) Biomarkers of cerebrovascular disease in dementia. Br J Radiol 80 Spec No 2:S128-145.

Mitrushina M, Drebing C, Uchiyama C, Satz P, Van Gorp W, Chervinsky A (1994) The pattern of deficit in different memory components in normal aging and dementia of Alzheimer's type. J Clin Psychol 50:591-596.

Moestrup SK, Gliemann J (1991) Analysis of ligand recognition by the purified alpha 2-macroglobulin receptor (low density lipoprotein receptor-related protein). Evidence that high affinity of alpha 2-macroglobulin-proteinase complex is achieved by binding to adjacent receptors. J Biol Chem 266:14011-14017.

Moir RD, Atwood CS, Romano DM, Laurans MH, Huang X, Bush AI, Smith JD, Tanzi RE (1999) Differential effects of apolipoprotein E isoforms on metal-induced aggregation of A beta using physiological concentrations. Biochemistry 38:4595-4603.

Moldes M, Feve B, Pairault J (1999) Molecular cloning of a major mRNA species in murine 3T3 adipocyte lineage. differentiation-dependent expression, regulation, and identification as semicarbazide-sensitive amine oxidase. J Biol Chem 274:9515-9523.

Monnier VM (2003) Intervention against the Maillard reaction in vivo. Arch Biochem Biophys 419:1-15.

Montine KS, Olson SJ, Amarnath V, Whetsell WO, Jr., Graham DG, Montine TJ (1997) Immunohistochemical detection of 4-hydroxy-2-nonenal adducts in Alzheimer's disease is associated with inheritance of APOE4. Am J Pathol 150:437-443.

Moossy J (1993) Pathology of cerebral atherosclerosis. Influence of age, race, and gender. Stroke 24:I22-23; I31-22.

Morin N, Lizcano JM, Fontana E, Marti L, Smih F, Rouet P, Prevot D, Zorzano A, Unzeta M, Carpene C (2001) Semicarbazide-sensitive amine oxidase substrates stimulate glucose transport and inhibit lipolysis in human adipocytes. J Pharmacol Exp Ther 297:563-572.

Morris NJ, Ducret A, Aebersold R, Ross SA, Keller SR, Lienhard GE (1997) Membrane amine oxidase cloning and identification as a major protein in the adipocyte plasma membrane. J Biol Chem 272:9388-9392.

Mullan M, Crawford F, Axelman K, Houlden H, Lilius L, Winblad B, Lannfelt L (1992) A pathogenic mutation for probable Alzheimer's disease in the APP gene at the N-terminus of beta-amyloid. Nat Genet 1:345-347.

Murphy DL, Wyatt RJ (1975) Neurotransmitter-related enzymes in the major psychiatric disorders: I. Catechol-O-methyl transferase, monoamine oxidase in the affective

disorders, and factors affecting some behaviorally correlated enzyme activities. Res Publ Assoc Res Nerv Ment Dis 54:277-288.
Muyllaert D, Terwel D, Borghgraef P, Devijver H, Dewachter I, Van Leuven F (2006) Transgenic mouse models for Alzheimer's disease: the role of GSK-3B in combined amyloid and tau-pathology. Rev Neurol (Paris) 162:903-907.
Naiki H, Nakakuki K (1996) First-order kinetic model of Alzheimer's beta-amyloid fibril extension in vitro. Lab Invest 74:374-383.
Naiki H, Higuchi K, Hosokawa M, Takeda T (1989) Fluorometric determination of amyloid fibrils in vitro using the fluorescent dye, thioflavin T1. Anal Biochem 177:244-249.
Narita M, Holtzman DM, Schwartz AL, Bu G (1997) Alpha2-macroglobulin complexes with and mediates the endocytosis of beta-amyloid peptide via cell surface low-density lipoprotein receptor-related protein. J Neurochem 69:1904-1911.
Naslund J, Haroutunian V, Mohs R, Davis KL, Davies P, Greengard P, Buxbaum JD (2000) Correlation between elevated levels of amyloid beta-peptide in the brain and cognitive decline. Jama 283:1571-1577.
Nazem A, Mansoori GA (2008) Nanotechnology solutions for Alzheimer's disease: advances in research tools, diagnostic methods and therapeutic agents. J Alzheimers Dis 13:199-223.
Neely MD, Sidell KR, Graham DG, Montine TJ (1999) The lipid peroxidation product 4-hydroxynonenal inhibits neurite outgrowth, disrupts neuronal microtubules, and modifies cellular tubulin. J Neurochem 72:2323-2333.
Neve RL, Robakis NK (1998) Alzheimer's disease: a re-examination of the amyloid hypothesis. Trends Neurosci 21:15-19.
Nilsson SE, Tryding N, Tufvesson G (1968) Serum monoamine oxidase (MAO) in diabetes mellitus and some other internal diseases. Acta Med Scand 184:105-108.
Nischwitz V, Berthele A, Michalke B (2008) Speciation analysis of selected metals and determination of their total contents in paired serum and cerebrospinal fluid samples: An approach to investigate the permeability of the human blood-cerebrospinal fluid-barrier. Anal Chim Acta 627:258-269.
Noda K, Miyahara S, Nakazawa T, Almulki L, Nakao S, Hisatomi T, She H, Thomas KL, Garland RC, Miller JW, Gragoudas ES, Kawai Y, Mashima Y, Hafezi-Moghadam A (2008a) Inhibition of vascular adhesion protein-1 suppresses endotoxin-induced uveitis. Faseb J 22:1094-1103.
Noda K, She H, Nakazawa T, Hisatomi T, Nakao S, Almulki L, Zandi S, Miyahara S, Ito Y, Thomas KL, Garland RC, Miller JW, Gragoudas ES, Mashima Y, Hafezi-Moghadam A (2008b) Vascular adhesion protein-1 blockade suppresses choroidal neovascularization. Faseb J 22:2928-2935.
Notkola IL, Sulkava R, Pekkanen J, Erkinjuntti T, Ehnholm C, Kivinen P, Tuomilehto J, Nissinen A (1998) Serum total cholesterol, apolipoprotein E epsilon 4 allele, and Alzheimer's disease. Neuroepidemiology 17:14-20.
Nunan J, Small DH (2000) Regulation of APP cleavage by alpha-, beta- and gamma-secretases. FEBS Lett 483:6-10.
Nunes SF, Figueiredo IV, Soares PJ, Costa NE, Lopes MC, Caramona MM (2008) Semicarbazide-sensitive amine oxidase activity and total nitrite and nitrate concentrations in serum: novel biochemical markers for type 2 diabetes? Acta Diabetol.
Nykjaer A, Willnow TE (2002) The low-density lipoprotein receptor gene family: a cellular Swiss army knife? Trends Cell Biol 12:273-280.

O'Rourke AM, Wang EY, Miller A, Podar EM, Scheyhing K, Huang L, Kessler C, Gao H, Ton-Nu HT, Macdonald MT, Jones DS, Linnik MD (2008) Anti-inflammatory effects of LJP 1586 [Z-3-fluoro-2-(4-methoxybenzyl)allylamine hydrochloride], an amine-based inhibitor of semicarbazide-sensitive amine oxidase activity. J Pharmacol Exp Ther 324:867-875.

Ono K, Hirohata M, Yamada M (2008) Alpha-synuclein assembly as a therapeutic target of Parkinson's disease and related disorders. Curr Pharm Des 14:3247-3266.

Opazo C, Huang X, Cherny RA, Moir RD, Roher AE, White AR, Cappai R, Masters CL, Tanzi RE, Inestrosa NC, Bush AI (2002) Metalloenzyme-like activity of Alzheimer's disease beta-amyloid. Cu-dependent catalytic conversion of dopamine, cholesterol, and biological reducing agents to neurotoxic H(2)O(2). J Biol Chem 277:40302-40308.

Ott A, Stolk RP, van Harskamp F, Pols HA, Hofman A, Breteler MM (1999) Diabetes mellitus and the risk of dementia: The Rotterdam Study. Neurology 53:1937-1942.

Paigen B, Morrow A, Brandon C, Mitchell D, Holmes P (1985) Variation in susceptibility to atherosclerosis among inbred strains of mice. Atherosclerosis 57:65-73.

Paigen B, Ishida BY, Verstuyft J, Winters RB, Albee D (1990) Atherosclerosis susceptibility differences among progenitors of recombinant inbred strains of mice. Arteriosclerosis 10:316-323.

Pallitto MM, Murphy RM (2001) A mathematical model of the kinetics of beta-amyloid fibril growth from the denatured state. Biophys J 81:1805-1822.

Palmer AM, Burns MA (1994) Selective increase in lipid peroxidation in the inferior temporal cortex in Alzheimer's disease. Brain Res 645:338-342.

Pamplona R, Dalfo E, Ayala V, Bellmunt MJ, Prat J, Ferrer I, Portero-Otin M (2005) Proteins in human brain cortex are modified by oxidation, glycoxidation, and lipoxidation. Effects of Alzheimer disease and identification of lipoxidation targets. J Biol Chem 280:21522-21530.

Pantoni L, Leys D, Fazekas F, Longstreth WT, Jr., Inzitari D, Wallin A, Filippi M, Scheltens P, Erkinjuntti T, Hachinski V (1999) Role of white matter lesions in cognitive impairment of vascular origin. Alzheimer Dis Assoc Disord 13 Suppl 3:S49-54.

Pappolla MA, Omar RA, Kim KS, Robakis NK (1992) Immunohistochemical evidence of oxidative [corrected] stress in Alzheimer's disease. Am J Pathol 140:621-628.

Paris D, Humphrey J, Quadros A, Patel N, Crescentini R, Crawford F, Mullan M (2003) Vasoactive effects of A beta in isolated human cerebrovessels and in a transgenic mouse model of Alzheimer's disease: role of inflammation. Neurol Res 25:642-651.

Parks JK, Smith TS, Trimmer PA, Bennett JP, Jr., Parker WD, Jr. (2001) Neurotoxic Abeta peptides increase oxidative stress in vivo through NMDA-receptor and nitric-oxide-synthase mechanisms, and inhibit complex IV activity and induce a mitochondrial permeability transition in vitro. J Neurochem 76:1050-1056.

Parsons MR, Convery MA, Wilmot CM, Yadav KD, Blakeley V, Corner AS, Phillips SE, McPherson MJ, Knowles PF (1995) Crystal structure of a quinoenzyme: copper amine oxidase of Escherichia coli at 2 A resolution. Structure 3:1171-1184.

Pasinetti GM, Eberstein JA (2008) Metabolic syndrome and the role of dietary lifestyles in Alzheimer's disease. J Neurochem 106:1503-1514.

Paulsson JF, Schultz SW, Kohler M, Leibiger I, Berggren PO, Westermark GT (2008) Real-time monitoring of apoptosis by caspase-3-like protease induced FRET reduction triggered by amyloid aggregation. Exp Diabetes Res 2008:865850.

Perez M, Cuadros R, Smith MA, Perry G, Avila J (2000) Phosphorylated, but not native, tau protein assembles following reaction with the lipid peroxidation product, 4-hydroxy-2-nonenal. FEBS Lett 486:270-274.

Petkova AT, Ishii Y, Balbach JJ, Antzutkin ON, Leapman RD, Delaglio F, Tycko R (2002) A structural model for Alzheimer's beta -amyloid fibrils based on experimental constraints from solid state NMR. Proc Natl Acad Sci U S A 99:16742-16747.

Petrovitch H, White LR, Izmirilian G, Ross GW, Havlik RJ, Markesbery W, Nelson J, Davis DG, Hardman J, Foley DJ, Launer LJ (2000) Midlife blood pressure and neuritic plaques, neurofibrillary tangles, and brain weight at death: the HAAS. Honolulu-Asia aging Study. Neurobiol Aging 21:57-62.

Pfeifer LA, White LR, Ross GW, Petrovitch H, Launer LJ (2002) Cerebral amyloid angiopathy and cognitive function: the HAAS autopsy study. Neurology 58:1629-1634.

Picklo MJ, Olson SJ, Markesbery WR, Montine TJ (2001) Expression and activities of aldo-keto oxidoreductases in Alzheimer disease. J Neuropathol Exp Neurol 60:686-695.

Picklo MJ, Montine TJ, Amarnath V, Neely MD (2002) Carbonyl toxicology and Alzheimer's disease. Toxicol Appl Pharmacol 184:187-197.

Picklo MJ, Amarnath V, McIntyre JO, Graham DG, Montine TJ (1999) 4-Hydroxy-2(E)-nonenal inhibits CNS mitochondrial respiration at multiple sites. J Neurochem 72:1617-1624.

Pietrzik CU, Busse T, Merriam DE, Weggen S, Koo EH (2002) The cytoplasmic domain of the LDL receptor-related protein regulates multiple steps in APP processing. Embo J 21:5691-5700.

Pietrzik CU, Yoon IS, Jaeger S, Busse T, Weggen S, Koo EH (2004) FE65 constitutes the functional link between the low-density lipoprotein receptor-related protein and the amyloid precursor protein. J Neurosci 24:4259-4265.

Pitschke M, Prior R, Haupt M, Riesner D (1998) Detection of single amyloid beta-protein aggregates in the cerebrospinal fluid of Alzheimer's patients by fluorescence correlation spectroscopy. Nat Med 4:832-834.

Precious E, Gunn CE, Lyles GA (1988) Deamination of methylamine by semicarbazide-sensitive amine oxidase in human umbilical artery and rat aorta. Biochem Pharmacol 37:707-713.

Prelli F, Castano E, Glenner GG, Frangione B (1988) Differences between vascular and plaque core amyloid in Alzheimer's disease. J Neurochem 51:648-651.

Prevot D, Soltesz Z, Abello V, Wanecq E, Valet P, Unzeta M, Carpene C (2007) Prolonged treatment with aminoguanidine strongly inhibits adipocyte semicarbazide-sensitive amine oxidase and slightly reduces fat deposition in obese Zucker rats. Pharmacol Res 56:70-79.

Priller C, Bauer T, Mitteregger G, Krebs B, Kretzschmar HA, Herms J (2006) Synapse formation and function is modulated by the amyloid precursor protein. J Neurosci 26:7212-7221.

Qahwash IM, Boire A, Lanning J, Krausz T, Pytel P, Meredith SC (2007) Site-specific effects of peptide lipidation on beta-amyloid aggregation and cytotoxicity. J Biol Chem 282:36987-36997.

Qin Z, Hu D, Han S, Reaney SH, Di Monte DA, Fink AL (2007) Effect of 4-hydroxy-2-nonenal modification on alpha-synuclein aggregation. J Biol Chem 282:5862-5870.

Qiu C, Winblad B, Fratiglioni L (2005) The age-dependent relation of blood pressure to cognitive function and dementia. Lancet Neurol 4:487-499.

Qiu WQ, Walsh DM, Ye Z, Vekrellis K, Zhang J, Podlisny MB, Rosner MR, Safavi A, Hersh LB, Selkoe DJ (1998) Insulin-degrading enzyme regulates extracellular levels of amyloid beta-protein by degradation. J Biol Chem 273:32730-32738.

Qiu Z, Strickland DK, Hyman BT, Rebeck GW (1999) Alpha2-macroglobulin enhances the clearance of endogenous soluble beta-amyloid peptide via low-density lipoprotein receptor-related protein in cortical neurons. J Neurochem 73:1393-1398.

Racchi M, Baetta R, Salvietti N, Ianna P, Franceschini G, Paoletti R, Fumagalli R, Govoni S, Trabucchi M, Soma M (1997) Secretory processing of amyloid precursor protein is inhibited by increase in cellular cholesterol content. Biochem J 322 (Pt 3):893-898.

Rao GN, Berk BC (1992) Active oxygen species stimulate vascular smooth muscle cell growth and proto-oncogene expression. Circ Res 70:593-599.

Ray JL, Leach R, Herbert JM, Benson M (2001) Isolation of vascular smooth muscle cells from a single murine aorta. Methods Cell Sci 23:185-188.

Razay G, Vreugdenhil A, Wilcock G (2007) The metabolic syndrome and Alzheimer disease. Arch Neurol 64:93-96.

Rebeck GW, Harr SD, Strickland DK, Hyman BT (1995) Multiple, diverse senile plaque-associated proteins are ligands of an apolipoprotein E receptor, the alpha 2-macroglobulin receptor/low-density-lipoprotein receptor-related protein. Ann Neurol 37:211-217.

Reches M, Gazit E (2003) Casting metal nanowires within discrete self-assembled peptide nanotubes. Science 300:625-627.

Refolo LM, Malester B, LaFrancois J, Bryant-Thomas T, Wang R, Tint GS, Sambamurti K, Duff K, Pappolla MA (2000) Hypercholesterolemia accelerates the Alzheimer's amyloid pathology in a transgenic mouse model. Neurobiol Dis 7:321-331.

Riekse RG, Leverenz JB, McCormick W, Bowen JD, Teri L, Nochlin D, Simpson K, Eugenio C, Larson EB, Tsuang D (2004) Effect of vascular lesions on cognition in Alzheimer's disease: a community-based study. J Am Geriatr Soc 52:1442-1448.

Robinson-White A, Baylin SB, Olivecrona T, Beaven MA (1985) Binding of diamine oxidase activity to rat and guinea pig microvascular endothelial cells. Comparisons with lipoprotein lipase binding. J Clin Invest 76:93-100.

Rogaeva E, Meng Y, Lee JH, Gu Y, Kawarai T, Zou F, Katayama T, Baldwin CT, Cheng R, Hasegawa H, Chen F, Shibata N, Lunetta KL, Pardossi-Piquard R, Bohm C, Wakutani Y, Cupples LA, Cuenco KT, Green RC, Pinessi L, Rainero I, Sorbi S, Bruni A, Duara R, Friedland RP, Inzelberg R, Hampe W, Bujo H, Song YQ, Andersen OM, Willnow TE, Graff-Radford N, Petersen RC, Dickson D, Der SD, Fraser PE, Schmitt-Ulms G, Younkin S, Mayeux R, Farrer LA, St George-Hyslop P (2007) The neuronal sortilin-related receptor SORL1 is genetically associated with Alzheimer disease. Nat Genet 39:168-177.

Rogers J, Luber-Narod J, Styren SD, Civin WH (1988) Expression of immune system-associated antigens by cells of the human central nervous system: relationship to the pathology of Alzheimer's disease. Neurobiol Aging 9:339-349.

Rogers J, Webster S, Lue LF, Brachova L, Civin WH, Emmerling M, Shivers B, Walker D, McGeer P (1996) Inflammation and Alzheimer's disease pathogenesis. Neurobiol Aging 17:681-686.

Rogers J, Cooper NR, Webster S, Schultz J, McGeer PL, Styren SD, Civin WH, Brachova L, Bradt B, Ward P, et al. (1992) Complement activation by beta-amyloid in Alzheimer disease. Proc Natl Acad Sci U S A 89:10016-10020.

Roher AE, Lowenson JD, Clarke S, Woods AS, Cotter RJ, Gowing E, Ball MJ (1993) beta-Amyloid-(1-42) is a major component of cerebrovascular amyloid deposits: implications for the pathology of Alzheimer disease. Proc Natl Acad Sci U S A 90:10836-10840.

Roher AE, Esh C, Kokjohn TA, Kalback W, Luehrs DC, Seward JD, Sue LI, Beach TG (2003) Circle of willis atherosclerosis is a risk factor for sporadic Alzheimer's disease. Arterioscler Thromb Vasc Biol 23:2055-2062.

Roher AE, Chaney MO, Kuo YM, Webster SD, Stine WB, Haverkamp LJ, Woods AS, Cotter RJ, Tuohy JM, Krafft GA, Bonnell BS, Emmerling MR (1996) Morphology and toxicity of Abeta-(1-42) dimer derived from neuritic and vascular amyloid deposits of Alzheimer's disease. J Biol Chem 271:20631-20635.

Roman GC, Royall DR (2004) A diagnostic dilemma: is "Alzheimer's dementia" Alzheimer's disease, vascular dementia, or both? Lancet Neurol 3:141.

Ronicke R, Klemm A, Meinhardt J, Schroder UH, Fandrich M, Reymann KG (2008) Abeta mediated diminution of MTT reduction--an artefact of single cell culture? PLoS ONE 3:e3236.

Rosenberg RN (2000) The molecular and genetic basis of AD: the end of the beginning: the 2000 Wartenberg lecture. Neurology 54:2045-2054.

Rottkamp CA, Raina AK, Zhu X, Gaier E, Bush AI, Atwood CS, Chevion M, Perry G, Smith MA (2001) Redox-active iron mediates amyloid-beta toxicity. Free Radic Biol Med 30:447-450.

Sagare A, Deane R, Bell RD, Johnson B, Hamm K, Pendu R, Marky A, Lenting PJ, Wu Z, Zarcone T, Goate A, Mayo K, Perlmutter D, Coma M, Zhong Z, Zlokovic BV (2007) Clearance of amyloid-beta by circulating lipoprotein receptors. Nat Med 13:1029-1031.

Salmi M, Jalkanen S (2006) Developmental regulation of the adhesive and enzymatic activity of vascular adhesion protein-1 (VAP-1) in humans. Blood 108:1555-1561.

Salmi M, Kalimo K, Jalkanen S (1993) Induction and function of vascular adhesion protein-1 at sites of inflammation. J Exp Med 178:2255-2260.

Salmi M, Hellman J, Jalkanen S (1998) The role of two distinct endothelial molecules, vascular adhesion protein-1 and peripheral lymph node addressin, in the binding of lymphocyte subsets to human lymph nodes. J Immunol 160:5629-5636.

Salmi M, Tohka S, Berg EL, Butcher EC, Jalkanen S (1997) Vascular adhesion protein 1 (VAP-1) mediates lymphocyte subtype-specific, selectin-independent recognition of vascular endothelium in human lymph nodes. J Exp Med 186:589-600.

Salmi M, Yegutkin GG, Lehvonen R, Koskinen K, Salminen T, Jalkanen S (2001) A cell surface amine oxidase directly controls lymphocyte migration. Immunity 14:265-276.

Salminen TA, Smith DJ, Jalkanen S, Johnson MS (1998) Structural model of the catalytic domain of an enzyme with cell adhesion activity: human vascular adhesion protein-1 (HVAP-1) D4 domain is an amine oxidase. Protein Eng 11:1195-1204.

Salter-Cid LM, Wang E, O'Rourke AM, Miller A, Gao H, Huang L, Garcia A, Linnik MD (2005) Anti-inflammatory effects of inhibiting the amine oxidase activity of semicarbazide-sensitive amine oxidase. J Pharmacol Exp Ther 315:553-562.

Sartori G, Snitz BE, Sorcinelli L, Daum I (2004) Remote memory in advanced Alzheimer's disease. Arch Clin Neuropsychol 19:779-789.

Saunders AM, Strittmatter WJ, Schmechel D, George-Hyslop PH, Pericak-Vance MA, Joo SH, Rosi BL, Gusella JF, Crapper-MacLachlan DR, Alberts MJ, et al. (1993) Association of apolipoprotein E allele epsilon 4 with late-onset familial and sporadic Alzheimer's disease. Neurology 43:1467-1472.

Savaskan E, Hock C, Olivieri G, Bruttel S, Rosenberg C, Hulette C, Muller-Spahn F (2001) Cortical alterations of angiotensin converting enzyme, angiotensin II and AT1 receptor in Alzheimer's dementia. Neurobiol Aging 22:541-546.

Sayre LM, Zelasko DA, Harris PL, Perry G, Salomon RG, Smith MA (1997) 4-Hydroxynonenal-derived advanced lipid peroxidation end products are increased in Alzheimer's disease. J Neurochem 68:2092-2097.

Schayer RW, Smiley RL, Kaplan EH (1952) The metabolism of epinephrine containing isotopic carbon. II. J Biol Chem 198:545-551.

Scheibel AB (1987) Alterations of the cerebral capillary bed in the senile dementia of Alzheimer. Ital J Neurol Sci 8:457-463.

Scheuner D, Eckman C, Jensen M, Song X, Citron M, Suzuki N, Bird TD, Hardy J, Hutton M, Kukull W, Larson E, Levy-Lahad E, Viitanen M, Peskind E, Poorkaj P, Schellenberg G, Tanzi R, Wasco W, Lannfelt L, Selkoe D, Younkin S (1996) Secreted amyloid beta-protein similar to that in the senile plaques of Alzheimer's disease is increased in vivo by the presenilin 1 and 2 and APP mutations linked to familial Alzheimer's disease. Nat Med 2:864-870.

Selkoe DJ (1991) The molecular pathology of Alzheimer's disease. Neuron 6:487-498.

Selkoe DJ (1994) Amyloid beta-protein precursor: new clues to the genesis of Alzheimer's disease. Curr Opin Neurobiol 4:708-716.

Selkoe DJ (2008) Soluble oligomers of the amyloid beta-protein impair synaptic plasticity and behavior. Behav Brain Res 192:106-113.

Serpell LC, Berriman J, Jakes R, Goedert M, Crowther RA (2000) Fiber diffraction of synthetic alpha-synuclein filaments shows amyloid-like cross-beta conformation. Proc Natl Acad Sci U S A 97:4897-4902.

Shah GN, Mooradian AD (1997) Age-related changes in the blood-brain barrier. Exp Gerontol 32:501-519.

Shankar GM, Li S, Mehta TH, Garcia-Munoz A, Shepardson NE, Smith I, Brett FM, Farrell MA, Rowan MJ, Lemere CA, Regan CM, Walsh DM, Sabatini BL, Selkoe DJ (2008) Amyloid-beta protein dimers isolated directly from Alzheimer's brains impair synaptic plasticity and memory. Nat Med 14:837-842.

Shen Y, Sullivan T, Lee CM, Meri S, Shiosaki K, Lin CW (1998) Induced expression of neuronal membrane attack complex and cell death by Alzheimer's beta-amyloid peptide. Brain Res 796:187-197.

Sherry RL, Baker GB, Coutts RT (1990) Effects of low-dose 4-fluorotranylcypromine on rat brain monoamine oxidase and neurotransmitter amines. Biol Psychiatry 28:539-543.

Shi XP, Tugusheva K, Bruce JE, Lucka A, Wu GX, Chen-Dodson E, Price E, Li Y, Xu M, Huang Q, Sardana MK, Hazuda DJ (2003) Beta-secretase cleavage at amino acid residue 34 in the amyloid beta peptide is dependent upon gamma-secretase activity. J Biol Chem 278:21286-21294.

Shibata M, Yamada S, Kumar SR, Calero M, Bading J, Frangione B, Holtzman DM, Miller CA, Strickland DK, Ghiso J, Zlokovic BV (2000) Clearance of Alzheimer's amyloid-ss(1-40) peptide from brain by LDL receptor-related protein-1 at the blood-brain barrier. J Clin Invest 106:1489-1499.

Shih JC, Chen K, Ridd MJ (1999) Monoamine oxidase: from genes to behavior. Annu Rev Neurosci 22:197-217.

Shuvaev VV, Laffont I, Serot JM, Fujii J, Taniguchi N, Siest G (2001) Increased protein glycation in cerebrospinal fluid of Alzheimer's disease. Neurobiol Aging 22:397-402.
Sibon I, Mercier N, Darret D, Lacolley P, Lamaziere JM (2008) Association between semicarbazide-sensitive amine oxidase, a regulator of the glucose transporter, and elastic lamellae thinning during experimental cerebral aneurysm development: laboratory investigation. J Neurosurg 108:558-566.
Sibon I, Larrieu D, El Hadri K, Mercier N, Feve B, Lacolley P, Labat C, Daret D, Bonnet J, Lamaziere JM (2004) Semicarbazide-sensitive amine oxidase in annulo-aortic ectasia disease: relation to elastic lamellae-associated proteins. J Histochem Cytochem 52:1459-1466.
Siegel SJ, Bieschke J, Powers ET, Kelly JW (2007) The oxidative stress metabolite 4-hydroxynonenal promotes Alzheimer protofibril formation. Biochemistry 46:1503-1510.
Silverberg GD, Mayo M, Saul T, Rubenstein E, McGuire D (2003) Alzheimer's disease, normal-pressure hydrocephalus, and senescent changes in CSF circulatory physiology: a hypothesis. Lancet Neurol 2:506-511.
Simm A, Casselmann C, Schubert A, Hofmann S, Reimann A, Silber RE (2004) Age associated changes of AGE-receptor expression: RAGE upregulation is associated with human heart dysfunction. Exp Gerontol 39:407-413.
Simons K, Ikonen E (1997) Functional rafts in cell membranes. Nature 387:569-572.
Simons M, Keller P, De Strooper B, Beyreuther K, Dotti CG, Simons K (1998) Cholesterol depletion inhibits the generation of beta-amyloid in hippocampal neurons. Proc Natl Acad Sci U S A 95:6460-6464.
Singh B, Tschernig T, van Griensven M, Fieguth A, Pabst R (2003) Expression of vascular adhesion protein-1 in normal and inflamed mice lungs and normal human lungs. Virchows Arch 442:491-495.
Skoog I, Kalaria RN, Breteler MM (1999) Vascular factors and Alzheimer disease. Alzheimer Dis Assoc Disord 13 Suppl 3:S106-114.
Skoog I, Lernfelt B, Landahl S, Palmertz B, Andreasson LA, Nilsson L, Persson G, Oden A, Svanborg A (1996) 15-year longitudinal study of blood pressure and dementia. Lancet 347:1141-1145.
Smith DJ, Vainio PJ (2007) Targeting vascular adhesion protein-1 to treat autoimmune and inflammatory diseases. Ann N Y Acad Sci 1110:382-388.
Smith DJ, Salmi M, Bono P, Hellman J, Leu T, Jalkanen S (1998) Cloning of vascular adhesion protein 1 reveals a novel multifunctional adhesion molecule. J Exp Med 188:17-27.
Smith MA (1998) Alzheimer disease. Int Rev Neurobiol 42:1-54.
Smith MA, Sayre LM, Monnier VM, Perry G (1995) Radical AGEing in Alzheimer's disease. Trends Neurosci 18:172-176.
Snowdon DA, Greiner LH, Mortimer JA, Riley KP, Greiner PA, Markesbery WR (1997) Brain infarction and the clinical expression of Alzheimer disease. The Nun Study. Jama 277:813-817.
Sole M, Hernandez M, Boada M, Unzeta M (2007) Characterization of A7r5 cell line transfected in a stable form by hSSAO/VAP-1 gene (A7r5 hSSAO/VAP-1 cell line). J Neural Transm 114:763-767.
Somfai GM, Knippel B, Ruzicska E, Stadler K, Toth M, Salacz G, Magyar K, Somogyi A (2006) Soluble semicarbazide-sensitive amine oxidase (SSAO) activity is related to oxidative

stress and subchronic inflammation in streptozotocin-induced diabetic rats. Neurochem Int 48:746-752.
Sommer B (2002) Alzheimer's disease and the amyloid cascade hypothesis: ten years on. Curr Opin Pharmacol 2:87-92.
Soto C (2003) Unfolding the role of protein misfolding in neurodegenerative diseases. Nat Rev Neurosci 4:49-60.
Sparks DL (1997) Coronary artery disease, hypertension, ApoE, and cholesterol: a link to Alzheimer's disease? Ann N Y Acad Sci 826:128-146.
Sparks DL, Woeltz VM, Markesbery WR (1991) Alterations in brain monoamine oxidase activity in aging, Alzheimer's disease, and Pick's disease. Arch Neurol 48:718-721.
Sparks DL, Scheff SW, Hunsaker JC, 3rd, Liu H, Landers T, Gross DR (1994) Induction of Alzheimer-like beta-amyloid immunoreactivity in the brains of rabbits with dietary cholesterol. Exp Neurol 126:88-94.
St John PA (2007) Differential binding and activation of caspase-3 in cultured hippocampal neurons by assembly forms of A beta 1-42. J Neurosci Res 85:1205-1214.
Stanyer L, Betteridge DJ, Smith CC (2002) An investigation into the mechanisms mediating plasma lipoprotein-potentiated beta-amyloid fibrillogenesis. FEBS Lett 518:72-78.
Stanyer L, Betteridge DJ, Smith CC (2004a) Potentiation of beta-amyloid polymerisation by low-density lipoprotein enhances the peptide's vasoactivity. Biochim Biophys Acta 1670:147-155.
Stanyer L, Betteridge DJ, Smith CC (2004b) Exaggerated polymerisation of beta-amyloid 40 stimulated by plasma lipoproteins results in fibrillar Abeta preparations that are ineffective in promoting ADP-induced platelet aggregation. Biochim Biophys Acta 1674:305-311.
Stefani M, Dobson CM (2003) Protein aggregation and aggregate toxicity: new insights into protein folding, misfolding diseases and biological evolution. J Mol Med 81:678-699.
Steinberg D (2002) Atherogenesis in perspective: hypercholesterolemia and inflammation as partners in crime. Nat Med 8:1211-1217.
Steventon G, Humfrey C, Sturman S, Waring RH, Williams AC (1990) Monoamine oxidase B and Parkinson's disease. Lancet 335:180.
Stolen CM, Yegutkin GG, Kurkijarvi R, Bono P, Alitalo K, Jalkanen S (2004) Origins of serum semicarbazide-sensitive amine oxidase. Circ Res 95:50-57.
Stolz M, Stoffler D, Aebi U, Goldsbury C (2000) Monitoring biomolecular interactions by time-lapse atomic force microscopy. J Struct Biol 131:171-180.
Stone JR, Collins T (2002) The role of hydrogen peroxide in endothelial proliferative responses. Endothelium 9:231-238.
Strickland DK, Bhattacharya P, Olson ST (1984) Kinetics of the conformational alterations associated with nucleophilic modification of alpha 2-macroglobulin. Biochemistry 23:3115-3124.
Strittmatter WJ, Saunders AM, Schmechel D, Pericak-Vance M, Enghild J, Salvesen GS, Roses AD (1993) Apolipoprotein E: high-avidity binding to beta-amyloid and increased frequency of type 4 allele in late-onset familial Alzheimer disease. Proc Natl Acad Sci U S A 90:1977-1981.
Strolin Benedetti M, Tipton KF (1998) Monoamine oxidases and related amine oxidases as phase I enzymes in the metabolism of xenobiotics. J Neural Transm Suppl 52:149-171.

Struijs JN, van Genugten ML, Evers SM, Ament AJ, Baan CA, van den Bos GA (2005) Modeling the future burden of stroke in The Netherlands: impact of aging, smoking, and hypertension. Stroke 36:1648-1655.

Su JH, Nichol KE, Sitch T, Sheu P, Chubb C, Miller BL, Tomaselli KJ, Kim RC, Cotman CW (2000) DNA damage and activated caspase-3 expression in neurons and astrocytes: evidence for apoptosis in frontotemporal dementia. Exp Neurol 163:9-19.

Subbarao KV, Richardson JS, Ang LC (1990) Autopsy samples of Alzheimer's cortex show increased peroxidation in vitro. J Neurochem 55:342-345.

Suo Z, Humphrey J, Kundtz A, Sethi F, Placzek A, Crawford F, Mullan M (1998) Soluble Alzheimers beta-amyloid constricts the cerebral vasculature in vivo. Neurosci Lett 257:77-80.

Suzuki N, Iwatsubo T, Odaka A, Ishibashi Y, Kitada C, Ihara Y (1994) High tissue content of soluble beta 1-40 is linked to cerebral amyloid angiopathy. Am J Pathol 145:452-460.

Syme CD, Nadal RC, Rigby SE, Viles JH (2004) Copper binding to the amyloid-beta (Abeta) peptide associated with Alzheimer's disease: folding, coordination geometry, pH dependence, stoichiometry, and affinity of Abeta-(1-28): insights from a range of complementary spectroscopic techniques. J Biol Chem 279:18169-18177.

Tabor CW, Tabor H, Rosenthal SM (1954) Purification of amine oxidase from beef plasma. J Biol Chem 208:645-661.

Tatsch MF, Bottino CM, Azevedo D, Hototian SR, Moscoso MA, Folquitto JC, Scalco AZ, Louza MR (2006) Neuropsychiatric symptoms in Alzheimer disease and cognitively impaired, nondemented elderly from a community-based sample in Brazil: prevalence and relationship with dementia severity. Am J Geriatr Psychiatry 14:438-445.

Terry RD, Masliah E, Salmon DP, Butters N, DeTeresa R, Hill R, Hansen LA, Katzman R (1991) Physical basis of cognitive alterations in Alzheimer's disease: synapse loss is the major correlate of cognitive impairment. Ann Neurol 30:572-580.

Thal DR, Ghebremedhin E, Orantes M, Wiestler OD (2003) Vascular pathology in Alzheimer disease: correlation of cerebral amyloid angiopathy and arteriosclerosis/lipohyalinosis with cognitive decline. J Neuropathol Exp Neurol 62:1287-1301.

Thomas T, Thomas G, McLendon C, Sutton T, Mullan M (1996) beta-Amyloid-mediated vasoactivity and vascular endothelial damage. Nature 380:168-171.

Thornalley PJ, Langborg A, Minhas HS (1999) Formation of glyoxal, methylglyoxal and 3-deoxyglucosone in the glycation of proteins by glucose. Biochem J 344 Pt 1:109-116.

Thunecke M, Lobbia A, Kosciessa U, Dyrks T, Oakley AE, Turner J, Saenger W, Georgalis Y (1998) Aggregation of A beta Alzheimer's disease-related peptide studied by dynamic light scattering. J Pept Res 52:509-517.

Tickler AK, Smith DG, Ciccotosto GD, Tew DJ, Curtain CC, Carrington D, Masters CL, Bush AI, Cherny RA, Cappai R, Wade JD, Barnham KJ (2005) Methylation of the imidazole side chains of the Alzheimer disease amyloid-beta peptide results in abolition of superoxide dismutase-like structures and inhibition of neurotoxicity. J Biol Chem 280:13355-13363.

Tohka S, Laukkanen M, Jalkanen S, Salmi M (2001) Vascular adhesion protein 1 (VAP-1) functions as a molecular brake during granulocyte rolling and mediates recruitment in vivo. Faseb J 15:373-382.

Trommsdorff M, Borg JP, Margolis B, Herz J (1998) Interaction of cytosolic adaptor proteins with neuronal apolipoprotein E receptors and the amyloid precursor protein. J Biol Chem 273:33556-33560.
Uchida K, Stadtman ER (1992) Selective cleavage of thioether linkage in proteins modified with 4-hydroxynonenal. Proc Natl Acad Sci U S A 89:5611-5615.
Ulery PG, Beers J, Mikhailenko I, Tanzi RE, Rebeck GW, Hyman BT, Strickland DK (2000) Modulation of beta-amyloid precursor protein processing by the low density lipoprotein receptor-related protein (LRP). Evidence that LRP contributes to the pathogenesis of Alzheimer's disease. J Biol Chem 275:7410-7415.
Unzeta M, Sole M, Boada M, Hernandez M (2007) Semicarbazide-sensitive amine oxidase (SSAO) and its possible contribution to vascular damage in Alzheimer's disease. J Neural Transm 114:857-862.
Urbanc B, Cruz L, Yun S, Buldyrev SV, Bitan G, Teplow DB, Stanley HE (2004) In silico study of amyloid beta-protein folding and oligomerization. Proc Natl Acad Sci U S A 101:17345-17350.
Uversky VN (2003) Protein folding revisited. A polypeptide chain at the folding-misfolding-nonfolding cross-roads: which way to go? Cell Mol Life Sci 60:1852-1871.
Vainio PJ, Kortekangas-Savolainen O, Mikkola JH, Jaakkola K, Kalimo K, Jalkanen S, Veromaa T (2005) Safety of blocking vascular adhesion protein-1 in patients with contact dermatitis. Basic Clin Pharmacol Toxicol 96:429-435.
Valente T, Sole M, Unzeta M (2008) SSAO/VAP-1 protein expression during mouse embryonic development. Dev Dyn 237:2585-2593.
van Dijk EJ, Breteler MM, Schmidt R, Berger K, Nilsson LG, Oudkerk M, Pajak A, Sans S, de Ridder M, Dufouil C, Fuhrer R, Giampaoli S, Launer LJ, Hofman A (2004) The association between blood pressure, hypertension, and cerebral white matter lesions: cardiovascular determinants of dementia study. Hypertension 44:625-630.
Varadarajan S, Kanski J, Aksenova M, Lauderback C, Butterfield DA (2001) Different mechanisms of oxidative stress and neurotoxicity for Alzheimer's A beta(1--42) and A beta(25--35). J Am Chem Soc 123:5625-5631.
Vekrellis K, Ye Z, Qiu WQ, Walsh D, Hartley D, Chesneau V, Rosner MR, Selkoe DJ (2000) Neurons regulate extracellular levels of amyloid beta-protein via proteolysis by insulin-degrading enzyme. J Neurosci 20:1657-1665.
Verbeek MM, Ruiter DJ, de Waal RM (1997) The role of amyloid in the pathogenesis of Alzheimer's disease. Biol Chem 378:937-950.
Vermeer SE, Prins ND, den Heijer T, Hofman A, Koudstaal PJ, Breteler MM (2003) Silent brain infarcts and the risk of dementia and cognitive decline. N Engl J Med 348:1215-1222.
Vidrio H (2003) Semicarbazide-sensitive amine oxidase: role in the vasculature and vasodilation after in situ inhibition. Auton Autacoid Pharmacol 23:275-283.
Vincent B, Smith JD (2001) Astrocytes down-regulate neuronal beta-amyloid precursor protein expression and modify its processing in an apolipoprotein E isoform-specific manner. Eur J Neurosci 14:256-266.
Vitek MP, Bhattacharya K, Glendening JM, Stopa E, Vlassara H, Bucala R, Manogue K, Cerami A (1994) Advanced glycation end products contribute to amyloidosis in Alzheimer disease. Proc Natl Acad Sci U S A 91:4766-4770.
Vlad SC, Miller DR, Kowall NW, Felson DT (2008) Protective effects of NSAIDs on the development of Alzheimer disease. Neurology 70:1672-1677.

Voisin T, Lugardon S, Balardy L, Vellas B (2003) [Vascular risk factors and Alzheimer's disease]. Rev Med Interne 24 Suppl 3:288s-291s.

Wahrle S, Das P, Nyborg AC, McLendon C, Shoji M, Kawarabayashi T, Younkin LH, Younkin SG, Golde TE (2002) Cholesterol-dependent gamma-secretase activity in buoyant cholesterol-rich membrane microdomains. Neurobiol Dis 9:11-23.

Waldstein SR, Katzel LI (2006) Interactive relations of central versus total obesity and blood pressure to cognitive function. Int J Obes (Lond) 30:201-207.

Walsh DM, Klyubin I, Fadeeva JV, Cullen WK, Anwyl R, Wolfe MS, Rowan MJ, Selkoe DJ (2002) Naturally secreted oligomers of amyloid beta protein potently inhibit hippocampal long-term potentiation in vivo. Nature 416:535-539.

Walsh DM, Townsend M, Podlisny MB, Shankar GM, Fadeeva JV, El Agnaf O, Hartley DM, Selkoe DJ (2005) Certain inhibitors of synthetic amyloid beta-peptide (Abeta) fibrillogenesis block oligomerization of natural Abeta and thereby rescue long-term potentiation. J Neurosci 25:2455-2462.

Walsh DM, Hartley DM, Kusumoto Y, Fezoui Y, Condron MM, Lomakin A, Benedek GB, Selkoe DJ, Teplow DB (1999) Amyloid beta-protein fibrillogenesis. Structure and biological activity of protofibrillar intermediates. J Biol Chem 274:25945-25952.

Walther M, Popratiloff A, Lachnit N, Hofmann N, Streppel M, Guntinas-Lichius O, Neiss WF, Angelov DN (2001) Exogenous antigen containing perivascular phagocytes induce a non-encephalitogenic extravasation of primed lymphocytes. J Neuroimmunol 117:30-42.

Wanecq E, Bour S, Verwaerde P, Smih F, Valet P, Carpene C (2006) Increased monoamine oxidase and semicarbazide-sensitive amine oxidase activities in white adipose tissue of obese dogs fed a high-fat diet. J Physiol Biochem 62:113-123.

Wang Q, Walsh DM, Rowan MJ, Selkoe DJ, Anwyl R (2004a) Block of long-term potentiation by naturally secreted and synthetic amyloid beta-peptide in hippocampal slices is mediated via activation of the kinases c-Jun N-terminal kinase, cyclin-dependent kinase 5, and p38 mitogen-activated protein kinase as well as metabotropic glutamate receptor type 5. J Neurosci 24:3370-3378.

Wang X, Desai K, Clausen JT, Wu L (2004b) Increased methylglyoxal and advanced glycation end products in kidney from spontaneously hypertensive rats. Kidney Int 66:2315-2321.

Wang X, Desai K, Chang T, Wu L (2005) Vascular methylglyoxal metabolism and the development of hypertension. J Hypertens 23:1565-1573.

Watson GS, Craft S (2003) The role of insulin resistance in the pathogenesis of Alzheimer's disease: implications for treatment. CNS Drugs 17:27-45.

Weiss HG, Klocker J, Labeck B, Nehoda H, Aigner F, Klingler A, Ebenbichler C, Foger B, Lechleitner M, Patsch JR, Schwelberger HG (2003) Plasma amine oxidase: a postulated cardiovascular risk factor in nondiabetic obese patients. Metabolism 52:688-692.

Wekerle H (2002) Immune protection of the brain--efficient and delicate. J Infect Dis 186 Suppl 2:S140-144.

Wenk GL (2003) Neuropathologic changes in Alzheimer's disease. J Clin Psychiatry 64 Suppl 9:7-10.

Wentworth P, Jr., Nieva J, Takeuchi C, Galve R, Wentworth AD, Dilley RB, DeLaria GA, Saven A, Babior BM, Janda KD, Eschenmoser A, Lerner RA (2003) Evidence for ozone formation in human atherosclerotic arteries. Science 302:1053-1056.

White AR, Bush AI, Beyreuther K, Masters CL, Cappai R (1999) Exacerbation of copper toxicity in primary neuronal cultures depleted of cellular glutathione. J Neurochem 72:2092-2098.
Whitmer RA, Sidney S, Selby J, Johnston SC, Yaffe K (2005) Midlife cardiovascular risk factors and risk of dementia in late life. Neurology 64:277-281.
Wilhelmus MM, Otte-Holler I, van Triel JJ, Veerhuis R, Maat-Schieman ML, Bu G, de Waal RM, Verbeek MM (2007) Lipoprotein receptor-related protein-1 mediates amyloid-beta-mediated cell death of cerebrovascular cells. Am J Pathol 171:1989-1999.
Wingender W (1983) High-performance liquid chromatographic method for the quantitative analysis of a synthetic copolymer with antitumor activity (copovithane) and methylamine in human blood plasma and urine. J Chromatogr 273:319-326.
Wolfe MS (2006) The gamma-secretase complex: membrane-embedded proteolytic ensemble. Biochemistry 45:7931-7939.
Wolfe MS, Xia W, Ostaszewski BL, Diehl TS, Kimberly WT, Selkoe DJ (1999) Two transmembrane aspartates in presenilin-1 required for presenilin endoproteolysis and gamma-secretase activity. Nature 398:513-517.
Wolozin B, Kellman W, Ruosseau P, Celesia GG, Siegel G (2000) Decreased prevalence of Alzheimer disease associated with 3-hydroxy-3-methyglutaryl coenzyme A reductase inhibitors. Arch Neurol 57:1439-1443.
Xiang Z, Ho L, Valdellon J, Borchelt D, Kelley K, Spielman L, Aisen PS, Pasinetti GM (2002) Cyclooxygenase (COX)-2 and cell cycle activity in a transgenic mouse model of Alzheimer's disease neuropathology. Neurobiol Aging 23:327-334.
Xiao S, Yu PH (2009) A fluorometric high-performance liquid chromatography procedure for simultaneous determination of methylamine and aminoacetone in blood and tissues. Anal Biochem 384:20-26.
Xu HL, Salter-Cid L, Linnik MD, Wang EY, Paisansathan C, Pelligrino DA (2006) Vascular adhesion protein-1 plays an important role in postischemic inflammation and neuropathology in diabetic, estrogen-treated ovariectomized female rats subjected to transient forebrain ischemia. J Pharmacol Exp Ther 317:19-29.
Yaffe K, Blackwell T, Kanaya AM, Davidowitz N, Barrett-Connor E, Krueger K (2004) Diabetes, impaired fasting glucose, and development of cognitive impairment in older women. Neurology 63:658-663.
Yaffe K, Lindquist K, Penninx BW, Simonsick EM, Pahor M, Kritchevsky S, Launer L, Kuller L, Rubin S, Harris T (2003) Inflammatory markers and cognition in well-functioning African-American and white elders. Neurology 61:76-80.
Yamada M, Tsukagoshi H, Otomo E, Hayakawa M (1987) Cerebral amyloid angiopathy in the aged. J Neurol 234:371-376.
Yamagishi S, Nakamura K, Imaizumi T (2005) Advanced glycation end products (AGEs) and diabetic vascular complications. Curr Diabetes Rev 1:93-106.
Yamashita K, Miyakawa T, Katsuragi S (1991) Vascular changes in the brains with Alzheimer's disease. Jpn J Psychiatry Neurol 45:79-84.
Yan SD, Chen X, Schmidt AM, Brett J, Godman G, Zou YS, Scott CW, Caputo C, Frappier T, Smith MA, et al. (1994) Glycated tau protein in Alzheimer disease: a mechanism for induction of oxidant stress. Proc Natl Acad Sci U S A 91:7787-7791.

Yan SD, Zhu H, Zhu A, Golabek A, Du H, Roher A, Yu J, Soto C, Schmidt AM, Stern D, Kindy M (2000) Receptor-dependent cell stress and amyloid accumulation in systemic amyloidosis. Nat Med 6:643-651.

Yan SD, Chen X, Fu J, Chen M, Zhu H, Roher A, Slattery T, Zhao L, Nagashima M, Morser J, Migheli A, Nawroth P, Stern D, Schmidt AM (1996) RAGE and amyloid-beta peptide neurotoxicity in Alzheimer's disease. Nature 382:685-691.

Yan SD, Fu J, Soto C, Chen X, Zhu H, Al-Mohanna F, Collison K, Zhu A, Stern E, Saido T, Tohyama M, Ogawa S, Roher A, Stern D (1997) An intracellular protein that binds amyloid-beta peptide and mediates neurotoxicity in Alzheimer's disease. Nature 389:689-695.

Yanagisawa K, Odaka A, Suzuki N, Ihara Y (1995) GM1 ganglioside-bound amyloid beta-protein (A beta): a possible form of preamyloid in Alzheimer's disease. Nat Med 1:1062-1066.

Yang F, Sun X, Beech W, Teter B, Wu S, Sigel J, Vinters HV, Frautschy SA, Cole GM (1998) Antibody to caspase-cleaved actin detects apoptosis in differentiated neuroblastoma and plaque-associated neurons and microglia in Alzheimer's disease. Am J Pathol 152:379-389.

Yankner BA, Mesulam MM (1991) Seminars in medicine of the Beth Israel Hospital, Boston. beta-Amyloid and the pathogenesis of Alzheimer's disease. N Engl J Med 325:1849-1857.

Yasuda M, Ohzeki Y, Shimizu S, Naito S, Ohtsuru A, Yamamoto T, Kuroiwa Y (1999) Stimulation of in vitro angiogenesis by hydrogen peroxide and the relation with ETS-1 in endothelial cells. Life Sci 64:249-258.

Ye S, Huang Y, Mullendorff K, Dong L, Giedt G, Meng EC, Cohen FE, Kuntz ID, Weisgraber KH, Mahley RW (2005) Apolipoprotein (apo) E4 enhances amyloid beta peptide production in cultured neuronal cells: apoE structure as a potential therapeutic target. Proc Natl Acad Sci U S A 102:18700-18705.

Yip CM, Elton EA, Darabie AA, Morrison MR, McLaurin J (2001) Cholesterol, a modulator of membrane-associated Abeta-fibrillogenesis and neurotoxicity. J Mol Biol 311:723-734.

Youdim MB (1989) Brain monoamine oxidase (MAO) B: a unique neurotoxin and neurotransmitter producing enzyme. Prog Neuropsychopharmacol Biol Psychiatry 13:363-371.

Young-Pearse TL, Bai J, Chang R, Zheng JB, LoTurco JJ, Selkoe DJ (2007) A critical function for beta-amyloid precursor protein in neuronal migration revealed by in utero RNA interference. J Neurosci 27:14459-14469.

Young SN, Davis BA, Gauthier S (1982) Precursors and metabolites of phenylethylamine, m and p-tyramine and tryptamine in human lumbar and cisternal cerebrospinal fluid. J Neurol Neurosurg Psychiatry 45:633-639.

Yu PH (1990) Oxidative deamination of aliphatic amines by rat aorta semicarbazide-sensitive amine oxidase. J Pharm Pharmacol 42:882-884.

Yu PH (2001) Involvement of cerebrovascular semicarbazide-sensitive amine oxidase in the pathogenesis of Alzheimer's disease and vascular dementia. Med Hypotheses 57:175-179.

Yu PH, Zuo DM (1993) Oxidative deamination of methylamine by semicarbazide-sensitive amine oxidase leads to cytotoxic damage in endothelial cells. Possible consequences for diabetes. Diabetes 42:594-603.

Yu PH, Zuo DM (1996) Formaldehyde produced endogenously via deamination of methylamine. A potential risk factor for initiation of endothelial injury. Atherosclerosis 120:189-197.
Yu PH, Zuo DM (1997) Aminoguanidine inhibits semicarbazide-sensitive amine oxidase activity: implications for advanced glycation and diabetic complications. Diabetologia 40:1243-1250.
Yu PH, Deng YL (1998) Endogenous formaldehyde as a potential factor of vulnerability of atherosclerosis: involvement of semicarbazide-sensitive amine oxidase-mediated methylamine turnover. Atherosclerosis 140:357-363.
Yu PH, Dyck RF (1998) Impairment of methylamine clearance in uremic patients and its nephropathological implications. Clin Nephrol 49:299-302.
Yu PH, Deng Y (2000) Potential cytotoxic effect of chronic administration of creatine, a nutrition supplement to augment athletic performance. Med Hypotheses 54:726-728.
Yu PH, Lai CT, Zuo DM (1997) Formation of formaldehyde from adrenaline in vivo; a potential risk factor for stress-related angiopathy. Neurochem Res 22:615-620.
Yu PH, Wang M, Deng YL, Fan H, Shira-Bock L (2002) Involvement of semicarbazide-sensitive amine oxidase-mediated deamination in atherogenesis in KKAy diabetic mice fed with high cholesterol diet. Diabetologia 45:1255-1262.
Yu PH, Wang M, Fan H, Deng Y, Gubisne-Haberle D (2004) Involvement of SSAO-mediated deamination in adipose glucose transport and weight gain in obese diabetic KKAy mice. Am J Physiol Endocrinol Metab 286:E634-641.
Yu PH, Lu LX, Fan H, Kazachkov M, Jiang ZJ, Jalkanen S, Stolen C (2006) Involvement of semicarbazide-sensitive amine oxidase-mediated deamination in lipopolysaccharide-induced pulmonary inflammation. Am J Pathol 168:718-726.
Zandi PP, Anthony JC, Hayden KM, Mehta K, Mayer L, Breitner JC (2002) Reduced incidence of AD with NSAID but not H2 receptor antagonists: the Cache County Study. Neurology 59:880-886.
Zeisel SH, Wishnok JS, Blusztajn JK (1983) Formation of methylamines from ingested choline and lecithin. J Pharmacol Exp Ther 225:320-324.
Zerbinatti CV, Cordy JM, Chen CD, Guillily M, Suon S, Ray WJ, Seabrook GR, Abraham CR, Wolozin B (2008) Oxysterol-binding protein-1 (OSBP1) modulates processing and trafficking of the amyloid precursor protein. Mol Neurodegener 3:5.
Zhang Q, Powers ET, Nieva J, Huff ME, Dendle MA, Bieschke J, Glabe CG, Eschenmoser A, Wentworth P, Jr., Lerner RA, Kelly JW (2004) Metabolite-initiated protein misfolding may trigger Alzheimer's disease. Proc Natl Acad Sci U S A 101:4752-4757.
Zhang X, McIntire WS (1996) Cloning and sequencing of a copper-containing, topa quinone-containing monoamine oxidase from human placenta. Gene 179:279-286.
Zhou Y, Gopalakrishnan V, Richardson JS (1996) Actions of neurotoxic beta-amyloid on calcium homeostasis and viability of PC12 cells are blocked by antioxidants but not by calcium channel antagonists. J Neurochem 67:1419-1425.
Zipfel GJ, Han H, Ford AL, Lee JM (2009) Cerebral amyloid angiopathy: progressive disruption of the neurovascular unit. Stroke 40:S16-19.
Zlokovic BV (1996) Cerebrovascular transport of Alzheimer's amyloid beta and apolipoproteins J and E: possible anti-amyloidogenic role of the blood-brain barrier. Life Sci 59:1483-1497.
Zlokovic BV (2004) Clearing amyloid through the blood-brain barrier. J Neurochem 89:807-811.

Zlokovic BV (2005) Neurovascular mechanisms of Alzheimer's neurodegeneration. Trends Neurosci 28:202-208.
Zlokovic BV (2008a) New therapeutic targets in the neurovascular pathway in Alzheimer's disease. Neurotherapeutics 5:409-414.
Zlokovic BV (2008b) The blood-brain barrier in health and chronic neurodegenerative disorders. Neuron 57:178-201.
Zuo DM, Yu PH (1994) Semicarbazide-sensitive amine oxidase and monoamine oxidase in rat brain microvessels, meninges, retina and eye sclera. Brain Res Bull 33:307-311.

VITA

Kun Chen was born in Shijiazhuang, China, July 8, 1980. He received a Bachelor of Engineering in Bioengineering from the Beijing Institute of Technology in 2003. Throughout his undergraduate education, he obtained knowledge and training on both engineering and biology. From 2002 to 2003, he conducted some studies on the pathology of Parkinson's disease in Dr. Yulin Deng's laboratory, where triggered his strong interest in neurodegenerative diseases. In 2004, he continued to persue a Master's degree in Neuropsychiatry in the Department of Psychiatry, University of Saskatchewan. In 2007, he transferred to the PhD program in the Department of Pharmacology. Under the supervision of Dr. Peter Yu, he studied the involvement of a vascular enzyme, SSAO, in the development of Alzheimer's disease. He has been awarded the scholarships from College of Medicine, University of Saskatchewan and from Alzheimer Society of Saskatchewan. Courses included Cellular Biochemistry, Neuropsychiatry, Neuropharmacology, Development of the Nervous System, and Graduate Pharmacology.

Publications

Refereed Papers

- M Kazachkov, **K Chen**, S Babiy, P H Yu Evidence for in vivo scavenging by aminoguanidine of formaldehyde produced via semicarbazide-sensitive amine oxidase-mediated deamination. *J Pharmacol Exp Ther.* 2007; 322 (3): 1201-7.
- **K Chen**, M Kazachkov, P H Yu Effect of aldehydes derived from oxidative deamination and oxidative stress on beta-amyloid aggregation; pathological implications to Alzheimer's disease. *J Neural Transm.* 2007; 114 (6): 835-9.
- **K Chen**, J Maley, P H Yu Potential implications of endogenous aldehydes in β-amyloid misfolding, oligomerization and fibrillogenesis. *J Neurochem.* 2006; 99 (5): 1413-24.

Abstracts

- **K Chen**, Z Jiang and P H Yu 6th International Congress on Vascular Dementia (Barcelona, Spain, 2009)
- **K Chen**, Z Jiang and P H Yu Spotlight on Research: Alzheimer's Disease and Related Dementia Research by the Alzheimer Society of Saskatchewan (Saskatoon, Canada, 2009)

- **K Chen**, Z Jiang and P H Yu The Canadian Society of Pharmacology and Therapeutics 2009 Conference (Saskatoon, Canada 2009)
- **K Chen**, Z Jiang and P H Yu The 13th Amine Oxidases and Related Diseases Workshop (Beijing, China, 2008)
- **K Chen** and P H Yu Alzheimer's Disease in the Keystone Symposia (Keystone, USA, 2008)
- **K Chen** and P H Yu The 12th Amine Oxidase and Trace Amines Workshop (Rotterdam, Netherlands, 2006)

Journal of Neurochemistry, 2006, **99**, 1413–1424 doi:10.1111/j.1471-4159.2006.04181.x

Potential implications of endogenous aldehydes in β-amyloid misfolding, oligomerization and fibrillogenesis

Kun Chen,* Jason Maley† and Peter H. Yu*

**Neuropsychiatry Research Unit, Department of Psychiatry; and †Saskatchewan Structural Sciences Centre, University of Saskatchewan, Saskatoon, Saskatchewan, Canada*

Abstract

Aldehydes are capable of inducing protein cross-linkage. An increase in aldehydes has been found in Alzheimer's disease. Formaldehyde and methylglyoxal are produced via deamination of, respectively, methylamine and aminoacetone catalyzed by semicarbazide-sensitive amine oxidase (SSAO, EC 1.4.3.6. The enzyme is located on the outer surface of the vasculature, where amyloidosis is often initiated. A high SSAO level has been identified as a risk factor for vascular disorders. Serum SSAO activity has been found to be increased in Alzheimer's patients. Malondialdehyde and 4-hydroxynonenal are derived from lipid peroxidation under oxidative stress, which is also associated with Alzheimer's disease. Aldehydes may potentially play roles in β-amyloid aggregation related to the pathology of Alzheimer's disease. In the present study, thioflavin-T fluorometry, dynamic light scattering, circular dichroism spectroscopy and atomic force microscopy were employed to reveal the effect of endogenous aldehydes on β-amyloid at different stages, i.e. β-sheet formation, oligomerization and fibrillogenesis. Formaldehyde, methylglyoxal and malondialdehyde and, to a lesser extent, 4-hydroxynonenal are not only capable of enhancing the rate of formation of β-amyloid β-sheets, oligomers and protofibrils but also of increasing the size of the aggregates. The possible relevance to Alzheimer's disease of the effects of these aldehydes on β-amyloid deposition is discussed.

Keywords: Alzheimer's disease, β-amyloid oligomerization, atomic force microscopy, formaldehyde, methylglyoxal, semicarbazide-sensitive amine oxidase.

J. Neurochem. (2006) **99**, 1413–1424.

Extracellular β-amyloid (Aβ) deposition in the brain is a major hallmark of Alzheimer's disease (reviewed in Selkoe 2002; Tanzi & Bertram 2005). Aβ peptides, comprising heterogeneously truncated fragments from amyloid precursor protein, readily form β-sheets, which assemble to oligomers, protofibrils, and fibrils, and subsequently coaggregate with other proteins, such as lipoproteins, to form senile plaques (Ma *et al.* 1994; Wisniewski *et al.* 1994; Cotman *et al.* 2000; Taylor *et al.* 2003). Aβ is toxic and capable of triggering a cascade of events including induction of oxidative stress and inflammatory responses leading to neurodegeneration (Loo *et al.* 1993; Morishima *et al.* 2001). Recently, Aβ oligomers (5–10 Aβ molecules) have been shown to be the most cytotoxic (Kayed *et al.* 2003; Klein *et al.* 2004). The roles of the advanced Aβ aggregates, i.e. fibrils and plaques, in the neurodegeneration of Alzheimer's disease have not been clearly defined.

A large body of literature suggests that vascular disorders are involved in the pathogenesis of vascular dementia and Alzheimer's disease (see reviews by Jellinger 2002; Kalaria and Ballard. 1999). Indeed, a variety of types of microvascular changes have been observed in aging and in Alzheimer's disease brains (Farkas & Luiten. 2001). Aβ depositions were found closely associated with the degenerated cerebral vasculature (Coria *et al.* 1988; Kawai *et al.* 1993). Aβ isolated from the vascular tissues contains significantly less isomerized and racemized aspartyl residues than those Aβ in the neuritic plaques, suggesting that the vascular amyloid is 'younger' (Roher *et al.* 1993). The cerebral vascular basement membrane has even been considered to play an important role in

Received April 12, 2006; revised manuscript received July 16, 2006; accepted July 17, 2006.

Address correspondence and reprint requests to Peter H. Yu, Neuropsychiatry Research Unit, University of Saskatchewan, Saskatoon, Saskatchewan, S7N 5E4 Canada. E-mail: YUP@USASK.CA

Abbreviations used: Aβ, β-amyloid; AFM, atomic force microscope; CD, circular dichroism spectroscopy; DLS, dynamic light scattering; FA, formaldehyde; HFIP, 1,1,1,3,3,3-hexafluoro-2-propanol; HNE, 4-hydroxy-2-nonenal; MG, methylglyoxal; MDA, malondialdehyde; PBS, phosphate-buffered saline; SSAO, semicarbazide-sensitive amine oxidase; ThT, thioflavin-T fluorescence assay.

J Neural Transm (2007) 114: 835–839
DOI 10.1007/s00702-007-0697-5
Printed in the Netherlands

Journal of Neural Transmission

Effect of aldehydes derived from oxidative deamination and oxidative stress on β-amyloid aggregation; pathological implications to Alzheimer's disease

K. Chen, M. Kazachkov, P. H. Yu

Neuropsychiatry Research Unit, Department of Psychiatry, University of Saskatchewan, Saskatoon, Saskatchewan, Canada

Received: November 3, 2006 / Accepted: December 1, 2006 / Published online: March 31, 2007

Summary Formaldehyde and methylglyoxal are generated *via* deamination from methylamine and aminoacetone respectively catalyzed by semicarbazide-sensitive amine oxidase (SSAO). Malondialdehyde (MDA) and 4-hydroxynonenal (HNE) are end products of lipid peroxidation due to oxidative stress. These aldehydes are capable of inducing protein cross-linkage. Elevated levels of aldehydes were found in Alzheimer's disease (AD). These reactive metabolites may potentially play important roles in β-amyloid (Aβ) aggregation related to the pathology of AD. In the present study thioflavin-T (ThT) fluorometry, an immuno-dot-blot assay and atomic force microscopy (AFM) were employed to reveal the effect of aldehydes on Aβ aggregation *in vitro*. The target on Aβ for interaction with formaldehyde was identified. The results support the involvement of endogenous aldehydes in amyloid deposition related to AD.

Keywords: Alzheimer's disease, β-amyloid, aldehydes, SSAO, AFM, fibrillogenesis

Introduction

Extracellular β-amyloid (Aβ) deposition is a major pathological hallmark of Alzheimer's disease (AD) (Selkoe, 2002). Aβ peptides readily form β-sheets structure, oligomers, protofibrils, fibrils, and subsequently co-aggregate with other proteins to produce senile plaques (Stanyer et al., 2004; Ma et al., 1994). Aβ is cytotoxic and capable of triggering oxidative stress and neurodegeneration (Loo et al., 1993). Its oligomers (i.e. 5–10 Aβ monomers) are the most toxic forms (Klein et al., 2004; Kayed et al., 2003). AD shares common pathological features and risk factors with other vascular disorders, such as atherosclerosis and diabetes mellitus (Messier, 2003). A large body of literature suggests that vascular disorders are involved in the pathogenesis of AD (Jellinger, 2002). Substantial Aβ deposits were found to be associated with cerebral vasculature degeneration (Coria et al., 1988; Kawai et al., 1993). Aβ isolated from the vascular tissues contains significantly less isomerized and racemized aspartyl residues than does the neuritic Aβ plaques suggesting that the vascular amyloid is "younger" (Roher et al., 1993).

Semicarbazide-sensitive amine oxidase (SSAO), an enzyme located on the plasma membrane surface of vascular smooth muscle and endothelial cells, may contribute to the pathogenesis of vascular disorders (Yu and Zuo, 1993; Yu and Deng, 1998). Increased SSAO activity is considered a potential risk factor for vascular disorders (Boomsma et al., 2000). SSAO catalyzes the deamination of endogenous substrates methylamine and aminoacetone producing toxic formaldehyde and methylglyoxal respectively, as well as hydrogen peroxide and ammonia. Formaldehyde derived from SSAO-mediated deamination of methylamine cross-links with proteins *in vivo* (Gubisne-Haberle et al., 2004). The enzyme is co-localized with cerebral vascular Aβ deposits in Alzheimer brains (Ferrer et al., 2002). Serum SSAO activity is elevated in different conditions of vascular disorders (see review by Yu et al., 2003) including AD (del Mar Hernandez et al., 2006). Methylglyoxal can also be synthesized *via* other metabolic pathways and is well known to contribute to advanced protein glycation in diabetes (Thornalley, 2002). Diabetes mellitus is a well-known risk factor for AD (Luchsinger et al., 2001). Interestingly, CSF samples from the AD patients exhibit significantly increased levels of methylglyoxal than that of the control

Correspondence: Dr. Peter H. Yu, Neuropsychiatry Research Unit, University of Saskatchewan, Saskatoon, Saskatchewan, S7N 5E4 Canada
e-mail: YUP@USASK.CA